THE UNIVERSITY
of EDINBURGH

Investigating myelination and remyelination in zebrafish

E. Jolanda Muenzel

Doctor of Philosophy

University of Edinburgh

2013

PREFACE

The work for this doctoral thesis was conducted at the Centre for Neuroregeneration and the Centre for Regenerative Medicine at the University of Edinburgh. I declare that the research described within this thesis is my own work and that this thesis was composed by myself unless otherwise specified in the text or the acknowledgements.

Neither this dissertation nor part thereof has been submitted for academic merit at another educational institution. Data within this thesis have been submitted for the following publication:

Münzel EJ, Schaefer K, Obirei B, Kremmer E, Burton EA, Kuscha V, Becker CG, Brösamle C, Williams A, Becker T. Claudin k is specifically expressed in cells that form myelin during development of the nervous system and regeneration of the optic nerve in adult zebrafish. Glia 2012 Feb;60(2):253-70

June 2013

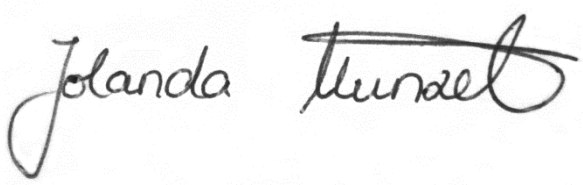

ACKNOWLEDGEMENTS

I would like to extend my gratitude to my supervisors Dr Anna Williams, Dr Catherina Becker, Dr Thomas Becker and Prof Charles ffrench-Constant for their guidance and continuous support throughout the experimental work, the composition and submission of manuscripts and the writing of my doctoral thesis.

I would like to thank the Centre for Clinical Brain Sciences for funding my work through the award of a PhD studentship.

A special thank you to all the members of the labs I have worked in over the past years for the support and motivation. It was great to have been part of an environment full of enthusiasm, and I am grateful for the many fun times spent together and the friendships that will remain.

Last, but by no means least, I would like to thank my family and my fiancé Kunal who have given me their undivided support and interest, and encouraged me at every step of the way.

ABSTRACT

Central nervous system (CNS) myelination is important for proper nervous system function in vertebrates. In demyelinating diseases such as multiple sclerosis, autoimmune-mediated myelin destruction results in neurological impairment; and although remyelination does occur spontaneously, it is poorly understood and insufficient in humans. Zebrafish (*Danio rerio*) are known to harbour tremendous regenerative capacity of various CNS tissues; however, there is presently only little knowledge of their myelin repair efficiency. An experimental model of myelin injury in zebrafish would permit study of the mechanisms involved in successful remyelination and could potentially guide the development of novel therapeutic agents for mammalian remyelination. This doctoral thesis describes the characterisation of the novel myelin protein Claudin k in zebrafish, demonstrates the establishment of adult zebrafish as an experimental model for CNS de- and remyelination and explores some mechanisms underlying myelin repair.

A variety of myelin markers have previously been investigated in zebrafish, including myelin basic protein and myelin protein zero. However, the use of these is limited by either late developmental expression or presence in compact myelin only. Claudin k is a novel tight junction protein specific to zebrafish CNS and PNS, which can be observed early in development and throughout nervous system regeneration. Utilising specific antibodies and a novel transgenic zebrafish line, in which the *claudin k* promoter drives the expression of green fluorescent protein in myelinating cells, the studies herein characterise the expression of Claudin k, demonstrate the fidelity of the transgenic construct, and investigate the relationship of Claudin k with established myelin and CNS inflammation markers. Data demonstrate that Claudin k expression closely resembles expression patterns of the endogenous gene, and as such provides a key tool for examining CNS myelination in zebrafish.

For the study of de- and remyelination in the zebrafish, the experiments herein describe the use of lysophosphatidylcholine (LPC), a detergent-like myelin toxin, which is used widely in rodent models to demyelinate axons. Its application to the adult zebrafish optic nerve induced focal demyelinating lesions, critically without detectable axonal injury, and permitted the study of time course and efficiency of remyelination. Myelin in the lesion area was reduced as detected by both immunohistochemistry and electron microscopy at 8 days post lesion (dpl), and return of the markers to control levels suggested regeneration by 28 dpl. In addition microglial activation was observed along the optic pathway, which also returned to levels compared to unlesioned control by 28 dpl. In young zebrafish (aged 4-6 months), the myelin thickness of remyelinated fibres showed no difference to the pre-lesion state, which is different to mammals, where the myelin thickness is reduced. However, in old fish (aged 18+ months), remyelinated fibres presented with thinner myelin, suggesting that the regenerative capacity of zebrafish declines with age.

While the zebrafish as an experimental system has tremendous benefits, such as potential for drug screens using the transparent larvae, capacity for transgenesis and live imaging, experimental models in zebrafish potentially bear several limitations, in particular their distant relationship to humans. To determine whether zebrafish remyelination involves homologous signalling mechanisms to mammals, demyelinated zebrafish optic nerves were treated with human recombinant Semaphorin 3A, an axonal guidance molecule which is well known to inhibit oligodendrocyte precursor cell (OPC) recruitment and remyelination in mammals. Results demonstrated fewer oligodendroglial cells at 14 dpl and less myelinated fibres at 28 dpl in the optic nerve lesion area compared to control treated animals, supporting the hypothesis that zebrafish remyelination may indeed respond to human signalling molecules.

Taken together, the findings in this doctoral thesis suggest that this new experimental zebrafish-based model of CNS remyelination can be added to the suite of current models to better understand the remyelination process and that some

signalling mechanisms observed in mammals around myelination and OPC recruitment are likely conserved in the zebrafish. In addition, it could potentially be used to discover novel therapeutic targets that promote myelination in injury.

CONTENTS

Chapter 2: Materials and methods

Chapter 6: Discussion

CHAPTER 1 – Introduction

Myelination is critical for neuronal function in mammals and destruction of myelin impairs neurological function. In certain chronic neurodegenerative disorders, repeated myelin injury eventually leads to failure of remyelination. In contrast to human remyelination, zebrafish possess a high regenerative capacity and I wondered whether zebrafish would be able to repair their myelin following injury and perhaps serve as a model organism to investigate signalling mechanisms underlying successful remyelination. In this doctoral thesis, 1) I characterised a novel myelin protein in zebrafish, Claudin k, and investigated its expression during zebrafish development and regeneration, 2) I developed an adult zebrafish model of CNS de- and remyelination and 3) I used this model to determine whether remyelination efficiency can be manipulated. In the introduction I will discuss the importance of myelin, its relevance for nerve conduction and its pathology in human demyelinating disease. I will further describe the experimental platforms developed to study hypotheses around de- and remyelination.

1.1 Myelin

Myelin was first described in the early 19th century by Rudolf Virchow (Virchow, 1854), who reported the finding of a white substance around the nerve fibres. It is a plasma membrane extension of glial cells – oligodendrocytes in the CNS and Schwann cells in the PNS – and is wrapped around the axon of neuronal cells in a spiral fashion (Geren and Schmitt, 1954). The myelin around an axon is not a single tube, but rather many areas of myelin ensheathment – internodes – are separated by non-myelinated nodes of Ranvier, which are important for nerve impulse propagation (Figure 1.1). While the myelin composition in the PNS and CNS is thought to be somewhat similar, the main difference lies in the myelinating cells

and how they myelinate. In the peripheral nervous system, Schwann cells form internodes on a one-to-one ratio, meaning that one cell will generate one internode only, and hence the cell is closely associated with the axon it myelinates. By contrast, oligodendrocytes in the CNS are able to form many internodes on multiple axons and are therefore usually located at some distance from the axons they myelinate (Figure 1.1). An oligodendrocyte can produce approximately $50x10^3$ μm^2 myelin membrane surface area per day (Pfeiffer et al., 1993) and myelinate up to 40 axons (discussed in Baumann and Pham-Dinh, 2001). In the human brain, myelination begins in midgestation (Inder and Huppi, 2000); at birth only a few areas of the brain are myelinated and this process continues until at least 25-30 years of age. Histological and magnetic resonance imaging studies in humans have showed that the myelinated fibre density in various cortical regions was extremely low at birth but continued to grow until well into the third decade (reviewed in Baumann and Pham-Dinh, 2001; Miller et al., 2012). It has been suggested that oligodendrocytes are the cell type generated last during nervous system development (reviewed in Thomas et al., 2000).

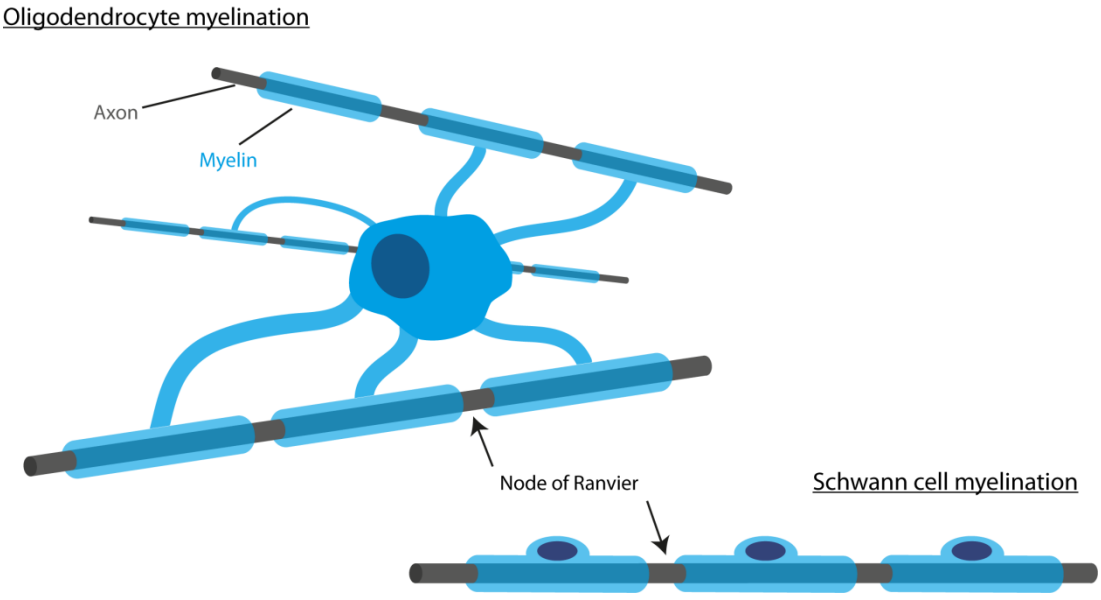

Figure 1.1: Schwann cell vs. oligodendrocyte myelination. While Schwann cells can only form one internode per cell and are therefore located immediately adjacent to the axon, oligodendrocytes are able to generate multiple internodes on many different axons through process extension.

Origin of oligodendrocytes

During embryogenesis and early postnatal life, oligodendrocytes originate from multipotent neural stem cells, which can form neurons, astrocytes and oligodendrocytes (McKay, 1997; Rao, 1999). The origin of these oligodendrocyte precursors has been widely debated (reviewed in Richardson et al., 2006); early studies suggested that oligodendrocyte precursors were formed under the influence of sonic hedgehog (Shh) and restricted to ventral regions of the ventricular progenitor zone from where they would migrate dorsally and laterally (Noll and Miller, 1993; Pringle et al., 1996; Warf et al., 1991). However, recent investigations provided evidence of an additional dorsal source of oligodendrocytes in the spinal cord, in which the specification of oligodendrocyte precursors is independent of Shh but involves BMP and FGF (Cai et al., 2005; Fogarty et al., 2005; Vallstedt et al., 2005). NG2+ cells (described in more detail lateron) have also been discussed as a source of multipotent neural stem cells capable of forming oligodendrocytes during development and in the adult CNS (Richardson et al., 2011). The initial discovery of the O-2A progenitor cell, which was found throughout the mature brain (Dawson et al., 2003), comprised 5% of all cells in the CNS and could generate both oligodendrocytes and type-2-astrocytes in vitro (Raff et al., 1983) gave rise to the possibility that these cells could contribute to the generation of oligodendroglial lineage cells in vivo. However, type-2-astrocytes could not be identified in vivo and recent studies using an inducible NG2-transgenic mouse line showed that there are distinct subtypes of NG2+ cells that either form astrocytes or oligodendrocytes, but not both (Zhu et al., 2011). NG2+ cells are therefore thought to be a population of slowly cycling progenitor cells in the CNS, which contributes to the formation of oligodendroglial lineage cells in the developing and adult brain, and may also play an important role for myelin repair after injury (reviewed in Zuo and Nishiyama, 2013).

Myelin function

Myelination is a very important process in the nervous system as it is needed for fast nerve conduction velocity in mammals. At early stages of evolution, organisms possessed only unmyelinated nerve fibres, which would have led to decreased conduction velocity and the need of incredibly thick axons as organisms increased in size throughout evolution (reviewed in Hartline and Colman, 2007). Myelination allowed them to grow while maintaining sufficient nerve conduction velocity by only permitting depolarisation at the intersegmental nodes of Ranvier and leading to fast, saltatory nerve impulse conduction (from the Latin "*saltare*" – to jump), which was first discovered in the 20th century (Huxley and Stampfli, 1949; Tasaki, 1939). Most axons in the central nervous system are myelinated for fast conduction, with some unmyelinated axons present in the hippocampus and cerebellum (Debanne et al., 2011). In the corpus callosum, approximately 80% of axons are myelinated; the unmyelinated fibres are mostly of sensory modality and are small enough to conduct action potentials at sufficient speed without myelination (personal communication Dr. Anna Williams). In unmyelinated axons, voltage dependent ion channels are present along the length of the axon, causing the electrical impulse or area of depolarisation to slowly travel along the axon. The formation of internodes however, leads to clustering of depolarisation machinery to the nodes of Ranvier; this allows much faster impulse propagation as the area of depolarisation can jump from one node of Ranvier to the next (Ritchie and Rogart, 1977; Waxman and Ritchie, 1985) (Figure 1.2). The basis of electrical signalling in nerve fibres was discovered by Hodgkin and Huxley and is discussed in more detail elsewhere (Catterall, 2012; Vandenberg and Waxman, 2012). Briefly, the nodes of Ranvier contain voltage-gated Na^+-channels, which are normally shut but rapidly open if there is a rise in membrane potential above the threshold maximum. This allows an inward flow of Na^+-ions, and a potentiation of this effect leads to a reversal of the membrane polarity upon which the channels rapidly inactivate. Na^+-ions no longer enter the axon and activated voltage-gated paranodal K^+-channels open to generate an outward flow of K^+ in order to restore the membrane potential. During repolarisation, the voltage-gated Na^+-channels remain inactivated

to prevent the action potential from expanding bidirectionally until the membrane hyperpolarises. Active transporters (Na^+/K^+ ATPases and Na^+/Ca^{2+} exchangers) then pump Na^+-ions back out of and K^+-ions into the axon until the electrochemical gradient is back at resting levels. If nerve fibres are demyelinated, these ion voltage-gated ion channels are no longer clustered around the nodes of Ranvier (England et al., 1990), leading to decreased nerve conduction velocity and neurological impairment. Histopathological analysis of tissue from demyelinating MS lesions, which contain demyelinated axons, Na^+-channels are no longer clustered to allow saltatory conduction but rather have been found in a patchy distribution along the axons (Black et al., 2007). It is thought that due to this changed distribution in demyelinated fibres, an increase of Na^+-ions in the axon leads to an axonal accumulation of Ca^{2+}-ions through reversal of the Na^+/Ca^{2+} exchanger (Stys et al., 1991). This causes activation of Ca^{2+}-dependent proteases, such as calpains, which degrade cytoskeletal proteins and result in disruption of axonal transport (Hassen et al., 2008). Sodium channels therefore present a possible therapeutic target to prevent axonal damage in demyelinating disease (reviewed in Smith, 2007). Blockage of the Na^+-channels with anti-epileptics such as Lamotrigine have shown decreased neurodegeneration in mice with experimental autoimmune encephalitis, an experimental model of MS (Bechtold et al., 2006). However, a clinical trial investigating the effect of Lamotrigine in MS patients with secondary progressive disease reported decreasing brain volume and rebound inflammation in patients receiving the treatment led to discontinuation of further clinical trials with Lamotrigine. Instead other anti-epileptics acting on sodium channels are being explored for their value in preventing axonal damage in neuroinflammatory disease, for example optic neuritis (http://clinicaltrials.gov, identifier number NCT01451593).

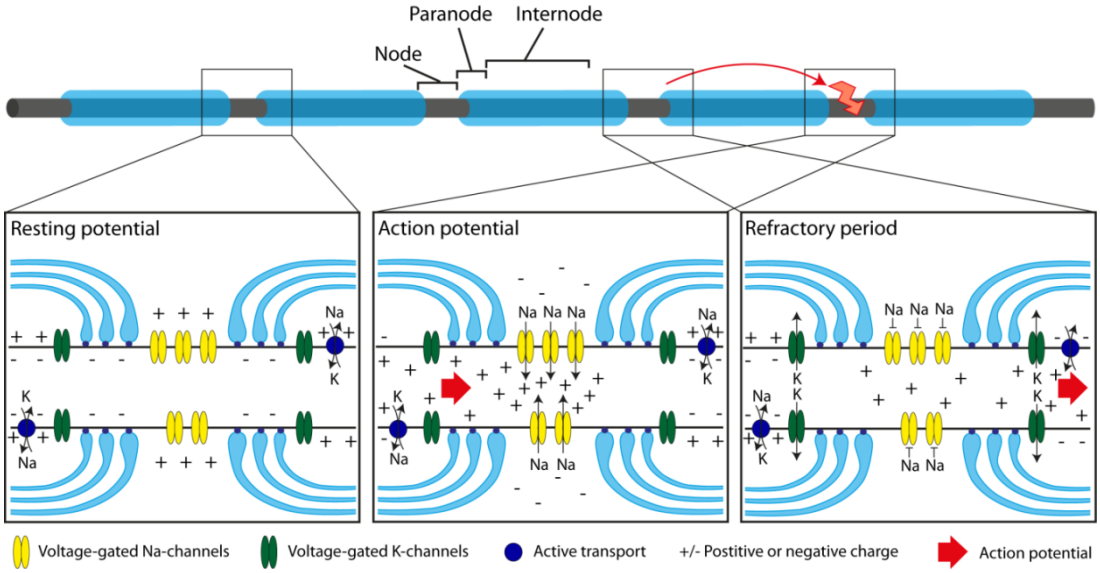

Figure 1.2: Action potential transmission in myelinated nerve fibres. Voltage-gated Na^+-channels are clustered at the node. Upon rise in membrane potential above the threshold maximum, these open, thereby creating an inward flow of Na^+ and a change in membrane polarity. When the peak of the action potential is reached, the Na^+-channels inactivate and voltage-gated K^+-channels in the paranodes open to allow an outward flow of K^+ and to repolarise the membrane potential. Na^+ and K^+ levels on both sides of the membrane are then restored by active transport through Na^+/K^+ ATPases and Na^+/Ca^{2+} exchangers.

Besides playing an important role in impulse propagation velocity and providing structural support, myelin is also important for trophic and metabolic support of the axon. It has been suggested that oligodendrocytes produce various trophic factors, which can promote neuronal survival (reviewed in Bankston et al., 2013). Neuronal cultures have showed increased survival if treated with conditioned medium from differentiated oligodendrocytes that contained glial cell line-derived neurotrophic factor (GDNF), and appeared to be dependent on phosphoinositide-3 kinase-Akt signalling, as a specific inhibitor resulted in poor neuronal survival (Wilkins et al., 2003). Rat embryonic cortical neurons survived better when co-cultured with oligodendrocytes and this was abolished upon treatment with a neutralising antibody to insulin-like growth factor 1 (IGF1), suggesting that this is also important for the survival of neurons (Wilkins et al., 2001). The brain-derived neurotrophic factor (BDNF) has also been associated with functions around neuronal survival when it is expressed in glial cells particularly following injury (Dougherty et al.,

2000). A recent *in vivo* study provides evidence for the importance of BDNF for axon protection, as mice deficient for BDNF in immune cells exhibited a decreased immune response, a more severe course of experimental autoimmune encephalomyelitis and progressive disability with enhanced axonal loss (Linker et al., 2010). Moreover, human embryonic stem cell-derived oligodendrocyte progenitor cells have been shown to express neurotrophic factors, which are thought to stimulate neurite outgrowth of rat neurons *in vitro* (Zhang et al., 2006).

In addition, oligodendrocytes do not just offer support to the axon by secreting pro-survival trophic factors, but also by providing metabolic support. When the myelin sheath is formed, the cytoplasmic channels come to lie within close proximity to the axon and it has been suggested that the lactate transporter provides one of the main gates through which the metabolic support from glial cells to axon is carried out (Lee et al., 2012). Lee et al. showed that the monocarboxylate transporter 1 (MCT1), which is highly expressed in oligodendrocytes in the white matter and serves to supply the axon with energy in form of lactate, is required for neuronal survival *in vitro*. Heterozygous MCT1-null mice develop an axonopathy in the CNS with axonal swelling but critically no change in myelination; upon selective down-regulation of MCT1 in oligodendrocytes, similar axonopathy was observed. Moreover, Fünfschilling and colleagues demonstrated that myelinating oligodendrocytes are able to supply axons with energy in the form of lactate in the absence of mitochondrial function and full glucose metabolism (Funfschilling et al., 2012). Cox10 mutant mice lacking the terminal electron transport chain complex in oligodendroglial mitochondria (cytochrome c oxidase, COX), which is normally required for full glucose metabolism, exhibit no dysmyelination phenotype. Proton magnetic resonance spectroscopy showed increased levels of lactate in mutant mice white matter during isoflurane anaesthesia with rapid normalisation after anaesthesia cessation and suggests that lactate is efficiently metabolised by myelinated neurons as an alternative energy source. These results highlight the importance of oligodendrocytes not just for saltatory conduction, but also for structural and metabolic support of neurons, which may lead to severe axonopathy if altered or defective.

Oligodendrocyte markers

For myelination to occur in the central nervous system, oligodendrocytes need to be developed from precursor cells and differentiate into mature cells with the capacity to myelinate. Throughout their development along the oligodendrocyte lineage, mammalian oligodendroglial cells express different markers, with which they can be identified (Figure 1.3). Neural precursor cells express nestin, an intermediate filament protein related to other neurofilaments, which distinguishes them from more differentiated cell types and is also expressed by glial precursors such as radial glia (Lendahl et al., 1990). Oligodendrocyte precursor cells also express the platelet-derived growth factor alpha (PDGF-α) receptor, the polysialated-neural cell adhesion molecule (PSA-NCAM) and the chondroitin sulphate proteoglycan NG2 (reviewed in Baumann and Pham-Dinh, 2001). As OPCs differentiate and become immature oligodendrocytes with processes but no associated myelin sheaths, they can be labelled by antibodies to O4, a surface antigen on pre-myelinating oligodendrocytes (Sommer and Schachner, 1981). Mature oligodendrocytes actively wrap axons and synthesise structural proteins of myelin, hence they can be visualised by markers for myelin such as myelin basic protein (MBP), proteolipid protein (PLP), myelin-associated glycoprotein (MAG) or myelin oligodendrocyte glycoprotein (MOG) (reviewed in Grinspan, 2002). In addition, the transcription factors *olig1*, *olig2* and *nkx2.2* are expressed throughout all stages of oligodendrocyte maturation, which are induced by sonic hedgehog signalling from the notochord and floorplate during development and are important for oligodendrocyte specification (Orentas et al., 1999; Pringle et al., 1996). Some motor neuron progenitors also express *olig2* and it has been demonstrated that the fate switch between motor neuron and oligodendrocyte generation is regulated by dephosphorylation of Serine 147 in the *olig2* domain in mice, chicks and *in vitro* (Li et al., 2011). The transcription factor *sox10* is expressed by early oligodendroglial cells and it has been demonstrated to play an important role during terminal differentiation in mammals (Stolt et al., 2002). More specifically, the basic helix-loop-transcription factors *olig1* and *olig2* both bind to *sox10* in mice to initiate the expression of MBP (Li et al., 2007). In zebrafish, *sox10* is only bound by *olig1*(Li et

al., 2007) and has been established as an important factor for survival of myelinating oligodendrocytes, as precursor cells in zebrafish lacking *sox10* proliferate, migrate and begin to myelinate but then die (Takada et al., 2010). Once precursor cells have committed to the oligodendrocyte lineage, *nkx2.2* appears to be important for their differentiation to mature oligodendrocytes; studies in *nkx2.2* null mice show severely retarded expression of mature myelin markers such as MBP and PLP (Qi et al., 2001). Oligodendrocyte specification and development is therefore a tightly regulated system, which shows severe effects if signals are slightly altered.

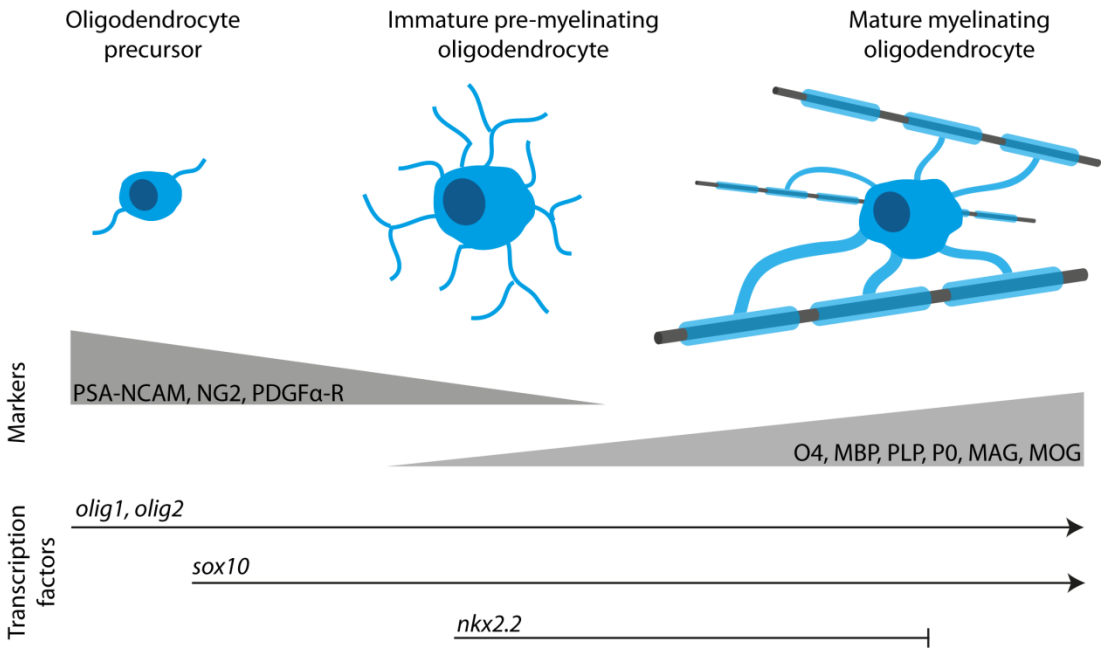

Figure 1.3: Expression of markers of oligodendrocyte lineage cells during various stages of oligodendrocyte differentiation. Oligodendrocyte precursor cells express stem cell markers such as nestin, but also oligodendrocyte lineage markers like PSA-NCAM, NG2 and PDGFα-receptor. As precursor cells mature, they begin to express myelin markers including O4, MBP, MAG and MOG. The transcription factors olig1 and olig2 are active early in oligodendrocyte lineage cells, whereas Nkx2.2 is only active from a pre-myelinating state and is transiently expressed. Cell schematics are not to scale.

Regulation of myelination

The process of myelin ensheathment of axons in the peripheral and central nervous system has been much studied. It has been established that there is a threshold for

myelination, meaning that only axons above a certain diameter will be myelinated. In the peripheral nervous system, myelination appears to be regulated by one main signalling pathway involving neuregulin-1 signalling through ErbB receptors, which allows Schwann cells to myelinate axons with the right myelin thickness (reviewed by Birchmeier and Nave, 2008). However the regulation of myelin ensheathment of central nervous system axons appears more complex and is currently poorly understood; especially which axons are myelinated by a particular oligodendrocyte and how the formation of the internodes is achieved remains unclear (reviewed in Emery, 2010). It has been well established that oligodendrocytes *in vitro* can differentiate and express myelin proteins in the absence of axons (Knapp et al., 1987; Raff et al., 1985). However, *in vivo* it is not clear whether extend and timing of myelination is regulated by intrinsic properties of oligodendrocytes or extracellular axonal signals. Time-lapse live imaging of oligodendrocytes in the spinal cord of zebrafish show a very dynamic behaviour, with multiple cell process extensions and retractions while the cells migrate and finally settle into their final position (Kirby et al., 2006). Furthermore Almeida et al. demonstrated that oligodendrocytes in the zebrafish spinal cord either myelinate several small calibre axons or associate with one axon of large diameter (Mauthner axon), however in the presence of supernumerary large diameter Mauthner axons, these oligodendrocytes are able to myelinate more than one Mauthner axon or ensheathe Mauthner axons in addition to small calibre fibres (Almeida et al., 2011). These observations support the theory that oligodendroglial cells are able to recognise their target axons by particular cues, which will guide them to establish the axon-glial contact at the right place. These signals could be:

a) Cell adhesion molecules PSA-NCAM, integrins, L1 and contactin

Certain cell adhesion molecules like PSA-NCAM, integrins, L1 and contactin have been investigated for their potential role in regulating CNS myelination. The abundance of the polysialic acid (PSA) modification of the neuronal cell adhesion molecules (NCAM) present on oligodendrocytes in culture is reduced during

myelination suggesting a function for PSA in regulating myelination and *in vivo* studies showed that only PSA-NCAM-negative axons were myelinated in the mouse optic nerve (Charles et al., 2002). Transgenic mice expressing the polysialtransferase ST8SialV driven by the *PLP* promoter did not exhibit down-regulation of PSA synthesis and showed decreased myelination in the forebrains during active myelination associated with abnormalities like redundant myelin and axonal degeneration (Fewou et al., 2007). However, more detailed studies to confirm the role of PSA-NCAM in myelination have not yet been conducted. Other neuron-glial signalling mechanisms which may be important for CNS myelination are integrins expressed by oligodendrocytes and their interaction with the neuronal laminins. The integrin receptor contains eight subunits, which all follow a different expression pattern throughout the course of oligodendrocyte development and maturation (reviewed in O'Meara et al., 2011). It is thought that in particular beta-1-integrin plays an important role in oligodendrocyte proliferation and survival through downstream signalling molecules such as phosphoinositide-3 kinase (PI3K) and mitogen-activated protein kinase (MAPK). More specifically it has been shown that in transgenic mice expressing dominant negative beta-1-integrin in oligodendrocytes, axons remain unmyelinated in the spinal cord and optic nerve and this is accompanied by altered MAPK activity and fewer oligodendrocytes (Lee et al., 2006). *In vitro* studies also confirm that beta-1-integrin signalling appears to be important but not sufficient for oligodendrocyte survival, as beta-1-integrin expressing oligodendrocytes survived better when plated on a plate coated with the beta- 1-integrin ligand laminin compared to alpha-integrin specific coatings in a growth-factor deprived environment, but they did not survive as well as control cells in a control medium (Frost et al., 1999). Beta-1-integrin knockout mice exhibit a myelination deficit that appears to be caused by the inability of oligodendrocytes to extend their myelin sheath due to failure of Akt activation, an essential kinase for axon ensheathment (Barros et al., 2009). These data were confirmed by expressing a constitutively active Akt or inhibiting the negative Akt regulator PTEN in beta-1-integrin deficient oligodendrocytes *in vitro*, which restored myelin sheath outgrowth. Further studies show that beta-1-integrin is in fact able to regulate

translation of the myelin protein MBP by binding to the inhibitory mRNA binding protein hnRNP-K and reversing its inhibitory effects (Laursen et al., 2011). Integrins can also form complexes with the cell adhesion molecule contactin, which is expressed in oligodendrocytes and neurons (De Benedictis et al., 2006; Gennarini et al., 1989; Ranscht, 1988). Zebrafish studies showed that Contactin is normally only detectable during development however is re-expressed in differentiating oligodendrocytes in optic nerve and spinal cord following lesioning of these structures and suggests a possible role for Contactin in myelinating cells (Schweitzer et al., 2007). *In vitro* studies have further demonstrated the importance of Contactin in oligodendrocyte survival, as interaction with the Contactin ligand L1 promoted myelination in neuron-oligodendroglial co-cultures through the control of Fyn phosphorylation (Laursen et al., 2009). L1 is expressed on the neuronal surface *in vitro* (van den Pol and Kim, 1993) and its expression *in vivo* peaks at the onset of myelination (Joosten and Gribnau, 1989). Studies in murine co-cultures showed that L1 expression was down-regulated in axons after they had been myelinated and that myelination could be inhibited by a blocking antibody to L1 (Barbin et al., 2004). However, as L1 knockout mice show no defect in developmental myelination, it is not clear what role this cell adhesion molecule plays in regulating CNS myelination (Cohen et al., 1998).

As such, signalling through adhesion molecules such as PSA-NCAM, integrin, contactin and L1 is involved in regulating myelin formation in the central nervous system; however, there appears to be no sole regulator of CNS myelination.

b) Neuregulin

In the peripheral nervous system, the signals regulating myelination are clearer; it has been demonstrated that the neuronal produced protein neuregulin-1 type 3 is able to bind to ErbB2/3 receptors on Schwann cells and by activating several downstream signalling pathways including PI3K/Akt, Erk1/2, FAK and Rac/Cdc42 can mediate a specific Schwann cell behaviour leading to axonal sorting and myelination including regulation of myelin thickness (reviewed in Newbern and Birchmeier,

2010). In the central nervous system, neuregulin appears to have no direct effect on the behaviour of oligodendrocytes, as mutant mice lacking the oligodendroglial ErbB receptors during development myelinate normally (Brinkmann et al., 2008). It has also been shown that overactivation of the Akt/mTOR pathway or knockdown of PI3K/PTEN in oligodendrocytes leads to increased relative myelin sheath thickness (Flores et al., 2008; Harrington et al., 2010); however, this effect of neuregulin signalling is not observed after demyelination and may only suggest a role in developmental myelination (Brinkmann et al., 2008). *In vitro* co-culture studies demonstrate that absence of neuregulin-1 type 3 in neurons does not affect differentiation of oligodendrocytes, but leads to significantly reduced internode formation (Taveggia et al., 2008). Furthermore, heterozygous neuregulin-3 type 1 knockout mice exhibit thinner myelin and fewer myelin wraps in the corpus callosum with normal myelin appearance in spinal cord and optic nerve, suggesting possible regional differences of neuregulin-3 type-1 effect on myelination. It appears therefore that Schwann cell and oligodendrocyte signalling is very different and in the central system not exclusively dependent on neuregulin, leaving questions regarding the regulation of myelination and remyelination in the CNS.

c) LINGO-1

The transmembrane protein and nogo-receptor interacting protein LINGO-1 is expressed by oligodendrocytes and appears to be a negative regulator of myelination, as functional inhibition leads to increased differentiation of oligodendrocytes *in vitro* and an increased proportion of myelinated fibres in Lingo-1 knockout mice compared to wild-type littermates (Mi et al., 2005). This is thought to be mediated through decreased downstream signalling of RhoA GTP and increased Fyn phosphorylation, both of which have been associated with effects on oligodendrocyte differentiation (Jepson et al., 2012; Liang et al., 2004). Furthermore it was found that LINGO-1 is also expressed on neurons and that inhibition of either, the oligodendrocyte LINGO-1 or the neuronal one, could promote oligodendrocyte differentiation and myelination (Lee et al., 2007).

d) Notch

Another inhibitory signal for oligodendrocyte differentiation and myelination is Notch1. During development, the Notch1-receptor is expressed by oligodendrocytes and interacts with its ligand Jagged1 on neuronal axons. Jagged1 expression decreases with a time course that is consistent with increasing appearance of myelination markers, and suggests a regulating inhibitory function of Notch1-Jagged1 signalling for myelination (Wang et al., 1998). This was confirmed by studies reporting Jagged1 expression only in unmyelinated axons during development and an increased number of myelinated axons in specific parts of the CNS of Notch1-mutant mice compared to wild type mice (Givogri et al., 2002). Notch/Jagged signalling therefore appears to be actively involved in the regulation of central nervous system myelination during development; however, it is not clear whether and how the Notch-receptor interacts with any other ligands, such as delta, to affect central nervous system myelination as the Notch-Delta signalling pathway has already been reported as important for oligodendrocyte specification and differentiation during development in zebrafish (Park and Appel, 2003).

e) Wnt/ß-Catenin

Similarly, the Wnt pathway appears to play a role in regulating developmental myelination, mainly through inhibitory signalling. The conditional activation of ß-catenin, which is a protein complex acting as an intracellular signal transducer in the Wnt pathway, does not impair the embryonic development of oligodendrocytes but rather affects their differentiation as fewer numbers of oligodendrocytes expressing mature myelin markers (PLP) were observed in the white matter of these transgenic mice (Fancy et al., 2009). Consequently, electron microscopic analysis at postnatal day 15 (P15) showed hypomyelination and higher G-ratios, a measure of myelin thickness in relation to axon diameter, which becomes higher with thinner myelin. However by P50 no difference to wild type mice was found. This suggests that Wnt signalling does not block oligodendrocyte differentiation but rather delays it. Studies using a heat shock-inducible dominant repressor of Wnt-mediated

transcription in larval zebrafish also demonstrated reduced levels of myelin basic protein, myelin protein zero and proteolipid protein highlighting the importance for Wnt signalling in developmental myelination (Tawk et al., 2011). Interestingly, Glycogen synthase kinase 3ß (GSK-3ß), which is known to stimulate the nuclear translocation of ß-catenin and signals via the Wnt pathway, has been shown to stimulate oligodendrocyte precursor proliferation and survival if inhibited, and hence seems to override the negative effect of Wnt-signalling (Azim and Butt, 2011). It seems therefore, that the Wnt/ß-catenin pathway occupies a complex role in regulating developmental myelination.

Taken together, it appears that compared to the peripheral nervous system, regulation of myelination in the central nervous system is more complex and remains poorly understood. No single mechanism responsible for regulating developmental myelination in the central nervous system *in vivo* has been described hitherto. However, research over recent years has identified several factors that appear to influence oligodendrocyte myelination mainly through inhibitory signalling, such as the Notch1/Jagged and Wnt pathways and several cell adhesion molecules; and neuronal activity also seems to at least partly drive the myelination process (Barres and Raff, 1993). It therefore remains unclear which pathways exactly control myelination in the CNS *in vivo* and if these different signalling mechanisms link together.

Myelin sheath formation

Although the regulation of myelin formation is rather complex, the process itself has been well studied (reviewed in Sherman and Brophy, 2005). Once oligodendrocytes have determined and established contact with their target axons, the myelin membrane begins to wrap around the axon and form the myelin sheath. Live *in vivo* imaging has revealed evidence that the initial contact only occurs between the tip of an oligodendrocyte process and a very small part of the axon,

and as more myelin layers are formed, the further the internode extends along the axon (Sobottka et al., 2011). To generate the myelin sheath, the oligodendrocyte must produce vast amounts of myelin proteins and evidence shows that in the case of myelin basic protein, the transcribing machinery is not membrane-bound but rather allows translation distant from the cell body in the cell processes and close to the edge of the growing myelin sheath (Colman et al., 1982). As multiple layers of myelin are formed, structural myelin proteins interact between adjacent membrane layers, resulting in a compaction of the myelin sheath with formation of major dense lines with the exception of areas containing cytoplasmic channels in the mesaxon and paranodal loops in the CNS and Schmidt-Lanterman incisures in the PNS, which are believed to be important for axonal nourishment (Lee et al., 2012).

Myelin components

As an extension of the glial cell membrane, myelin is characterised by a high proportion (70-85%) of lipids and especially cholesterol has been shown to be essential for myelin sheath formation (Saher et al., 2005). The other 15-30% comprises of different proteins, which are embedded within the lipid bilayer or attached to its surface and play a role in the structure or function of myelin. The most abundant proteins are myelin basic protein (MBP) and proteolipid protein (PLP), making up about 60-80% of the protein composition. Other myelin proteins in the central nervous system include myelin associated glycoprotein (MAG) and myelin/oligodendrocyte protein (MOG), with myelin protein zero (P0) and the peripheral nerve myelin protein 22 (PMP22) in the peripheral nervous system in mammals. Every protein has a specific function within the myelin sheath; these are described below and are visually illustrated in Figure 1.4.

a) Proteolipid protein (PLP/DM20)

PLP is the major constituent of myelin in the central nervous system. It is a structural myelin protein with 4 transmembrane domains and exists as two splice

variants, the longer PLP isoform (30 kDa) and the shorter DM20 (25 kDa). The *jimpy* mouse mutants, which carry a deletion in the *PLP* gene, exhibit relatively normal myelination and compaction; however, they do exhibit late axonopathy with axonal swelling and degeneration, suggesting a possible role of PLP in long-term integrity of axons (Griffiths et al., 1998). Human mutations in the *PLP* gene have been linked to Pelizaeus-Merzbacher disease presenting with severe dysmyelination in the central nervous system during early infancy. PLP is also produced by Schwann cells at low levels, but appears to not be actively integrated into the myelin sheath and therefore appears to have no major function in the peripheral nervous system myelin (Puckett et al., 1987).

b) Myelin basic protein (MBP)

This is the second most abundant myelin protein in the central and peripheral nervous system, which is required for compact myelin formation, and comprises about 30% of the total myelin proteins (Boggs, 2006). MBP is spliced into many isoforms ranging from 14-22 kDa; the major isoform in human CNS is 18.5 kDa compared to 14 kDa in rodents and recent research suggests that function might vary depending on the MBP isoform (Smith et al., 2013). It binds to negatively charged lipids on the cytosolic surface of the oligodendrocyte plasma membrane, thereby creating a stable interaction between two adjacent lipid bilayers. It is thought that MBP initiates myelin compaction and along with P0 stabilises the major dense lines as rodent models with mutations or deletions in the *MBP* gene – the *shiverer* mouse and the *Long Evans shaker* rat – exhibit strong defects in formation of compact myelin with absence of the major dense lines (Carre et al., 2002; Readhead et al., 1990). In the peripheral nervous system the mutants show a more subtle phenotype, presumably due to the cytoplasmic P0 domain, which may act as a functional substitute to MBP (Martini et al., 1995).

c) Myelin protein zero (P0)

With a single transmembrane domain, a small cytoplasmic domain and an extracellular IgG-like domain, myelin protein zero is a structural protein found in the peripheral nervous system (Eichberg, 2002). P0 proteins homophilically bind *in trans* to tightly connect adjacent myelin membrane layers, and thus are an integral part of compact myelin. Mouse mutants lacking P0 have shown major deficits in myelin compaction with dysmyelination and absence of major dense lines in peripheral nerves (Martini et al., 1995), highlighting the importance of the protein for proper myelin membrane formation. In mammals, P0 is present in the peripheral nervous system myelin only, while zebrafish express P0 in the myelin of the central and peripheral nervous system. This is thought to be due to the vertebrate evolution and is described in more detail later on. Deletions in the human *P0* gene have been associated with Charcot-Marie-Tooth disease type 1B (Hayasaka et al., 1993) and a wide variety of sub-classified syndromes, all of which share the common dysmyelinating pathology in the peripheral nervous system.

d) Peripheral nerve myelin protein 22 (PMP22)

This tetraspan myelin protein has a size of 22 kDa and is a major constituent in compact myelin of the peripheral nervous system. Studies show that PMP22 is able to form complexes with P0 in the peripheral nerve myelin, hence it is thought to be important for maintaining myelin structure (D'Urso et al., 1999). Dominant point mutations leading to duplication of the *PMP22* gene result the peripheral neuropathy Charcot-Marie-Tooth disease type 1A (Patel et al., 1992; Roa et al., 1993) and deletions cause hereditary liability to pressure palsy (Nicholson et al., 1994). PMP22-deficient *trembler* mice also exhibit a dysmyelinating phenotype with delayed myelination onset, production of hypermyelination at young age followed by demyelination, axonal loss and functional disability (Adlkofer et al., 1995).

e) Myelin associated glycoprotein (MAG)

Myelin associated glycoprotein is a 100kDa transmembrane myelin protein present in the central and peripheral nervous system but only constitutes 1% of the total myelin proteins. In the central nervous system MAG only localises to the periaxonal cytoplasmic channel (Trapp et al., 1989). The function of MAG has been studied in mice deficient of the protein and myelination appears to be mostly normal with the exception of the periaxonal cytoplasmic channel, which is impaired in most internodes (Li et al., 1994). In MAG-deficient mice, the onset myelination appears to be delayed with a reduced number of myelinated axons present in the optic nerve of 11 day old MAG-/- mice compared to wild type animals and is often associated with the presence of two or more myelin sheaths around one axon (Montag et al., 1994). MAG-deficient mice also show no abnormalities in their motor coordination and spacial learning, a subtle intention tremor has been reported (Li et al., 1994). This perhaps suggests a role of MAG in axon-glial contact and maintenance of the periaxonal space rather than a critical function during myelin formation (Li et al., 1998).

f) Myelin/oligodendrocyte glycoprotein (MOG)

Located on the outermost lamellae of the myelin sheath and on mature oligodendrocytes is the myelin/oligodendrocyte glycoprotein (Brunner et al., 1989), which is 26-28 kDa in size after glycosylation. MOG is thought to act as a cell adhesion molecule that interacts with a ligand to stabilise the compact myelin, however this function of MOG is not yet proven and a specific ligand for MOG remains to be identified (Johns and Bernard, 1999).

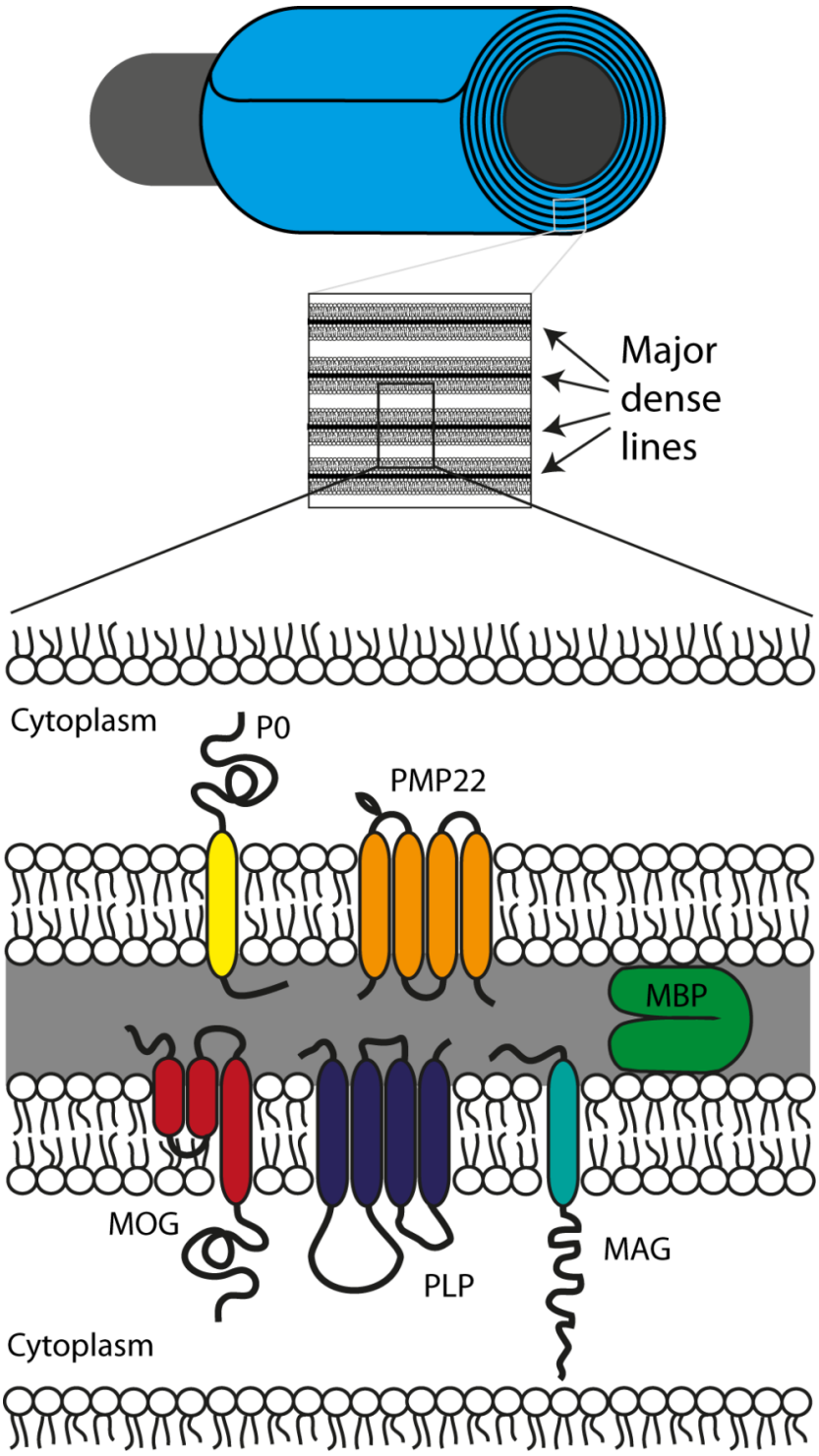

Figure 1.4: Major myelin proteins in the central and peripheral nervous system. Close apposition of adjacent myelin layers through interactions of myelin proteins with each other and the lipid bilayer form the major dense lines in the myelin sheath. The most common myelin proteins are: myelin basic protein (MBP), proteolipid protein (PLP), myelin protein zero (P0), peripheral myelin protein 22 (PMP22), myelin associated glycoprotein (MAG) and myelin/oligodendrocyte protein (MOG). Schematic is not to scale.

1.2 Multiple sclerosis

Clinical aspects

Multiple sclerosis (MS) is a chronic inflammatory disease of the CNS, which was first described in the late 19th century. Approximately 2.5 million people are affected worldwide (Pugliatti et al., 2002) and 1 in 500 people in Scotland. It is the most common cause of non-traumatic disability in young people and despite much scientific research effort its cause is still poorly understood. Neurological impairment in MS includes impaired visual function, sensory deficits and paresis (reviewed in Noseworthy et al., 2000). There is no single identified cause for MS, rather a multifactorial aetiology including genetic susceptibility, epigenetic regulation and environmental factors has been suggested (Costenbader et al., 2012).

The pathological hallmark is white matter lesions in the brain and spinal cord, which is thought to be caused by an autoimmune response to self-antigens (reviewed in Sriram, 2011; Wu and Alvarez, 2011). It has been proposed that MS shares the underlying pathology of autoimmune diseases, which originates from immunological molecular mimicry whereby a peptide antigen presented by MHC class II antigen presenting cells is indistinguishable from self-antigens within the body (for example components of the myelin) and cause T-cells to generate an inappropriate immunological response against these peptides (reviewed in Chastain and Miller, 2012). As a result, auto-reactive T-cells enter the circulation and induce a break-down of the blood-brain barrier through expression of inflammatory cytokines and reactive oxygen species, thereby allowing access to the central nervous system (reviewed in Larochelle et al., 2011). Other immune cells like macrophages can infiltrate the brain parenchyma, creating an irreversible loop of pro-inflammatory enhancement, which can, if it persists for extended periods or occurs frequently, set up mechanisms leading to axonal degeneration and neurological disability (reviewed in Compston and Coles, 2002). Transient gadolinium-enhancing brain lesions in MRI studies and oligoclonal immunoglobulin

G bands in the cerebrospinal fluid are commonly seen in MS patients, and are indicative of inflammatory nature of the disease and blood-brain barrier breakdown (Compston and Coles, 2008). Pathological analysis of post-mortem brains from MS patients demonstrated a positive correlation between the degree of inflammation and axonal transection, and as remyelinated lesions showed reduced axonal damage, it has been the widely accepted view that MS has a primary autoinflammatory aetiology, which may lead to secondary effects such as demyelination and neurodegeneration (Bitsch et al., 2000; Kuhlmann et al., 2002,Trapp, 1998 #646). However, recent evidence questions this hypothesis (reviewed in Stys et al., 2012). Wide spread lesions in the deep grey matter have been found in MS patients, which have fewer T-cells and less immune cell infiltration (Vercellino et al., 2009). In addition, studies have shown that cortical grey matter lesions and progressive brain atrophy correlate with irreversible cognitive impairment, which is thought to progress with disease progression (Calabrese et al., 2009). This raises the possibility of an underlying neurodegenerative disease, leading to primary axonal damage. However, the pathogenesis of MS and whether it is primarily an autoimmune or neurodegenerative process remains poorly understood and researchers continue to explore and link both possibilities (reviewed in Stys et al., 2012; van Noort et al., 2012).

Most patients in early stages of MS typically have relapsing-remitting disease, whereby the periods of functional deficits are thought to result from acute inflammation and demyelination within the CNS are followed by periods of functional recovery without significant clinical symptoms. These relapses can be treated by immunosuppressants such as oral and i.v. glucocorticoids to shorten acute symptomatic attacks, and immune modulatory treatments like interferons and glatiramer acetate, which decrease the frequency of relapses. Recent research has shown that approximately 65% of patients with initial relapsing-remitting MS enter the phase of secondary progressive disease, ultimately leading to irreversible functional disability (Compston and Coles, 2008). This, and primary progressive disease, is currently untreatable. The anti-inflammatory and immune suppressing

treatments available (including Fingolimod and Natalizumab which are more effective and recently licensed) do not appear to delay or slow MS progression. Recent research indicates that degeneration of axons is one of the key contributors of clinical decline in progressive MS and it is thought that intact myelin is essential for neuroprotection and maintenance of axonal integrity (Reynolds et al., 2011; Stadelmann and Bruck, 2008). Evidence suggests that demyelination leads to dysfunction of mitochondria in axons and that this is possible a key contributor to their degeneration (Andrews et al., 2005; Qi et al., 2007; Su et al., 2009). However, histopathological analysis of post-mortem brains from MS patients shows that axonal damage is already extensive in early stages of the diseases and decreases with time (Ferguson et al., 1997; Kuhlmann et al., 2002). Moreover, patients with secondary progressive disease appear to have more axonal injury than of those with primary progressive MS (Bitsch et al., 2000), suggesting that neurodegeneration is associated with the relapsing-remitting stage. As such, it is thought that axonal damage is not necessarily only a result of demyelination but may occur simultaneously and in association with the inflammatory process (reviewed in Bruck, 2005). Research shows that activated microglia can contribute to axonal loss by the secretion of possible mediators including but not limited to pro-inflammatory cytokines and free radicals (Hendriks et al., 2005), and that these reactive oxygen species inhibit axonal transport leading to axonal degeneration (Fang et al., 2012). It is therefore important to consider both the demyelinating and the inflammatory neurodegenerative aspect of MS in the development of potential treatment strategies (reviewed in Franklin and Ffrench-Constant, 2008; Franklin et al., 2012).

Failure of remyelination

In early stages of MS spontaneous remyelination does occur (Goldschmidt et al., 2009; Patrikios et al., 2006), however these myelin sheaths appear thinner and with shorter internodal lengths (Perier and Gregoire, 1965; Prineas and Connell, 1979; Raine and Wu, 1993) and one of the primary foci in MS research over the past

decades has been to understand how remyelination is regulated and what causes this remyelination failure.

Research in rodent experimental models of MS shows that following a demyelinating lesion, there is an increase of proliferating cells, which are mostly expressing markers of the oligodendrocyte lineage; and that in remyelinated areas increased numbers of mature oligodendrocytes, expressing markers of late myelin differentiation, have been found when compared to before demyelination (Prayoonwiwat and Rodriguez, 1993). Cre-lox fate mapping of PDGFα/NG2+ oligodendrocyte progenitor cells in mice showed very clearly that this population is responsible for generating almost all remyelinating cells in demyelinating lesions in the adult CNS (Zawadzka et al., 2010). Moreover, it has been demonstrated that once an oligodendrocyte is differentiated and myelinating, it does not contribute to the myelin repair, despite its survival within a demyelinated lesion or its transplantation from a normally myelinating area into a lesion site. Keirstead and Blakemore showed that demyelination of the adult rat spinal cord and additional irradiation of the same area to destroy proliferating cells, did not result in consequent myelin repair by post-mitotic oligodendrocytes, which survived the demyelinating insult (Keirstead and Blakemore, 1997; Targett et al., 1996). Similarly, studies by Targett and colleagues described a lack of remyelination in the adult rat spinal cord after transplantation of mature human oligodendrocytes into the demyelinated area (Targett et al., 1996). This ultimately leads to the assumption that although oligodendrocytes may survive the demyelination process, there must also be a mechanism for the production and recruitment of new remyelinating cells. Most evidence points to oligodendrocyte progenitor cells (OPCs), as they can proliferate, migrate, mature, attach to axons and form new myelin sheaths. Groves et al. showed that rat OPCs were able to differentiate into myelinating oligodendrocytes and produce robust myelin after transplantation into demyelinated areas (Groves et al., 1993). Furthermore, endogenous immature dividing cells in adult brain are able respond to demyelination by differentiating into oligodendrocytes, which then produce myelin and remyelinate axons (Gensert and Goldman, 1997). It is therefore thought that endogenous oligodendrocyte precursor

cells are capable of responding to demyelinated lesions and aid myelin repair. However, this is a very intricate process as has already been demonstrated during development and although most animal models show quite robust remyelination, in the human condition the remyelination capacity is limited. As such, the question whether this is due to a failure of OPC recruitment, differentiation or both, and why the extent of remyelination decreases with time, remains.

It has been suggested that one of the reasons remyelination is insufficient is because of a mismatch of axonal signalling and OPC response. This especially raises questions about the differences between developmental myelination when full myelin thickness is achieved and remyelination when this process is insufficient (reviewed in Fancy et al., 2011), and whether differential signalling mechanisms could explain the failure of sufficient remyelination. The “recapitulation versus delay”-hypothesis (reviewed in Franklin and Hinks, 1999), suggests that during myelination in development, an oligodendrocyte precursor cell contacting an axon with a diameter above myelinating threshold for the first time will myelinate it. As all axons during development are smaller, both axon and myelin will then mature together; the axon will become larger in diameter and the myelin proportionally thicker. After a demyelinating insult however, the axon already possesses its full-grown diameter and the precursor cells surrounding the lesion will be adult oligodendrocyte progenitor cells, suggesting that they might respond differently to myelination signals. Studies have demonstrated already that the adult progenitor cells show different behaviour, as NG2-positive progenitor cells in the developing system can differentiate into oligodendrocytes, astrocytes and neurons, while these adult NG2+ expressing progenitors will only differentiate into oligodendrocytes (Kang et al., 2010). Since they are halted in a precursor-like state from development onwards and will only reach the myelination stage with delay it might be more difficult for them to respond to signals and myelinate axons, especially if these already exist at full diameter. It could mean that there is a mismatch in the axon-glial signalling, caused by the axon which might not be able to signal its need for sufficient remyelination or the adult progenitor cell which might not be able to respond to the signals in a way it would during developmental myelination, or both.

Therapeutic strategies

As myelination is important for neuronal function and metabolic axon support, myelin repair in demyelinating diseases plays an important role in preventing axonal loss and associated neurological impairment, which is thought to occur secondary to immune-mediated demyelination. Axonal damage occurs most extensively at early stages of MS when acute demyelination is most active, and appears to be a major contributor to permanent disability (Kuhlmann et al., 2002; Trapp et al., 1999). To date it is unclear what mechanisms drive neurodegeneration; however it has been proposed that demyelinated axons have a higher metabolic demand as electrogenic machinery along the axons such as sodium channels no longer cluster at the nodes of Ranvier and nerve impulse conduction becomes less efficient. If this increased metabolic demand is not met by mitochondria, which also have to reorganise in a demyelinated axon, the production of nitric oxide is thought to further potentially compensate axonal integrity (reviewed in Campbell and Mahad, 2011; Su et al., 2009). This hypothesis is supported by the fact that in MS brain, axonal degeneration is most prevalent in active lesions where inflammation is greatest and that sodium channels in these areas are found diffusely located in demyelinated axons (Craner et al., 2004).

Prevention of axonal loss by remyelination has been explored in a murine experimental model, where irradiation following cuprizone-induced demyelinating lesions resulted in reduced remyelination (due to irradiated remyelinating cells) and increased axonal loss; this could be rescued by transplantation of neural progenitor cells into the irradiated and demyelinated area (Irvine and Blakemore, 2008). Compared to active demyelinating lesions in brain tissue from MS patients, remyelinated lesions also exhibited less axonal loss (Kuhlmann et al., 2002). Moreover, CNS remyelination in various experimental animal models has been associated with functional recovery, indicating prevention of axonal loss and associated neurological changes by myelin repair (Duncan et al., 2009; Liebetanz and Merkler, 2006; Murray et al., 2001). However, recent studies suggest that remyelination perhaps does not completely prevent axonal loss as late functional

decline in mice experimental models of demyelination has been observed after initial remyelination and functional recovery, and this was concurrent with axonal loss in affected white matter tracts and changes in myelin composition (Manrique-Hoyos et al., 2012). Taken together, these results support a clear association of remyelination with increased axonal survival and functional outcome, but also present the possibility of continuous processes leading to axonal loss independent of remyelination, which may in future elucidate putative pathological mechanisms in progressive disease.

In early stages of MS, spontaneous remyelination does take place, however it is often insufficient in humans (Hagemeier et al., 2012). The aim to protect axons as best as possible and to prevent disease progression has led to research around the development of novel therapeutic strategies.

As immune cells play a major role in the disease pathology of MS, much research has focussed on strategies to modulate the immune system. In fact, most of the currently used Food and Drug Association (FDA)-approved disease modifying therapies for MS, such as beta-interferon, glatiramer acetate and the newly licensed fingolimod, were discovered in animals with experimental autoimmune encephalomyelitis (EAE), which models the immunological aspect of MS (reviewed in Denic et al., 2011). While clinical studies clearly show that these therapies have the short-term benefit of reducing both the frequency of relapses and the development of new inflammatory lesions in MS; the long-term outcome remains much debated and it is thought that disease modifying therapy has only little to no impact on disease progression (Katrych et al., 2009; Trojano et al., 2011). Recently completed clinical trials investigating the monoclonal antibody alemtuzumab as a treatment for MS showed that treatment with this medication resulted in fewer relapses and this was also evident for patients with relapsing-remitting MS, which had failed on beta-interferon therapy. Moreover, alemtuzumab also demonstrates the effect of delayed disease progression in MS patients with the exception of cases with very early MS or progressive disease, and this is the first time this has been

reported of an anti-inflammatory agent (Cohen et al., 2012; Coles et al., 2012). However, it is not clear whether this is a long-lasting effect and why delayed disease progression is only observed in patients with certain disease courses.

Therapy strategies enhancing the remyelination process therefore seem promising to try and limit disease progression, and there are several possible approaches. One is the transplantation of remyelinating cells for the repair of focal lesions (Franklin, 2002a), however, there are significant hurdles associated with cell transplantation (Lindvall and Kokaia, 2010). Firstly, MS is a multifocal disease and would therefore probably require cell transplantation into all areas of demyelination as it has already been suggested in experimental animal models that transplanted glial progenitor cells may have limited migration potential (Blakemore et al., 2002). Secondly, controlling the proliferation and differentiation process of transplanted cells is very difficult; the cells could migrate inappropriately or proliferate excessively, and fail to remyelinate. Animal models, on which the transplantation would be tested first, may fail to reflect the exact human pathology, leading to different cell behaviour and effect in clinical trials. Thirdly, as these cells would be transplanted into the lesion sites in the human brain, they would have to be absolutely clean and could not be raised in animal serum, which makes the handling process extremely difficult. And finally, as with any transplantation procedure, patients receiving stem-cell transplants would have to be strongly immunosuppressed and as the disease is multifocal and on-going, repetitive cell transplantations may be required with the many associated risks for the patient. In addition, the source of stem cells also associates many ethical and safety issues, especially in the case of human embryonic stem cells, as concerns of a higher tumour formation risk are raised. Perhaps, some of these problems may be solved by the use of oligodendrocyte progenitor cells derived from patient-specific induced pluripotent stem cells; protocols for differentiating functional oligodendrocytes from induced pluripotent stem cells are already being investigated in mice (Czepiel et al., 2011). Recently, researchers reported their success in differentiating human induced pluripotent stem cells into OPCs, which then exhibited robust myelination upon transplantation

into dysmyelinated neonatal mouse brain (Wang et al., 2013). However, these techniques are still being developed and therefore the pharmacological promotion of endogenous remyelination currently presents a much more attractive approach (reviewed in Franklin and Ffrench-Constant, 2008).

For successful remyelination to take place, OPCs need to be able to respond to demyelination by proliferation and/or migration to the lesion site, followed by differentiation and ensheathment of axons. It has been shown that these most likely come from within the lesion or from the immediately surrounding white matter (Franklin et al., 1997), however other evidence suggests that precursor cells in the subventricular zone can also contribute to remyelination if the lesion site is within close proximity (Menn et al., 2006; Nait-Oumesmar et al., 1999). To enhance remyelination, research has therefore focussed on the two essential steps; to repopulate the demyelinated area with OPCs and to promote their remyelinating ability; and some factors/pathways have already been identified (Figure 1.5).

To aid the migration of OPCs to the demyelinated area, various signalling molecules seem to play important roles. Many chemokines, which are able to influence immune cell migration, have been detected in astrocytes around demyelinating lesions. Omari et al. found that immature and more mature OPCs expressed chemokine receptors CXCR1-3 *in vitro*. The respective ligands CXCL8,1 and 10 were absent from normal CNS tissue, but could be detected in reactive astrocytes bordering the lesion. Hence OPCs could respond to this cue for increased OPC recruitment (Omari et al., 2006; Omari et al., 2005). Similarly, it has been shown that OPCs express the platelet-derived-growth-factor alpha (PDGFα) receptor, and that more PDGFα receptor expressing OPCs repopulate the lesion site during the early remyelination process (Redwine and Armstrong, 1998). These findings indicate that PDGFα might be involved in OPC recruitment to demyelinating lesions and further research by Zhang et al. proposes that polysialic acid neural cell adhesion molecule (PSA-NCAM) is necessary for this directional OPC migration (Zhang et al., 2004). Other migratory molecules are the class 3 Semaphorins, in particular Sema3A

and 3F, which actively direct oligodendrocyte migration during development may also play a key role in regulation OPC migration following a demyelinating lesion (reviewed in Williams et al., 2007); these will be further discussed in Chapter 5.

When the demyelinated area has been repopulated with OPCs, these need to differentiate into myelinating oligodendrocytes in order to repair and regenerate the myelin sheath. This is a tightly regulated process, which is thought to possibly be impaired in MS (Chang et al., 2002; Fancy et al., 2010; Kuhlmann et al., 2008) and several key factors and potential therapeutic targets have been identified (reviewed in Huang and Franklin, 2011), which are described in more detail in the following paragraphs.

a) LINGO-1

LINGO-1 is a protein containing N-terminal leucine-rich repeat domains, which interacts with the Nogo receptor and has been shown to regulate axon outgrowth (Mi et al., 2004). Recent research suggests a key role of LINGO-1 as a potent negative regulator of OPC differentiation and remyelination in spinal cord of MOG-induced experimental autoimmune encephalomyelitis (EAE) and Lysophosphatidylcholine (LPC)/Cuprizone induced demyelination in rats. Treatment of LINGO-1 deficient mice with an anti-LINGO-1 antagonist resulted in functional recovery from EAE and also increased remyelination (Mi et al., 2007). Similarly, the anti-LINGO-1 antagonist also showed increased remyelination in LPC-induced demyelinating lesions in rats, by direct stimulation of OPC differentiation (Mi et al., 2009; Pepinsky et al., 2011). As such LINGO-1 is a potential target for MS therapy and specific antibodies could potentially promote remyelination in the clinical setting; a clinical trial in phase 1b has already been completed, however the results have not yet been reported (http://clinicaltrials.gov/ct2/show/NCT01244139).

b) Notch1

Also expressed by reactive astrocytes is the Notch1 receptor ligand Jagged1, which was first identified as a potential negative regulator of remyelination in a

microarray screen investigating putative astrocytic inhibitors of remyelination (John et al., 2002). During development Notch-Jagged signalling inhibits OPC differentiation and it has been shown that mouse models lacking of Notch1 in cells of the oligodendrocyte lineage leads to accelerated oligodendrocyte differentiation and myelination (Givogri et al., 2002; Wang et al., 1998). As such it has been proposed that Notch-signalling might be responsible for failure of remyelination. *In vivo* studies using experimental animal models show that Notch1 and its effector Hes5 are detected in OPCs in demyelinating lesions, and *in vitro* studies revealed that Notch signalling permitted expansion of OPCs but hindered their maturation and myelin formation (Zhang et al., 2009). Moreover, it has been shown that the transforming growth factor-beta (TGF-ß), a cytokine upregulated in MS, was able to trigger Jagged1 expression in reactive human astrocytes, which are known to border MS plaques lacking remyelination, while Notch1 and the downstream effector gene Hes5 localised to immature oligodendroglial cell (John et al., 2002; Zhang et al., 2010). This suggests a role of Notch1 in regulation of remyelination and makes it a target for potential therapeutic strategies.

c) Retinoid X receptor-ϒ

Recent microarray analysis of different remyelination stages identified the nuclear retinoid X receptor-ϒ (RXR-ϒ) as a positive regulator endogenous remyelination (Huang et al., 2011b). Huang et al. were able to show that RXR-ϒ is highly expressed in OPCs during remyelination and that inhibition of RXR-ϒ by siRNAs resulted in oligodendrocytes of a morphologically less differentiated phenotype *in vitro*. Focal demyelinating lesions in RXR-ϒ knockout mice showed accumulation of immature oligodendrocyte lineage cells and contained less differentiated oligodendrocytes. Treatment of OPCs with RXR-ϒ antagonist *in vitro* resulted in impaired OPC maturation, whereas incubation with 9-*cis*-retinoic acid, a RXR agonist, stimulated differentiation and formation of myelin membrane like sheaths in OPC cultures and cerebellar slice cultures (Huang et al., 2011b). These results therefore propose a key role of RXR-ϒ-signalling in the regulation of oligodendrocyte differentiation and RXR-agonists as potential promoters of endogenous remyelination.

d) Wnt/ß-Catenin

Signalling through the Wnt pathway has been shown to negatively affect developmental myelination. Transgenic mice which actively express a dominant active ß-catenin gene show exhibit delayed oligodendrocyte differentiation and hypomyelination during development but catches up eventually (Fancy et al., 2009). Similarly, experimental toxin-induced demyelination in these mice also resulted in delayed oligodendrocyte differentiation with no effect on OPC recruitment. Tcf4, a intranuclear binding partner of ß-catenin that is normally detected in developing mice but not in adult white matter, is re-expressed upon white matter demyelination in adult animals (Fancy et al., 2009; Ye et al., 2009). As Tcf4 locates to OPCs, which are being recruited to the lesion site in experimental models and it is also highly expressed in MS lesions, it is thought that Tcf4 could possibly play role in regulating oligodendrocyte differentiation and therefore myelin repair through active Wnt signalling.

e) Chemokines

The chemokine CXCL12 is known to influence migration, proliferation and differentiation of neural precursors during development. Studies have shown that in a rodent model of CNS demyelination, CXCL12 and its receptor CXCR4 we significantly upregulated in activated astrocytes and microglia and that *in vivo* RNA silencing resulted in decreased OPC differentiation and increased remyelination failure (Patel et al., 2010).

f) Hyaluronan

Hyaluronan is a glycosaminoglycan, which is currently being examined for its ability to block remyelination (reviewed in Hanafy and Sloane, 2011). It has been observed in MS lesion in human brain tissue, as well as in lesions of EAE mice (Back et al., 2005). Studies using both toxin-induced rodent demyelinating lesion and *in vitro* oligodendrocyte culture could show that upon presence of hyaluronan, there was no differentiation of OPCs, implicating a role in oligodendrocyte maturation. This

effect is thought to be mediated through the Toll-like receptors (TLR) 2, as this receptor is strongly expressed by oligodendrocytes and TLR2-agonists are able to inhibit OPC differentiation *in vitro* (Sloane et al., 2010). Moreover, neutralising antibodies of TLR2 have been shown to prevent the hyaluronan-mediated failure of OPC differentiation and TLR-null mice exhibit faster and more effective remyelination, suggesting an inhibitory signalling pathway, which may be influencing remyelination in the human condition.

g) Bone morphogenic protein (BMP)

Another group of cytokines, the bone morphogenic proteins (BMPs), were originally discovered by their ability to induce bone and cartilage formation, however are now believed to play a role in many more processes, including myelin repair. Upregulation of BMP 4,6 and 7 in demyelinating lesions of MOG-induced EAE mice has been demonstrated (Ara et al., 2008) and inhibition of BMP4 *in vivo* and could increase the number of remyelinated axons in areas of focal CNS demyelination in mice (Sabo et al., 2011). However, whether this is due to direct promotion of OPC differentiation or by inhibiting BMP-mediated astrogliosis (reviewed in See and Grinspan, 2009) is not yet known.

h) Sonic Hedgehog (Shh)

Sonic Hedgehog is essential for oligodendrocyte specification during embryonic development. Studies in the adult brain have shown that in Shh is still active in certain areas, mainly for maintenance of stem cell niches, which show reduced proliferation *in vivo* if Shh signal is blocked (Lai et al., 2003; Machold et al., 2003). Viral application of Shh into the lateral ventricle of adult mice showed an increase in proliferating oligodendrocyte progenitor cells and following OPC differentiation, suggesting that Shh can modify the stem cell niches to increase the production of precursor cells which will ultimately differentiate along the oligodendroglial lineage (Loulier et al., 2006). Very recently, Ferent and colleagues found that also in experimental demyelinating lesions, Shh upregulation in oligodendroglial cells

resulted in increased OPC proliferation and a Shh antagonist impaired myelin repair (Ferent et al., 2013).

Taken together, many pathways have been identified that evidently influence oligodendrocyte precursor migration to the site of injury and differentiation into myelinating oligodendrocyte and might affect remyelination *in vivo*. The advantage of having an array of possible pathways potentially involved in remyelination is that processes such as OPC migration and OPC differentiation may be influenced separately, which could be important bearing in mind that the majority of MS lesions contain plentiful OPCs, which appear to have stalled in their differentiation process but 30% of MS lesions lack undifferentiated OPCs, pointing towards insufficient OPC migration (Chang et al., 2002; Lucchinetti et al., 1999). LINGO-1 antibodies and RXR agonists both mainly affect differentiation of oligodendrocyte precursors into myelinating oligodendrocytes and could be used to enhance remyelination in those lesions containing OPCs with impaired differentiation, however, with not much effect in OPC-deficient lesions. On the other hand, molecules such as Semaphorins, which have been shown to affect OPC migration, could be helpful in treating lesions with a lack of progenitor cells. However, as MS patients mostly present with both types of lesions, potential systemic medication affecting only one particular pathway might not result in overall remyelination effects; and local treatment of individual lesions would be rather difficult as patients would require multiple intracranial injections to deliver the medication to the lesion site. In addition, pathways such as the Notch and ß-catenin pathway are widely involved in other body functions and systemic treatment might lead to severe undesirable side effects. Moreover, any treatment aiming to affect remyelination does not necessarily affect the underlying disease course, making the treatment symptomatic rather than curative. The current challenge of MS research therefore is to establish if and how these pathways act together to regulate remyelination and whether the underlying disease pathology can be altered to enhance myelin repair capacity and disease progression.

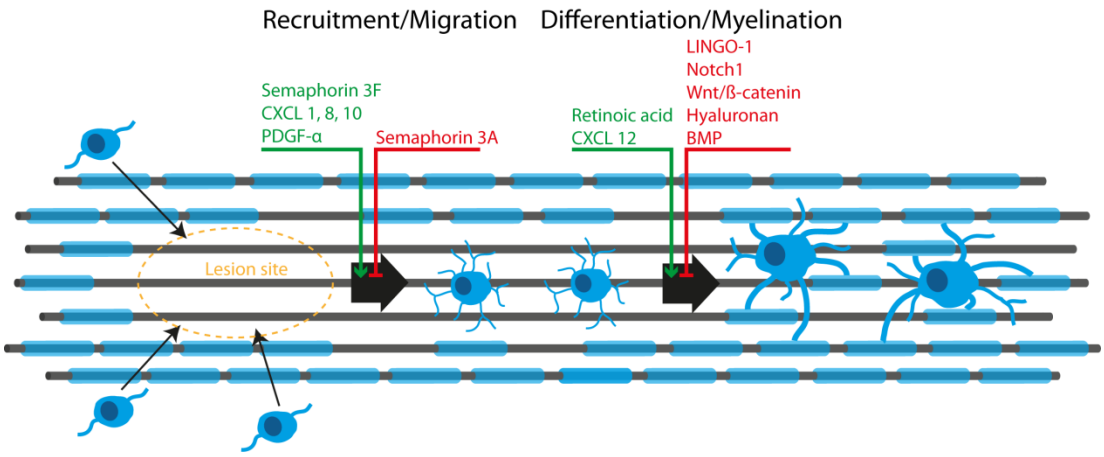

Figure 1.5: Schematic showing factors that influence remyelination. For successful remyelination, OPCs need to be recruited to the lesion site and then differentiate into myelinating oligodendrocytes. Some factors/signalling pathways have been identified, which positively (green) or negatively (red) influence remyelination by altering these steps.

1.3 Experimental models to study MS

As multiple sclerosis appears to be limited to humans and does not occur in animals, there is no natural model of MS and various experimental animal models have been established for research of CNS de- and remyelination. The difficulty is, however, that different model systems will only mimic certain aspects of the human disease and as such they have different benefits and limitations in studying MS pathology and therapeutic targets.

Experimental autoimmune encephalomyelitis (EAE)

Rodent EAE models are probably the most widely studied animal model for inflammatory CNS disease. To induce EAE, animals are actively immunised with CNS antigens such has spinal cord homogenate, common myelin proteins (mainly MBP, but also PLP and MOG) or peptides of these proteins emulsified in an adjuvant, which is needed to boost the immune response. The difficulty is that different antigens in combination with different host animals will produce a wide variety of disease courses and clinical phenotypes (reviewed in Kipp et al., 2012). When susceptible animals are immunised with CNS tissue they exhibit a monophasic but self-limiting episode with acute paralysis and full recovery or a chronic disease course with progressive paralysis without recovery. Immunisation of *Lewis* rats with MBP and Freund's adjuvant (antigen emulsified in mineral oil, which can also contain inactivated and dried mycobacteria to potentiate the immune response) for example results in an acute monophasic EAE disease course with minimal demyelination and recovery (Swanborg, 2001). In contrast, immunisation of *Biozzi ABH* mice with MOG, PLP or spinal cord homogenate in adjuvant leads to a relapsing disease pattern resembling relapsing remitting MS and secondary progressive MS, with minimal demyelination during the acute phase of EAE and more extensive myelin damage during chronic relapses (Amor et al., 1993; Amor et al., 1994; Baker et al., 1990). In addition, these mice also show axonal damage and neurological deficits, which increase with time and number of relapses. In particular

immunisation of *Biozzi ABH* mice with spinal cord homogenate and adjuvant results in a secondary progressive disease pattern with inflammation, extensive de- and remyelination, gliosis and axonal loss (Hampton et al., 2008). However, although a wide variety of EAE disease patterns can be induced in susceptible animal models and they resemble certain aspects of the MS disease courses, such as neurological impairment and extend of demyelination, the underlying pathogenesis is not identical. EAE is thought to be mediated through T-cells, in particular Th1 CD4+ cells as studies have been able to show that depletion of CD4+ cells inhibits EAE induction and prevents clinical disease in experimental models (Abdul-Majid et al., 2003). EAE is therefore the prototype to study CD4+ T-cell-mediated diseases such as MS. The experimental advantages are that it mimics the auto-immune pathogenic mechanisms involved in MS closely and as such permit investigation of T-cell mediated immune damage of the CNS and the exploration of pharmacological targets in this cascade of innate immunity. Moreover, as EAE also associates with different clinical stages, it is possible to evaluate functional outcome. The limitations include that like MS, various clinical disease courses are also present in EAE, depending on the auto-antigen, host species and their relative genetic background. EAE models also show parallel appearing inflammatory demyelination and remyelination, thereby making it difficult to detect direct changes in either de- or remyelination and amount of inflammation following drug treatment. Moreover, recent studies suggest that CD8+ T-cells are also emerging as a possible contributor to MS pathology (Friese and Fugger, 2009; Johnson et al., 2007), and EAE models with a CD8+ T-cell mediate autoimmune disease are being developed to study this further (Ji and Goverman, 2007). Similarly, the influence of B-cells in MS is not modelled in EAE either. Lastly, a primary progressive disease course where MS progresses from the beginning has been well described in MS patients; however, current EAE models fail to display this type of clinical progression.

Viral models

Similarities in the pathogenesis of MS and CNS viral diseases have led to hypothesis of a possible viral aetiology of MS. Although various viral infections such as Epstein-Barr virus have been linked to MS susceptibility, it is not thought that these are the direct causative agent for MS (reviewed in Owens and Bennett, 2012). The Theiler's murine encephalomyelitis virus (TMEV), which is one of the most commonly used and best studied in viral models, for example, was discovered by its ability to cause paralysis and encephalomyelitis in susceptible mouse strains (Theiler, 1934). It induces a biphasic disease of progressive CNS demyelination that shows similar pathology to MS (Dal Canto and Lipton, 1975, 1977; Lipton, 1975). The virus is persistent in oligodendrocytes and microglia, and infection of the CNS results in inflammation and concurrent demyelination, with further axonal damage and spinal cord atrophy in some mouse strains with chronic disease (Tsunoda and Fujinami, 2010). Remyelination in this model is often sparse, with thinner myelin sheaths months after the initial demyelinating event (Dal Canto and Lipton, 1975). *In vitro* studies suggest that TMEV leads to demyelination through direct effects on myelinating oligodendrocytes; by infecting early OPC precursors expressing NG2 and A2B5 as well as CNPase-positive immature oligodendrocytes, TMEV blocks their differentiation and is thought to delay or inhibit remyelination *in vivo* (Pringproa et al., 2010). The viral model benefits from the possibility to study the impact of immunosuppressive therapies on CNS infections, but limitations include the fact that disease only occurs after the virus is directly injected into the CNS, thereby not permitting the investigation of whether peripheral infections also play a role in the aetiology of CNS autoimmune diseases.

Toxin-induced demyelination in vivo

Over recent years, a variety of myelin toxins have been employed to induce focal demyelinating lesions or systemic disease depending on their mode of application. Lysophosphatidylcholine (LPC) and ethidium bromide are the most commonly used

and their local injection into spinal cord or brain causes a well-defined demyelinating lesion with a reduced detectability of myelin markers and fewer oligodendroglial cells in the lesion area (Woodruff and Franklin, 1999). A systemically applied toxin is cuprizone, which when fed to mice for several weeks results in demyelination of highly myelinated white matter tracts such as the corpus callosum (Blakemore, 1973a; Ludwin, 1978). The benefit of these toxin-based models is that through local stereotactic injection of a defined toxin volume, the lesion area remains constant, permitting the close analysis of how remyelination takes place including the exploration of the origin of remyelinating cells and their migration towards the defined lesion, which is useful for testing potential remyelination-enhancing target drugs. Limitations include toxicity to neurons at higher toxin concentrations in lesions and that the immunological aspect of MS cannot be studied due to missing T-cell recruitment. These toxin-induced models are further detailed in chapter 4.

In vitro cell culture systems

For exploring interactions between specific cell types, *in vitro* approaches have proven beneficial, as particular cells of interest can be grown and observed outside of the *in vivo* environment and can be easily manipulated. Cell cultures contain cells from various sources, most often from rodent or human origin, and therefore permit the testing of rodent findings in a human system. Various types of co-cultures have been described (reviewed in Jarjour et al., 2012); however, especially co-cultures of oligodendroglial cells and neurons have been useful in understanding how oligodendrocyte precursor cells differentiate into myelinating oligodendrocytes and single cell imaging has opened up new avenues to further explore the initiation of axon-glial contact and myelin formation (Ioannidou et al., 2012). Neuron-glial co-cultures also permit the exploration of possible factors that are able to influence the interaction between oligodendrocytes and neurons. For example, factors enhancing oligodendrocyte differentiation or myelin formation can be closely studied by treating co-cultures with chemical compounds, such as agonists or

antagonists of a specific signalling pathway, or by comparing the co-cultures from wild-type and knockout animals. However, although *in vitro* systems are useful to study cell-to-cell interaction, they are limited by the lack of environmental cues like growth factors and support through other cells, which are present in an *in vivo* system. Hence, cultured cells may behave quite differently to *in vivo* experimental models with an intact environment; for example it has been shown that a myelinating oligodendrocyte *in vivo* is able to produce approximately 500 times more myelin than an oligodendrocyte in culture (Pfeiffer et al., 1993). It is therefore important to take these limitations into consideration when extrapolating findings from *in vitro* studies to *in vivo* situations, in particular in the case of de- and remyelination, which occurs in the presence of inflammation and injury.

Ex vivo slice culture

An alternative to *in vitro* cell culture is the *ex vivo* slice culture model, which was initially developed for neurophysiological purposes. By creating slices from explanted animal CNS tissue and then keeping them in a culture environment, this method permits the exploration of cell-to-cell interactions and ease of manipulation with the added benefit of intact tissue architecture. This system has been refined throughout recent years; slices are commonly 200-500 µm thick and are grown on semiporous membranes, allowing survival of mouse cerebellum, brainstem, cerebral hemisphere and spinal cord slices for at least 4 weeks in culture (reviewed in Jarjour et al., 2012). *Ex vivo* slice cultures have also been well established in remyelination research, especially as myelin toxins can be added to the slice cultures to induce focal or global demyelinating lesions (Birgbauer et al., 2004; Zhang et al., 2011) and myelination can then be imaged using high resolution live imaging (Sobottka et al., 2011). As this is a culture system however, there are limitations for example in investigating cell migration from distant sources. In particular questions around the origin of remyelinating cells may be difficult to address in this model system and highlight the need for *in vivo* models with the potential for live imaging.

Zebrafish

Over the recent years, zebrafish (*Danio rerio*) have become increasingly significant in the field of biological research and are now regarded as one of the most important vertebrate model organisms. This ray-finned fish is a teleost of the cyprinid family, and has a genome of 1.7 gigabases in size, which is divided onto 25 chromosomes (Nüsslein-Volhard and Dahm, 2002). The advantage of the zebrafish in the scientific field is that external development of embryos can easily be observed through the chorion. During the first 24 hours of development, the embryos are completely transparent, but also at later stages, up to a few days of age, the larvae remain mostly transparent, allowing easy observation of the internally developing organs. This is particularly useful in transgenic zebrafish, in which the development of single fluorescent cells can be observed. Zebrafish embryos show a very rapid development; they progress from egg to larvae in 3-5 days. The breeding of fish also has many advantages compared to other vertebrates. Zebrafish can be mated daily, and have reliable egg production with quite a large clutch size all year around. Scientific work with zebrafish also benefits from the ease of genetic manipulation and high throughput embryo screening. Finally, global zebrafish networks, such as ZFIN (www.zfin.org), are developing rapidly, where genes, plasmids and probes are recorded and other relevant information is shared.

Zebrafish genetic and drug high throughput screens have been well established over the last decade and are now commonly used to screen chemical compound libraries for the identification of new drug targets and pathways (Hao et al., 2010; Hong, 2009). The rate at which screens can be conducted depends on many variables; these include whether the screening takes place at one particular time point or requires analysis of processes over time and also whether the read out is a particular phenotype (eg. expression of transgene) or an effect that requires more detailed analysis (eg. cell count, differentiation or function). Manual screening of chemical compounds allows examination of several 100 compounds per week, which can be increased manifold with the development of new automated read-out

systems and embryo sorting devices (Pfriem et al., 2012; Spomer et al., 2012). Many research laboratories are exploiting these advantages to perform zebrafish screens for the discovery of genes implicated in myelination (Pogoda et al., 2006; Simmons and Appel, 2012; Takada and Appel, 2010) and moreover to discover substances with potential pro-myelinating effect that could be useful for remyelination therapy (Buckley et al., 2010). These zebrafish screens focus on substances which may affect physiological myelination during larval development; however, it is unclear whether myelination in larvae is regulated in the same manner as in adult zebrafish, whether myelination during development accurately models myelination that occurs after myelin injury, and finally, it is currently unknown how processes involved in myelination and remyelination in zebrafish compare to those observed in mammals.

Orthologues for most human genes can be investigated in the zebrafish (Barbazuk et al. 2000; Postlethwait et al. 2000), which is also true for myelin genes and proteins. Most mammalian myelin proteins are present in fish and show a similar distribution; however, there are some notable differences as listed in Table 1.6. During evolution, duplications of the genome after the divergence of the tetrapods have resulted in the presence of multiple zebrafish genes for each mammalian gene. This is for example the case for the proteolipid protein and its splice variant DM20, which have multiple paralogues in teleost fish (Schweitzer et al., 2006). The main difference between zebrafish and mammalian myelin, however, is that myelin protein zero (P0) is the major structural myelin protein in zebrafish CNS, whereas in mammalian CNS this role is occupied by myelin proteolipid protein (PLP/DM20) and P0 is only present in peripheral Schwann cell-derived myelin. Evolutionary studies suggest that with the first appearance of myelin ~440 million years ago in cartilaginous fish (sharks and rays), P0 was the initial primary structural protein of myelin in the CNS and PNS (Kirschner et al., 1989; Kitagawa et al., 1993; Saavedra et al., 1989; Stratmann and Jeserich, 1995; Waehneldt et al., 1986). As P0 is co-expressed with PLP or DMα (the DM20 orthologue in fish) in the CNS and PNS of bony fish and amphibia, it is thought that a co-existence of DM20 and P0 was necessary in the CNS due to high mutation rates (Yoshida and Colman, 1996). The slightly longer isoform of DM20, PLP, with an additional 35 amino acids in exon 3

and first appeared ~400 million years ago after the divergence of bony fish (Macklin et al., 1987; Nave et al., 1987). It has been suggested that the evolution of this PLP-specific domain allowed stable integration of PLP into the mammalian CNS myelin and functional replacement of P0 (Waehneldt, 1990; Yoshida and Colman, 1996). These differences in the composition of zebrafish and mammalian myelin need to be kept in mind when findings made in zebrafish are extrapolated to other vertebrate systems, especially investigations concerning the function of particular myelin components and their interactions. However, despite evolutionary distance, zebrafish screens have led to the discovery of a g-coupled protein receptor (grp126), which is essential for myelin formation in the zebrafish PNS and has recently also been associated with significant functions in peripheral nerve development and myelination in mammals (Monk et al., 2009; Monk et al., 2011). These findings highlight the importance of zebrafish screens in identifying potential signalling pathways implicated in mammalian myelination.

Protein	**Function**	**Location**	
		Mammals	Zebrafish
Proteolipid protein (PLP, DM20)	Structural protein, necessary for the compaction and maintenance of myelin structure	CNS	CNS
Myelin basic protein (MBP)	Myelin adhesion protein	CNS and PNS	CNS and PNS
Myelin protein zero (MPZ, P0)	Structural protein, necessary for the compaction and maintenance of myelin structure	PNS	PNS and CNS
Peripheral myelin protein 22 (PMP22)	Structural protein, early PNS development and myelination	PNS	PNS
Myelin associated protein (MAG)	Structural protein, function unclear	CNS	?
Myelin/oligodendrocyte protein (MOG)	Structural protein, assumed role in axon-glial contact	CNS	?

Table 1.6: Major mammalian myelin proteins are also present in zebrafish, and similarly distributed. The main exception is myelin protein zero, which is only in the peripheral nervous system of mammals, but in both the CNS and PNS of zebrafish (Data modified from Bai et al., 2011; Baumann and Pham-Dinh, 2001; Brosamle and Halpern, 2002; Wulf et al., 1999).

Another difference between mammals and zebrafish is the regeneration of tissues. While regeneration in mammals seems to be somewhat limited, zebrafish possess an incredibly high capacity to regenerate. This was already observed in several different organ systems such as the heart (Poss et al., 2002), retina (Bernardos et al., 2007; Fausett and Goldman, 2006; Fimbel et al., 2007), spinal cord (Becker and Becker, 2008; Reimer et al., 2008) and brain (Kroehne et al., 2011), but knowledge about the ability of zebrafish to regenerate their myelin is limited. Previous studies in the closely related goldfish show that myelin can successfully be restored around regenerated axons; however by using nerve crush as an injury paradigm, these studies do not investigate remyelination, but rather de novo myelination of regenerating axons. These processes might comprise quite different signalling mechanisms especially as it has been proposed that an oligodendrocyte, which contacts a growing axon for the first time may be more successful in its myelination than an oligodendrocyte aiming to remyelinate a once myelinated axon (Fancy et al., 2011; Franklin and Hinks, 1999). I therefore sought to develop an adult zebrafish model, which would allow the study of myelin repair, including time course and mechanisms underpinning zebrafish de- and remyelination without axonal injury, in a highly regenerative environment, and determine possible similarities and/or differences between zebrafish and mammals.

1.4 Central hypothesis

The central hypothesis is that following focal demyelinating injury of the central nervous system, adult zebrafish are able to repair their myelin effectively.

1.5 Statement of aims

1) To characterise a myelin marker that can be used for quantification of myelin throughout all stages of myelination in developing and adult zebrafish
2) To develop a method for the induction of focal demyelinating lesions in the adult zebrafish central nervous system without concurrent axonal injury
3) To use this zebrafish-based model for the study of remyelination time course and efficiency in a highly regenerative environment
4) To test whether remyelination mechanisms in this zebrafish-based model show homologies to the mammalian system

CHAPTER 2 – Materials and methods

A list of materials and recipes for the solutions used are detailed at the end of this chapter. Abbreviations are listed from page 212 onwards.

2.1 Fish husbandry and housing

All zebrafish lines were kept and raised in our animal facility under standard conditions (Westerfield, 1995), with a 14 hour light and 10 hour dark cycle at 26.5°C. Embryos were obtained from natural spawning and kept at 28.5°C in embryo medium or conditioned aquarium water containing 0.00001% methylene blue; some embryos were raised in the presence of 0.003% n-phenylthiourea from 20 hours post fertilisation (hpf) to prevent pigmentation. All embryos were staged by days post fertilisation (dpf) using standard procedures (Kimmel et al., 1995).

2.2 Operational procedures

All experiments were performed under British Home Office regulations. For all operational procedures, young zebrafish aged between 4 – 7 months were used unless otherwise stated in the text.

Optic nerve crush

Optic nerve crush of adult zebrafish was performed as previously described (Becker et al., 2000). In short, fish were anaesthetised in tricane mesylate (MS222) (1:5000 in phosphate buffered saline (PBS)) and positioned under a stereomicroscope on an ice cold surface. Using fine forceps, the left eye was gently lifted from its socket and the exposed optic nerve was crushed behind the eyeball. A translucent strip across

the usually white opaque optic nerve indicated a successful lesion. The eye was rotated back into the socket and the fish placed back into the water.

Optic nerve injection

For optic nerve injections, the optic nerve of anaesthetised adult zebrafish was exposed as described above. Using a 5 µl Hamilton Injection Syringe (Hamilton®, Reno, USA) with an attached glass needle on a micromanipulator, 0.2 µl of 1% lysophosphatidylcholine (LPC) (weight/volume) was injected into the optic nerve. The eye was placed back into its socket and the fish returned back into the water.

Intraperitoneal injection of Bromodeoxyuridine (BrdU) / Ethynyl-deoxyuridine (EdU)

Adult zebrafish were anaesthetised in MS222 (1:5000 in PBS) and transferred onto a wet surface on ice. Using a 5 µl one-time use injection needle, 0.5 µl of a BrdU (5 mg/ml) or EdU (16.3 mM) solution was carefully injected intraperitoneally without damage of vital organs. The fish was then returned to the water.

Compound application to optic nerve

For application of compounds to the optic nerve, small pieces of absorbable gelatine foam (Gelfoam) soaked in specific compounds were prepared. Adult fish were anaesthetised in MS222 (1:5000 in PBS), placed on an ice cold surface under a stereo microscope and using fine forceps, the eye was gently rotated out of the socket. A small piece of gelatine foam was placed next to the optic nerve behind the eyeball, and the eye was placed back into the socket. Finally, the fish was returned to its tank. As described in chapter 4, demyelination was successfully achieved with gelfoam soaked with 5ul of 1% LPC.

Retrograde axonal tracing

Retrograde labelling of optic nerve axons has already been described (Becker et al., 2000). Briefly, the optic nerve was exposed as described above. The tracer was applied to severed axons of the optic nerve using small pieces of biocytin soaked gelatine foam and the tracer was allowed to be retrogradely transported along the optical projection for 4 hours. Fish were perfusion fixed and retrogradely labelled axons in the optic tectum were analysed in vibrating blade microtome sections.

Perfusion and fixation of tissue

Embryo and adult zebrafish were terminally anaesthetised in aminobenzoic acid ethylmethylester (MS222, 1:1000 in PBS) and fixed by immersion in 4% PFA in PBS (embryos) or perfusion with 4% paraformaldehyde (PFA) in PBS (adults) overnight. Tissue from *Tg(claudin k:GAL4,UAS:GFP)* transgenic fish was usually post-fixed for 2-3 days for technical reasons.

2.3 Sectioning of tissue

Cryostat sections

Fixed whole embryos or dissected tissue from fixed adult zebrafish were immersed in 30% sucrose in PBS overnight, embedded in O.C.T. cryostat embedding medium and flash frozen in liquid nitrogen cooled methyl-2-butane. The regions of interest were cut into 14 µm sections on a cryostat (CM3050 S, Leica, Wetzlar, Germany) and mounted on Superfrost coated glass slides.

Vibrating blade microtome sections

Dissected tissue from fixed adult zebrafish was embedded in 4% agar in PBS and cut into 50 µm sections on a vibrating blade microtome (Microtom HM650V, Zeiss, Oberkochen, Germany). Sections were collected in 24-well plates in PBS.

Semi-thin sections

For semi-thin sections, EPON embedded tissue blocks (see electron microscopy section for details) were mounted on a stage, cropped using carbon steel blades, cut into 0.5 µm thick sections on a microtome (Reichert Jung Ultracut Microtome, Leica, Wetzlar, Germany) and collected on microscope glass slides.

Ultra-thin sections

Ultra-thin sectioning was performed by Steven Mitchell in the Science Faculty Electron Microscope Facility, Daniel Rutherford Building, King's Buildings, Mayfield Road, Edinburgh EH9 3JH, United Kingdom.

2.4 Immunolabelling

Cryostat sections

For immunohistochemistry on cryostat sections, these were encircled with a hydrophobic PAP-pen, washed in 1x PBS, blocked in 5% donkey serum in 0.2% Triton X-100 in PBS (PBSTx) for 1 hour in a wet chamber at room temperature and incubated with primary antibody in 0.2% PBSTx at 4°C overnight. They were then washed in PBS, incubated with fluorescently labelled secondary antibody in 0.2% PBSTx in a wet chamber for 2 hours and washed in PBS again. Finally, the sections were mounted in 70% glycerol in PBS or Fluoromount-G.

For retinal sections of adult transgenic fish for myelin protein zero (P0) immunohistochemistry, the following modifications of the protocol were used: adult fish were terminally anesthetized as above. The unfixed tissue was then dissected, frozen and cut as above. The sections were treated in ice cold methanol for 10 min, then blocked in 1.5% donkey serum in PBS for 30 min and then incubated in primary antibody in PBS at 4°C overnight. The slides were then washed in PBS, incubated in secondary antibody in PBS for 45 min at room temperature and washed in PBS again before being mounted as above.

For retinal sections of transgenic fish lines the following protocol was used: The tissue was dissected from terminally anaesthetised and perfused zebrafish, incubated in sucrose, embedded, frozen, and cut as above. The sections were fixed in ice cold ethanol for 10 min, washed in PBS and heated in 10 mM sodium citrate (pH 6.5) for 10 min at 80°C for antigen retrieval. Sections were then incubated in blocking solution (10% donkey serum in 0.3% PBStx) for 1 hour and then in primary antibody in blocking solution at 4°C overnight. They were then washed in PBS, incubated in secondary antibody in blocking solution for 90 min at room temperature and washed in PBS again before being mounted as above.

Vibratome sections

For vibrating blade microtome sections, the sections were washed in PBS, followed by antigen retrieval in 10 mM sodium citrate in PBS for 30min at 80°C and washed in PBS again. After a 10 min incubation in 50 mM glycine in 0.1% PBSTx at room temperature, the floating sections were washed in 0.1% PBStx, blocked in 2% donkey serum in PBS for 30 min at room temperature and incubated with primary antibody in 0.1% PBStx at 4°C overnight. The sections were then washed in 0.1% PBStx, followed by incubation with secondary antibody in 0.1% PBStx for 45 min at room temperature. After this, the sections were washed twice in 0.1% PBStx and once in PBS. If nuclear staining was required, 1 µg/ml Hoechst in PBS was added for a few minutes between the washes. Finally, the sections were mounted in 70% glycerol in PBS or Flouromount-G™.

Whole mount preparations

Following perfusion of adult zebrafish, desired tissue was dissected out and kept in PBS at 4°C. Just before the staining procedure, the tissue was digested with 2 mg/mL collagenase for 5 min and washed in PBS. The tissue was blocked in blocking buffer (1% goat serum, 1% bovine serum albumin (BSA), 1% dimethyl sulfoxide (DMSO), and 0.7% Triton X-100) for 30 min followed by incubation with the primary

antibody in blocking buffer at 4°C overnight. After washing in PBS, specimens were incubated with the fluorescently labelled secondary antibody in blocking buffer at 4°C overnight. Finally, specimens were washed again and mounted onto slides in 70% glycerol in PBS.

Bromodeoxyuridine (BrdU) immunohistochemistry

Tissue from adult perfused zebrafish was dissected, dehydrated in sucrose, embedded, frozen, and cut as above. The sections were washed in 0.1% PBStx for 5 min, then incubated in 2 M hydrochloric acid for 1 hour at room temperature. After washing the sections in 0.1% PBStx for 5 min, they were blocked in 1.5% donkey serum in 0.1% PBStx for 30 min and incubated in primary antibody in blocking solution overnight at 4°C. They were then intensively washed in 0.1% PBStx, incubated in secondary antibody in 0.1% PBStx for 45 min at room temperature, washed in 0.1% PBStx again and mounted in Fluoromount-G™.

Ethynyl-deoxyuridine (EdU) detection

Cryostat sections from perfused adult zebrafish were encircled with a PAP-pen, dehydrated and permeabilised in a methanol bath at -20°C for 10 min and washed in PBS for 10 min at room temperature. For EdU detection the Click-iT™ kit was used. The Click-iT™ reaction cocktail was prepared according to manufacturer's guidelines: For 100 µl total volume, 4.3 µl 10x Click-iT™ reaction buffer was combined with 88.7 µl dH_2O, 2 µl copper sulphate, 0.1 µl Alexa Fluor azide and 5 µl reaction buffer additive. 100µl of this reaction cocktail was added to each slide and covered with parafilm and the slides were incubated for 3 hours at room temperature in the dark. Next, the reaction cocktail was removed and the slides were washed in PBS, three times 10 minutes. Finally, the sections were mounted in Fluoromount-G™ or processed for further immunohistochemistry.

Anti-4C4 antibody generation

Hybridoma cell line 7.4.C4, producing 4C4 antibodies, was obtained from Health Protection Agency Cultures Collection, Salisbury, United Kingdom. The hybridoma cells were thawed upon arrival and then kept in suspension in cell culture medium at 37°C at the cell culture facility, Centre for Regenerative Medicine, Edinburgh, United Kingdom under the care of Judy Fletcher. Every 2-3 days more medium was added (normally 10 ml/flask) until cells became too dense and were split for further expansion. After 2-3 weeks, the cells were centrifuged (5000 rpm/5 min), the supernatant collected and the antibody tested on vibratome sections of zebrafish brain. For preservation, 0.2% sodium azide was added to the supernatant, which was then aliquoted and frozen at -80°C for further use.

Colorimetric immunolabelling using Vectastain ABC kit

After the vibratome sections have been collected in 24-well plates in PBS they were treated with hydrogen peroxide (0.5% in 0.1% PBStx) for 20min followed by 20 min incubation with 50 mM glycine and a quick wash in 0.1% PBStx. The sections were then incubated in complex A+B solution from the Vectastain ABC kit for 90 min the dark and washed again in 0.1% PBStx and PBS. Washing solutions were replaced by 500 µl/well DAB working solution and incubated for 30 min at 4°C, then 50 µl/well hydrogen peroxide (30%, 1:1000) was added to the wells and reaction stopped with PBS when sufficient staining was present (usually 2-5min). The sections were kept in PBS at 4°C until further processing. After sorting the sections they were mounted and dried on chromalaungelatine coated glass slides and then counter stained.

For counterstaining, dried sections on the coated glass slides were sorted into racks and incubated in a series of solutions at room temperature: 1) distilled water (1-2 min), 2) neutral red solution (6 min), 3) distilled water (briefly), 4) distilled water (briefly), 5) 70% ethanol (2-5 min), 6) 95% ethanol (2-5 min), 7) 100% acetone (15 sec), 8) 100% acetone (15 sec), 9) 100 xylene (5 min), 10) xylene (5 min). Finally the sections were embedded with Eukitt mounting medium.

For coating of glass slides, the slides were sorted into racks, incubated with washing solution (500 ml 95% ethanol/10 ml 100% acetic acid) for 5 min, then dried in the oven at 65°C. Subsequently they were coated with chromalaungelatine solution for 1 min and dried in the oven as before. This coating process with chromalaungelatine solution was then repeated and slides dried again.

2.5 Western blot analysis

Lysis of tissue

Embryo and adult zebrafish were terminally anaesthetised in tricane mesylate (MS222) (1:1000 in PBS). Desired tissue was dissected and collected in lysis buffer, homogenised and incubated on ice for 30 min before being centrifuged at 6000 rpm for 5 min. The supernatant was collected and transferred into new tubes, centrifuged again at 6000 rpm for 5 min, transferred again and finally frozen until further processing.

Protein Quantification

For protein quantification, the Pierce® BCA Protein Assay Kit was used according to manufacturer's guidelines. Briefly, the experimental samples were diluted to different concentrations and distributed in a 96-well plate; diluted bovine serum albumin (BSA) standards were used as control. Working solution was prepared for all samples and the plate was incubated at 37°C for 30 min, or until sufficient colour reaction occurred. Finally, the absorbance was measured at 562nm on a standard plate reader.

Western blot

Samples were diluted with 4x NuPage SDS Page sample buffer and distilled water and boiled at 80°C for 5 min. They were then loaded into polyacrylamide gels and

run in 1x hepes running buffer at 150 V for 45 min, or until loading line was sufficiently advanced. As a marker the Precision Pro Plus Protein marker was used. The gels were taken out of the holders and transferred onto polyvinylidene fluoride (PDVF) membranes, which had been fixed for 15 sec in each methanol and distilled water, in transfer buffer at 400 mA for 2 hours at 4°C. Then the membranes were blocked in blocking buffer (4% bovine serum albumin (BSA) in tris buffered saline (TBS) with 0.1% Tween 20) for 1 hour at room temperature on a shaker and incubated with primary antibody in blocking buffer on a shaker at 4°C overnight. Following three 10 min washes in TBST (0.1% Tween 20 in TBS), the membranes were incubated with secondary antibodies in blocking buffer for 30 min at room temperature, then washed in TBST again, developed with the Pierce ECL Western Blotting substrate Kit and exposed to film in the dark room.

2.6 In situ hybridisation

The in situ hybridisation protocol has been published previously (Lieberoth et al., 2003). Briefly, work surfaces were thoroughly cleaned with RNase Zap and vibratome sections of adult perfused zebrafish were washed twice in PBS with 0.1% Tween 20 (PBST), digested with Proteinase K in PBST (10 µg/ml) for 9 min at room temperature and reaction was stopped by washing the sections twice in glycine in PBST (2 mg/ml) for 5 min each and fixing them again in 4% PFA for 20 min at room temperature before washing them three times 5 min in PBST. The washing solution was replaced with hybridisation buffer and sections were incubated at 65°C for 5 min and after changing to new hybridisation buffer they were prehybridised for 4-5 hours at 65°C. Preheated digoxygenin-labelled probes (1:1000 in hybridisation buffer) were added, and the sections hybridised overnight at 65°C. The following washing steps were conducted at 65°C for 10 min each with pre-warmed solutions: once in each 75% hybridisation mix for washes (HMW) in 2xSSC/0.1% Tween 20, 40% HMW in 2xSSC/0.1% Tween 20, 100% 2xSSC/0.1% Tween 20, 100% 1xSSC/0.1% Tween 20 and then twice in 0.2xSSC for 30 min. Progressively, the 0.2xSSC was

replaces with PBST through a series of 10 min washes in 75% 0.2xSSC in PBST, 40% 0.2xSSC in PBST and 100% PBST. The sections were blocked for 3-4 hours in in situ blocking buffer at room temperature; anti-DIG conjugated antibody solution was diluted 1:10,000 in blocking buffer and left on the sections overnight at 4°C with gentle agitation. The sections were subsequently washed six times in PBST for 15 min at room temperature, three times alkaline tris buffer and then in 5-Bromo-4-chloro-3-indolyl phosphate (BCIP)/ Nitro blue tetrazolium chloride (NBT) staining solution (one tablet/10 ml dH_2O) in the dark until sufficient signal development. Finally when the desired staining intensity was reached, the reaction was stopped by washing the sections twice in stop solution for 15 min each and then twice in PBST for 10 min. The sections were mounted onto glass slides in Elvanol (Polyvinyl alcohol mounting medium) or kept in PBS at 4°C for further immunohistochemical processing.

2.7 Electron microscopy

Tissue preparation for electron microscopy

Adult zebrafish were perfused with primary fixative (2% glutaraldehyde/ 4% formaldehyde in 0.1 M sodium cacodylate buffer, pH 7.4) and kept in fixative for at least 2 hours at room temperature. The tissue was then dissected out and kept in fresh primary fixative at 4°C overnight. The tissue was rinsed in 0.1 M cacodylate buffer 3 times for 10 min at room temperature before being fixed in secondary fixative (2% osmium tetroxide in 0.1 M cacodylate buffer and 0.1 M imidazole, pH 7.5). For the secondary fixation, all microwave steps were performed in a water bath at 15°C ± 3°C, which was continuously adjusted throughout the following microwave steps. The samples were stimulated at 100 watts for 1 min, kept at room temperature for 1 min, and then stimulated again at 100 watts for 1 min. This was followed by another microwaving regime: stimulation at 450 watts for 20 sec/room temperature for 20 sec, which was repeated 5 times. Finally, the samples were left in secondary fixative for 1 hour at room temperature. The tissue was then rinsed in

distilled water 3-5 times for 10 min and stained en bloc with saturated (8%) uranyl acetate. To dehydrate the samples, they were microwave stimulated at 250 watts in a series of ethanol (50%, 70%, 95%, 100%), followed by stimulation at 250 watts with 100% EM grade acetone. For pre-infiltration, a 1:1 mix of EPON embedding medium and EM grade acetone was prepared and added to the samples and left overnight; and then pre-infiltrated in pure EPON for a minimum of 6 hours while the acetone was allowed to evaporate. Finally, the tissue samples were embedded in EPON in silicon moulds, properly aligned and the blocks were incubated at 60-65°C to polymerise for at least 24 hours.

EPON embedding medium was made with the EMbed 812 kit according to manufacturer's guidelines. Briefly, 100ml EMbed, 45 ml dodecenylsuccinic anhydride (DDSA) and 60ml methyl-5-Norbornene-2,3-Dicarboxylic Anhydride (NMA) were heated to 65°C in an oven and mixed. The mixture was allowed to cool down, while stirring, for 1 hour. Then, 6.15 ml benzyldimethylamine (BDMA) was added to the mixture and after thorough mixing, the embedding medium was aliquoted and frozen at -20°C.

Semi-thin sectioning

Semi-thin sections were cut as described above; the sections were stained with 1% toluidine blue staining solution.

Ultra-thin sectioning, lead staining and electron microscopy

Further processing of the samples prepared for electron microscopy was done by the Science Faculty Electron Microscope Facility, Daniel Rutherford Building, King's Buildings, Mayfield Road, Edinburgh EH9 3JH, United Kingdom.

2.8 Behavioural analysis

To record swimming behaviour, the fish were tested for their free swimming capability in a 175cm^2 arena. The fish was tracked with the EthoVision XT software (Noldus, Leesburg, USA), which also extracted and calculated the total distance moved and the average swimming velocity. Each fish was tracked 3 times for 10 minutes, with an acclimatisation of 5 min once it had been placed in the arena and a minimum of 30min between tracking sessions.

2.9 Image acquisition and processing

Imaging of live zebrafish larvae

Live embryos were anaesthetised in MS222 (1:5000 in PBS) and mounted on a glass slide in 1.5% low melting point (LMP) agarose. After imaging, they were removed from the agarose and transferred back into the water.

Microscopes

For imaging of fluorescent and calorimetric sections, the following microscopes were used: Zeiss LSM 710 confocal microscope, Zeiss Scope.A1 microscope, Zeiss Imager.Z Apotome (all from Zeiss, Oberkochen, Germany) and Leica DMI 4000B confocal microscope (Leica, Wetzlar, Germany) using 5x, 10x, 20, 40x and 63x lenses and using the Zen 2009 or Axio Vision (both from Zeiss, Oberkochen, Germany) software. Embryos were exclusively live imaged on the Zeiss LSM 710 confocal microscope. Fluorescent images of the adult zebrafish were taken on a Zeiss fluorescent stereo microscope. Electron microscope images were taken on a Philips CM120 electron microscope at the Science Faculty Electron Microscope Facility, Daniel Rutherford Building, King's Buildings, Mayfield Road, Edinburgh EH9 3JH, United Kingdom.

Images were processed using Image J (National institute of health, Bethesda, MD, USA) and Adobe Photoshop CS4 (Adobe, San Jose, CA, USA). Compilations of figure panels were done with Adobe Illustrator CS5.1 (Adobe, San Jose, CA, USA).

2.10 Protein sequence alignment and identity calculations

Protein sequences were determined using the NCBI database and aligned using the EMBL-EBI EMBOSS-Needle Pairwise Sequence Alignment tool, which utilises the Needleman-Wunsch algorithm.

2.11 Quantification and statistical analysis

Pixel intensity measurements

For measurements of average pixel intensity, the randomly selected sections of one experiment were imaged with the same intensity settings on the confocal microscope; they were opened in Image J (National institute of health, Bethesda, MD, USA) and stacked using the "Z-Project" function. Using the "Analyze-histogram" command, I measured the pixel intensity of the desired marker/channel in a square in the area of interest (lesioned optic nerve) in a blinded fashion. This process was repeated for the unlesioned site with an equally sized square. Finally, a ratio was determined between lesioned-to-unlesioned sides for accurate comparison between animals. For technical replicates, multiple areas of interest were measured per lesion site.

Cell profile counts

Similarly, for cell profile counts, randomly selected sections of a lesion area were imaged on the confocal microscope. The images were opened in Image J (National institute of health, Bethesda, MD, USA) and cell profiles in a defined field of interest

(0.01 mm^2) were counted in a stereological fashion throughout the z-stack, taking into account half cut-off cells on two sides of the field of interest but not on the other two.

Myelinated/unmyelinated axons

The technique for determining the percentage of myelinated axons has also been described previously (Edgar et al., 2009). For this, the same images as analysed for the G-ratios were taken and blinded for further measurements. A grid with star-shaped lines (see below) was devised by Dr J Edgar, and using Adobe Photoshop (Adobe, San Jose, CA, USA), this was laid over the image. Any axon intersecting with any of these lines would be counted as myelinated or unmyelinated and an average percentage was determined. At least 100 axons were counted per animal, and at least 3 animals per condition (n=3).

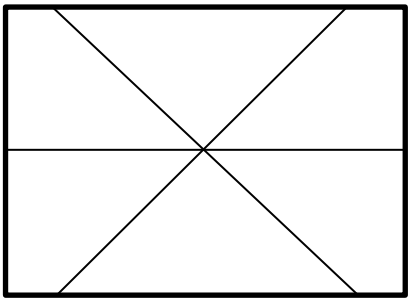

Grid used for counting of %myelinated/unmyelinated axons

G-ratios

The G-ratio is determined by dividing the diameter of the axon by the combined diameter of axon and myelin (see figure below). Previously described techniques were used for G-ratio measurements (Edgar et al., 2009). Generally, to obtain the axon diameter, the area of the axon was measured with a Bamboo Pen and Touch pad (Wacom, Vancouver, WA, USA), and assuming that every axon was perfectly circular, the diameter was calculated with the formula: diameter = 2*√(area/∏) (see figure below). The optic nerve lesion area was determined by visual cues, such as difference to the normal optic nerve, random myelin clusters not associated with

axons (“myelin debris”), and macrophages with engulfed myelin droplets. Randomly selected areas in the lesion area were imaged on the electron microscope at a fixed magnification (x4800). Images were blinded for further measurement. A 0.5 µm-sized grid was overlaid using Image J (National institute of health, Bethesda, MD, USA), and any axon that intersected with lines of the grid was measured. The grid size was chosen so that the largest axons would fit inside a grid square (and not create bias towards these larger axons) and approximately 15 axons were selected at random. Pre-calculations demonstrated that the average axon diameter calculated from the randomly selected axons (0.50 ± 0.13, mean ± SD) was not different to when all axons in an image were measured (0.49 ± 0.12, mean ± SD). At least 200 axons were measured per animal, and at least 3 animals were analysed per condition (n=3).

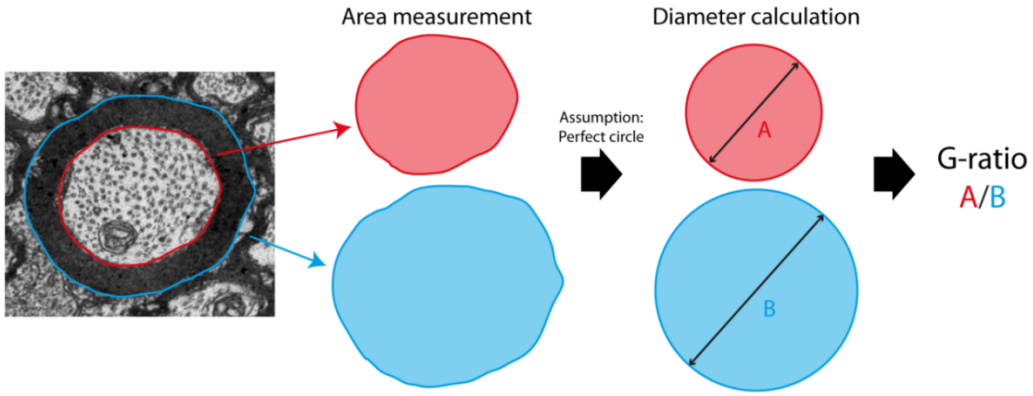

Technique used for measuring G-ratios

Western blot quantifications

Intensity of bands was measures using the “Analyze - Gel” command in Image J (National institute of health, Bethesda, MD, USA). Values were normalised to those obtained for anti-ß-tubulin immunolabelled bands from the same protein isolations.

Statistical analysis

The software Graphpad Prism 5 (GraphPad Software Inc., San Diego, CA, USA) was used for statistical analysis. The tests chosen were dependant on experimental setup and are specified in the test/figure legends. Generally experiments with two

variables were analysed by t-test or Mann Whitney U-test (in case normality could not be shown) and experiments with three or more variables by ANOVA with Bonferroni post-test or Kruskal Wallis test with Dunn's post-test (in case normality could not be shown). A p value of 0.05 or less was considered statistically significant. Throughout the thesis, * denotes $p<0.05$, ** denotes $p<0.01$ and *** denotes $p<0.001$). Error bars represent mean ± standard deviation (SD) or standard error of the mean (SEM) as specified in the text or figure legends.

2.12 Materials

Solutions and buffers

Acetate buffer	75 ml 0.1M sodium acetate 50 ml 0.1M acetic acid
Alkaline Tris buffer for in situ hybridisation	100 mM Tris buffer (1 M stock, pH 9.0) 50 mM $MgCl_2$ 100 mM NaCl 0.1% Tween 20
Blocking buffer for in situ hybridisation	1x PBS 0.1% Tween 20 2% Normal sheep serum 2 mg/ml Albumin (BSA)
Blocking buffer for western blot	1x TBS 0.1% Tween 20 4% Albumin (BSA)

Blocking buffer for whole mount immunohistochemistry	0.7% Triton X-100 1% Dimethyl sulfoxide (DMSO) 1% Albumin (BSA) 1% Goat serum
Cell culture medium	Dulbecco's modified eagle medium 2 mM Glutamine 1% Hypoxanthine, Thymidine (HT) supplement 10% Foetal Bovine Serum (FBS)
Chromalaungelatine solution	2.5 g gelatine 250 ml dH_2O This was warmed to 50°C and 0.13 g Chromium (III) potassium sulphate dodecahydrate was added
DAB (diaminobenzidine) solution	1:120 in PBS (from 6% stock solution) 2 µl/ml $NiCl_2$ (from 1% stock solution) 2 µl/ml $CoSO_4$ (from 1% stock solution)
Embryo medium	15 mM NaCl 0.5 mM KCl 1 mM $CaCl_2$ 1 mM $MgSO_4$ 0.15 mM KH_2PO_4 0.05 mM NaH_2PO_4 0.7 mM $NaHCO_3$
Glutaraldehyde 2%/paraformaldehyde 4% Primary	For 10ml: 2.5 ml 16% paraformaldehyde (EM grade)

EM fixative	0.8 ml 25% glutaraldehyde (EM grade) 1 ml 1M cacodylate buffer, pH 7.4 5.7 ml ultra-pure dH_2O
Glycine, 50mM	For 10 ml: 0.0375g glycine in 10 ml PBS/PBStx
Hybridisation buffer	50% Formamide 5x SSC 0.1% Tween20 50 µg/ml heparin (50 mg/ml) 5 mg/ml tRNA from brewer's yeast in DEPC-H_2O, adjust pH to 6.0
Hybridisation mix for washes (HMW)	50% Formamide 5x SSC in DEPC-H_2O
Imidazole 0.2 M	700mg imidazole 50 ml dH_2O
Lysis buffer	20 mM Tris base, pH 7 150 mM NaCl 5 mM EGTA 1% Triton X-100 0.1% SDS 1:100 Protease Inhibitor cocktail mix
Neutral red staining solution	4 ml acetate buffer (pH 4.8) 100 ml 1% neutral red in dH_2O

Osmium-Imidazole solution (EM grade), secondary EM fixative	1 part 4% OsO_4 solution 1 part buffer: 0.2 M imidazole and 0.2 M sodium cacodylate
Paraformaldehyde 4%	16 g paraformaldehyde 40 ml 10x PBS Make to 400 ml with dH_2O
Phosphate buffered saline (PBS), 10x pH 5.5	80 g NaCl 10.8 g Na_2HPO_4 65 g NaH_2PO_4 2 g KCl In 1L dH_2O Adjust pH to 5.5
Phosphate buffered saline (PBS) 10x, pH 7.4	80 g NaCl 14.16 g Na_2HPO_4 2 g KCl 2.4 g KH_2PO_4 In 1L dH_2O Adjust pH to 7.4
Running buffer for western blot	20x Hepes buffer, diluted with dH_2O to 1x
SSC 20x pH 7.0	175.3 g NaCl 88.2 g Sodium citrate in 1L DEPC-H_2O Adjust pH to 7.0
Sodium Cacodylate Buffer 1 M	8.56 g sodium cacodylate 40 ml dH_2O

Sodium citrate (10 mM) 1 L	2.94 g Sodium citrate 1L dH_2O Adjust pH to 6.5
Stop solution for in situ hybridisation	1x PBS, pH 5.5 1 mM EDTA 0.1% Tween 20
Tris buffered saline (TBS) 10x 1 L	50 g NaCl 2 g KCl 30 g Tris base Adjust pH to 7.5
Transfer buffer for western blot 10x 1L	30.3 g Tris base 144 g Glycine Adjust pH to 8.0
Uranyl acetate	Saturated solution which is about 8%. 8 g uranyl acetate 100 ml dH_2O

Primary antibodies

Primary antibody	Host species	Origin/Reference	Dilution
α-4C4	mouse	Hybridoma cell line from HPC Cell Cultures (92092321), Salisbury, United Kingdom	1:50
α-Acetylated tubulin	mouse	Sigma-Aldrich, St Louis, MO, USA (T6793)	1:1000
α-ß-tubulin	rabbit	Abcam, Cambridge, MA, USA (ab6046)	1:1000
α-BrdU	rat	Serotec, Oxford, United Kingdom	1:500
α-Claudin k	rabbit	Eurogentec, Seraing, Belgium	1:1000
α-Claudin k	rat	(Schaefer, 2009)	1:1000
α-GFP	chicken	Abcam, Cambridge, MA, USA (ab13970)	1:500
α-GFP	rabbit	Invitrogen, Carlsbad, CA, USA (A11122)	1:200
LINC (supernatant)	mouse	Developmental studies hybridoma bank, Iowa City, IA, USA	1:5
α-Myelin Basic Protein	rabbit	(Lyons et al., 2005)	1:50
α-Myelin Protein Zero	rabbit	(Bai et al., 2011)	1:1000
α-Pan-sodium channel	mouse	Sigma-Aldrich, St Louis, MO, USA (S8809)	1:200
α-Proliferating Cell Nuclear Antigen (PCNA)	mouse	Dako, Sigma-Aldrich, St Louis, MO, USA (M0879)	1:1000
α-Semaphorin 3A	mouse	Abcam, Cambridge, MA, USA (23393-50)	1:1000

Secondary antibodies for immunohistochemical analysis

Fluorescent coupled antibodies were obtained from Stratech Scientific, Sydney, Australia and all were used at a dilution of 1:200.

Secondary antibody	**Catalogue #**
Donkey anti-mouse Cy 3	715-165-151-JIR
Donkey anti-mouse Alexa Fluor 647	715-605-151-JIR
Donkey anti-rat Cy 3	712-165-153-JIR
Donkey anti-rat Alexa Fluor 647	712-605-153-JIR
Donkey anti-rabbit Cy3	711-165-152-JIR
Donkey anti-rabbit Alexa Fluor 647	711-605-152-JIR
Anti-chicken Alexa Fluor 488	703-545-155-JIR

Secondary antibodies for western blot

All antibodies were obtained from Amersham, GE Life Sciences, Little Chalfont, United Kingdom.

Secondary antibody	**Catalogue #**	**Dilution**
ECL Anti-rat IgG	323640	1:5000
ECL Anti-mouse IgG	399402	1:5000
ECL Anti-rabbit	4646554	1:10000

In situ hybridisation oligonucleotide probes

The generation of the probes for *P0* and *Sema3Aa/3Ab* and their sequences are described elsewhere (*P0:* (Schweitzer et al., 2003); *Sema3Aa:* (Feldner, 2005); *Sema3Ab:* (Roos et al., 1999)).

Transgenic fish lines and mutants

Tg(claudin k:GAL4,UAS:mGFP)	(Schaefer, 2009)
Tg(claudin k:GAL4,UAS:mGFP) x Tg(olig2:DsRed)	(Münzel et al., 2012)
Tg(UAS:nfsB-mCherry)	(Davison et al., 2007)
Tg(claudin k:GAL4,UAS:mGFP) x Tg(UAS:nfsB-mCherry)	(Münzel et al., unpublished)
Tg(olig2:GFP)	(Shin et al., 2003)
Tg(olig2:DsRed)	(Kucenas et al., 2008)
Tg(FoxD3:GFP)	(Gilmour et al., 2002)
Tg(MBP:EGFP)	(Almeida et al., 2011)
sox10$_{t3}$(colourless) mutant	(Dutton et al., 2001)

Chemicals reagents and products

Acetic acid >99%	Sigma-Aldrich, St Louis, MO, USA (45762)
Acetone, EM grade	Electron microscope sciences, Hatfield, PA, USA (10012)
Agarose	Oxoid, Basingstroke, United Kingdom (LP0028)
Agarose, Hi-Strength LMP	BioGene Ltd, Kimbolton, United Kingdom (300-800)
Albumin (BSA)	Sigma-Aldrich, St Louis, MO, USA (A3912)
Albumin (BSA) standard, fraction V	Thermo Fisher Scientific, Waltham, MA, USA (23209)

Aminobenzoic acid ethylmethylester (MS222)	Sigma-Aldrich, St Louis, MO, USA (A5040)
BCIP/NBT tablet	Sigma-Aldrich, St Louis, MO, USA (B5655)
Biocytin hydrochloride	Sigma-Aldrich, St Louis, MO, USA (13758)
Blades, carbon steel	Sigma-Aldrich, St Louis, MO, USA (T585)
Bromodeoxyuridine (BrdU)	Sigma-Aldrich, St Louis, MO, USA (B9285)
Calcium Chloride, $CaCl_2$	Sigma-Aldrich, St Louis, MO, USA (223506)
Chromium (III) potassium sulphate	Sigma-Aldrich, St Louis, MO, USA (24331)
Copper (II) sulphate $CoSO_4$	Sigma-Aldrich, St Louis, MO, USA (451657)
DEPC-treated H_2O, ultra-pure	Invitrogen, Carlsbad, CA, USA (750023)
Diaminobenzidine 99% (DAB)	Thermo Fisher Scientific, Waltham, MA, USA (112080250)
α-Digoxygenin-AP conjugate	Roche Diagnostics Ltd, Burgess Hill, United Kingdom (11093274910)
Dimethyl sulfoxide (DMSO)	Sigma-Aldrich, St Louis, MO, USA (D2650)
Dulbecco's Modified Eagle Medium (DMEM), low glucose	Thermo Fisher Scientific, Waltham, MA, USA (SH30021.01)
DPX mounting medium	Thermo Fisher Scientific, Waltham, MA, USA (D/5319/05)
ECL 2 western blotting substrate, Pierce	Thermo Fisher Scientific, Waltham, MA, USA (80196)

Ethanol	VWR International, Radnor, PA, USA (20821-330)
Ethanol absolute	Sigma-Aldrich, St Louis, MO, USA (E7023)
Ethylene glycol tetraacetic acid (EGTA)	Sigma-Aldrich, St Louis, MO, USA (34596)
Ethylenediaminetetraacetic acid (EDTA)	Sigma-Aldrich, St Louis, MO, USA (EDS)
Ethynyl-deoxyuridine (Edu)	Invitrogen, Carlsbad, CA, USA (A10044)
Eukitt mounting medium	Sigma-Aldrich, St Louis, MO, USA (03989)
Fetal bovine serum (FBS)	Invitrogen, Carlsbad, CA, USA (16000044)
Fluoromount-G™	Southern Biotech, Birmingham, AL, USA (0100-01)
Formamide	Sigma-Aldrich, St Louis, MO, USA (F7508)
Gelatine from porcine skin	Sigma-Aldrich, St Louis, MO, USA (G1890)
Gelfoam®, absorbable gelatine sponge	Pfizer, New York, NY, USA
Glutaraldehyde 25% EM grade	Agar Scientific, Stansted, United Kingdom (R1020)
Glutamine	Thermo Fisher Scientific, Waltham, MA, USA (119951000)
Glycine	Sigma-Aldrich, St Louis, MO, USA (G8898)
Glycerol	Sigma-Aldrich, St Louis, MO, USA (G5516)
Heparin sodium salt	Sigma-Aldrich, St Louis, MO, USA (H3393)
Histoacryl® Tissue seal	Braun, Melsungen, Germany
Hoechst 33342, Biotium	Cambridge Bioscience, Cambridge, United Kingdom (40046)

Hydrochloric acid, HCl	Sigma-Aldrich, St Louis, MO, USA (320331)
Hydrogen peroxide 30%, H_2O_2	Sigma-Aldrich, St Louis, MO, USA (216763)
Hypoxanthine, Thymidine (HT) supplement 50x	Invitrogen, Carlsbad, CA, USA (41065012)
Imidazole	Sigma-Aldrich, St Louis, MO, USA (I5513)
Lysophosphatidylcholine (LPC)	Sigma-Aldrich, St Louis, MO, USA (L1381)
Magnesium sulfate, $MgSO_4$	Sigma-Aldrich, St Louis, MO, USA (208094)
Methanol	Sigma-Aldrich, St Louis, MO, USA (179957)
Methylene Blue	VWR International, Radnor, PA, USA (3470.0025)
Methyl-2-butane	Sigma-Aldrich, St Louis, MO, USA (320404)
Metronidazole Sigma Ultra	Sigma-Aldrich, St Louis, MO, USA (M1547)
Neutral red	Thermo Fisher Scientific, Waltham, MA, USA (SDS254-2)
Nickel (II)-chloride, $NiCl_2$	Thermo Fisher Scientific, Waltham, MA, USA (38732-0500)
Normal donkey serum	Millipore, Billerica, MA, USA (S30)
Normal goat serum	Abcam, Cambridge, MA, USA (ab7481)
Normal sheep serum	Covance, Princeton, NJ, USA (SMI-6050C)

N-Phenylthriourea (PTU) 98%	Sigma-Aldrich, St Louis, MO, USA (P7629)
NuPAGE LDS Sample buffer	Invitrogen, Carlsbad, CA, USA
O.C.T Cryo embedding medium	Thermo Fisher Scientific, Waltham, MA, USA
Osmium tetroxide 2%	Electron microscope sciences, Hatfield, PA, USA
PAP-Pen for immunohistochemistry	Sigma-Aldrich, St Louis, MO, USA (Z377821)
Paraformaldehyde (PFA)	Sigma-Aldrich, St Louis, MO, USA (P6148)
Paraformaldehyde (PFA) 16% EM grade	Agar Scientific, Stansted, United Kingdom (R1026)
PDVF membrane for western blotting	Millipore, Billerica, MA, USA
Polyvinyl alcohol mounting medium with DABCO®, pH 8.7 (Elvanol)	Sigma-Aldrich, St Louis, MO, USA (10981)
Potassium chloride, KCl	Sigma-Aldrich, St Louis, MO, USA (P5404)
Potassium dihydrogen orthophosphate, KH_2PO_4	VWR International, Radnor, PA, USA (2321820)
Precise protein gels 4-20%, Pierce	Thermo Fisher Scientific, Waltham, MA, USA (0025 224)
Precision Pro Plus Marker “Kaleidoscope”	Bio Rad, Hercules, CA, USA
Protease inhibitor cocktail set III	Calbiochem, Millipore, Billerica, MA, USA (539134)
RNaseZAP	Sigma-Aldrich, St Louis, MO, USA (R2020)

Semaphorin 3A, human recombinant	R&D Systems, Minneapolis, MN, USA
Sodium azide	VWR International, Radnor, PA, USA (1155190)
Sodium acetate, CH_3COONa	Sigma-Aldrich, St Louis, MO, USA (S2889)
Sodium bicarbonate, $NaHCO_3$	Sigma-Aldrich, St Louis, MO, USA (S8875)
Sodium cacodylate	Agar Scientific, Stansted, United Kingdom (R1102)
Sodium chloride, NaCl	Sigma-Aldrich, St Louis, MO, USA (S7653)
Sodium citrate	Sigma-Aldrich, St Louis, MO, USA (S1804)
Sodium dodecyl sulphate (SDS)	Sigma-Aldrich, St Louis, MO, USA (L4909)
Sodium hydroxide, NaOH	Sigma-Aldrich, St Louis, MO, USA (S5881)
Sodium phosphate dibasic, Na_2HPO_4	Sigma-Aldrich, St Louis, MO, USA (S0876)
Sodium dihydrogen phosphate, NaH_2PO_4	Sigma-Aldrich, St Louis, MO, USA (S5011)
Sucrose 98%	Sigma-Aldrich, St Louis, MO, USA (179949)
Superfrost coated glass slides	VWR International, Radnor, PA, USA
Super RX x100 Fuji Xray film	Fujifilm, United Kingdom (47410 19236)
Toluidine blue	Sigma-Aldrich, St Louis, MO, USA (89640)
Tris-Base	Sigma-Aldrich, St Louis, MO, USA (93362)
Tris-HEPES-SDS Buffer, 20x, Pierce	Thermo Fisher Scientific, Waltham, MA, USA (28368)
Triton X-100	Sigma-Aldrich, St Louis, MO, USA (93426)

tRNA from brewer's yeast	Roche Diagnostics Ltd, Burgess Hill, United Kingdom (10109517001)
Tween 20	Sigma-Aldrich, St Louis, MO, USA (274348)
Uranyl acetate	Taab, Aldermaston, United Kingdom (U008)
Whatman chromatography paper	Thermo Fisher Scientific, Waltham, MA, USA (FB59065)
Xylene	VWR International, Radnor, PA, USA (305756G)

All dissection tools were purchased from Fine Science Tools, Heidelberg, Germany.

Plastic ware

24-well plates	Greiner Bio-One Inc., Germany (T-3026-1)
Corning® 10 cm petri dishes	Sigma-Aldrich, St Louis, MO, USA (CLS430588)
Corning® 3.5 cm petri dishes	Sigma-Aldrich, St Louis, MO, USA (CLS430591)
Centrifuge tubes (15 + 50 ml)	Greiner Bio-One Inc. Germany (188271/227261)
Plastipak syringe 1ml disposable	Scientific Lab supplies, Augustine, FL, USA (SYR6001)

Kits

EdU Click-iT™ kit	Invitrogen, Carlsbad, CA, USA (C10340)
EMbed 812 kit	Electron microscope sciences, Hatfield, PA, USA (14120)
BCA Protein Assay kit, Pierce	Thermo Fisher Scientific, Waltham, MA, USA (23228/23224)
Vectastain ABC Kit	Vector Laboratories Ltd, Burlingame, CA, USA (PK-4000)

Enzymes

Collagenase	Sigma-Aldrich, St Louis, MO, USA (C9891)
Proteinase K	Roche Diagnostics Ltd, Burgess Hill, United Kingdom (03 115 887 001)

CHAPTER 3 – Claudin k as a tool to study myelination in zebrafish

3.1 Introduction

To observe and measure myelination and regeneration of myelin in the zebrafish, it is important to have a reliable myelin marker. In zebrafish, Claudin k is strongly and exclusively expressed in autotypic tight junctions of oligodendrocytes and Schwann cells; it was discovered in a microarray expression screen investigating differential expression of myelin specific genes, which was performed by Karin Schaefer for her dissertation at the Ludwig-Maximilan University in Munich (Schaefer, 2009). She also began the characterisation of Claudin k expression in the zebrafish using both a rat monoclonal and rabbit polyclonal antibody that she generated against Claudin k, as well as a transgenic zebrafish line expressing membrane-bound GFP under the Claudin k promoter - *tg(Claudin k:Gal4,UAS:mGFP)* - that she developed for this purpose. I used these tools as the basis of my PhD project, and will first summarise relevant key findings from Karin's work, before proceeding to my own results.

Claudins are tetraspan transmembrane proteins and major components of tight junctions, which are present in various vertebrate tissues (reviewed in Findley and Koval, 2009), including myelin. Tight junctions are areas of a cell, where the membranes of two adjacent cells are closely connected and thus creating an impermeable barrier. Typically, transmembrane proteins such as claudins, junction adhesion molecules (JAM) or occludins are connected to the cytoskeleton on the adjacent cell via adapter proteins such as zonula occludens proteins 1-3 or cingulin (Figure 3.1-A). Their function is to hold the cells together, but they also play an important role in material transport and osmotic balance: As tight junctions prevent material from passing in-between the cells, molecules and ions can only pass this barrier by entering the cells through diffusion or active transport. Depending on the

composition of the tight junctions, the barrier can be selective for molecule size and/or charge, thereby allowing close regulation of fluid composition on either side of the barrier.

Tight junctions in myelinating glia are known as autotypic tight junctions because they connect two adjacent layers of myelin. These autotypic tight junctions are present along the inner and outer mesaxon as well as in Schmidt-Lanterman incisures and paranodal loops of myelin sheaths (Figure 3.1-B). Electron microscope studies of autotypic tight junctions appear as close associations of adjacent myelin sheaths (Figure 3.1-C).

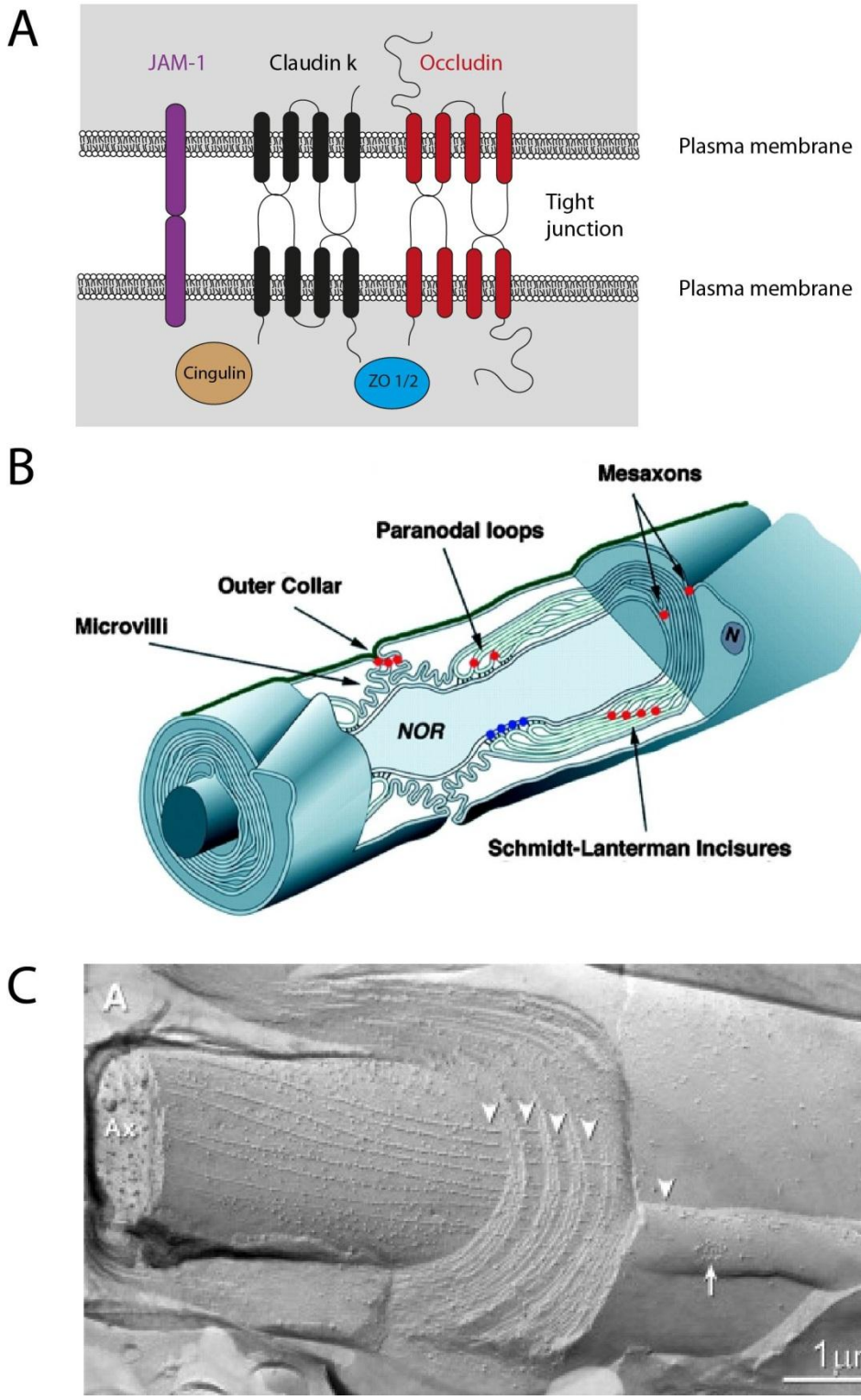

Figure 3.1: Tight junctions in myelin form a diffusion barrier between adjacent cells. (A) Typical adhesion molecules in tight junctions are junctional adhesion molecules (JAM), Claudins and Occludins and they interact with intracellular adaptor proteins such as the zona occludens molecule and cingulin. (B) A schematic of a myelinated nerve at the node of Ranvier (NOR) is shown. Red dots mark the tight junctions. Modified from (Poliak et al., 2002). (C) Tight junctions between myelin lamellae can be clearly observed (arrowheads) in freeze-fracture processed myelinated nerve tissue. Arrow points out the outer cytoplasmic tongue. Modified from (Rash, 2010). Scale bar: C = 1 µm.

Many claudin family genes have been identified to date; 24 types in humans and more than twice the number in teleost fish (Lal-Nag and Morin, 2009; Loh et al., 2004). The *claudin k* gene lies on chromosome 3 at 48,270,951-48,274,629 bp and consists of two exons, with the entire 648 bp open reading frame on the second exon (Figure 3.2-A). The Claudin k protein is 216 aa long and has a calculated molecular weight of 22.8 kDa. Computational analysis predicts the typical Claudin topology with 4 transmembrane domains, a short intracellular N-terminus, a long intracellular C-terminus and a long first extracellular loop (Figure 3.2-B). Phylogenetic analysis suggests that Claudin k clusters with other claudins (Figure 3.2-C); in particular the orthologues of *Takifugu rubripes* Claudin 31 (80% aa identity) and *Salmo salar* Claudin 6 (82% aa identity) show a high sequence homology. Claudins have also been previously described in mammals: Claudin 11, known as oligodendrocyte specific protein, in the CNS and Claudin 19 in the PNS are both expressed in tight junctions and are thought to play a role in regulating nerve conduction velocity (Devaux and Gow, 2008; Miyamoto et al., 2005). However, these proteins are not closely related to Claudin k and the mammalian claudin with the highest sequence homology is mouse and human Claudin 6 (54% aa identity). Due to an evolutionary duplication in zebrafish genome, most genes are present as two paralogues, however Claudin k has no paralogue. The zebrafish claudin with the highest homology to Claudin k is Claudin g (47% aa identity), which is an orthologue of the mammalian Claudin 4.

The *claudin k* mRNA can be observed from 2 days post fertilisation (dpf) in the hindbrain and spinal cord (Figure 3.2-D I, II), the areas where myelination by oligodendrocytes first occurs (Brosamle and Halpern, 2002), and from 3 dpf the mRNA is also present in the zebrafish posterior lateral line nerve (Schaefer, 2009). This suggests that it is selectively expressed by both oligodendrocytes in the CNS and Schwann cells in the PNS from early in the myelination process. For the generation of the Claudin k antibodies, two peptides from the cytosolic C-terminus were chosen because this is the most divergent part of Claudin family proteins. The two peptides (PTFSSDESSPRRAGV and SPRRAGVSSQVKGYV) were each injected into two rabbits (performed by Eurogentec, Southamton, United Kingdom), giving rise to

a polyclonal serum. The rat monoclonal antibody was generated by using the peptide SPRRAGVSSQVKGYV and was generated in the SFB 596 antibody facility (E. Kremmer, Helmholtz-Zentrum, Munich, Germany). The specificity of both antibodies was confirmed by western blot analysis and specific labelling of the CNS and PNS in whole mounted zebrafish larvae (Schaefer, 2009). On a subcellular level, Claudin k localises to the autotypic tight junctions and specifically labels the paranodal loops, mesaxon and Schmidt-Lanterman incisures in the PNS (Figure 3.2-E). It also co-labels with the tight junction zona occludens-1 protein in preparations of single nerve fibres indicating that it is indeed a tight junction protein (Figure 3.2-F). However, as Claudin k immunoreactivity can only be demonstrated in fixed material and does not label the entire morphology of myelinating cells, K. Schaefer generated a transgenic zebrafish line, in which the *claudin k* promoter drives the expression of a membrane-bound GFP utilising the previously described GAL4:UAS system (Figure 3.2-G) (Asakawa and Kawakami, 2008). I then studied the developmental expression of Claudin k in embryonic zebrafish and the expression pattern in adult zebrafish to evaluate its use as a marker of myelin in zebrafish.

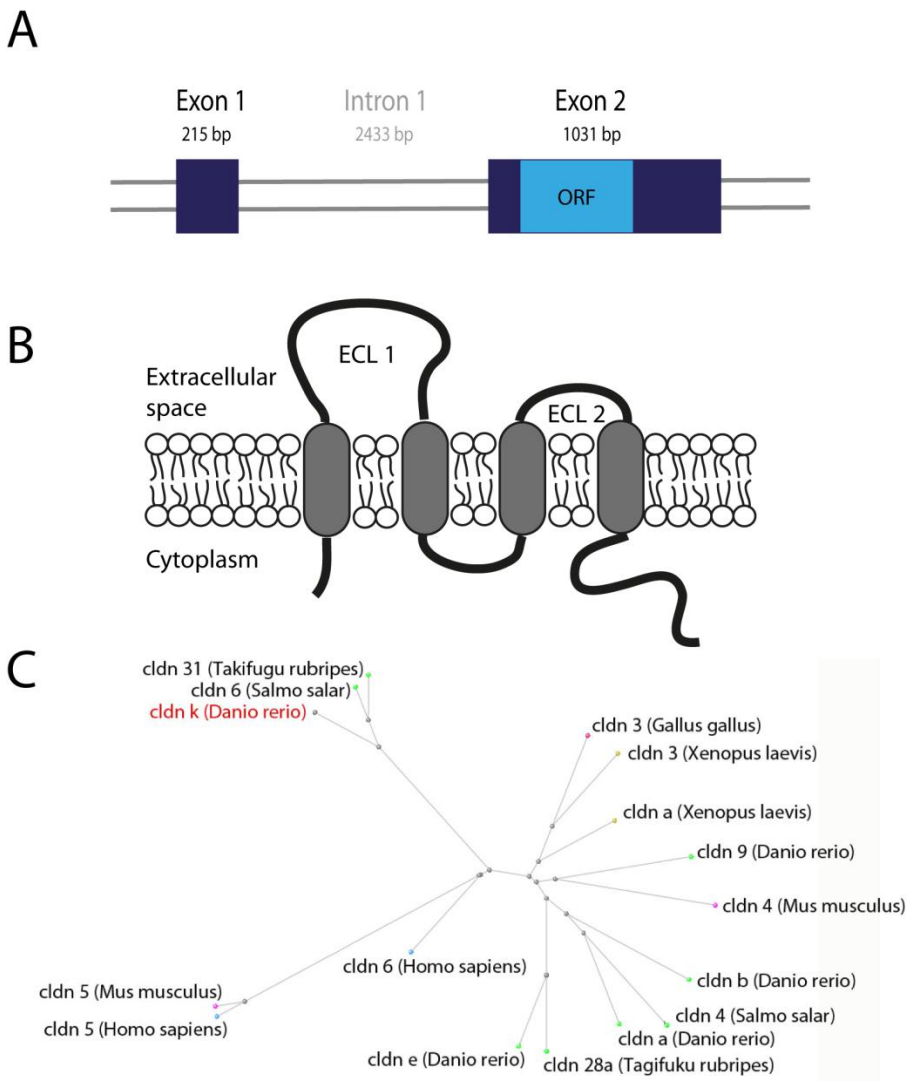

Figure 3.2 (A-C): The *claudin k* gene. (A) The zebrafish *claudin k* consists of two exons (dark blue, 215 and 1031bp) separated by an intron (2433bp); the entire open reading frame (light blue region) lies on the second exon. (B) The predicted membrane topology of Claudin k protein is typical of the claudin family with 4 transmembrane domains, a short intracellular N-terminus, a long intracellular C-terminus and two extracellular loops. (C) A phylogenetic tree of *Danio rerio* Claudin k (red) shows close homology with other claudins, in particular the *salmo salar* Claudin 6 and *Takifugu rubripes* Claudin 31. The mammalian claudin with the closest homology is Claudin 6.

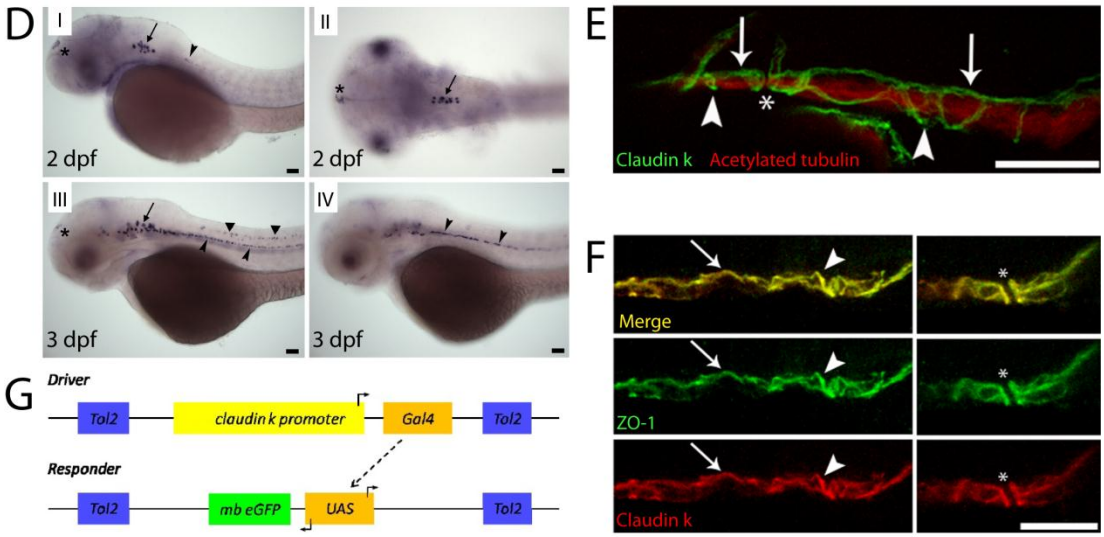

Figure 3.2 (D-F) The *claudin k* gene. (D) *Claudin k* mRNA is can be observed in the hindbrain (arrows) and spinal cord (arrowheads) from 2 dpf (I, II, III), in the dorsal spinal cord from (triangles, III) and in the posterior lateral line (arrowhead, IV) from 3 dpl. Expression in the epiphysis was detected in the rostral part of the zebrafish head (asterisk). I, II and III show larvae from lateral, II from dorsal. Rostral is left. (E) Preparation of a single teased peripheral nerve fibre shows that Claudin k localises to the mesaxon (arrows), Schmidt-Lanterman incisures (arrowheads) and paranodal loops (node indicated by asterisk). (F) Immunolabelling with Claudin k (red) and the tight junction marker ZO-1 (green) in single peripheral nerve fibres shows overlapping localisation in mesaxon (arrow), Schmidt-Lanterman incisures (arrowhead) and paranodal looks (node indicated by asterisk). (G) Schematic of Driver and responder construct used to make the transgenic zebrafish line. Scale bars: C = 50 µm, E,F = 10 µm. D,E,F and G were modified from results obtained by Karin Schaefer (Schaefer, 2009).

3.2 Results

Claudin k labels myelin in the CNS and PNS

To confirm that the previously generated antibodies worked in my hands, I repeated some of the experiments performed by K. Schaefer. Using western blotting, I could show that both the monoclonal and the polyclonal antibody recognise a single band of protein at ~20 kDa in peripheral nerve and brain tissue, which was not present in the negative control tissue (ovaries), confirming the specific expression of Claudin k in nervous tissue (Figure 3.3-A). To validate the specificity of the rat monoclonal anti-Claudin k antibody in tissue sections, I used immunohistochemistry to co-label Claudin k+ brain sections of zebrafish larvae with other myelin markers, such as myelin basic protein (MBP) and myelin protein zero (P0). I could show that all three myelin markers label the same structures during development in the larval brain, however, the onset of labelling differed: Claudin k could be detected in the medial longitudinal fascicle from as early as 3 dpf, whereas MBP immunoreactivity in the same structure was only present from 4 dpf and P0 from 5 dpf (Figure 3.3-C). To investigate whether this staggered expression was also true for other myelinated areas in the zebrafish CNS, I examined the optic chiasm and found a similar differential expression in time (Figure 3.3-D). The reason for this is perhaps that these different myelin proteins have different functions in myelin, which are only needed successively throughout myelin formation in development. Alternatively, the antibodies may also have different sensitivities for their target protein, leading to differential expression.

As antibody specificity was confirmed, I further aimed to investigate whether it could be used to quantify myelination. I therefore labelled brain cross sections of wild type and *sox10*^{t3} *(colourless)* mutant larvae with different myelin markers (Figure 3.4-A,B). *Sox10*^{t3} *(colourless)* mutant larvae have reduced myelination (Takada et al., 2010) and *in situ* hybridization indicates fewer GFP-expressing cells in sox10 mutants compared to wild type fish (Schaefer, 2009). Indeed, Claudin k, MBP

and P0 immunoreactivity was significantly lower in the mutant larvae at 8 dpf compared to wild type larvae of the same age (Figure 3.4-C). This confirms that Claudin k is expressed in myelinating cells and that it can be used to quantify myelination.

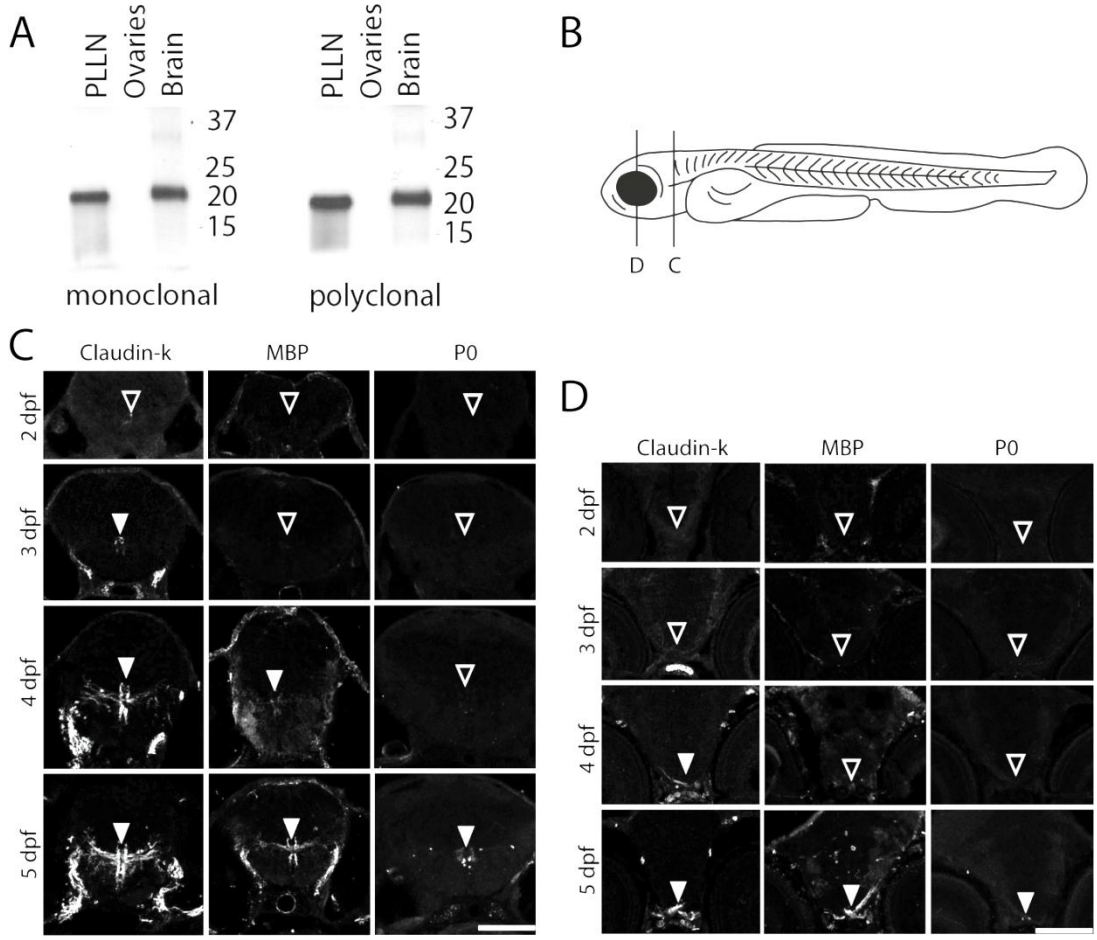

Figure 3.3: Claudin k antibodies specifically label myelinated tracts in the zebrafish. (A) Specific bands for Claudin k are detected with the monoclonal and polyclonal antibody at ~20kDa in the CNS (brain) and PNS (posterior lateral line nerve, PLLN). The negative control (ovaries) shows no Claudin k band. (B) Schematic of a larval zebrafish indicates locations of cross sections displayed in C and D. (C,D) Cross sections of zebrafish larvae at various dpf are shown (dorsal is up). Immunolabelling with Claudin k, MBP and P0 of cross sections through the larval brain (C) show that Claudin k labels myelinated tracts such as the medial longitudinal fascicle from 3 dpf, MBP and P0 label these structures later at 4 and 5 dpf respectively (full arrowheads). No immunolabelling can be detected earlier in these locations (empty arrowheads). Similarly, Claudin k labels the optic chiasm (D) from 4 dpf, while MBP and P0 are only detectable from 5 dpf (full arrows). No immunoreactivity is seen in the optic chiasm before these time points (empty arrows). Scale bars: 100 µm.

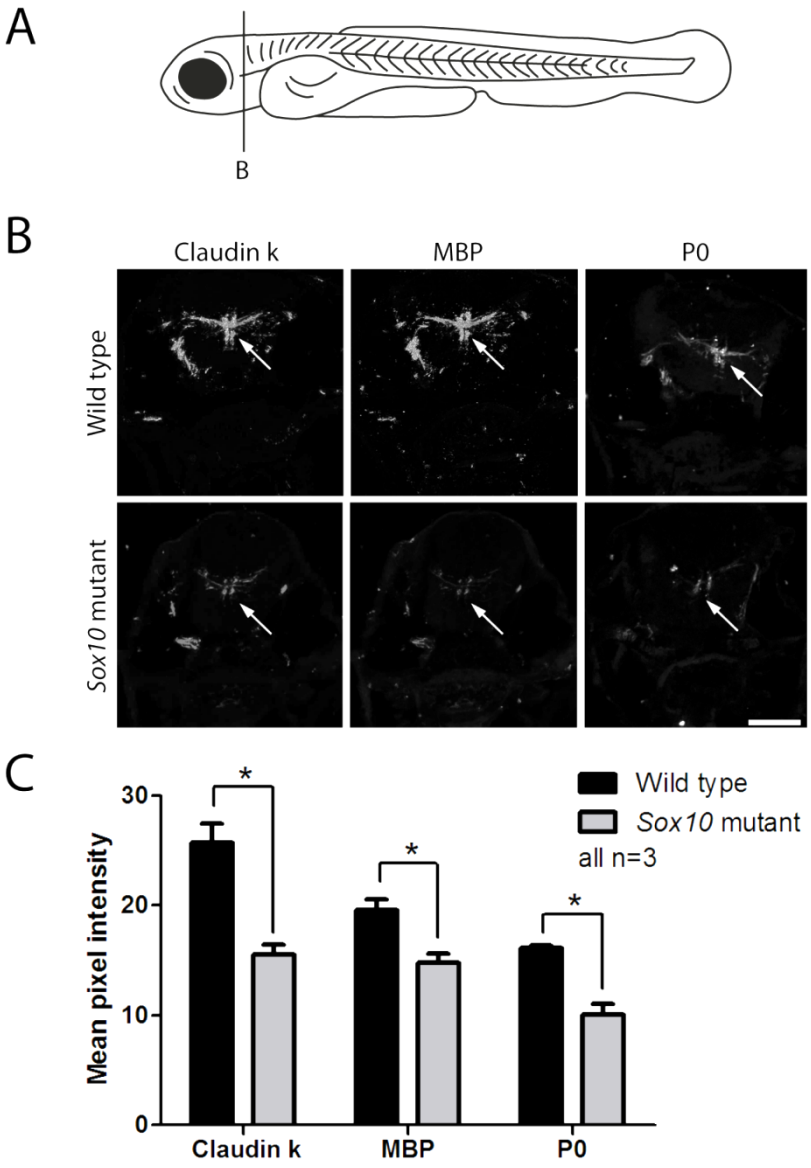

Figure 3.4: Claudin k expression is reduced in *sox10* mutant larvae. (A) Schematic of a larval zebrafish indicates location of cross sections displayed in B. (B) Immunolabelling of different myelin markers in hindbrain cross sections of 8 dpf zebrafish larvae is shown. Labelling of Claudin k, MBP and P0 in the hindbrain (arrows) is severely reduced in sox10 mutant larvae compared to age matched wild type controls. (C) Quantification of immunofluorescence in the hindbrain of sox10 mutants compared to wild type fish is shown ($p<0.05$, Mann Whitney U-test, n=3). Error bars represent mean ± SEM. Scale bar: B = 100 µm.

Developmental expression of Claudin k and tg(Claudin k:Gal4,UAS:mGFP) in fixed and live larvae

To study Claudin k expression during zebrafish development, I utilised the rat monoclonal anti-Claudin k antibody as well as the transgenic line *tg(Claudin k:Gal4,UAS:mGFP)*. I analysed cryostat sections of developing larvae at 1-5 dpf and found that Claudin k was first detectable at 3 dpf in the medial longitudinal fascicle in the hindbrain, the spinal cord and the posterior lateral line nerve (PLLN) (Figure 3.5-A-C) and over time, labelling increased in these locations and throughout the CNS and PNS. The *claudin k* transgene was already present at 24 hours post fertilisation (hpf) in cells in the rostral head (Figure 3.5-D), reflecting early *claudin k* mRNA expression as described by K. Schaefer (Schaefer, 2009), however these labelled cells are unlikely to be oligodendrocytes at this early developmental stage. The onset of GFP expression in presumed oligodendrocytes in the hindbrain was detected at 2 dpf (Figure 3.5-A,B). At this time point, labelling in the Mauthner axons of the spinal cord was also found, and the PLLN was GFP-positive from 3 dpf (Figure 3.5-A,C). Thus, the transgene labelling appeared in the same structures as Claudin k immunoreactivity and *claudin k* mRNA, but was detectable slightly earlier than Claudin k immunoreactivity.

Next, I tested whether the *claudin k* transgene could be used to identify and analyse differentiation of myelin-forming cells in individual live larvae. To investigate if the transgene expression occurred in oligodendrocytes, I crossed this transgenic fish with a previously characterised line, which expresses cytoplasmic DsRed under the control of the *olig2* promoter in oligodendrocytes and motor neurons. Migrating *olig2*:DsRed+ cells in the dorsal spinal cord of these fish have been identified as oligodendrocytes (Kucenas et al., 2008). I found that some of these DsRed+ cells were also surrounded by a cell membrane labelled with the membrane-tethered GFP, which was also observed the cell processes and myelinated internodes (Figure 3.6-A). It was notable that not all DsRed+ cells co-labelled with a GFP+ cell membrane, a phenomenon that is likely due to variegated transgene expression, which is discussed later on.

In dorsal (Figure 3.6-B) and lateral (Figure 3.6-C) live imaged views of the same larva, the first transgene expression was detected at 54–66 hpf in the medial longitudinal fascicle in the hindbrain, in structures medial to the otic cavity, as well as in the rostral spinal cord and PLLN. Wild-type embryos did not show such fluorescence. As individual larvae developed, GFP expression extended along the spinal cord and PLLN in a rostral to caudal pattern (Figure 3.6-C) between 60 and 90 hpf, similarly to previously published myelination patterns (Brosamle and Halpern, 2002). Motor axons were associated with GFP fluorescence suggestive of myelination from 78 hpf onward (Figure 3.6-C). GFP expression was also detected in the fins of the zebrafish larvae (Figure 3.6-B), but this expression could not be co-labelled with anti-Claudin k antibody (data not shown), and therefore was deemed ectopic. However, this expression did not affect observation of oligodendrocytes and Schwann cells in the nervous system. Thus, the progress of differentiation of oligodendrocytes and Schwann cells can be followed in live *tg(Claudin k:Gal4,UAS:mGFP)* animals.

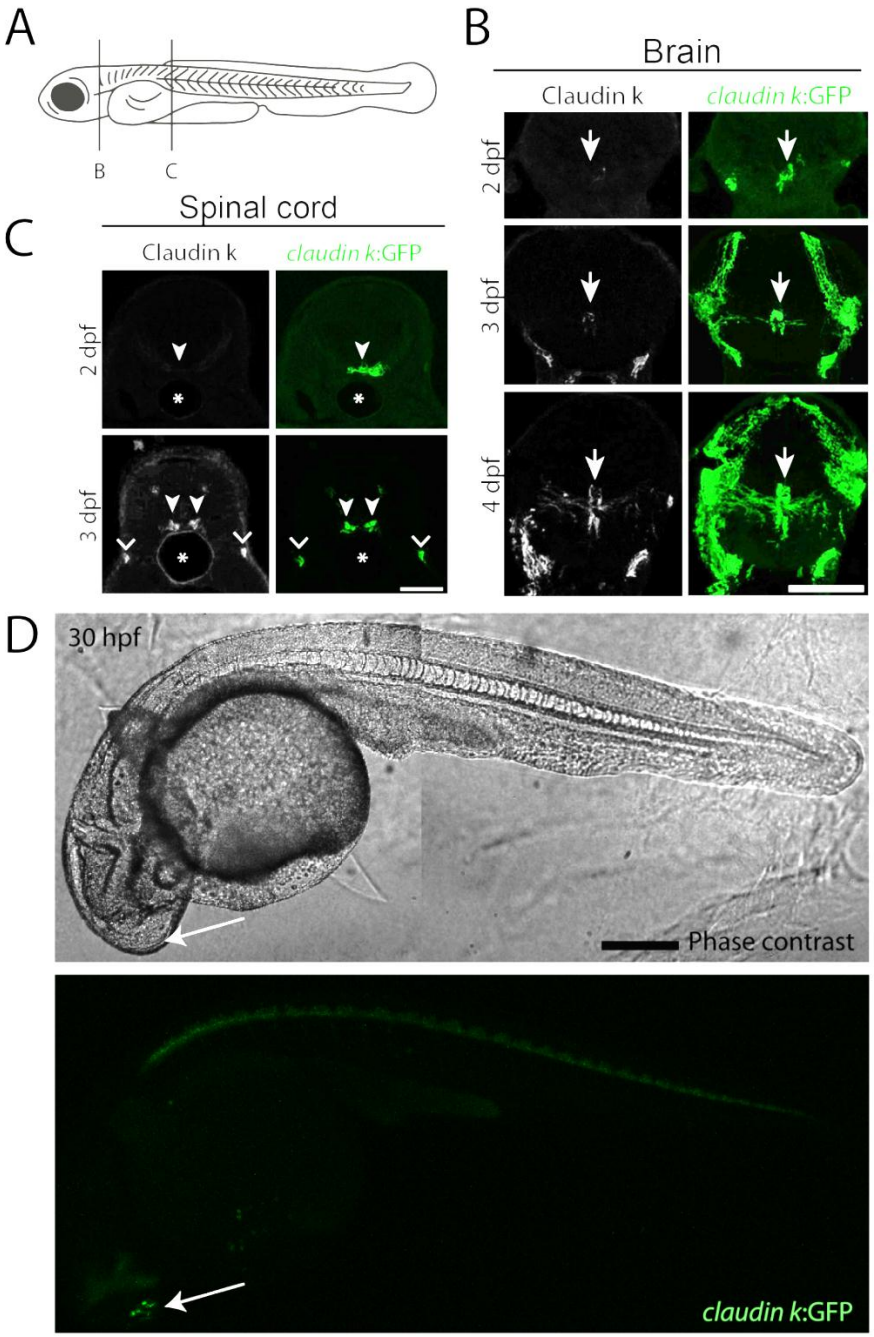

Figure 3.5: Developmental Claudin k and *tg(Claudin k:Gal4,UAS:mGFP)* expression in sectioned embryonic zebrafish. (A) Schematic of larval zebrafish indicates locations of cross sections shown in B and C. (B) Cryostat cross sections through hindbrain at different ages were double labelled with the anti-Claudin k antibody and *claudin k* transgene. First expression of Claudin k is observed at 3 dpf in the medial longitudinal fascicle of the hindbrain (arrows). Dorsal is up. (C) Cryostat cross sections of spinal cord at different ages were double labelled with the Claudin k antibody and *claudin k* transgene. First expression of Claudin k is observed at 3 dpf the spinal cord Mauthner axons (arrowheads) and the PLLN (open arrows) at 3 dpf, *claudin k* transgene expression in the spinal cord Mauthner axons is already present from 2 dpf. The ventricle is marked by the asterisk. Dorsal is up.(D) Images of a whole mounted *tg(Claudin k:Gal4,UAS:mGFP)* zebrafish at 30 hpf shows a few GFP labelled cells in the rostral head (arrow). Rostral is left. Scale bars: A = 50 µm, B = 100 µm, D = 200 µm.

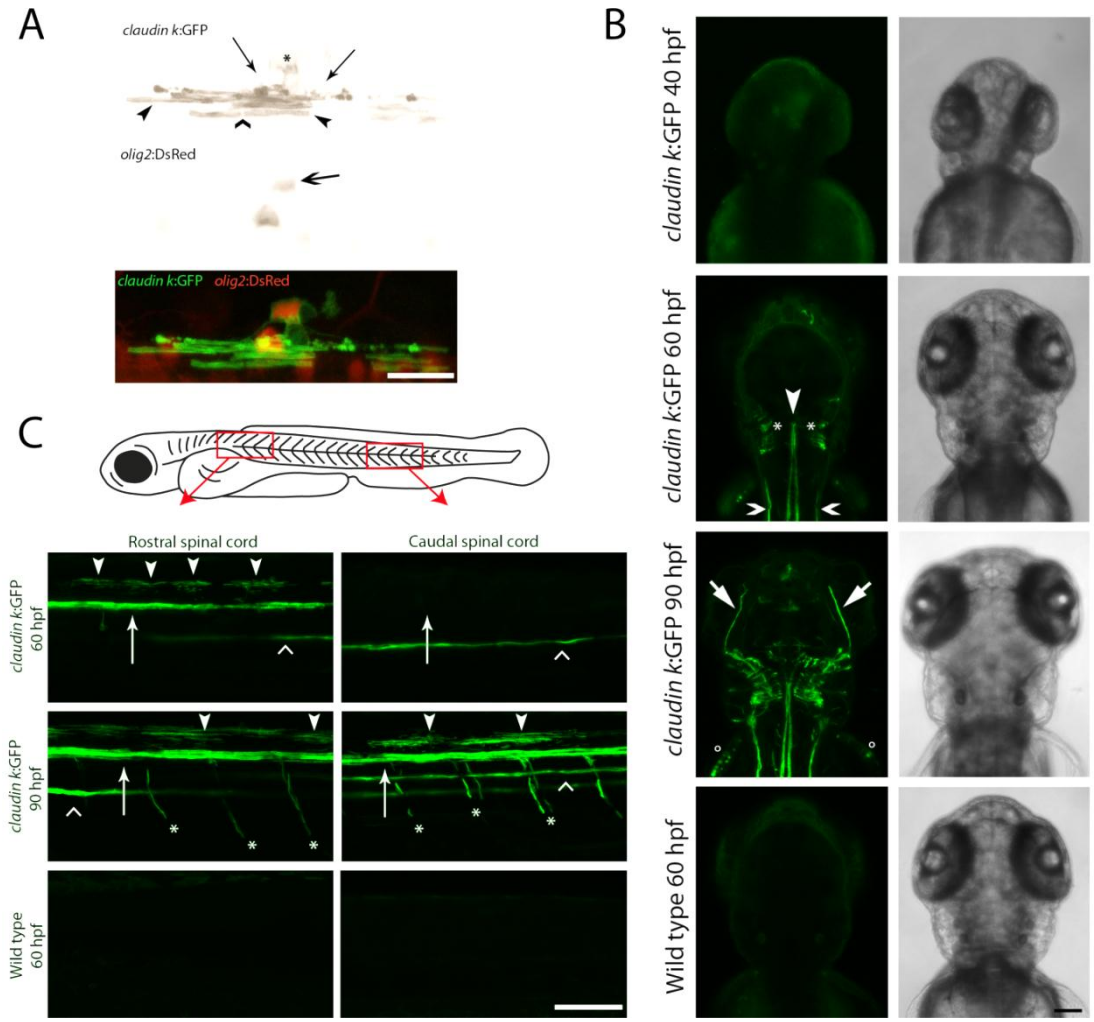

Figure 3.6: Developmental Claudin k and *tg(Claudin k:Gal4,UAS:mGFP)* expression in live imaged embryonic zebrafish. (A) An oligodendrocyte in a *tg(Claudin k:Gal4,UAS:mGFP)* x *tg(olig2:DsRed)* live zebrafish at 4 dpf in the dorsal spinal cord is shown. GFP expression can be observed in the cell membrane (asterisk), cell processes (arrows) and myelinating internodes (arrowheads). The open arrowhead indicated a putative Node of Ranvier between two internodes. (B) GFP expression time course of a single live transgenic zebrafish is shown (view from dorsal, rostral is up). No expression can be detected at 40 hpf. At 60 hpf, GFP expression associated with the Mauthner axons (arrowhead), fibres of the ventral commissure (asterisk) and PLLN (open arrow) can be observed. No GFP expression is detected in wild-type larva at this time. GFP expression increases in these structures and also labels nerves innervating the eye at 90 hpf (arrow). Ectopic expression in the fins is observed (circles). (C) A time course of the rostral and caudal trunk region of a single transgenic zebrafish is shown (dorsal is up, rostral is left). At 60 hpf, GFP expression was observed in the ventral (arrow) and dorsal (arrowheads) aspects of the rostral, but not the caudal spinal cord. The PLLN already shows GFP expression in the rostral as well as the caudal trunk region at 60 hpf (open arrows). No GFP expression is detectable in the wild-type larvae at this time point. At 90 hpf, GFP expression is now present in the caudal spinal cord as well (arrows), including the dorsal spinal cord fibres (arrowheads). GFP expression is associated with motor axons leaving the spinal cord, which is suggestive of myelination, was also observed in both regions (asterisks). Scale bars: A = 20 µm; B,C= 100 µm.

Expression of Claudin k and tg(Claudin k:Gal4,UAS:mGFP) in adult zebrafish

To investigate whether Claudin k is also a usable marker for myelin in adult zebrafish, I double-labelled sections of the adult *tg(Claudin k:Gal4,UAS:mGFP)* zebrafish with the anti-Claudin k antibody. Claudin k and transgenic GFP expression were detectable throughout the CNS, in particular myelinated white matter tracts in the optic tectum (Figure 3.7-A) showed co-labelling. While myelinated tracts, such as the tectobulbar tract were labelled by the anti-Claudin k antibody and the transgenic GFP, oligodendroglial cell bodies in the CNS were only labelled by the *claudin k* transgene (Figure 3.7-A). Moreover, these GFP positive cell bodies could be double-labelled with P0 mRNA, confirming the oligodendroglial-specific labelling of the transgenic GFP (Figure 3.7-B). This difference in labelling between the anti-Claudin k antibody and the *claudin k* transgene is due to a membrane tag of the transgenic GFP, which means it will be incorporated into any membrane in the cell. In contrast, the Claudin k antibody only recognises the protein in its final location, ie the myelin membrane sheath. This difference, however, allows the visualisation of myelinating oligodendroglial cells as well as their membrane sheath, and as such the anti-Claudin k antibody and the *claudin k* transgenic zebrafish line *tg(Claudin k:Gal4,UAS:mGFP)* are very powerful tools for myelination studies in zebrafish.

To confirm the specificity of the Claudin k antibody and GFP transgene, I double labelled sections of CNS tissue with another myelin marker, P0 antibody. Claudin k and P0 immunostaining in spinal cord sections showed a high degree of overlap, and confirm the myelin-specific labelling pattern of the Claudin k antibody in adult zebrafish (Figure 3.7-C). However, I observed that the transgenic GFP did not label all myelinated fibres that could be detected with the P0 antibody (Figure 3.7-D). P0 is only present in compact myelin sheaths, but Claudin k can be found in both non-compacted and compacted myelin wraps and therefore would be expected to co-label all P0-positive myelinated fibres. As this is not the case, these results suggest that the *tg(Claudin k:Gal4,UAS:mGFP)* fish exhibits a variegated transgenic expression pattern. To quantify the extent of this variegated expression, I counted GFP positive glial cells in the outer layers of the tectum in *tg(olig2:GFP)* and

tg(Claudin k:Gal4,UAS:mGFP) fish. I found that the membrane-bound GFP in *tg(Claudin k:Gal4,UAS:mGFP) fish* only labelled approximately half the number of cells compared to the *tg(olig2:GFP*) fish (*claudin k* transgenic fish: 16.3 ± 3.3 cells per field, *olig2* transgenic fish: 37.2 ± 6.8 cells per field, $p<0.01$, Mann Whitney U test, n=3). Thus, Claudin k immunoreactivity quantitatively labels myelin sheaths, whereas transgenic GFP exhibits a variegated expression pattern in oligodendroglial cells in the adult zebrafish CNS.

In the peripheral nervous system, as exemplified by the posterior lateral line nerve, co-labelling of the *claudin k* transgene and the antibody was also detected (Figure 3.7-E); and peripheral nerves surrounding the eyes of live adult zebrafish were visible through the skin (Figure 3.7-F). Variegated transgene expression in the peripheral nervous system was not quantified.

These results thus suggest that both the Claudin k antibody and transgenic GFP can be used to visualise myelin and myelinating glial cells in the adult zebrafish, but only the antibody immunoreactivity should be used for quantification as the *claudin k* transgene exhibits a variegated expression.

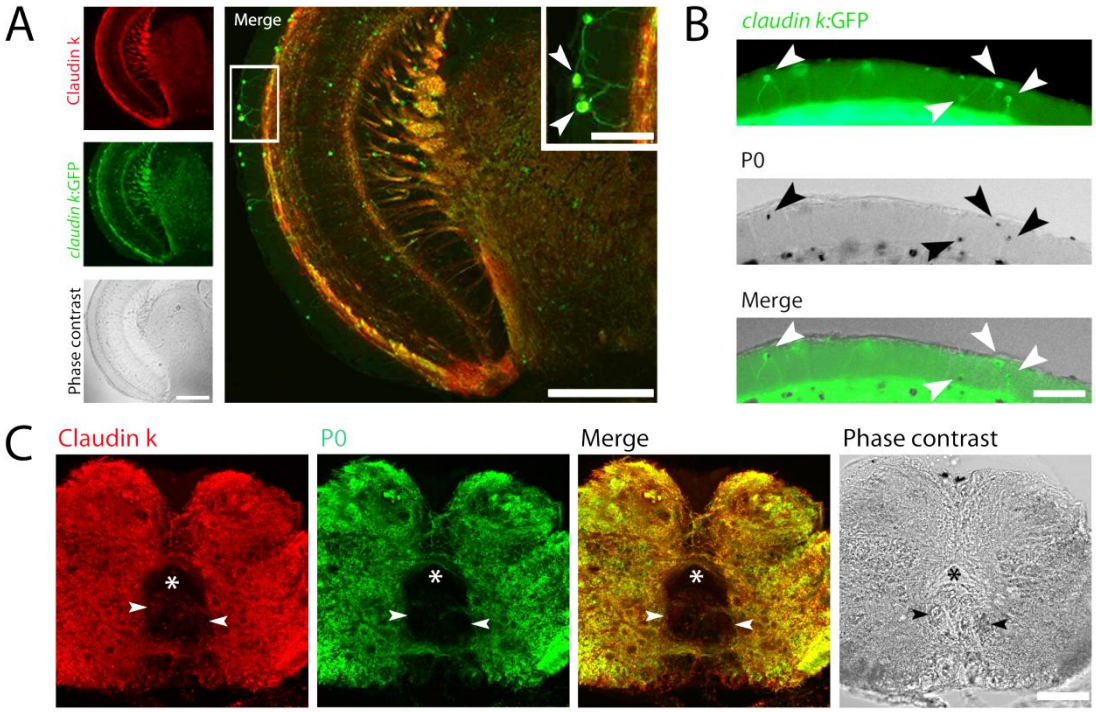

Figure 3.7 (A-C): Claudin k and *tg(Claudin k:Gal4,UAS:mGFP)* expression in adult zebrafish. (A) Cryostat cross sections of adult optic tectum shows co-labelling of the Claudin k antibody and the transgenic GFP, however oligodendroglial cell bodies are only labelled by the transgene as it contains a membrane tag (inset, arrowheads). Dorsal is up. (B) In the outer layers of the optic tectum, GFP-positive cells in the *tg(Claudin k:Gal4,UAS:mGFP)* transgenic zebrafish are also positive for *P0* mRNA (arrowheads), indicating that they are oligodendrocytes. (C) Double labelling of spinal cord cross-sections with Claudin k and P0 antibodies shows an overlapping staining pattern. Labelling of myelin sheaths around the Mauthner axons can be observed (arrowheads). Asterisk marks the ventricle. Dorsal is up. Scale bar: A = 200 µm; Inset = 60 µm, B = 50 µm, C = 100 µm.

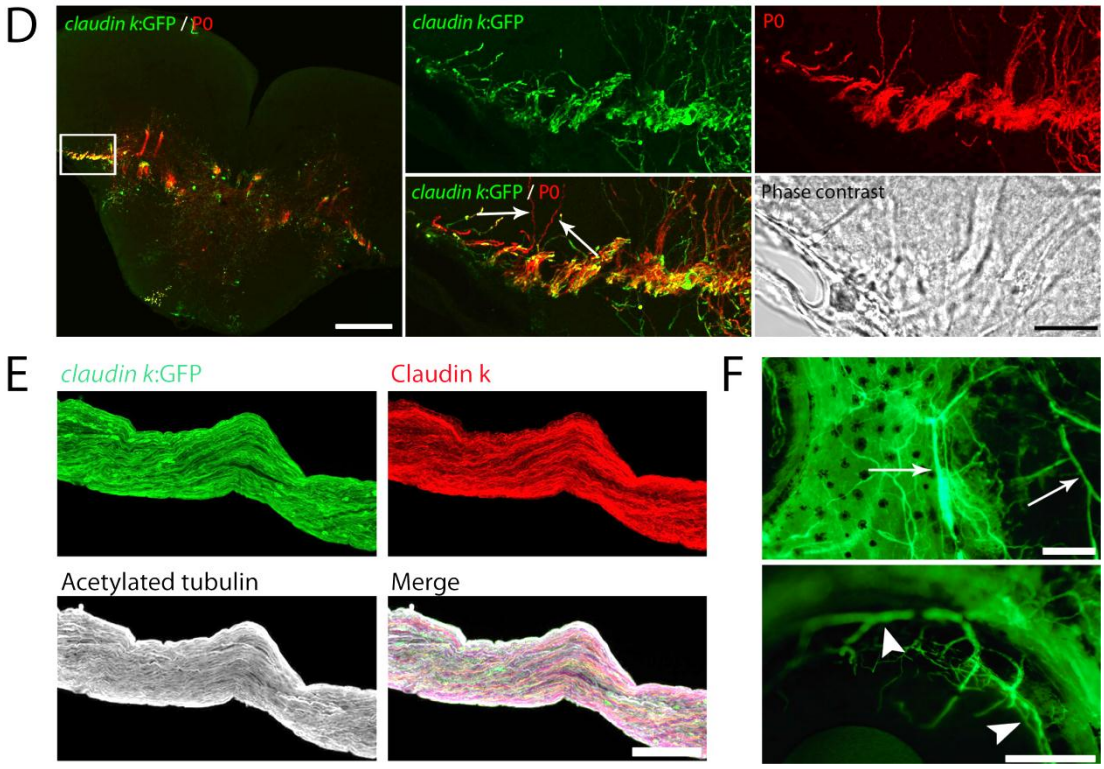

Figure 3.7 (D-F): Claudin k and *tg(Claudin k:Gal4,UAS:mGFP)* expression in adult zebrafish. (D) In cross sections of the adult telencephalon transgenic GFP expression largely co-labels with P0 antibody immunoreactivity, however there are some P0 positive/GFP-negative myelin sheaths (arrows). The boxed area in the left image is shown in higher magnification on the right. (E) A whole mounted PLLN shows co-labelling of GFP expression, Claudin k antibody and acetylated tubulin immunoreactivity. (F) Transgenic GFP expression in peripheral nerves around the eye is visible in anaesthetised live adult zebrafish under a fluorescent stereomicroscope. Rostral is left, dorsal is up. Scale bars: D = 100 µm (low magnification, left); 10 µm (high magnification, right), E = 100 µm, F = 0.5 mm.

Claudin k expression in the visual system of adult zebrafish

The optic nerve in adult zebrafish is ideal for experimental lesions as it is easily accessible through the large orbita. Previous studies in goldfish use the optic nerve for myelination studies; however differential myelination patterns along retinal ganglion cell (RCG) axons between species prompted detailed analysis of Claudin k expression in the optic system of zebrafish. In rodents, the optic nerve contains myelinated fibres, while axons of the retinal fibre layer remain unmyelinated, presumably to allow sufficient light to reach the photoreceptors in the inner layers of the retina. Evidence has shown that in these species a barrier (the glia limitans) prevents oligodendrocytes from migrating into and myelinating the retinal fibre layer (Ffrench-Constant et al., 1988). Previous studies of the zebrafish optic system indicated the presence of loose myelin wraps in the intraretinal part of the retinal ganglion cell axons, and that glial cells of the RGC layer express *contactin 1a* mRNA, which is usually only found in actively differentiating oligodendrocytes (Schweitzer et al., 2007). As *P0*, a marker of compact myelin is only found in the optic nerve and tract but not in the retinal fibre layer (Schweitzer et al., 2003), I hypothesised that the adult zebrafish retina may contain oligodendrocytes that have retained a somewhat immature differentiation status. However, such cells have not been directly visualised previously.

By using the Claudin k antibody and the *tg(Claudin k:Gal4,UAS:mGFP)* fish line, I could show that Claudin k is indeed expressed in the retina and optic nerve of adult zebrafish, and that the staining pattern was similar to that of MBP (Figure 3.8-A). By comparison, the P0 antibody only labelled the optic nerve and optic nerve head and no immunoreactivity could be detected in the retina, confirming earlier *in situ* hybridisation results (Schweitzer et al., 2003). However, when I investigated the retinal fibre layer in *olig2*:GFP transgenic zebrafish, I found *olig2*-positive cells in the retina and optic nerve, confirming that oligodendroglial cells are present in both locations (Figure 3.8-B). To visualise these oligodendroglial cells in retina and optic nerve, I used the variegated transgene labelling in *tg(Claudin k:Gal4,UAS:mGFP)* fish to my advantage as then positive cells were more separated and could be

distinguished from each other. In whole mounted retina and optic nerve, I found *claudin k* transgene-positive cells, which were also *olig2*-positive, confirming their oligodendroglial origin (Figure 3.8-C,D). Moreover, their morphology was typical for oligodendrocytes with multiple processes ending in longitudinal structures, reminiscent of internodes (Grinspan, 2002). The identity and morphology of these intraretinal oligodendroglial cells has not been described before in teleosts; and confirms the hypothesis that these are indeed responsible for loose wraps of myelin around retinal ganglion cell axons. However, why they are only present in fish and do not form *P0+* compact myelin sheaths remains unknown.

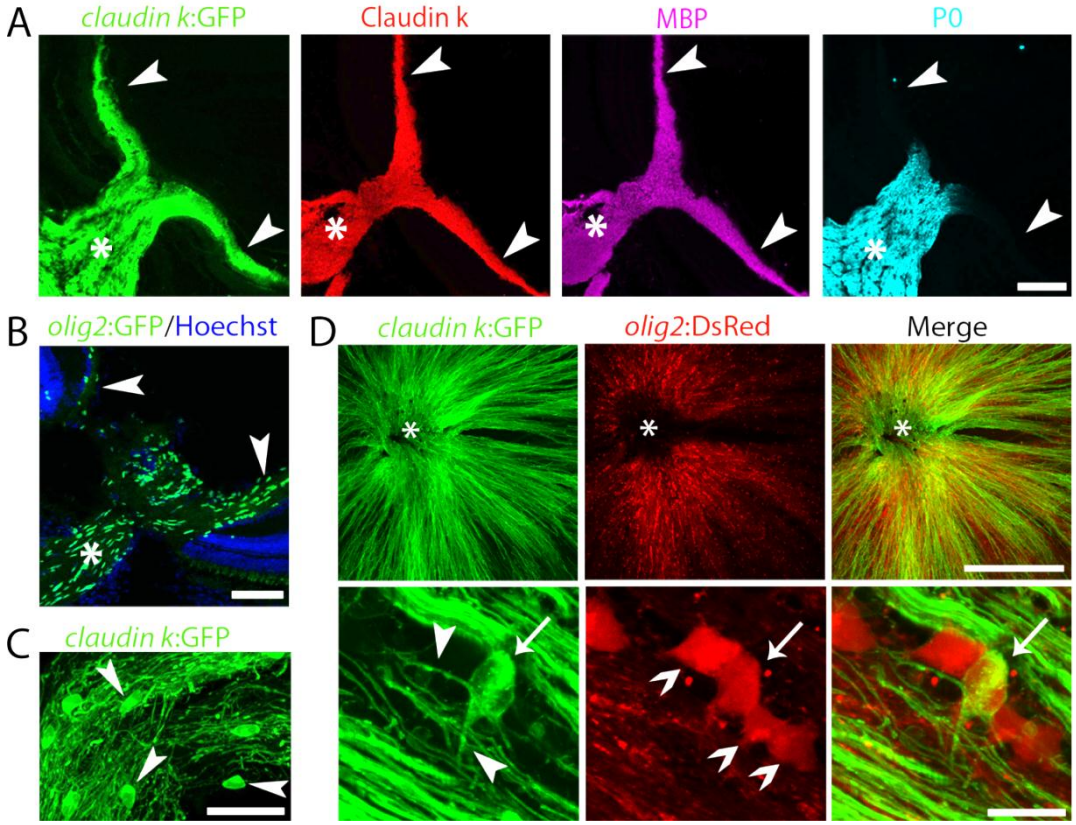

Figure 3.8: Claudin k and *tg(Claudin k:Gal4,UAS:mGFP)* expression in the adult zebrafish optic nerve and retinal fibre layer. (A) Cross sections through adult zebrafish eyes show co-labelling of GFP, Claudin k and MBP in the central retina (arrowheads) and optic nerve (asterisks), while P0 immunoreactivity can only be detected in the optic nerve. (B) *Olig2*:GFP are present in the optic nerve (asterisk) and throughout the retina (arrowheads). (C) Single GFP-positive cells are visible in a whole-mounted optic nerve of *tg(Claudin k:Gal4,UAS:mGFP)* zebrafish. (D) A whole-mounted retina of adult *tg(Claudin k:Gal4,UAS:mGFP) x tg(olig2:DsRed)* double transgenic fish at low magnification (top row) and single oligodendrocytes therein at high magnification (bottom row) are shown. GFP-positive processes in the retinal optic fibre layer orientate around the optic disk (asterisk). Single oligodendroglial cells (arrow) with processes (arrowheads) co-label with transgenic GFP and DsRed, while other oligodendroglial cells are only *olig2*:DsRed positive (open arrows). Scale bars: A, B = 200 µm, C = 40 µm, D = 300 µm (low magnification); 20 µm (high magnification).

Oligodendrocyte and myelin regeneration after adult optic nerve lesion

Due to its easy access, the zebrafish optic system is ideal to study nerve regeneration and related changes in oligodendrocyte differentiation. It has been shown previously that following an optic nerve crush in adult zebrafish, severed axons degenerate along the optic tract within hours, and newly formed axons repopulate the entire optic pathway already by day 16 post lesion (Wyatt et al., 2010), and fully reinnervate the tectum within 4 weeks (Becker et al., 2000). To investigate the dynamics of claudin k-positive oligodendroglial cells during optic nerve regeneration, I performed optic nerve crushes in adult *tg(Claudin k:Gal4,UAS:mGFP)* transgenic zebrafish and quantified Claudin k immunoreactivity and GFP as a marker for differentiating oligodendrocytes and LINC immunoreactivity as a marker for axons (Figure 3.9). Claudin k, LINC and transgenic GFP were significantly reduced in the lesion site at 3 days post lesion (dpl), the earliest time point analysed. These findings indicate loss of oligodendrocytes and axons. Proximal (towards the retina) and distal (towards the brain) of the lesion, immunofluorescence persisted, likely due to the presence of intact axonal segments (proximal) and fibre debris (distal), which prevented me from further quantifying changes in these regions. At 7 dpl, Claudin k immunoreactivity and transgenic GFP was still significantly less than in controls, however, GFP-positive cell bodies were observed in the lesion site. LINC immunoreactivity showed increased and no longer significantly different levels from the 3 dpl time point, suggesting that axonal regrowth was in progress. At 14 dpl, GFP-positive oligodendrocytes with varying morphologies were observed in the lesion area, ie some with more and some with less processes (suggesting more and less mature cells) (Figure 3.9-A), and by 28 dpl all investigated markers had returned to normal levels and were comparable to those in unlesioned control nerve, suggesting that both axons and oligodendrocytes had regenerated (Figure 3.9-B,C).

Variegated expression in the *tg(Claudin k:Gal4,UAS:mGFP)* fish allowed more detailed analysis of oligodendroglial morphology during this regenerative process as single transgenic cells could be visualised in the regenerating optic nerve (Figure

3.10-A,B). I therefore quantified GFP-positive cells 200 µm proximal and distal of the lesion epicentre in longitudinal nerve sections at the same time points as described before. There was an overall significant increase of GFP-positive oligodendroglial cells in the lesion from 3.0 ± 2.0 cells at 3 dpl to 17.7 ± 3.5 cells at 28 dpl (mean ± SD, $p<0.05$, n=3, Mann Whitney U-test). GFP-positive cells with a simple morphology (≤ 2 processes, Figure 3.10-A) were present in the lesion site at 3 dpl (3.0 ± 2.0 cells), significantly increased at 7 dpl (13.3 ± 3.1 cells, $p<0.01$, n=3, Kruskal Wallis test, Dunn's post-test) and became fewer in number again at 14 dpl (4.0 ± 3.6 cells) and 28 dpl (0.3 ± 0.6 cells). By comparison, cells with a more complex morphology that resemble that of differentiated and myelinating oligodendrocytes with more than 2 processes (Figure 3.10-A) were not found in the lesion at 3 dpl. They were observed in the lesion site at 7 dpl (3.3 ±1.5 cells) and 14 dpl (14.7 ± 9.8 cells), and were significantly increased toward the end of the regeneration process at 28 dpl (17.3 ± 3.5 cells, $p<0.01$, n=3, Kruskal Wallis test, Dunn's post-test) This increased morphological complexity and number of axon-associated processes of oligodendrocytes in the lesion site is suggestive of myelination of the regenerated axons.

In mammalian studies, the majority of oligodendrocytes associated with myelination after axonal regeneration is generated by proliferation of oligodendrocyte precursor cells (OPCs) (Blakemore and Keirstead, 1999; Gensert and Goldman, 1997). To determine whether regenerated axons in zebrafish are also myelinated by newly generated oligodendrocytes, the animals received daily injections of bromodeoxyuridine (BrdU at 2,3 and 4 days post lesion. In contrast to the contralateral unlesioned nerve, there was a significant increase of BrdU labelled/GFP-positive cells in the lesion site of the crushed nerve at 14 dpl (26.7% ± 5.6% in the lesioned vs. 5.7% ± 8.6% in the control nerve, mean ± SD, $p<0.05$, n=4, Mann Whitney-U test, Figure 3.10-C,D,E). This increased uptake of the proliferation marker BrdU in myelinating GFP-positive oligodendrocytes suggests a lesion-induced generation and differentiation of oligodendrocytes during regeneration of the adult zebrafish optic nerve.

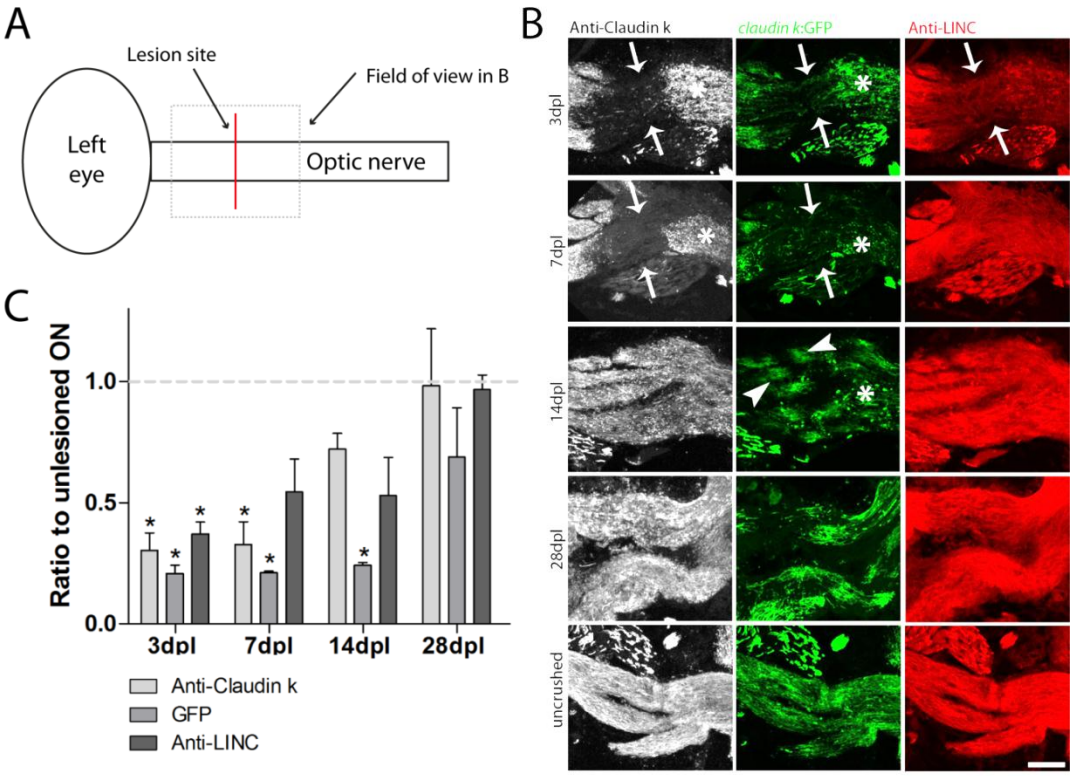

Figure 3.9: Claudin k and *tg(Claudin k:Gal4,UAS:mGFP)* expression during optic nerve regeneration. (A) A schematic shows the site of crush and the part of the nerve imaged in B. (B) Immunolabelling of the lesion area shows decreased Claudin k, transgenic GFP and LINC (marking axons) immunoreactivity at 3 and 7 dpl (arrows) Myelin debris is detected distal (toward the brain) of the lesion site (asterisks). By 28 dpl, GFP fluorescence, Claudin k and LINC immunoreactivity have returned to similar levels as observed in the unlesioned nerve, suggesting successful regeneration. GFP-positive oligodendroglial cells with varying number of processes were detected in the lesion site at 14 dpl (arrowheads). (C) Quantification of immunoreactivity in the lesion site, described as a ratio to the signal intensity in the contra-lateral unlesioned control nerve is shown. ($p < 0.05$, Two-way ANOVA, Bonferroni post-test, n = 3). Error bars represent mean ± SD. Scale bar: B = 300 µm.

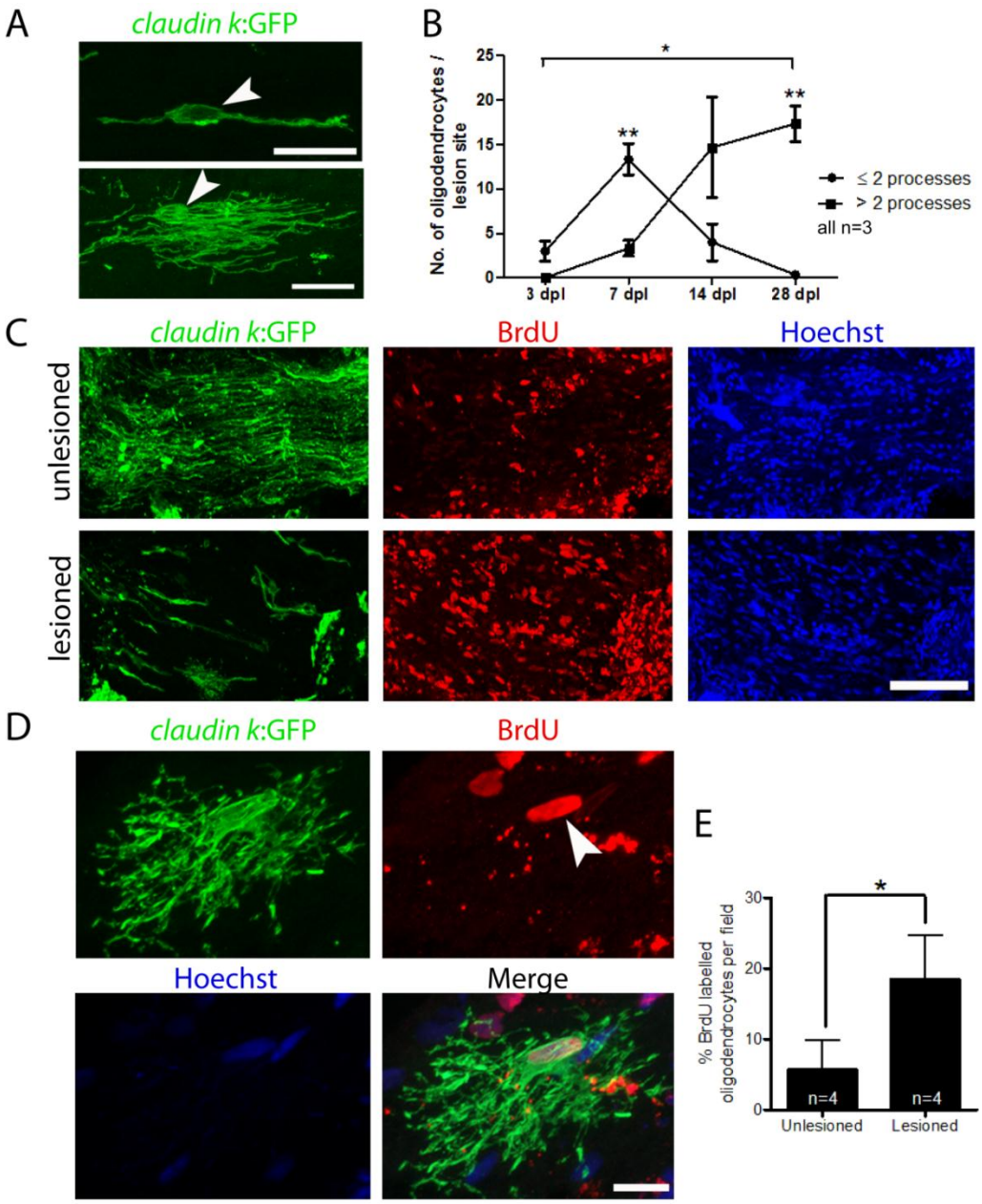

Figure 3.10: Oligodendroglial morphology and BrdU labelling during optic nerve regeneration. (A) Variegated GFP expression labels single oligodendrocytes (cell bodies indicated by arrowheads) with varying number of processes in the lesion site at 14 dpl. (B) There is an overall significant increase in total number of labelled oligodendrocytes in the lesion site over the time points analysed ($p<0.05$, n=3, Mann Whitney U-test). The number of GFP-positive cells with two or fewer processes in the lesion site peaks at 7 dpl ($p<0.01$, n=3, Kruskal Wallis test, Dunn's post-test). The number of GFP-positive cells with more than two processes in the lesion site increases during the regeneration process until 28 dpl ($p<0.01$, n=3, Kruskal Wallis test, Dunn's post-test). (C) Coronal cross sections of adult *tg(Claudin k:Gal4,UAS:mGFP)* transgenic zebrafish optic nerves 14 dpl and BrdU injections at 2,3 and 4 dpl show reduced GFP expression in the lesioned optic nerve and an increase in BrdU+ cells. (D) A single differentiating oligodendrocyte (arrowhead) in the optic nerve shows positive BrdU labelling at 14 dpl. (E) The proportion of GFP+/BrdU+ cells is significantly increased in the lesioned optic nerve ($p<0.05$, Mann Whitney-U test, n=4). Error bars represent mean ± SD. Scale bars: A = 20 µm, C = 80 µm, D = 10 µm.

3.3 Discussion

Claudin k is a myelin associated protein, which is expressed in the zebrafish central and peripheral nervous system. Analysis of Claudin k by specific antibody immunolabelling and transgenic GFP expression showed a dynamic expression pattern during development and optic nerve regeneration that is similar to previously described myelination patterns (Brosamle and Halpern, 2002; Schweitzer et al., 2003). Moreover, the transgenic zebrafish line, which expresses membrane-bound GFP under the *claudin k* promoter, allowed the morphological characterisation of single oligodendrocytes and their myelin sheaths around the retinal ganglion axons, and during the process of optic nerve regeneration following crush injury.

During development, Claudin k is detectable from 3 dpf in the hindbrain, which is consistent with detectable mRNA in the same location from 2 dpf (Schaefer, 2009), and the onset of other myelination markers such as P0, DM20 (proteolipid protein) and MBP (Brosamle and Halpern, 2002). It is as such one of the earliest markers for differentiating oligodendrocytes found in zebrafish. Claudin k immunolabelling and transgenic GFP expression are lower in the hypomyelinating *sox10^{t3}(colourless)* mutant zebrafish larvae compared to wild type, and after an optic nerve crush both markers are initially reduced in the lesion area and re-appear in a time course that is consistent with optic nerve regeneration. Hence, both Claudin k immunoreactivity and transgenic GFP can be used effectively to quantify the level of myelination and to track myelin-forming cells in development and in lesioned adult zebrafish.

Throughout my studies with the transgenic *tg(Claudin k:Gal4,UAS:mGFP)* line, I observed variegated GFP expression patterns as indicated by some transgenic animals showing more and brighter fluorescence than others. I also found that even in the fish with the most labelled cells, GFP was not consistently expressed in all oligodendrocyte processes labelled with Claudin k or P0 antibody nor in all cell membranes of *olig2*:GFP expressing cells. This may be due to a variance in the loci where the transgene was integrated or the number of integrated transgene copies

in the individual animal. To stabilise expression patterns in this transgenic line, I used in- and out-crossing breeding strategies, however I continued to observe this variegated expression pattern. This perhaps suggests another reason, such as the GAL4/UAS system, which was used to generate the *tg(Claudin k:Gal4,UAS:mGFP)* line. The GAL4/UAS system was first utilised in *drosophila* for easy and effective transgenesis, and commonly uses 14 repetitive upstream activating sequences (UAS) (Brand and Perrimon, 1993). It allows an enhanced expression of fluorescent proteins even if the promoters are very weak, as the binding of GAL4 to repetitive UAS leads to increased production of fluorescent protein. Recent studies in transgenic zebrafish with this system have shown that because the UAS is present in multiple identical repeats, parts become silenced through methylation (Akitake et al., 2011), and therefore present an explanation for the variegated expression I observed in the *tg(Claudin k:Gal4,UAS:mGFP)* line. However, although only a proportion of oligodendrocytes are labelled in the transgenic line, these cells are visible in their entire morphology and as such this provides a unique opportunity to use the *tg(Claudin k:Gal4,UAS:mGFP)* line for the study of individual oligodendrocytes.

As differential myelin patterns in the adult zebrafish retina had been described previously, I used the *tg(Claudin k:Gal4,UAS:mGFP)* line to visualise individual myelinating cells in this area. Earlier electron microscope studies of the adult zebrafish retina showed that intraretinal ganglion axons are ensheathed only by loose wraps of cell membrane; the optic nerve by comparison showed compact myelination (Schweitzer et al., 2007). This is different to mammals, which do not possess a myelinated retina, with exception of the rabbit (Morcos and Chan-Ling, 1997), and is consistent with findings in goldfish and other teleosts (Easter et al., 1984; Wolburg, 1980). Previous studies have demonstrated that *contactin 1a* mRNA, which is normally only expressed by actively differentiating oligodendrocytes and neurons, is present in the adult zebrafish retinal fibre layer, whereas P0, a marker for compact protein is not detectable in the retina (Schweitzer et al., 2003). Thus it was not clear whether the loose myelin wraps of intraretinal axons originated indeed from oligodendrocytes. By investigating whole-

mounted retinae of *tg(Claudin k:Gal4,UAS:mGFP) x tg(olig2:DsRed)* double transgenic fish, I could demonstrate that intraretinal myelinating cells indeed exhibit an oligodendrocyte-like morphology with several processes emanating from the cell body to associate with axons. This strongly supports the hypothesis that the cells ensheathing axons in the adult zebrafish retina are indeed oligodendrocytes.

In mammalian retinae, a barrier prevents OPCs from migrating into the retina from the optic nerve head (Ffrench-Constant et al., 1988). However, when OPCs are injected into the normally non-myelinated rat retina, they are able to form compact myelin (Laeng et al., 1996; Setzu et al., 2004; Setzu et al., 2006), indicating that also in mammals, intraretinal axons are fully myelination competent. This raises the intriguing possibility that in fishes, other factors may prevent retinal oligodendrocytes from forming compact myelin. What these factors may be is unknown, but this model may be a useful tool to further investigate factors that could be involved in preventing oligodendrocytes from forming compact myelin, which as previously discussed in the context of MS, may be highly relevant in investigating the failure of oligodendroglial cells to fully mature into myelinating oligodendrocytes, one cause of remyelination failure in MS (reviewed in Piaton et al., 2009).

To explore myelination in regeneration, I used the previously established optic nerve crush injury in adult zebrafish. I could show that at 3 days after the lesion, Claudin k and transgenic GFP are severely reduced and become re-detectable as the nerve regenerates within 4 weeks. This corresponds to earlier findings of other myelin markers; *contactin 1a* mRNA marks early differentiating oligodendrocytes and is most strongly up-regulated at 7 dpl, followed by P0 at 28 dpl, which marks the reappearance of compact myelin (Schweitzer et al., 2003). Moreover, studies in goldfish demonstrate the presence of the myelin molecules 36 kDa protein, galactocerebroside and MBP from 3.5 weeks after optic nerve crush (Ankerhold and Stuermer, 1999). These results suggest, that zebrafish are capable of not only regenerating their retinal ganglion cell axons, but can also myelinate them.

To gain further insight into these newly myelinating cells, I used the transgenic *tg(Claudin k:Gal4,UAS:mGFP)* line to identify GFP-positive cells in the lesion site at early time points following the crush injury. These cells had a simple, bipolar morphology and were reminiscent of oligodendrocyte precursor cells (Grinspan, 2002). At later time points, they had a more complex morphology with multiple processes; this is a clear indication of oligodendroglial identity. Thus, these cells were unlikely to be Schwann cells, which have been shown to invade the regenerating optic nerve of goldfish (Nona et al., 1992). In addition, I could show that ~25% of oligodendrocytes in the lesion site took up the proliferation marker BrdU, suggesting that these cells had been newly generated. Goldfish studies using dye fills of oligodendrocytes have previously demonstrated, that these are capable of de- and re-differentiation following optic nerve crush and only a minority (7.5%) are newly generated (Ankerhold and Stuermer, 1999). However, due to the differential nature of the dye fill and BrdU protocols, it is not possible to compare these findings quantitatively. Other studies also highlight the possibility that oligodendrocyte lineage cells could be capable of de- and redifferentiation. Using *in vitro* studies of primary cell cultures enriched in oligodendrocytes, Grinspan and colleagues were able to show the dedifferentiating potential of mature oligodendrocytes as they observed an increase in oligodendrocyte progenitor cells upon basic fibroblast growth factor treatment of the cultures (Grinspan et al., 1993). Further, the authors could demonstrate that this effect of basic fibroblast growth factor was direct and not mediated through other cell types, and also required the oligodendrocytes to re-enter the cell cycle (Grinspan et al., 1996). Other studies investigating the role of voltage-gated potassium channels, which are known to be involved in growth-factor induced cell proliferation of oligodendrocyte lineage cells, suggest that these channels are upregulated in NG2-positive oligodendrocyte progenitor cells within MS lesions (Tegla et al., 2011). In addition, they seem to regulate cell cycle activation and oligodendrocyte dedifferentiation *in vitro* by controlling the activation of complement and the assembly of the terminal complement complex (C5b-9), which has been shown to play an important role in the pathogenesis of neurodegenerative CNS diseases like MS (Rus et al., 2006).

Mature oligodendrocytes *in vivo* therefore appear to be capable of dedifferentiation; however, *in vivo* approaches investigating the origin of remyelinating oligodendrocytes indicate that while in the mammalian CNS only oligodendrocytes that newly arise from OPCs appear capable of remyelination (reviewed in Blakemore and Keirstead, 1999; Franklin and Ffrench-Constant, 2008), Schwann cells in the PNS seem to be able to de- and re-differentiate (Mirsky et al., 2008). Bearing in mind that fish oligodendrocytes have some similarities with mammalian Schwann cells, such as de-differentiation in culture (Jeserich and Rauen, 1990) and expression of P0 (Schweitzer et al., 2003), it would be interesting to further investigate whether this could be the reason for successful CNS regeneration in fish. The results from the BrdU studies are also compatible with dedifferentiation, division and re-differentiation of oligodendrocytes following optic nerve injury and as such don't answer the question about the origin of the cells that myelinate newly generated optic nerve fibres. To investigate this closer, one would need to design a transgenic line which would allow colour conversion of cells after the lesion. This is further discussed in chapter 5.

CHAPTER 4 – Establishing a model of myelin injury in adult zebrafish

---

4.1 Introduction

As highlighted in the main introduction of this dissertation, various experimental animal models to study demyelinating disease have already been established. Zebrafish are transparent during embryonic development and this advantage is widely used to investigate the process of myelination more closely (Almeida et al., 2011; Czopka and Lyons, 2011; Kirby et al., 2006; Raphael and Talbot, 2011; Takada et al., 2010), with the goal of potentially extrapolating important findings to the mammalian system. Large scale screens for genes involved in myelination and for the discovery of pro-myelinating substances have been conducted in zebrafish larvae (Buckley et al., 2010; Pogoda et al., 2006; Simmons and Appel, 2012), and zebrafish have also been investigated as potential model organisms to study demyelinating diseases (Buckley et al., 2008). As such, they could be very useful to study promotion of myelin repair for clinical translation; however it is unclear whether the mechanisms of myelination in developing zebrafish are similar to remyelination in adult zebrafish in which developmental myelination has largely finished, and whether the process of remyelination in teleost fish is in fact similar to that in mammals. I therefore thought it important to generate an adult zebrafish de/remyelination model to compare with mammalian remyelination and to validate potential drug candidates identified in prior zebrafish screens for further testing in rodent or non-human primate models of demyelination and possible clinical translation.

Adult zebrafish are able to regenerate various CNS tissues after injury, including retina, spinal cord and brain (Becker and Becker, 2008; Fimbel et al., 2007; Kroehne et al., 2011), however there is only limited knowledge about the regenerative

capacity of myelin. Previous studies investigating myelination following nerve crush injury in goldfish demonstrate that regenerated axons are myelinated successfully (Wolburg, 1978, 1981) and that this is most likely achieved by previously present de- and re-differentiated oligodendroglial cells (Ankerhold and Stuermer, 1999). However by applying a nerve crush injury, these studies effectively investigated de novo myelination of regenerated axons rather than remyelination of existing axons which have been stripped of their myelin. Hence a more accurate model system to study de- and remyelination without axonal injury in fish could give valuable insight into the processes of successful myelin regeneration.

Methods to induce demyelinating lesions

As outlined in the general introduction, studies exploring mechanisms underpinning myelin repair use different experimental animal models and depending on the preference for focal or global demyelination, mode of application or timeframe of recovery, various methods to induce demyelination are available. I reviewed these in other species in order to choose the most appropriate for the adult zebrafish. These include:

- Local toxin induced demyelinating lesions with substances such as ethidium bromide or lysophosphatidylcholine
- Dietary intake of substances known to cause CNS demyelination such as Cuprizone
- Targeting single cells of interest by laser phototoxicity
- Transgenic conditional cell ablation by use of heat shock promoters or tamoxifen/diphtheria toxin inducible systems
- Experimental autoimmune encephalitis

Local application of toxins

Ethidium bromide (EtBr): Previous studies investigating remyelination in rodents and cats locally injected the intercalating agent EtBr and could demonstrate a toxic effect on myelinating cells (Blakemore, 1982; Bondan et al., 2009). While not much axonal damage has been reported with this model, presumably as most neuronal cell bodies which could be subject to EtBr intercalation are located outside of the white matter, the disadvantages of EtBr includes that it exhibits auto fluorescent qualities, which may limit the use of immunohistochemical methods following demyelinating injury. In addition, EtBr is highly carcinogenic and this toxic effect makes it impractical to handle.

Lysophosphatidylcholine (LPC): Many experimental models of demyelinating disease in rodents use the detergent-like substance LPC, also known as lysolecithin, to demyelinate axons. It is unclear how the substance leads to demyelination; it is thought that like a detergent, it dissolves the myelin sheaths and leads to apoptotic death of oligodendrocytes. However, there is also a hypothesis that LPC has direct influence on immune cells. LPC results from the hydrolysis of naturally occurring cell membrane derived phosphatidylcholines, whereby one of the fatty acid groups is removed by the enzyme phospholipase A_2 (PLA_2). PLA_2 activation is associated with multiple stimuli, in particular stress and inflammatory signals, and leads to the production of multiple pro-inflammatory lipids. The secreted form of PLA_2 is released from macrophages and other cell types at the site of injury (Bingham and Austen, 1999), and by producing extracellular LPC promotes inflammatory effects such as the up-regulation of endothelial cell adhesion molecule and growth factors (Kume and Gimbrone, 1994), chemotaxis of monocytes and T-lymphocytes (McMurray et al., 1993; Rong et al., 2002) and activation of macrophages, which is thought to be T-cell mediated (Ghasemlou et al., 2007). Recent research has identified the G-protein-coupled receptors G2A and GPR4 in macrophages and dendritic cells as specific targets of LPC. Activation of these receptors leads to ERK MAP kinase phosphorylation, intracellular calcium increase via Gαi g-proteins and transcriptional activation of serum response factor (Kabarowski et al., 2002). Using

local application of LPC in the rat brain striatum, researchers could show an initial increase in number of immune cells, and chemotactic functions of LPC could be confirmed in *in vitro* cultures with microglia and astrocytes (Sheikh et al., 2009). This suggests that LPC may directly influence the innate immune response and antigen presentation prior to the LPC-induced demyelination. It is currently not clear if LPC primarily causes demyelination, which then triggers the immune response, or whether LPC mainly attracts microglia, which then lead to demyelination. However LPC remains a beneficial tool in remyelination research, as the process of de- and remyelination can be observed separately from the adaptive immune response.

LPC is commonly used to induce focal demyelinating lesions *in vivo* and its ability to demyelinate axons was established as early as the 1980's (Foster et al., 1980; Waxman et al., 1979). Following injection of LPC *in vivo* or application to slices of CNS tissue *in vitro* a reduction in immunolabelling of myelin-associated proteins such as myelin basic protein has been observed, while detectability of axonal markers such as neurofilament in immunohistochemistry remained largely unchanged (Birgbauer et al., 2004; Nait-Oumesmar et al., 1999; Zhang et al., 2011). Hence LPC can be used to induce focal demyelinating lesions. Advantages include the possibility of local injection and safe use for the investigator; however higher doses can be toxic to axons.

It appeared possible to use both EtBr and LPC for the induction of focal demyelinating lesions in adult zebrafish, but as EtBr is highly toxic and LPC likely safer to use, I decided to trial this method.

General application of toxin in diet

Cuprizone diet-induced demyelination: Cuprizone-induced demyelination is commonly used in rodent experimental models and involves the feeding with a copper chelator, which results in demyelination of well-defined regions in the mouse brain (mainly the corpus callosum) within several weeks of commencing the

diet (Matsushima and Morell, 2001; Steelman et al., 2012). To date it is not known how Cuprizone leads to demyelination and what the subcellular processes are, however it may involve mitochondrial pathology and copper deficiency (Acs and Komoly, 2012; Benetti et al., 2010). Cuprizone also has a neurotoxic effect, which is thought to be mediated through its ability to chelate copper (Benetti et al., 2010). This method of demyelination has not been tried in zebrafish previously and as the food is fed through the water, it would be difficult to determine a) the dose of Cuprizone to be given to the fish and b) possible side effects as it dissolves in the water.

Demyelination using laser ablation

Another method to specifically target myelinating cells is laser-induced phototoxic apoptosis, whereby phototoxicity could induce apoptosis in specific cells of interest expressing a certain transgene. This method has been applied to zebrafish embryos and larvae before (Kirby et al., 2006), however as adult zebrafish are much bigger and, more importantly, not transparent, this method may only have limited potential in the generation of an adult zebrafish demyelination model.

Transgenic conditional cell ablation

Various methods are available for the generation of a transgenic model permitting an inducible ablation of specific cells of interest. As the activity of a particular gene can be controlled in space and time in almost any tissue, these techniques open up many possibilities to study the influence of single genes in specific cells in animal models of human disease.

The inducible Cre/lox site-specific recombination system is widely used in rodent experimental models and has emerged as a powerful tool for the generation of mutant animals (Hayashi and McMahon, 2002). In this system, the inducible gene inactivation is based on tamoxifen-inducible excision of a gene of interest flanked

by loxP sites in cells expressing a tamoxifen dependent Cre recombinase (Figure 4.1-A). Briefly, the Cre recombinase is fused to a mutated ligand binding domain of the oestrogen receptor (ER), and while CreER normally remains in the cytoplasm, on binding of tamoxifen to the ligand binding domain (ER), the recombinase is relocated into the nucleus. As oestrogen receptors normally act in the nucleus, application of tamoxifen, and its binding to the ER fused to Cre recombinase allows temporal control of its translocation into the nucleus and recombination of the gene of interest. It can then recombine its loxP-flanked DNA substrate containing parts of the gene of interest, leaving the animal with a mutated gene. A variation of this method uses a loxP-flanked stop cassette followed by a gene of interest to selectively switch on this gene. Under normal conditions, transcription would stop at the stop signal and the gene of interest would remain untranscribed, however upon Cre recombinase translocation into the nucleus, excision of the stop cassette would lead to transcription of the gene of interest. To generate an inducible targeted cell ablation in adult zebrafish, this method could be used to create a transgenic line in which cells contained a loxP-flanked stop cassette followed by an apoptotic signal such as caspase signalling, and crossing it with another line that expressed tissue specific CreER. The addition of tamoxifen in animals containing both transgenic constructs would then cause an excision of the stop cassette and the tissue specific promoter could drive the expression of apoptotic signals for specific death of oligodendrocytes (Figure 4.1-B). Apoptosis, also known as programmed cell death, is mediated through caspase (cysteine aspartatic proteases) signalling. Caspases have been assigned a major role in programmed cell death; they are synthesized as inactive procaspases and participate in the cell death cascade once activated (reviewed in Thornberry and Lazebnik, 1998). The caspase cascade is executed via the initiating caspases (2,8,9 and 10) and the effector caspases (3,6 and 7). Overexpression or activation of caspases in this signalling cascade is associated with increased cell death (Druskovic et al., 2006; Yang et al., 2007), and this can be used to specifically target cells of interest (Chelur and Chalfie, 2007; Mallet et al., 2002).

Similarly, a Cre inducible diphtheria toxin receptor can mediate cell lineage specific cell death (Buch et al., 2005). This system could be successfully employed in the fish by generating a transgenic line with a loxP-flanked stop cassette prohibiting diphtheria toxin receptor (DTR) expression, which is removed when crossed with a fish line expressing Cre in the specific tissue of interest. Expression of the diphtheria toxin receptor sensitises the tissue to cell death induced by application of diphtheria toxin (Figure 4.1-C). In addition, Cre could also be expressed under the heatshock promoter, which would permit temporal control of Cre expression, as a heatshock promoter is only activated upon incubation of the animal carrying the construct at higher temperature. This would allow the generation of a zebrafish line which could be raised in normal conditions and only when Cre expression is desired, the fish could be incubated at higher temperatures. These inducible systems, where Cre recombinase leads to expression of the diphtheria toxin, are already used in zebrafish with success in ablating cardiomyocytes (Wang et al., 2011b), however transgenic zebrafish lines allowing central nervous system specific cell death would have to be generated.

A relatively new method for transgenic conditional cell ablation that is widely and successfully used in zebrafish is the nitroreductase/metronidazole (NTR/MTZ) system (Curado et al., 2008). Metronidazole is an antibiotic medication normally used to treat infections with anaerobic organisms. When it is taken up by bacteria, it is non-enzymatically reduced and deactivates critical bacterial enzymes. Metronidazole metabolites can also be taken up into bacterial DNA to form unstable molecules and harm bacterial survival. In transgenic models using this system for conditional cell ablation, a tissue specific promoter drives NTR, a bacterial enzyme, which converts the compound MTZ from an inactive metabolite to its active cytotoxic form. As a result, the application of MTZ leads to toxic ablation of specific cells containing the enzyme NTR (Figure 4.1-D). This method shows reproducible results, and as it is only dependent on the addition of MTZ, it is also reversible. A clear advantage of this system is that metronidazole can be applied locally or globally, as such resulting in different extents of cell ablation. Recent research shows that this system can be used successfully in larval *Xenopus*

laevis to specifically ablate oligodendroglial cells and to investigate the events of demyelination and myelin repair (Kaya et al., 2012), however this is not known for zebrafish. Moreover, there is yet no evidence that this transgenic inducible system is retained into adulthood in any species and could be useful for the generation of an adult demyelination model.

As I aimed to investigate whether the previously described *tg(Claudin k:Gal4,UAS:mGFP)* transgenic zebrafish line, *Tg(claudin k:GAL4,UAS:GFP)* could be used to generate offspring in which cells of the oligodendrocyte lineage could be specifically ablated, I chose to trial this system.

Experimental autoimmune encephalomyelitis (EAE)

EAE is commonly used to study de- and remyelination in rodent experimental models as described in chapter 1. Although it is useful for investigation of inflammation due to its immunological component in disease pathogenesis, the de- and remyelination in this model is ongoing as the disease pattern is often relapsing or chronic, making it more complicated to separate the remyelination process for closer examination. Limitations also include associated axonal damage and the many different disease courses described in murine EAE (Kipp et al., 2012). While it has been described that immunisation of zebrafish with central nervous system homogenate was able to trigger inflammation of the CNS (Quintana et al., 2010), it is unclear how the immune system of fish and mammals compares and whether this method would lead to demyelinating lesions in the fish brain.

To study de- and remyelination in adult zebrafish, I therefore chose to generate a zebrafish line for transgenic conditional cell ablation utilising the NTR/MTZ technique. In addition I sought to determine whether LPC can be used to generate focal demyelinating lesion in the adult zebrafish optic nerve, as this is a part of the central nervous system which is very easily accessible for operative procedures.

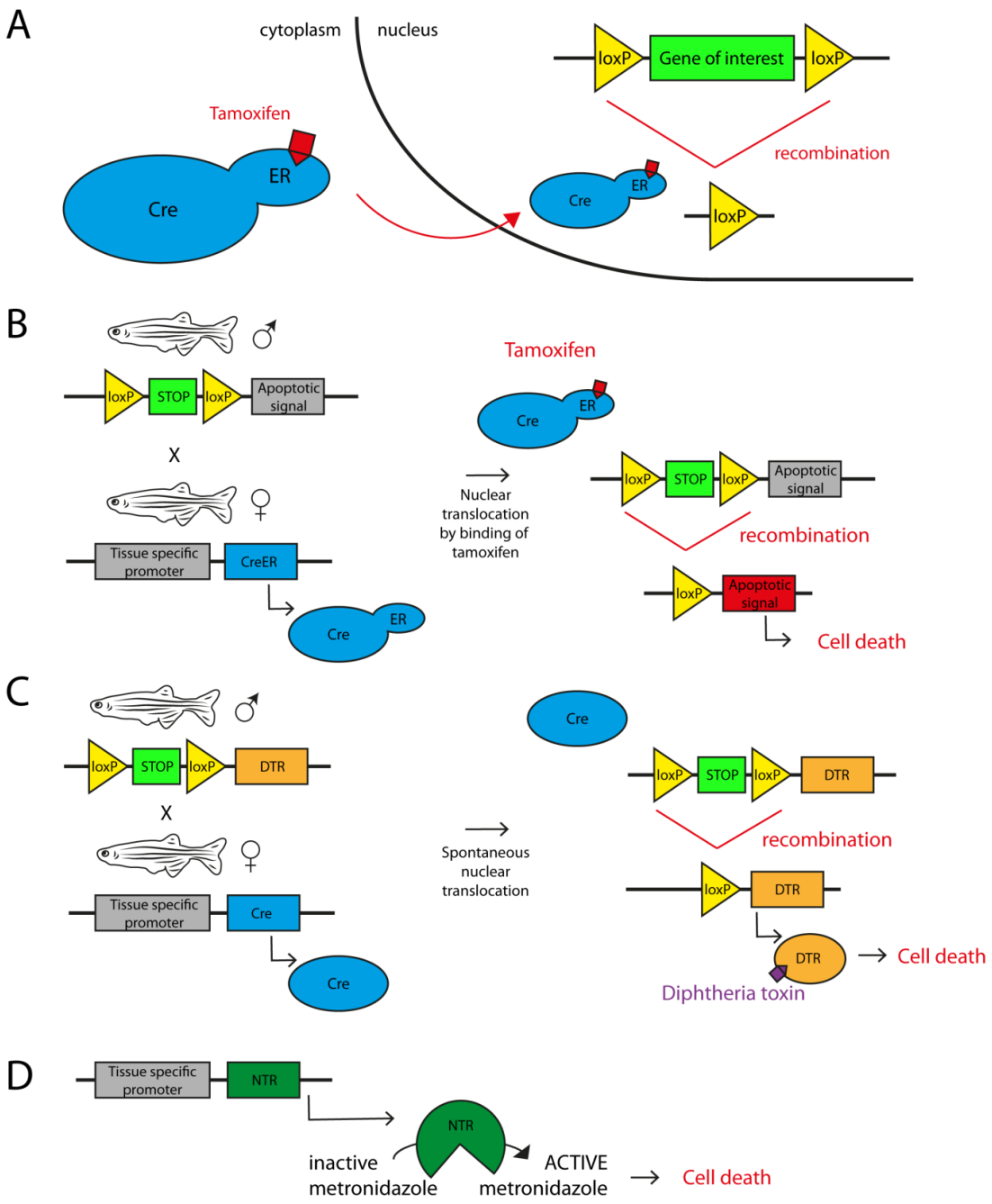

Figure 4.1: Outline of methods available to generate tools for transgenic conditional cell ablation. (A) Cre/lox-site specific recombination controlled by the steroid tamoxifen. When tamoxifen binds to the ligand binding domain of the oestrogen receptor (ER) fused to the Cre, CreER translocates to the nucleus and recombines loxP sites within a gene of interest. (B) In fish this system could be used to drive an apoptotic signal under a tissue specific promoter after recombination of the loxP-flanked stop-cassette. (C) Similarly, Cre could excise a stop-cassette under a tissue specific promoter to drive the expression of diphtheria toxin receptor, rendering specific cells sensitive to the toxin. (D) In the nitroreductase (NTR)/metronidazole(MTZ) cell ablation method, NTR is expressed under a tissue specific promoter, allowing to convert inactive MTZ to its active form and resulting in toxic death of particular cells of interest.

4.2 Results

Transgenic conditional cell ablation in larval zebrafish using the nitroreductase/ metronidazole method

A transgenic line making use of the NTR/MTZ system can be generated either by injecting a direct construct into zebrafish embryos, for example where a tissue specific promoter drives NTR and a fluorescently tagged protein directly, or by crossing two transgenic lines containing the driver and responder constructs. To explore the usefulness of my previously characterised driver line, I chose to use the zebrafish line described in chapter 2, in which the glial cell promoter *claudin k* drives the expression of GFP via the Gal4-UAS system, *Tg(claudin k:GAL4,UAS:GFP)*. The responder line expressing NTR linked to a mCherry fluorescent protein under the control of UAS, *Tg(UAS:nfsb-mCherry)* was generously provided by Dr Hitoshi Okamoto, Japan and has been described previously (Davison et al., 2007). After crossing these lines, some of the offspring contained all constructs, allowing *claudin k* to drive the expression of Gal4, which should bind to the UAS of both other constructs, one driving expression of GFP and the other NTR and mCherry *Tg(claudin k:GAL4,UAS:GFP) x Tg(UAS:nfsb-mCherry)* (Figure 4.2-A). Double transgenic offspring showed glial cells expressing GFP and mCherry (Figure 4.2-B). However, as noted in the previous chapter, although the Gal4/UAS system was designed to enhance expression particularly in the presence of a weak promoter, multiple identical repetitive UAS sequences lead to silencing of the transgene through methylation (Akitake et al., 2011). As a result, the offspring I generated in the facility from the driver and responder lines described showed very variegated GFP and mCherry expression, where some glial cells expressed either GFP or mCherry, and others expressed both or neither. This implied some difficulties in generating a reliable tool for oligodendroglial cell ablation in zebrafish, and will be discussed further in the discussion section of this chapter. To investigate whether glial cells in this transgenic line could be specifically ablated, I treated zebrafish larvae with MTZ for 48 hours from 4-6 dpf and performed live imaging of the same fish at various time points (Figure 4.2-C). The treatment onset at 4 dpf was chosen

based on the observation that this was the earliest time point at which a sufficient number of cells were mCherry-positive in the spinal cord, suggesting that these would be sensitive to metronidazole; the treatment length of 48 hours was chosen based on the complete disappearance of mCherry transgene, which was still present in many spinal cord cells after only 24 hours of MTZ treatment (checked visually under the fluorescent stereomicroscope). I observed that at 4 dpf, transgenic zebrafish larvae had an average of 12.8 ± 4.6 (mean ± SD) mCherry-positive cells over 6 segments, which significantly dropped to 0.3 ± 0.8 cells (mean ± SD, $p<0.001$, n=6, Kruskal Wallis test, Dunn's post-test) after 48 hours of treatment with MTZ and partially recovered until 12 dpf (the latest time point analysed due to poor survival, $p<0.05$, n=6, Kruskal Wallis test, Dunn's post-test, Figure 4.2-D). This means that the system is able to recover once MTZ is withdrawn, however, the question whether the recovery was a response to the pathological insult, or rather normal development (albeit delayed) remained.

To investigate this further, I treated another clutch of transgenic offspring with MTZ and compared the number of mCherry-positive cells in the spinal cord before and after treatment to the number of cells in siblings of the same clutch, which had not received MTZ treatment (Figure 4.2-E,G). This clutch showed fewer mCherry-positive cells in the spinal cord before treatment. As before, the treated group showed a marked decrease of mCherry-positive cells in the spinal cord after 48 hours of MTZ treatment (3.9 ± 2.4 cells to 0.4 ± 0.5 cells, mean ± SD), with partial recovery to 2.1 ± 1.4 cells seen at the 10 dpf time point. The number of cells in 6 segments of the spinal cord in the control group increased from 3.8 ± 2.3 at 4 dpf to 5.9 ± 2.0 mCherry+ cells (mean ± SD) at 10 dpf and indicates normal development. These finding indicate that while there is some recovery and generation of new mCherry+ cells in the treated group, these do not reach control levels within 4 days of treatment cessation. The rate of mCherry+ oligodendrocyte addition between 6 dpf and 10 dpf was not different in the MTZ-treated group compared to the control group and suggesting a normal developmental generation, which is not accelerated due to previous ablation. To determine whether the cell number in the treated group catches up to normal levels again, I attempted live imaging at longer time

points after treatment, however this was severely hindered by the poor survival of the zebrafish larvae. Whether this was due to the treatment or to the conditions they were kept in during the analysis is unclear.

Throughout my analysis, I noticed that mCherry-positive cells in the PNS, specifically the posterior lateral line nerve (PLLN), were also reduced after treatment, however as I was aiming to ablate oligodendrocytes in the CNS, I did not investigate this any further. To determine whether the ablation of mCherry-positive cells would lead to a deficit in myelination, I measured Claudin k pixel intensity before and after MTZ treatment (Figure 4.2-F), and found that there was no difference in the Claudin k pixel intensity in the spinal cord after MTZ treatment, indicating that probably not sufficient numbers of oligodendroglial cells were ablated to cause a detectable myelin deficiency.

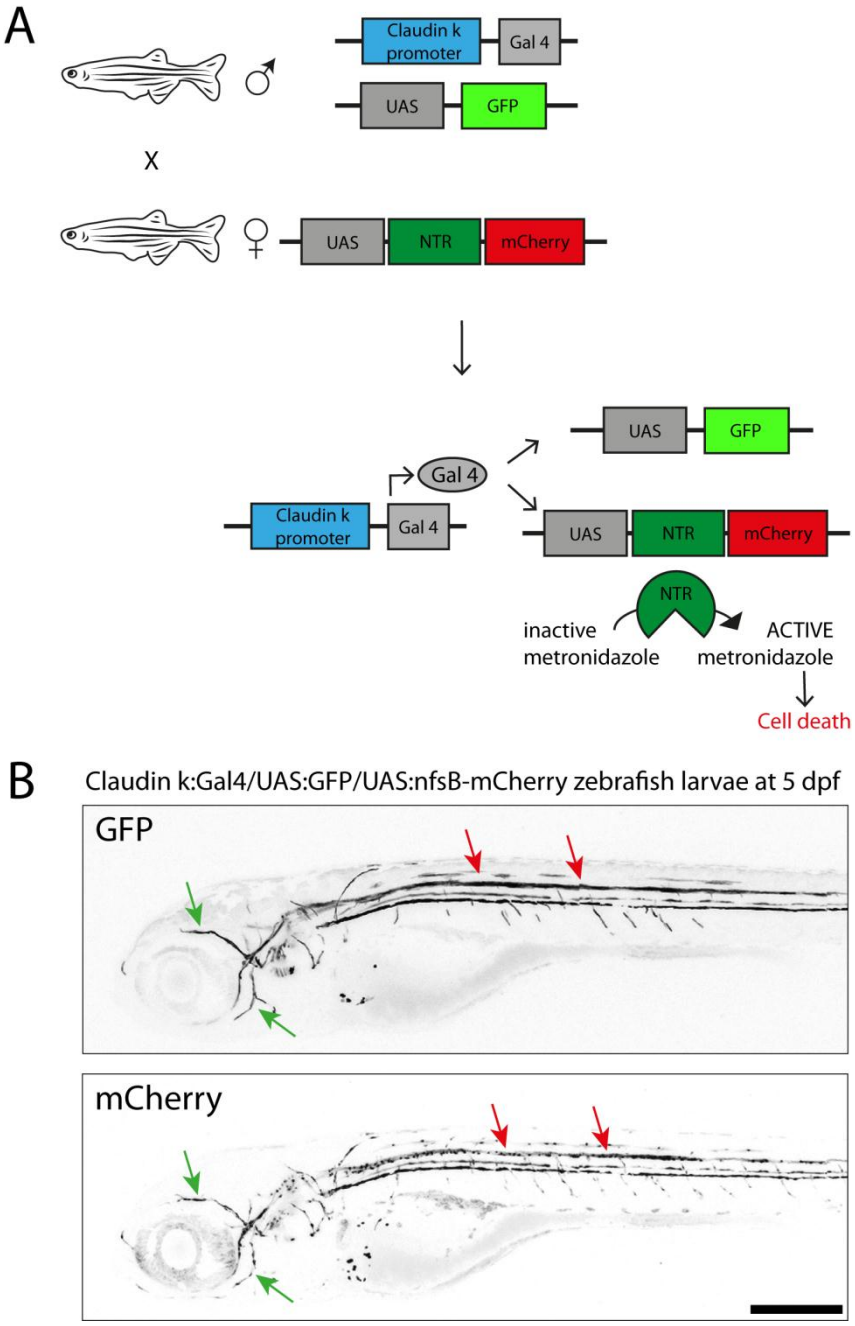

Figure 4.2 (A-B): Investigating the efficiency of the nitroreductase/metronidazole (NTR/MTZ) system in zebrafish larvae. (A) Schematic of driver and responder zebrafish lines used to generate transgenic offspring in which targeted cell ablation is inducible by treatment with MTZ. (B) Live imaging of transgenic offspring from lateral show GFP and mCherry expression in cells of the central (red arrows) and peripheral (green arrows) nervous system. Scale bars: B = 0.5 mm.

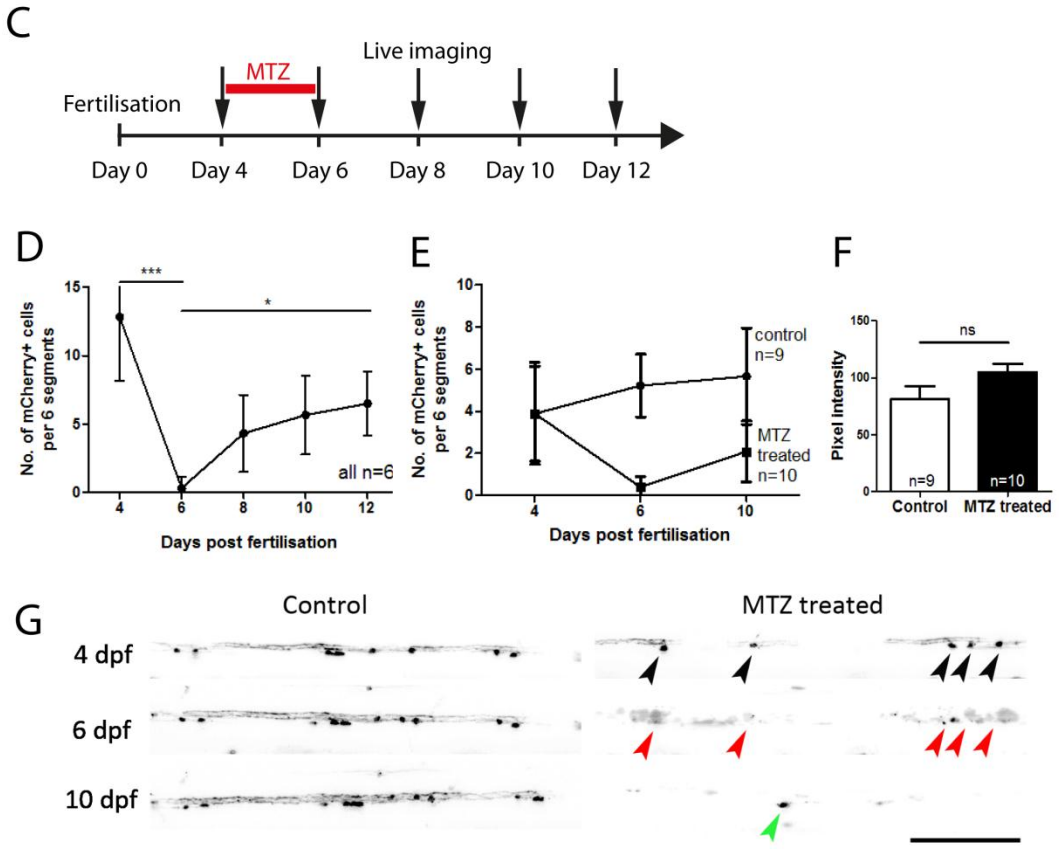

Figure 4.2 (C-G): Investigating the efficiency of the nitroreductase/metronidazole (NTR/MTZ) system in zebrafish larvae. (C) Schematic of MTZ treatment and live imaging time points in transgenic larvae. (D, E) Cell counts of mCherry-positive cells over 6 spinal cord segments in live imaged transgenic zebrafish larvae from different clutches are shown. (D) mCherry-positive cells are notably decreased after 48 hours of MTZ treatment and recover following the treatment cessation ($p<0.05$, n=6, Kruskal Wallis test, Dunn's post-test). (E) Live imaging of transgenic zebrafish larvae with and without MTZ treatment shows that some mCherry-positive cells are generated after cessation of MTZ treatment, however the amount of cells recovered do not reach control levels by 10 dpf. (F) Claudin k pixel intensity measurements in the spinal cord of MTZ treated transgenic ZF larvae shows no difference to control indicating that not sufficient cells were ablated to cause myelin deficiency. (G) Live imaging of one control and one MTZ treated fish at time points shows mCherry-positive cells in the spinal cord before MTZ treatment (black arrowheads), disappearance of these cells after 48 hours of MTZ treatment (red arrowheads) and the appearance of new mCherry expressing cells at 10 dpf (green arrowhead). Error bars represent mean ± SD. Scale bars: G = 100 µm.

Transgenic conditional cell ablation in adult zebrafish using the nitroreductase/ metronidazole method

To determine whether this system could be used in adult zebrafish to specifically ablate cells of oligodendroglial lineage, I generated NTR-transgenic zebrafish offspring as before, sorted them for the strongest mCherry expression and raised them to adulthood. At this time, I treated them with MTZ until I could see less mCherry-positive transgene in superficial nerves of anaesthetised adult zebrafish under a fluorescent stereomicroscope. I observed that after 1 week of treatment, the mCherry-positive transgene was largely absent in the superficial skin nerves (data not shown). In addition, the MTZ treated NTR transgene-positive group showed less active swimming behaviour compared to the non-treated control group carrying the NTR transgene, and this was confirmed with behavioural testing, which showed a decreased mean velocity and total distance moved (Figure 4.3-A,B). However, the NTR transgene-negative group, which also received MTZ treatment showed similar changes in swimming behaviour and hence, I concluded that this was probably a toxic effect of MTZ.

Upon histological analysis of the brain of the NTR transgene-positive adult zebrafish, which had not been treated with MTZ, I was surprised to find no mCherry expression in the brain at all (Figure 4.3-C). However, sections of the posterior lateral line nerve (PLLN) of the same fish suggested that the NTR transgene was still expressed in the PNS, as I observed many mCherry+ cells in cross sections of the PLLN (Figure 4.3-D). In fish, which had been treated with MTZ for 1 week, mCherry immunofluorescence in the PLLN was reduced and appeared very clumpy (Figure 4.3-D). Thus, the system appears to be working in the PNS, not the CNS; possible reasons for this include an inactive promoter in adulthood or transgene silencing.

These findings highlight the difficulties with variegated transgenic expression and potential silencing in specific tissues. As my aim was to create an experimental model to explore myelin injury in the central nervous system of adult zebrafish, this genetic cell ablation method proved insufficient for my purposes and I focussed on using focal application of LPC.

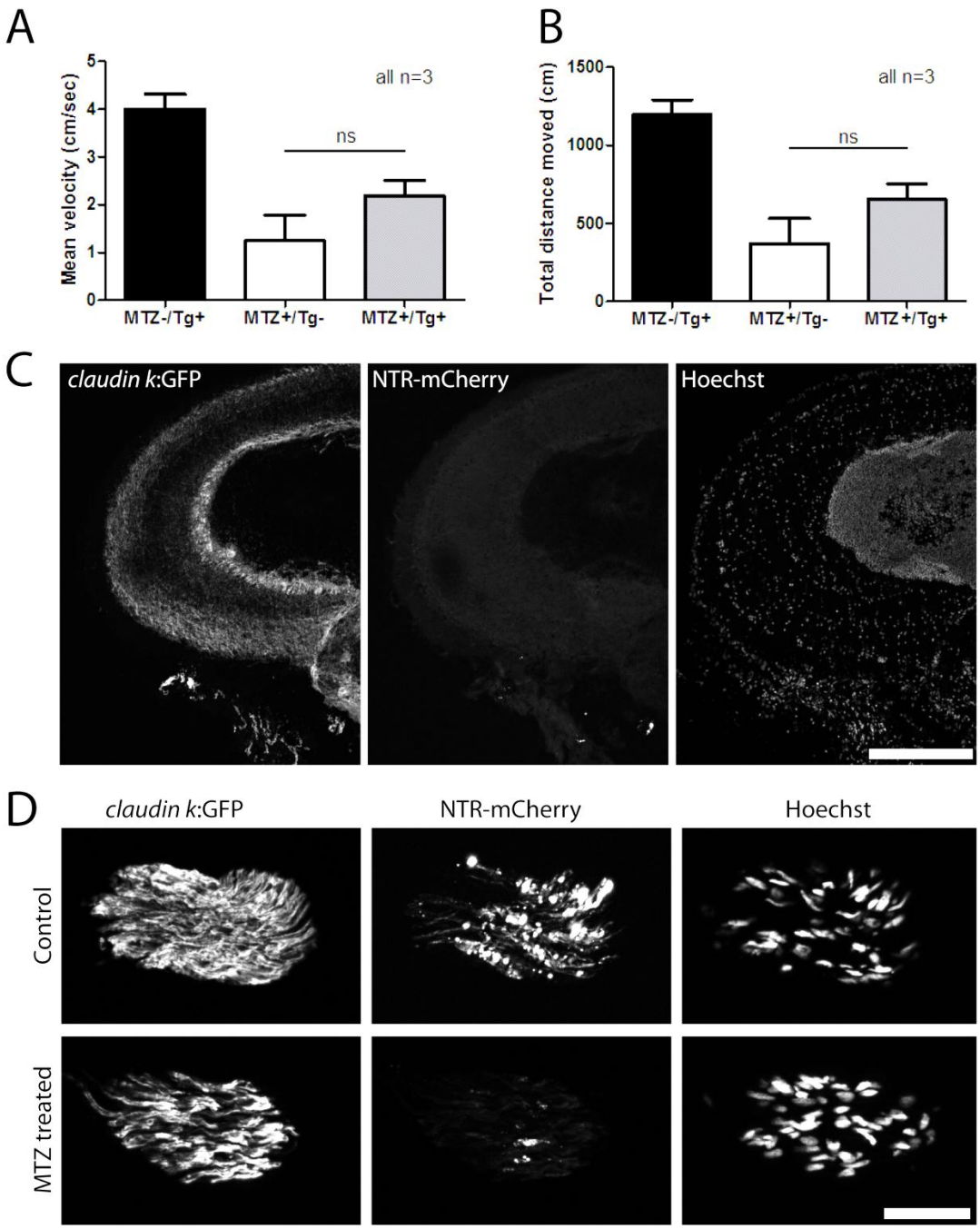

Figure 4.3: Targeted cell ablation in adult zebrafish using the NTR/MTZ technique. (A,B) Adult zebrafish were treated with MTZ for 1 week. Behavioural analysis shows a difference between the control group and the MTZ treated group in the mean velocity and total distance moved. A group treated with MTZ but not transgenic for NTR showed no difference to the MTZ treated group containing the transgene ($p>0.05$, n=3, Mann Whitney-U test) indicating that this was a toxic effect of MTZ. (C) Immunohistochemical analysis of vibratome cross sections of adult zebrafish brain show that NTR-mCherry is not expressed. (D) Cryostat cross sections of adult zebrafish PLLN indicate that NTR-mCherry is expressed in the peripheral nervous system, and is reduced after 1 week of MTZ treatment. Error bars represent mean ± SEM. Scale bar: C = 200 µm, D = 50 µm.

Toxin-induced demyelinating lesions by LPC injection

As genetic targeted cell ablation in the central nervous system of adult zebrafish was insufficient with the transgenic line I had generated, I chose a different method to induce demyelinating lesions. Lysophosphatidylcholine (LPC) is a detergent-like substance, which is used widely in rodent models to induce demyelinating lesions, usually administered by injection into the corpus callosum or other strongly myelinated tracts within the brain or spinal cord (Foster et al., 1980). In the zebrafish optic nerve approximately 95% of the fibres are myelinated. Hence I injected the optic nerve of adult zebrafish with 2µl of 1% LPC, the standard concentration used in rodents, and within 8 days I observed a much reduced immunohistochemical myelin staining in longitudinal sections of the lesioned optic nerve, while the axonal marker LINC was present across the lesion site (Figure 4.4-A,B). At this time point 4C4+ microglia were also increased in the lesioned optic nerve (Figure 4.4-C).

To investigate the time course of myelin injury and repair using this method of LPC injections, I performed multiple immunohistochemical analyses of optic nerve cross sections at various time points following the LPC injection (Figure 4.5-A). To quantify myelin and axons, I measured pixel intensity of Claudin k and LINC immunofluorescence and calculated a ratio of lesioned to unlesioned optic nerve, hence the closer the ratio was to 1 the more similar the signal was to that in unlesioned optic nerve. This method was chosen to account for any differences of the immunohistochemical staining between the different animals.

I found that Claudin k immunoreactivity was significantly reduced at 8 dpl (compared to 2dpl and 28dpl, $p<0.05$, n=3-6, Kruskal Wallis test, Dunn's post-test) and had returned to control levels within 4 weeks, while the axonal stain LINC remained constant throughout the time course (Figure 4.5-B,C). Counts of 4C4-positive cells in the optic nerve, representative of microglia, showed a significant increase at early time points ($p<0.05$, n=3, Kruskal Wallis test, Dunn's post-test), which also returned to control levels within 4 weeks (Figure 4.5-D). To confirm that this increase of microglia number was an effect of the LPC rather than the injection

process, I compared the numbers of 4C4-positive cells in the optic nerve after LPC injection to PBS injection and unlesioned control (Figure 4.5-E,F). The number of 4C4-positive cells at 8 days following the lesion was significantly larger in the optic nerve of LPC injected animals than in those injected with PBS ($p<0.05$, $n=3$, Mann Whitney U-test), hence this increase in cell number is probably due to the direct effect of LPC rather than the injection. However, the number of 4C4-positive cells in PBS injected animals was also higher than compared to unlesioned control optic nerves, indicating that the injection process is also associated with an immune response ($p<0.05$, $n=3$, Mann Whitney U-test).

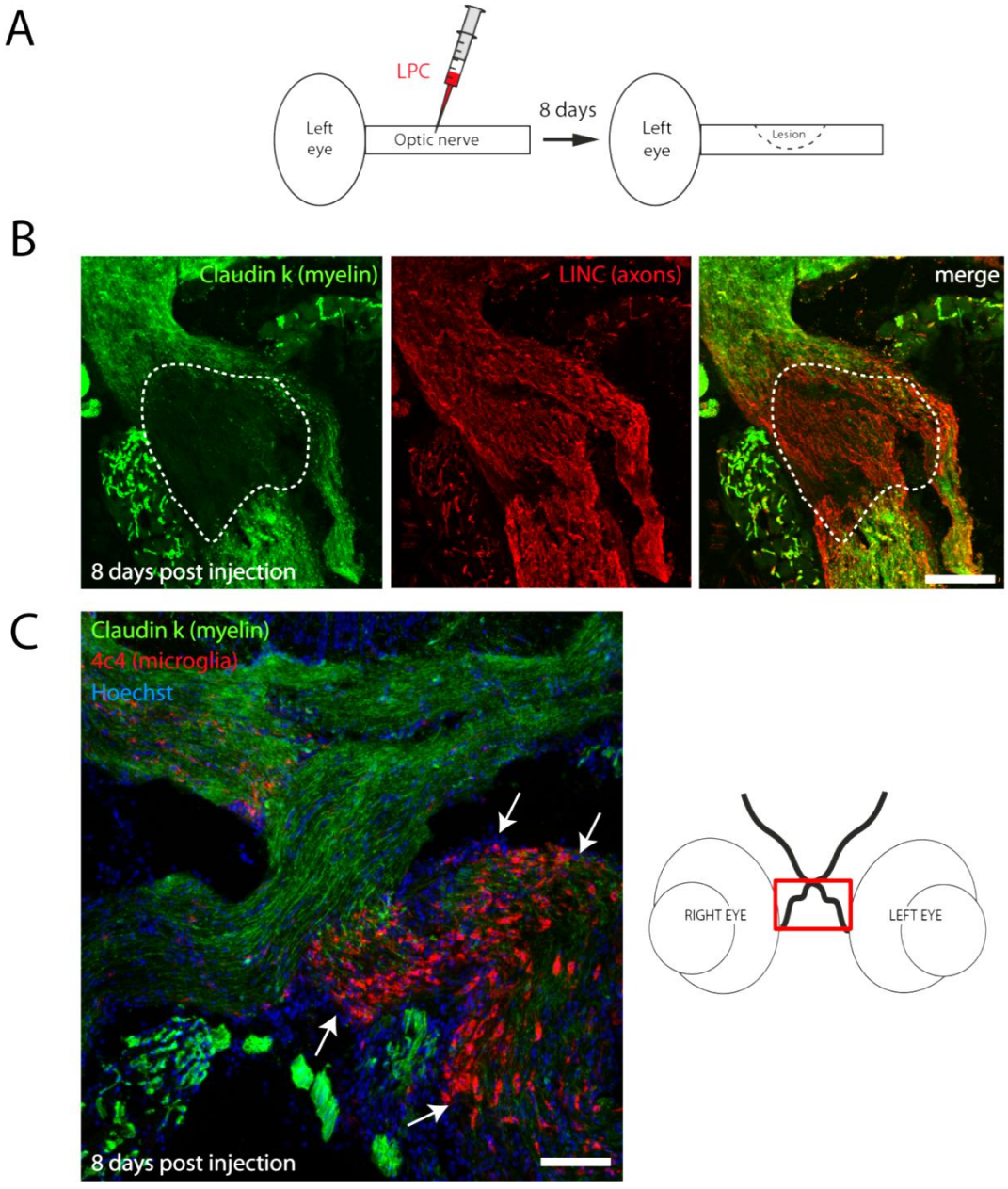

Figure 4.4: LPC injection into adult zebrafish optic nerve. (A) LPC was injected into the optic nerve as shown on this schematic. (B) Immunohistochemical analysis of longitudinal optic nerve sections at 8 dpl shows reduced Claudin k immunoreactivity while the axonal stain LINC is present across the lesion site. (C) Immunohistochemical analysis of a section through the optic chiasm at 8 dpl shows an increase in 4C4-positive microglia in the lesioned optic nerve (arrows). Schematic shows the region where the cross section was taken. Scale bars: B,C = 100 µm.

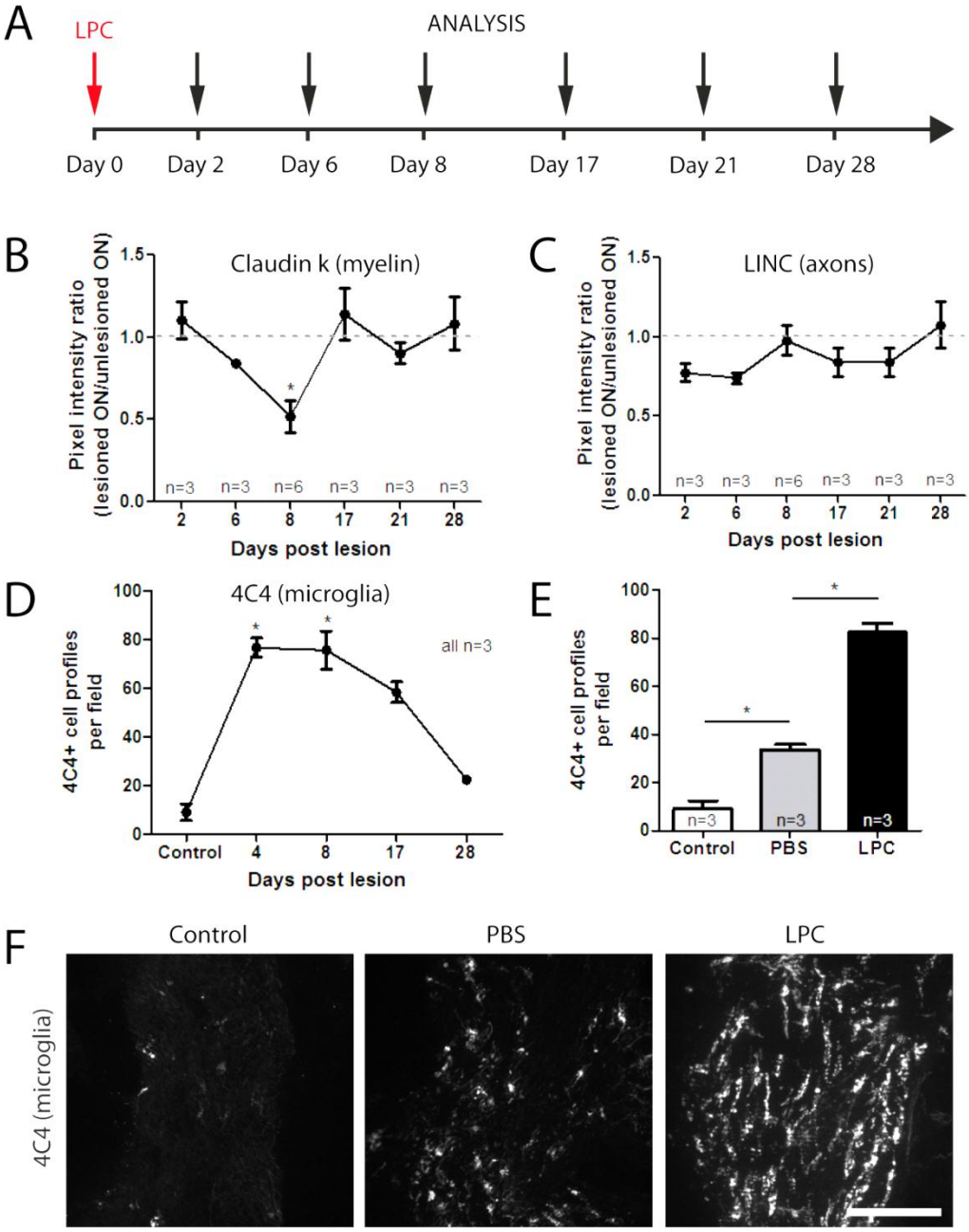

Figure 4.5: Analysis of regeneration following LPC injection into adult zebrafish optic nerve. (A) Schematic of time course performed to investigate regeneration is shown. (B) Claudin k immunofluorescence is maximally decreased at 8 dpl ($p<0.05$, n=3-6, Kruskal Wallis test, Dunn's post-test). (C) LINC immunofluorescence does not show differences throughout the time course. (D) 4C4-positive cells are significantly increased at early time points after the lesion and return to normal levels within 4 weeks ($p<0.001$, n=3, Kruskal Wallis test, Dunn's post-test). (E) Numbers of 4C4-positive cells in longitudinal sections of the optic nerve were significantly higher 8 days after LPC injection compared to PBS injected controls ($p<0.05$, n=3, Mann Whitney U-test). Numbers of 4C4-positive cells in PBS injected optic nerves are also higher than unlesioned controls indicating that the injection is associated with an immune response as well ($p<0.05$, n=3, Mann Whitney U-test). (F) Images of optic nerve cross sections stained for 4C4+ cells are representative for data shown in E. Error bars represent mean ± SEM. Scale bar: F = 100 µm.

To further investigate myelination of optic nerve fibres and myelin regeneration, I performed electron microscopy studies. Analysis of optic nerve cross sections showed many unmyelinated axons at 8 dpl compared to contralateral unlesioned optic nerves, but after 28 dpl most were ensheathed by myelin again (Figure 4.6-A,B,C). More specifically, in the unlesioned control optic nerve 93% ± 2.3% (mean ± SEM) of axons were myelinated and this was reduced significantly to 17% ± 11.9% at 8 dpl (mean ± SEM, $p<0.05$, n=3, Kruskal Wallis test, Dunn's post-test) and not different to unlesioned controls at 28 dpl with 84% ± 9.6% myelinated axons (mean ± SEM, Figure 4.6-D). In the lesion site at 8 dpl, I also observed myelin debris around bare axons and many macrophages/microglia with ingested myelin droplets (Figure 4.6-E,F). For further examination of myelin regeneration after LPC injection, I measured G-ratios in the unlesioned control, lesioned and regenerated optic nerve and found that while the average G-ratio was significantly increased at 8 dpl due to many non-myelinated fibres ($p<0.01$, n=3, Kruskal Wallis test, Dunn's post-test), the regenerated axons showed no difference to unlesioned controls (Figure 4.6-G). As it is difficult to determine the location of the lesion site in a fully regenerated optic nerve I performed serial sections every 100µm for the first 400µm from the distal side (near chiasm) of each regenerated optic nerve (Location A-D). By immunohistochemistry for Claudin k, the lesion could always be found within this distance from the chiasm and ensured that the lesion site was also sectioned and analysed in electron microscopy. By electron microscopic analysis, the average G-ratio was not different at any of the optic nerve locations analysed at 28 dpl, suggesting full myelin regeneration (Figure 4.6-G). Correlations of G-ratio and axon diameter show similar populations at 28 dpl and in unlesioned control, while most axons at 8 dpl have larger G-ratios indicating thinner myelin (Figure 4.6-H-M).

These results suggest that zebrafish optic nerve axons are able to fully regenerate their myelin sheath after LPC injection. However, on closer evaluation of the images at 8 dpl, it seemed that there were many more small diameter axons, which appeared closely clustered together and reminiscent of regenerated fibres or axon sprouts. I therefore wondered whether these fibres had possibly been damaged during the injection process and not primarily demyelinated, and so also not

remyelinated but just myelinated for the first time, similarly to the optic nerve crush situation. Previous studies in fish show that severed axons in the optic nerve are capable of re-growing and re-innervating the optic tectum (Becker et al., 2000). These regenerated fibres are known to be small calibre axons, which run in bundles of close axonal density (Nona, 1994). A frequency distribution of axonal diameter was significantly different in lesioned optic nerves compared to unlesioned controls ($p<0.05$, Kolmogorov-Smirnov test), with more small calibre axons (0.2-0.29 µm) present in the LPC-injected optic nerves ($p<0.05$, n=3, Mann Whitney U-test, Figure 4.7-B). This might indicate that some of the axons were indeed damaged and the unmyelinated, small calibre axons seen may be sprouts. The previous finding of microglia activation upon PBS injection supports the hypothesis of mechanical axon damage.

To further investigate whether axonal damage was induced during the injection process and to which extent, I performed neuronal tracer experiments. For this I injected biocytin tracer into the optic nerve, which would only be taken up and transported along the optic pathway by damaged axons, and I assessed labelling of the optic tectum after 4 hours (Figure 4.7-C). In zebrafish, like in other fish, almost all optic nerve fibres cross the midline at the chiasm. This is different to mammals where 50% of fibres cross the midline to the contralateral side and 50% remain ipsilateral. I could therefore measure the uptake of the biocytin tracer in the contralateral tectum in zebrafish after tracer application and make a quantitative statement about the percentage of damaged optic nerve fibres. Compared to the positive control in which all axons had been severed and traced, and as a result the entire optic tectum of the contralateral side showed tracer uptake, there was only partial labelling in the tracer injected animals (Figure 4.7-D). Measuring the length of the tectum and the percentage labelled by the neuronal tracer permitted quantification of these findings. In the injected animals, approximately one-third of the tectum was labelled with tracer, indicating that the process of injecting into the optic nerve damaged approximately one-third of the axons (Figure 4.7-E). As the injection of LPC into the zebrafish optic nerve led to axonal damage, this was not the optimal model for demyelination.

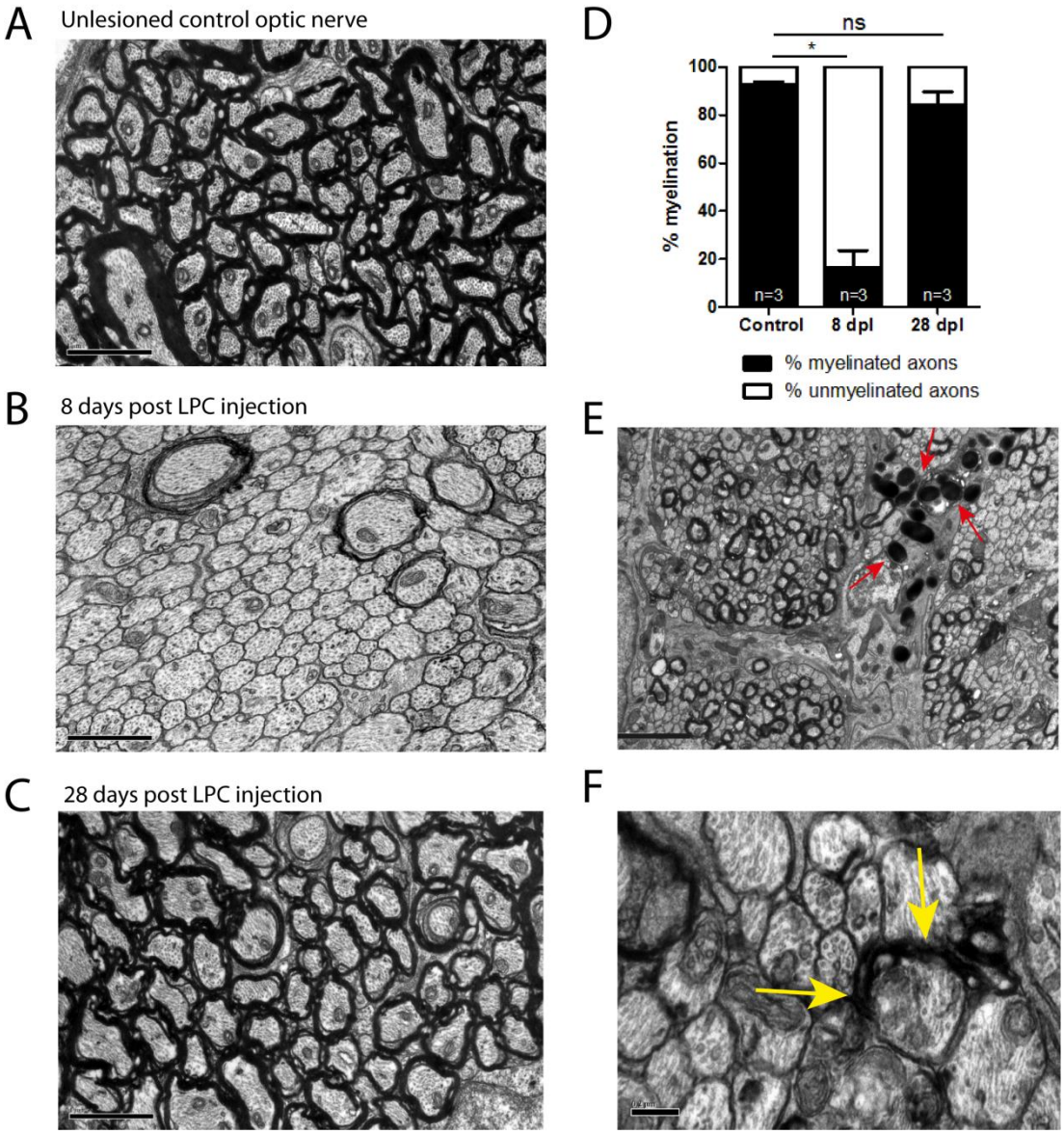

Figure 4.6 (A-F): Electron microscopy studies of optic nerve cross sections before and after LPC injection. (A-C) Electron microscopy analysis of optic nerve cross sections shows myelinated fibres in unlesioned nerves (A), many non-myelinated fibres at 8 dpl (B), and fibres with regenerated myelin at 28 dpl (C). (D) Quantification of myelinated and non-myelinated fibres show a significant decrease in myelinated fibres at 8 dpl and regeneration within 4 weeks ($p<0.05$ n=3, Kruskal Wallis test, Dunn's post-test). (E-F) Areas of demyelination at 8 dpl presented with microglia/macrophages with ingested myelin droplets (red arrows) and myelin debris around axons (yellow arrows). Scale bars: A,B,C = 1 µm; E = 2 µm, F = 0.2 µm.

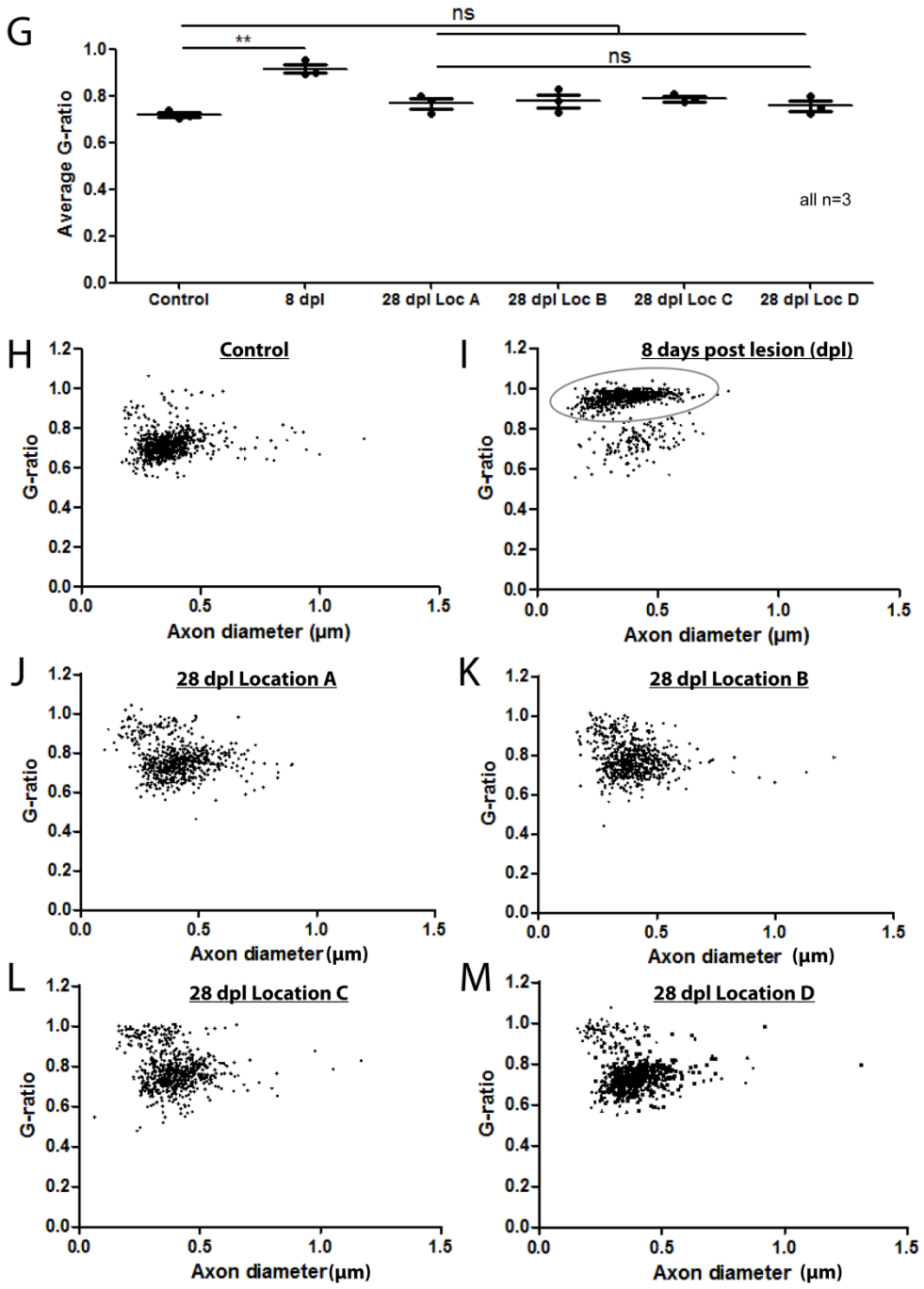

Figure 4.6 (G-M): Electron microscopy studies of optic nerve cross sections before and after LPC injection. (G) Quantification of average G-ratios showed significant differences at 8 dpl compared to unlesioned controls ($p<0.01$, n=3, Kruskal Wallis test, Dunn's post-test). The optic nerve at 28 dpl was cut in 4 different locations each 100 µm apart to ensure the lesion site was sectioned. The average G-ratio in all locations at 28 dpl was not different to unlesioned controls, suggesting full myelin regeneration. Error bars represent mean ± SEM. (H-M) Correlations of G-ratio and axon diameter show similar populations at 28 dpl (all locations) and in unlesioned control, while most axons at 8 dpl have a much larger G-ratio indicating thinner myelin (circle).

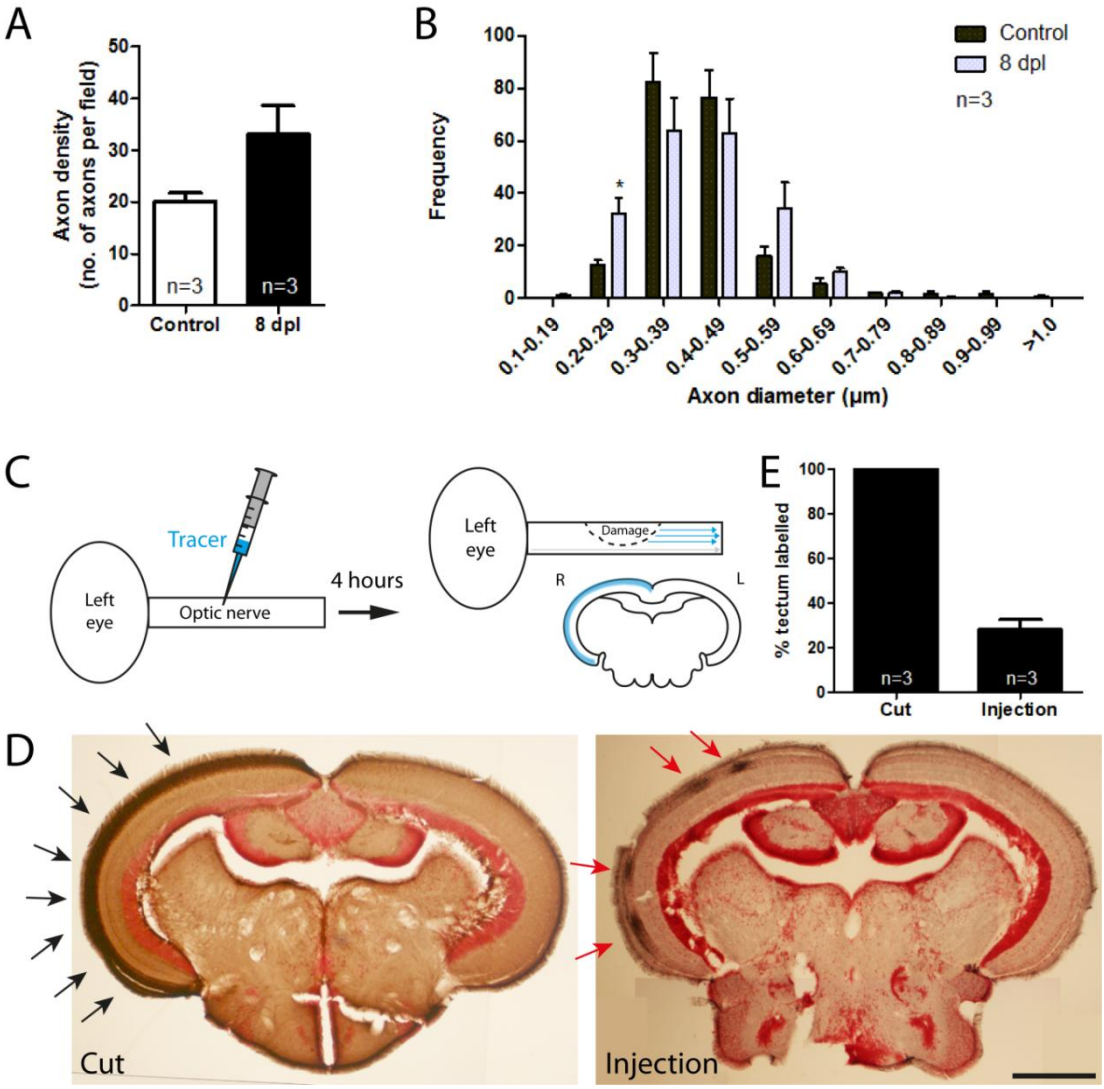

Figure 4.7: Investigation of axonal damage after LPC injection into adult zebrafish optic nerve. (A) **A**xon density in lesioned optic nerves higher than unlesioned controls. (B) A frequency distribution analysis of axon diameter in lesioned optic nerves is significantly different to that found in control optic nerves ($p<0.05$, Kolmogorov-Smirnov test). Moreover, it suggests more small calibre axons in the lesioned optic nerve (0.2-0.29 µm diameter) compared to non-lesioned controls ($p<0.05$, n=3, Mann Whitney U test). (C) The schematic shows how tracer experiments were performed: Tracer was injected into the optic nerve and assessed by positive labelling of the tectum. (D) Vibratome cross sections of an adult zebrafish brain after neuronal tracing are shown. The control group in which all axons were severed and traced shows full tectal labelling (black arrows), while the tracer injected group only shows partial labelling (red arrows). Neutral red staining labels neuronal cell bodies. Dorsal is up. (E) Quantification of tracer labelled area in the tectum (length of tectum labelled was measured) suggests that one-third of the axons are damaged during the injection process. Error bars represent mean ± SEM. Scale bar: D = 400 µm.

Toxin-induced demyelinating lesions by local LPC application

As injections of LPC result in partial axonal damage and therefore could be used to investigate pure de- and remyelination, I applied LPC by soaking a medical sponge (Gelfoam®) in the LPC solution and placing it next to the optic nerve in order to prevent manual axonal damage during the application process. I then also performed neuronal tracer experiments to check for axonal damage (Figure 4.8-A). For this, I placed a small piece of gelfoam soaked with different amounts of a 1% LPC solution next to the optic nerve. The axons were traced at 8 days after the placement of the LPC-sponge, which is the time point at which I had observed a reduction in the immunoreactivity of myelin-associated proteins with LPC injection and this method. The nerve was cut proximal to the lesion side and the neuronal tracer biocytin applied to the end of the severed optic nerve to allow for uptake into the axons. Two possible outcomes were considered: in the event of no axonal damage, all axons would transport the tracer to the optic tectum and I would observe full labelling of the contralateral side, whereas in case of damaged axons some would not transport the tracer to the tectum, and only partial labelling would be visible. To control for all axons remaining intact, I soaked the gelfoam with PBS instead of LPC, and as a control for partial axon damage I performed a partial crush of the optic nerve where only a fraction of optic nerve axons were severed.

As expected, full tectal labelling was visible in the control animals treated with the PBS-soaked gelfoam and animals, which received the partial optic nerve crush showed only partial labelling (Figure 4.8-B). To quantify this, I measured pixel darkness in the optic tectum and calculated a ratio to the unlesioned/untraced side to normalise for varying tissue darkness across different sections; hence a ratio of 1.0 would indicate no tracer uptake and equal darkness to the unlesioned/untraced side. After 5 µl LPC on gelfoam the labelling was not different to the PBS treated controls, while 10 µl of LPC on gelfoam resulted in a clear reduction in tectal labelling darkness and was similar to that of the partial crush ($p<0.05$, $n=3$, Kruskal Wallis test, Dunn's post-test, Figure 4.8-B,C). These results indicate that larger amounts of LPC lead to axonal damage and that the optimal amount for

demyelination has to be determined for this model. Hence I analysed longitudinal sections of optic nerves demyelinated with different amounts of LPC. For this, the widest diameter of a Claudin k-negative demyelinated lesion in optic nerve sections was measured and expressed as a percentage of total nerve diameter. I found that 5 µl and 10 µl both demyelinated approximately 70% of the optic nerve, compared to only ~15% demyelination with 1 µl LPC ($p<0.01$, n=3, Kruskal Wallis test, Dunn's post-test, Figure 4.8-D). Pixel intensity measurements of Claudin k and LINC in the lesion area and compared to the non-lesioned contralateral optic nerve representing myelination and axons respectively demonstrated a significant decrease in optic nerve myelination with 5 µl and 10 µl LPC ($p<0.05$, n=3, Kruskal Wallis test, Dunn's post-test) while axonal immunoreactivity only appeared reduced with 10 µl LPC ($p<0.01$, n=3, Kruskal Wallis test, Dunn's post-test, Figure 4.8-E).

Taken together these results show that 1 µl LPC is not sufficient for demyelination, 5 µl LPC leads to demyelination and 10µl LPC causes loss of myelin and axonal damage. Hence I chose to proceed with 5µl LPC on gelfoam to establish the time course for de-and remyelination in the adult zebrafish optic nerve, which are described in chapter 5.

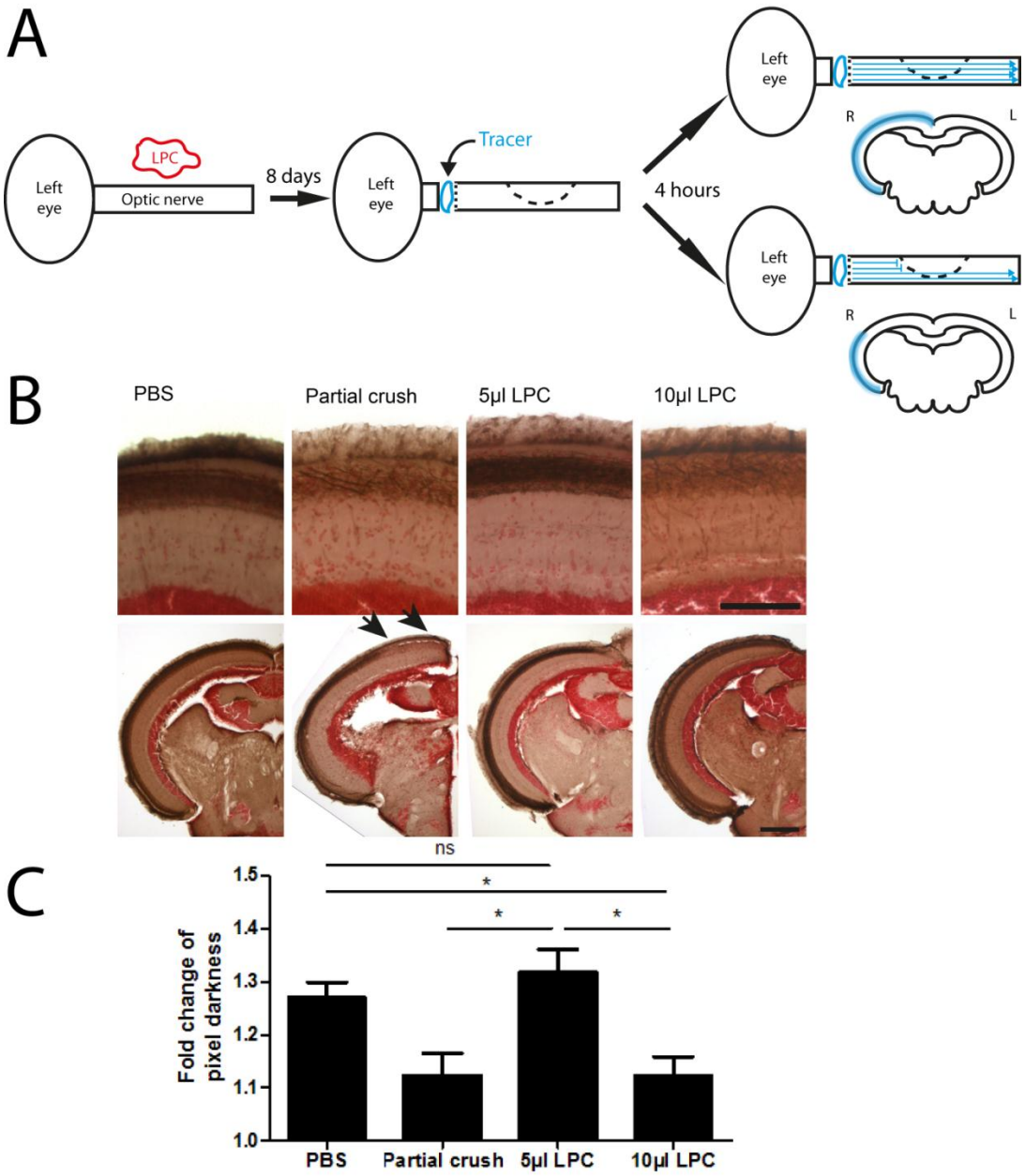

Figure 4.8 (A-C): Assessing neuronal damage after lesioning the optic nerve with LPC on gelfoam. (A) Schematic shows how neuronal tracing experiments were performed: The optic nerve was lesioned with LPC on a gelfoam sponge and after 8 days the nerve was cut proximal to the lesion for the application of a tracer. If no axons were damaged, the tracer would be expected to travel along the optic pathway and label the entire tectum of the contralateral side. In case of axonal damage only part of the axons would take up the tracer and partial tectal labelling would be observed. (B) Vibratome sections of adult zebrafish brains after LPC lesions and neuronal tracer application are shown. Treatment with PBS leads to labelling of the entire optic tectum, whereas a partial crush results in partial labelling (black arrows). Tracer uptake is also much reduced after 10 µl LPC, indicating axonal damage. Dorsal is up. (C) Quantification of tectal labelling was done by calculating a ratio of pixel darkness between lesioned/traced and unlesioned/untraced side. PBS and 5 µl LPC treatment show no difference, while partial crush and 10 µl LPC treatment result in reduced tracer uptake suggesting axonal damage ($p<0.05$, n=3, Kruskal Wallis test, Dunn's post-test). Error bars represent mean ± SEM. Scale bars: B = 100 µm (top row), 200 µm (bottom row).

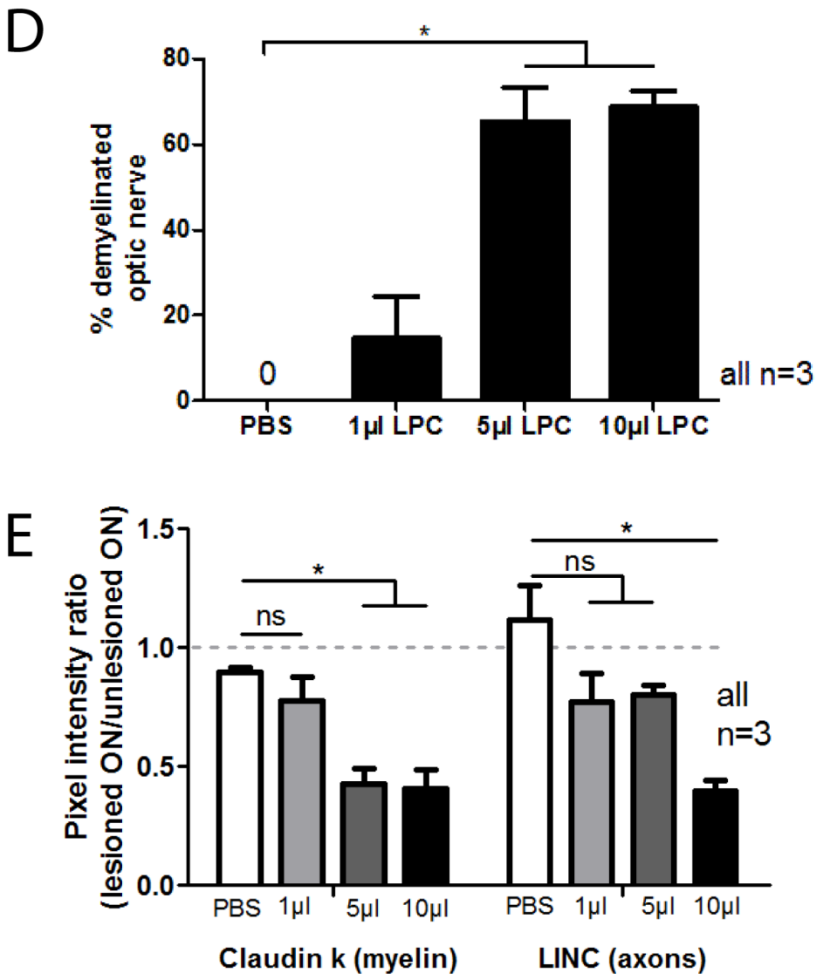

Figure 4.8 (D-E): Assessing neuronal damage after lesioning the optic nerve with LPC on gelfoam. (D) To quantify the amount of demyelination, the widest diameter of a demyelinated optic nerve lesion marked by reduced Claudin k immunoreactivity was measured and expressed as a percentage of total nerve diameter. While 1µl LPC did not cause any notable demyelination, 5 µl and 10 µl demyelinated approximately 70% of the optic nerve fibres ($p<0.05$, n=3, Kruskal Wallis test, Dunn's post-test). (E) Pixel intensity quantification of Claudin k (myelin) and LINC (axons) show reduced Claudin k immunoreactivity with 5 µl and 10 µl treatment and reduced LINC immunoreactivity with 10µl treatment suggesting demyelination with 5 µl LPC and axonal damage with 10 µl LPC ($p<0.05$, n=3, Kruskal Wallis test, Dunn's post-test). Error bars represent mean ± SD (D) and ± SEM (E).

4.3 Discussion

Regeneration of myelin is often insufficient in humans and as zebrafish demonstrate a remarkably high capacity to fully repair various tissues I aimed to generate a model in adult zebrafish that would allow analysis of myelin de- and regeneration without concurrent axon injury.

Various ways to induce demyelinating lesions in experimental animal models have been described in literature, including the use of ethidium bromide (Blakemore, 1982), Cuprizone (Matsushima and Morell, 2001) and inducible transgenic methods (Kaya et al., 2012), however to date none have been established in zebrafish, and therefore I tried and compared different approaches.

Transgenic conditional cell ablation has only been developed in recent years and relies on transgenic expression of a toxin receptor to which a cell toxic substance can bind or an enzyme which can convert inactive substances to active cell toxic metabolites. If these constructs are driven by a promoter specific to the cells of interest, targeted cell death can be induced. The nitroreductase/metronidazole method has already been successfully employed in zebrafish to ablate cells in specific tissues (Ariga et al., 2010; White et al., 2011; Zhou and Hildebrandt, 2012), however targeted ablation of oligodendroglial cells in zebrafish has not been described. As I wanted to investigate whether my previously described line, *Tg(claudin k:GAL4,UAS:GFP)* could be used to generate offspring in which cells of the oligodendrocyte lineage could be specifically ablated, I crossed it with the driver line *Tg(UAS:nfsb-mCherry)*. While many offspring showed some expression of driver and responder transgenes there was a highly variable expression pattern across different siblings from the same clutch and amongst clutches from the same parents. This was mainly visible in the number of cells labelled with GFP and/or mCherry, as some only expressed GFP or mCherry and others expressed both or neither, despite the fact that all transgenic fluorescent proteins were driven by the same promoter *claudin k*. This variegated expression in the *Tg(claudin k:GAL4,UAS:GFP)* zebrafish line has been described before (Chapter 3 and Münzel et

al., 2012). One of the possible reasons for this is DNA methylation due to the 14x repetitive UAS sequences causing gene silencing and attempts have been made to develop constructs which do not contain repetitive sequences to alleviate this problem (Akitake et al., 2011). DNA methylation is a process whereby a methyl group is added to the cytosine or adenine in the DNA, thereby suppressing the expression of genes (for example viral genes), which could be harmful to the cell. The presence of 14 identical UAS sequences in the responder lines to enhance transgene expression is therefore probably recognised as potentially harmful and methylation prevents further expression, along with silencing of the transgene. Akitake and colleagues have developed non-repetitive UAS sequences, which have been shown to result in less DNA methylation, and are also associated with less transgene silencing (Akitake et al., 2011).

As a result of using a transgenic line with repetitive UAS sequences, only a limited number of oligodendroglial cells, namely the ones expressing the NTR transgene, could be ablated with the MTZ treatment and although live imaging showed clearly that NTR-mCherry-positive cells were destroyed and new ones generated, this was not sufficient to cause disruption of myelin in MTZ treated zebrafish larvae. As such, this system could be useful to investigate glial cell ablation and regeneration on a single cell level, but cannot be used to induce local demyelinating lesions or global ablation of glial cells. Due to this reason, this system is also not ideal for drug screening, in particular to evaluate the pro-myelinating effects of chemical compounds, as the number of oligodendroglial cells varies between clutches and siblings of the same clutch and does not offer a stable read-out.

In adult zebrafish, I found that the NTR-mCherry transgene was not expressed at all in oligodendroglial cells in the brain and only appeared in a clumpy distribution in cells of the posterior lateral line nerve, which is part of the peripheral nervous system. The lack of expression is presumably due to transgene silencing, rather than a switched-off promoter in adulthood, as I could demonstrate that *claudin k*-driven GFP expression in the adult zebrafish brain was still present. The clumpy distribution of NTR-mCherry in the posterior lateral line nerve could be due to the

size of the fluorescent protein as similar non-homogenous distribution patterns of the similar sized fluorescent protein DsRed have been described previously (Okita et al., 2004).

In summary, the zebrafish line that I generated for conditional cell ablation is not useful for adult demyelination studies. To use the transgenic embryos for further investigation of the cellular events following destruction of single oligodendroglial cells, it would be necessary to determine what occurs during normal development as it is difficult to investigate the response to injury in a developing system. It could also be useful to explore whether there is a time point at which the generation of new NTR-mCherry-positive cells plateaus but NTR-mCherry is still expressed in oligodendroglial cells in the larval zebrafish, compared to adult zebrafish where the transgene is no longer visible in the CNS.

To bypass the problem of lack of NTR-mCherry transgene expression in the adult zebrafish, I investigated whether demyelinating lesions could also be induced by the myelin toxin LPC. Firstly I injected the toxin into the optic nerve and could show that there was reduced immunoreactivity of myelin and axons markers, both of which returned within 4 weeks. However, visual evaluation of the electron microscope images at 8 dpl also appeared to have more small calibre axons clustered together in bundles. This was reminiscent of what has been shown in studies investigating axonal regeneration in fish, as they describe axonal sprouting and the presence of many small calibre axons which regrow in bundles of high axonal density (Becker et al., 2000; Nona, 1995).

A frequency distribution of axonal diameter clearly indicates that the lesioned optic nerve contains a significant increase in number of small calibre axons, suggesting that some axons are damaged and are beginning to regrow at this stage following the lesion. There was also an increased frequency of larger diameter axons; this could be due to swelling as a result of the injury, which has been previously described in the context of traumatic axonal injury (Wang et al., 2011a). Studies in traumatic brain injury show that damaged axons are often swollen due to Neuronal tracing experiments clearly demonstrated that some axonal damage is caused by

the injection and that approximately one-third of the optic nerve axons are affected. As such, LPC injections are not ideal to induce demyelinating lesions without concurrent injury and I went on to investigate whether LPC could be applied differently to bypass this problem.

Gelfoam is used medically for patient care, is able to soak up liquid and disintegrate within the body. I wondered whether this could be used to induce demyelinating lesions in adult zebrafish as it has been used previously in a lesion context in the zebrafish optic nerve (Becker et al., 2000). Neuronal tracing experiments and immunohistochemical analysis of optic nerve sections suggested that a very small amount of LPC was not sufficient to demyelinate the optic nerve and very large amounts were toxic and caused diffuse axonal injury. The latter is undesirable when attempting to evaluate remyelination, as it would be difficult to differentiate between newly formed myelin around regenerated axons and remyelination of pre-existing, demyelinated axons, especially as these two processes may involve very different signalling mechanisms.

In summary, it is important to note that although there was no difference in tectal labelling after 5 µl LPC compared to control, this does not imply that there is no axonal damage at all. The neuronal tracing method is limited by the fact the only pixel intensity or area of tracer uptake can be measured rather than number of single traced fibres and so a few damaged fibres may not be detected. Moreover, as 5 µl LPC demyelinated approximately 70% of the optic nerve, with no detectable damaged axons by LINC immunohistochemistry and neuronal tracing, any subtle axon damage not detected by the methods used in this thesis may be disregarded because most fibres will be demyelinated only. Therefore, I have developed a method in adult zebrafish to reliably demyelinate optic nerve fibres in adult zebrafish permitting the study of remyelination. However, it has to be kept in mind that this is not a model of multiple sclerosis, as the demyelinating lesions do not occur naturally in zebrafish but have to be induced with the myelin toxin LPC. This does not allow the investigation of pathogenesis; however, signalling mechanisms involved in remyelination might be explored in this zebrafish-based model.

CHAPTER 5 – Remyelination in adult zebrafish optic nerve following toxin-induced demyelination

5.1 Introduction

LPC-induced demyelination has been studied extensively in rodents and was first used to lesion peripheral nerve in mice (Hall, 1973; Hall and Gregson, 1971). In the CNS, injection of 1µl of the standard 1% solution into the white matter of the rodent spinal cord leads to a defined demyelinating lesion (Hall, 1972). Within the lesion the majority of oligodendrocytes are lost due to LPC toxicity (Caillava et al., 2011), with some cells surviving the demyelinating injury. Remyelination studies in the cerebellar peduncle of rats have shown that at 8 days post injection most axons in the lesion area remained demyelinated and remyelination occurred as early as 6 weeks post lesion beginning from the outside perimeter of the lesion (Woodruff and Franklin, 1999). However, while most fibres are remyelinated with great efficiency, the myelin sheath is often thinner and with shorter internodes compared to myelin produced during developmental (Blakemore and Franklin, 2008). Zebrafish are highly effective in repairing various CNS tissues, including spinal cord (Becker and Becker, 2008), retina (Fimbel et al., 2007) and brain (Kroehne et al., 2011), but knowledge of myelin regeneration is limited. I therefore aimed to characterise toxin-mediated de- and remyelination in zebrafish and compare this to the processes evident in mammals.

For successful remyelination to take place, oligodendrocyte precursor cells (OPCs) need to be activated, migrate to the lesion area, and differentiate into myelinating oligodendrocytes. Alternatively, mature oligodendrocytes could de-differentiate, migrate to the lesion area and re-differentiate into myelinating oligodendrocytes. In multiple sclerosis (MS) lesions spontaneous remyelination does occur (Lassmann et al., 1997); however, failure to repair myelin is a prominent feature of MS pathology

and leads to axonal degeneration, which is thought to be a major contributor to clinical disability of patients and progressive disease (Reynolds et al., 2011). It has been postulated that reasons for this reduced remyelination capacity in MS include repeated demyelination, due to the relapsing-remitting nature of the disease, a hostile environment due to inflammatory debris and cytokine signalling and age-related insufficient repair mechanisms (reviewed in Franklin, 2002b; Franklin et al., 2002). OPCs are found in MS lesions in human post-mortem brain tissue (Chang et al., 2000) and evidence also indicates sufficient ability of OPCs to repopulate experimental demyelinating lesions in the rat spinal cord (Chari and Blakemore, 2002), suggesting that insufficient differentiation of progenitor cells rather than recruitment failure might be responsible for impaired remyelination. Closer analysis of OPCs in human chronic MS lesions showed that while they expressed markers of the early oligodendrocyte lineage, they appeared to be quiescent and lacking expression of proliferation and differentiation markers (Wolswijk, 1998). In experimental rat models, repeated focal toxin-mediated demyelination did not lead to depletion of OPCs in or around the lesion, nor a difference in percentage of demyelinated axons, or remyelination capacity (Penderis et al., 2003), and post mortem tissue from human MS patients even after many years of disease still showed plentiful OPCs (Chang et al., 2002). In contrast, differentiated oligodendrocytes *in vitro* present with an increased vulnerability to repeated demyelinating insults (Fressinaud, 2005). These results propose a possible mechanism for reduced myelin repair following chronic disease: differentiated oligodendrocytes die as a result of repeated demyelination insults, and although OPCs are present in and around lesions, they are not capable of differentiating into mature oligodendrocytes to repair the damage. In recent years, inflammation has been positively associated with remyelination; pathological studies in human MS lesions demonstrated that acute lesions with a high immune cell infiltrate, especially macrophages, showed much higher remyelination capacity than chronic demyelinated areas, which presented with reduced inflammation (Raine and Wu, 1993; Wolswijk, 2002). Moreover, depletion of macrophages in adult rats preceding a demyelination spinal cord lesion resulted in altered OPC response and decreased

remyelination (Kotter et al., 2005), and more specifically the presence of myelin debris in the lesion site has been identified as a factor adversely affecting remyelination (Kotter et al., 2006). Thus, macrophages and immune response are important for myelin repair, and are thought to affect rate and efficiency of remyelination at chronic disease stages and with increasing age. It has been noted that white matter injury is more extensive in old rats compared to young ones in a focal demyelination model and that remyelination in aged rats is not as effective, as many axons remain unmyelinated after 4 weeks when much remyelination has already occurred in younger rats (Hampton et al., 2012; Shields et al., 1999). In parabiosis studies, where old mice where joined to young ones, so that they share a blood supply, and a demyelinating lesion was placed in the old mouse's spinal cord, more differentiating oligodendrocytes were observed in the lesion site and remyelination took place much more effectively than in old mice joined to old ones. Further experiments suggested that the macrophages of a young mouse traversing into the lesion of the old animal are important for successful remyelination (Ruckh et al., 2012). As zebrafish show a much higher regenerative capacity than rodents and other experimental models, it will therefore be interesting to investigate whether old zebrafish also show a decreased remyelination efficiency.

The remyelination process involves many steps which can potentially be targeted and influenced in a way that promotes remyelination speed and capacity. Several signalling pathways involved in OPC differentiation, including Notch and Wnt signalling, the chemokine CXCL12 and the retinoid X receptor-ϒ, have already been described (Huang et al., 2011b; John et al., 2002; Patel et al., 2010) and are further summarised in the main introduction of this thesis. Studies investigating mechanisms underlying OPC recruitment focus on migratory cues, and in particular the Semaphorins 3A and 3F have been identified as potential key regulators of this process (Williams et al., 2007).

The semaphorins are a class of secreted and transmembrane proteins, which were primarily described as axonal guidance molecules with great importance for the developing nervous system (reviewed in Kolodkin, 1996). Class 3 semaphorins have

also been identified as chemotactic factors for oligodendroglial cells during development, in particular Semaphorin 3A (Sema 3A) and Semaphorin 3F (Sema 3F) aid the recruitment of glial precursor cells from the brain to the developing optic nerve by their repulsive and attractive properties (Spassky et al., 2002; Sugimoto et al., 2001). Signalling of class 3 semaphorins occurs through binding to receptor complexes containing Neuropilin 1 and 2 (NRP1/2) and the class A Plexins (reviewed in Sharma et al., 2012), however the Neuropilins exhibit different affinities for Sema 3A and 3F. While Neuropilin 1 binds Sema 3A with high affinity and Sema 3F as well as several other Semaphorins with low affinity (He and Tessier-Lavigne, 1997; Kolodkin et al., 1997), Neuropilin 2 shows high affinity for Sema 3F and 3C and lower affinity for Sema 3B and 3G (Chen et al., 1997). However, these affinities were observed in *in vitro* studies and may well be different *in vivo,* especially as observations in other laboratories have shown that in NRP2 knockout mice, no binding of Sema 3F could be detected, suggesting that it also does not bind to Neuropilin 1 *in vivo* (Giger et al., 2000). Moreover Neuropilins are also able to bind cytokines of the Vascular endothelial growth factor (VEGF) family, which bear different structural and functional properties to semaphorins (reviewed in Geretti et al., 2008). Structurally, Neuropilins are comprised of a large extracellular domain containing four sub-domains: 1) the N-terminal CUB domain (a1 and a2 sub-domain), which binds class 3 semaphorins amongst other ligands, 2) the coagulation factor domain, which is also known as b1/b2 sub-domain and binds VEGF, 3) and the C-terminal MAM-domain. While VEGF only binds to the b1b2 sub-domain, it has been shown that class 3 semaphorins can interact with both, the a1a2 and the b1b2 sub-domain, but the critical domain is the a1a2. Expression of NRPs has been demonstrated in the vascular system, and appear to play a central role in normal blood vessel development as NRP1 knockout mice are embryonic lethal with disorganised vascular formation and transposition of great vessels and NRP2 knockout mice displayed a severe reduction of small lymphatic vessels and capillaries (Kawasaki et al., 1999; Yuan et al., 2002). Class 3 semaphorins have been demonstrated to negatively regulate tumour growth; in particular Sema 3B and 3F have been shown to reduce tumour formation in mice and inhibit tumour

angiogenesis and metastasis (Bielenberg et al., 2004; Kessler et al., 2004; Tse et al., 2002). As class 3 semaphorins are unable to directly interact with plexins, the signal transducing subunits, it is thought that semaphorins bind to neuropilin/plexin receptor complexes (Sema3A/NRP1/PlexinA4 and Sema3F/NRP2/PlexinA3), which then mediate intracellular signalling (reviewed in Zhou et al., 2008). Upon semaphorin3 binding, FARP2 dissociates from plexinA, activates Rac1 which is thought to control actin dynamics via PAK and Cofilin. In addition, plexinA signalling is associated with RasGAP (Ras GTPase activating protein) stimulation and phosphoinositide 3-kinase (PI3K) inactivation ultimately leading to inhibition of integrin-mediated adhesion signalling and CRMP2 (collapsin response-mediated protein) inactivation via GSK3ß. CRMP2 is thought to be involved in microtubule dynamics and endocytosis through signalling via cyclin-dependent kinase 5 (Cdk5) and Fyn. The culminating effects of Sema3/NRP/Plexin signalling are changes in the actin cytoskeleton, permitting modulation in cell shape and motility.

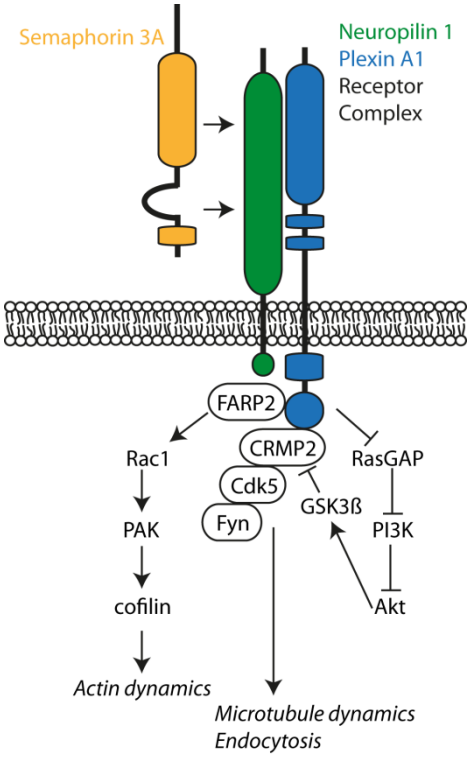

Schematic of semaphorin 3A signalling via neuropilin 1/plexin A1 receptor complex

In LPC-induced demyelinating lesions in rat spinal cord as well as in active plaques of MS brain transcripts of both Sema 3A and 3F are upregulated (Williams et al., 2007). Moreover, expression of the semaphorin receptors neuropilins and plexins is increased on oligodendrocyte precursor cells and upon Sema 3A/3F overexpression in a murine demyelination model OPC recruitment and remyelination rate could be manipulated (Piaton et al., 2011). These results suggest a key role of Sema 3A and 3F in OPC recruitment following a demyelinating insult and a possible target for promotion of remyelination.

In this chapter I aimed to determine if zebrafish are able to regenerate their myelin with the same capacity as they repair other CNS tissues. Furthermore, I sought to investigate if the mechanisms underpinning zebrafish remyelination are homologous to mammals and whether manipulation of these could alter myelin repair in a system with high regeneration capacity.

5.2 Results

Characterisation of LPC-induced demyelinating optic nerve lesions in adult zebrafish

The previous chapter details how focal demyelinating lesions were achieved in the adult zebrafish optic nerve through local application of the myelin toxin LPC, critically without concomitant axonal injury. A small piece of absorbable gelatine sponge was soaked in LPC and placed onto the optic nerve in a simple operative procedure (Figure 5.1-A). Eight days following the placement of the LPC sponge, the time point of maximum reduction in myelin after LPC injection, I quantified pixel intensity in cryostat cross sections of the optic nerves and chiasm and observed a reduction in Claudin k immunoreactivity in the lesion site representing a loss of myelin (Figure 5.1-B). Accordingly, I also found fewer olig2+ oligodendroglial cells in the lesion area and an increase of 4C4+ microglia/macrophages in the lesioned optic nerve, while the neuronal immunostaining with LINC indicated no axonal change (Figure 5.1-B).

To further investigate the events after myelin injury, I lesioned the animals as described above and then analysed cryostat sections of the optic nerve (as shown in Figure 5.1-B) at various time points after the lesion (Figure 5.2-A). By measuring pixel intensity of Claudin k in the lesion area and calculating a ratio to the unlesioned contralateral optic nerve to account for differences in labelling brightness, I could show that myelin is maximally reduced at 8 days following the lesion ($p<0.01$, n=6, Kruskal Wallis test, Dunn's post-test, Figure 5.2-B). Oligodendroglial cells marked by *olig2:*DsRed were also decreased at early time points after the lesion, with a significant decrease at 8 dpl compared to unlesioned control optic nerves ($p<0.05$, n=6, Kruskal Wallis test, Dunn's post-test, Figure 5.2-C). Both pixel intensity of Claudin k immunoreactivity and the number of *olig2:*DsRed-positive oligodendroglial cells in the lesion area had increased within 4 weeks (Figure 5.2-B,C). 4C4+ microglia were significantly increased in number at 4 dpl ($p<0.05$, n=6, Kruskal Wallis test, Dunn's post-test) and returned levels comparable to the unlesioned control at 14 dpl (Figure 5.2-D). Axons marked by

pixel intensity of LINC immunoreactivity were not different to the unlesioned contralateral optic nerve (pixel intensity of 1) at any time point, (Figure 5.2-E). These findings indicate that LPC leads to a demyelinating lesion in the optic nerve by 8 dpl, which is able to regenerate within 4 weeks.

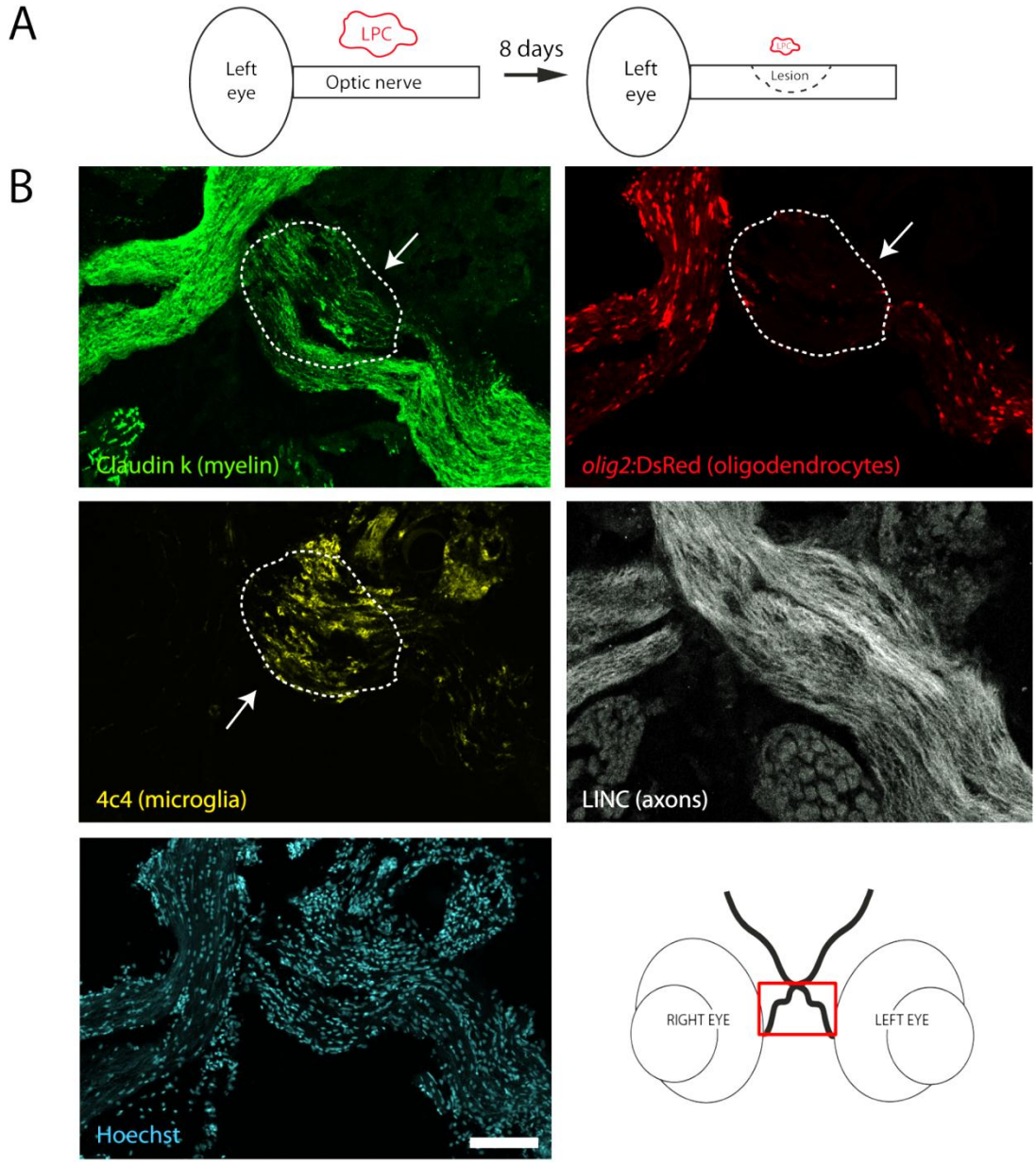

Figure 5.1: Characterisation of the toxin-induced demyelinating lesion. (A) Schematic shows how the demyelinating lesions were performed: A small sponge soaked in LPC was placed next to the optic nerve. Cross sections of the optic nerve were then evaluated at 8 days post lesion. (B) Cryostat cross sections of adult zebrafish optic nerves and chiasm showing a reduction in Claudin k (myelin) immunoreactivity and number of *olig2:*DsRed-positive oligodendroglial cells in the lesion site. 4C4+ microglial cells were increased around the lesion area and axons seemed intact by LINC immunohistochemistry. Sections showing *olig2*:DsRed, 4C4 and Hoechst are the same, Claudin k and LINC immunohistochemistry is shown on alternate sections. Dorsal is up. Schematic shows the where the cryostat sections were taken. Scale bars: B = 100 µm.

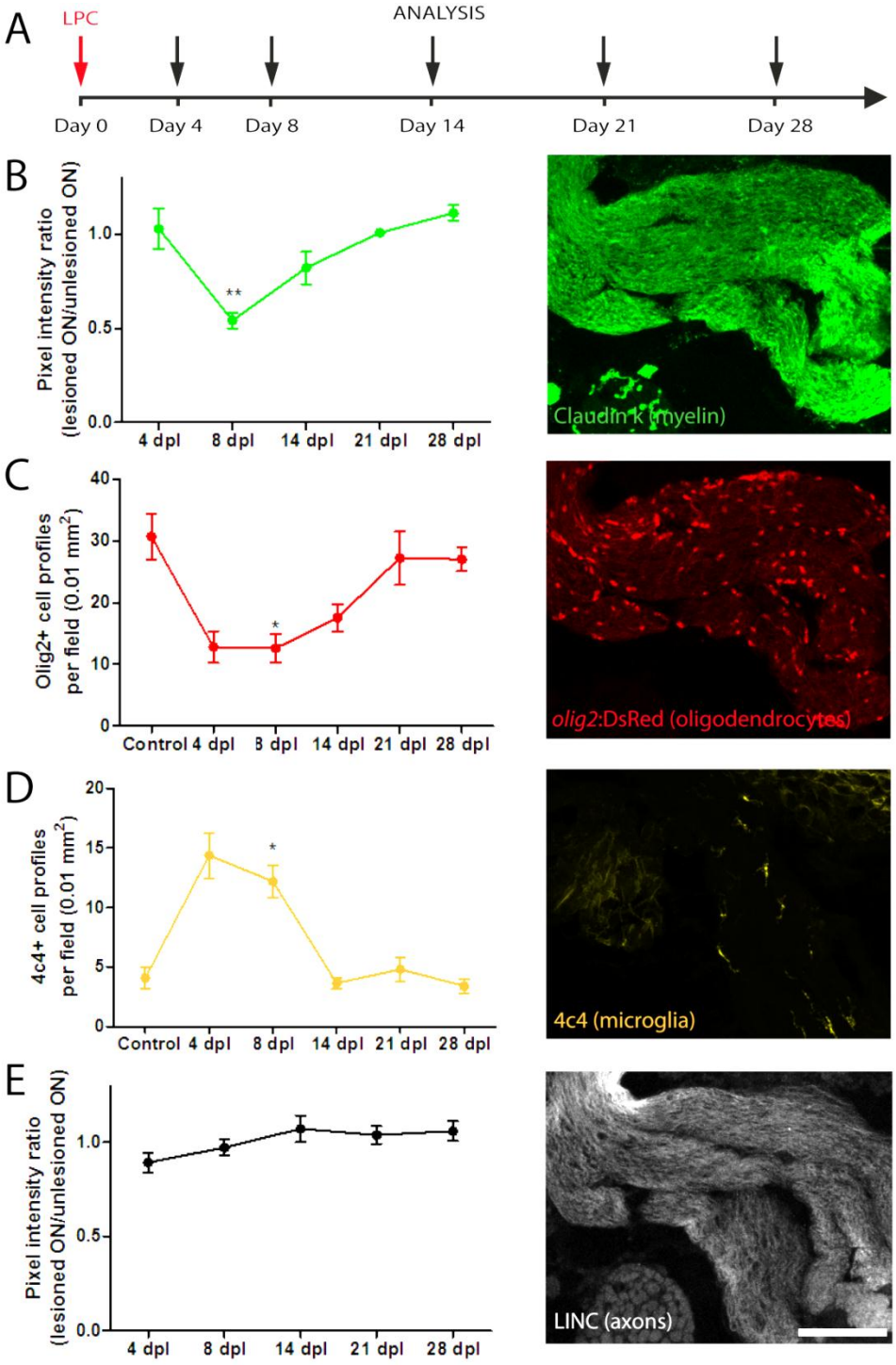

Figure 5.2: Investigation of myelin, oligodendroglial cells, microglia and axons following demyelinating injury. (A) Lesion and analysis time points are indicated in the schematic. (B) Pixel intensity measurements and cell profile counts in longitudinal cryostat sections of adult zebrafish optic nerves and chiasm show: (B) a significant reduction in Claudin k (myelin) immunoreactivity ($p<0.01$, n=6, Kruskal Wallis test, Dunn's post-test), (C) fewer olig2+ oligodendroglial cells in the lesion site ($p<0.05$, n=6, Kruskal Wallis test, Dunn's post-test), (D) up-regulated 4C4+ microglial cells at 4dpl ($p<0.05$, n=6, Kruskal Wallis test, Dunn's post-test) and (E) no change in LINC+ axon pixel intensity. Immunohistochemical analysis of longitudinal optic nerve sections at 28 dpl are representative of data shown in graphs. Error bars represent mean ± SEM. Scale bar: B-E = 100 µm.

Electron microscopic analysis of de- and remyelinated optic nerve

To further investigate myelin repair after toxin induced demyelinating lesions, I performed electron microscopy (EM) studies of the optic nerve. EM analysis of optic nerve cross sections showed that at 8 days post lesion, many axons had been stripped of their myelin sheath, leaving most axons unmyelinated compared to the unlesioned contralateral control optic nerve (24% ± 9% vs. 93% ± 1% myelinated axons, mean ± SEM, $p<0.05$, n=3, Kruskal Wallis test, Dunn's post-test). After 4 weeks most axons had regained their myelin sheath (92% ± 1%, mean ± SEM) and were not different from unlesioned controls, suggesting completion of myelin repair (Figure 5.3-A,B). Compared to in the unlesioned optic nerve, the remyelinated fibres appeared much further apart with longs strands of cytoplasm running through the lesioned area at 28 dpl. These are probably astroglial processes, which help to re-establish fascicular architecture of the optic nerve, as has been suggested previously in goldfish optic nerve regeneration (Nona et al., 1998). As remyelination results in thinner myelin sheaths in human brain (Perier and Gregoire, 1965) and rodent experimental demyelination models (Blakemore and Franklin, 2008), I wondered whether fish would also show this phenotype. Therefore I measured G-ratios in remyelinated optic nerves and compared them to unlesioned controls. Scatter graphs of G-ratio vs. axon diameter show clustering of axons with a diameter of 0.3-0.5µm and G-ratio of 0.6-0.8 in remyelinated optic nerves and unlesioned controls, while at 8 dpl axons of similar size present with a much larger G-ratio of 0.8-1.0 and clearly indicate demyelination (Figure 5.3-C). When I compared the average G-ratio of 28 dpl optic nerves and unlesioned controls (3 animals per condition and 200-300 measured axons per animal), I found no difference in average G-ratio (Figure 5.3-D). As the G-ratio only evaluates myelin thickness and not compactness, ie the G-ratio may appear the same even if the myelin wraps are looser and there are less of them, visual observations confirmed that the myelin sheaths was indeed compact. The quality of the electron microscope preparations did not allow closer analysis of myelin structure such as major dense lines. In summary, these data suggest that zebrafish are capable of regenerating their myelin sheath completely, both in number of axons remyelinated

and the thickness of the myelin sheath and this differs from what has been observed in rodent studies.

During EM analysis, I also noted that optic nerve cross sections after LPC-induced demyelination looked very different to those after optic nerve crush with severed axons (Figure 5.4-A). While after demyelination many axons of variable axon diameter without myelin were present in optic nerve cross sections, the average axon diameter after nerve crush was smaller (Figure 5.4-B). When I compared the axon diameter frequency of both conditions, I observed a left shifted curve in the nerve crush population with more small diameter axons compared to unlesioned controls and LPC treated optic nerves ($p<0.05$, $n=3$, Mann Whitney U-test, Figure 5.4-C). It is well established that following nerve transection axons in the nerve stump will sprout in an effort to regenerate (Nona, 1995; Wolburg, 1981), and while mammals are only able to regrow peripheral nerves, zebrafish can regrow their optic projection and other central nervous system axons with high efficiency (Becker and Becker, 2007). Moreover I noted some axons that appeared to have continuous cytoplasm suggestive of branching/sprouting, and these were not present in the optic nerve after demyelination (Figure 5.4-A, inset); this has been observed previously after nerve crush in the goldfish optic nerve (Nona, 1995; Wolburg, 1981). As such, these results provide further evidence that no major axonal damage is present in the optic nerve after demyelination.

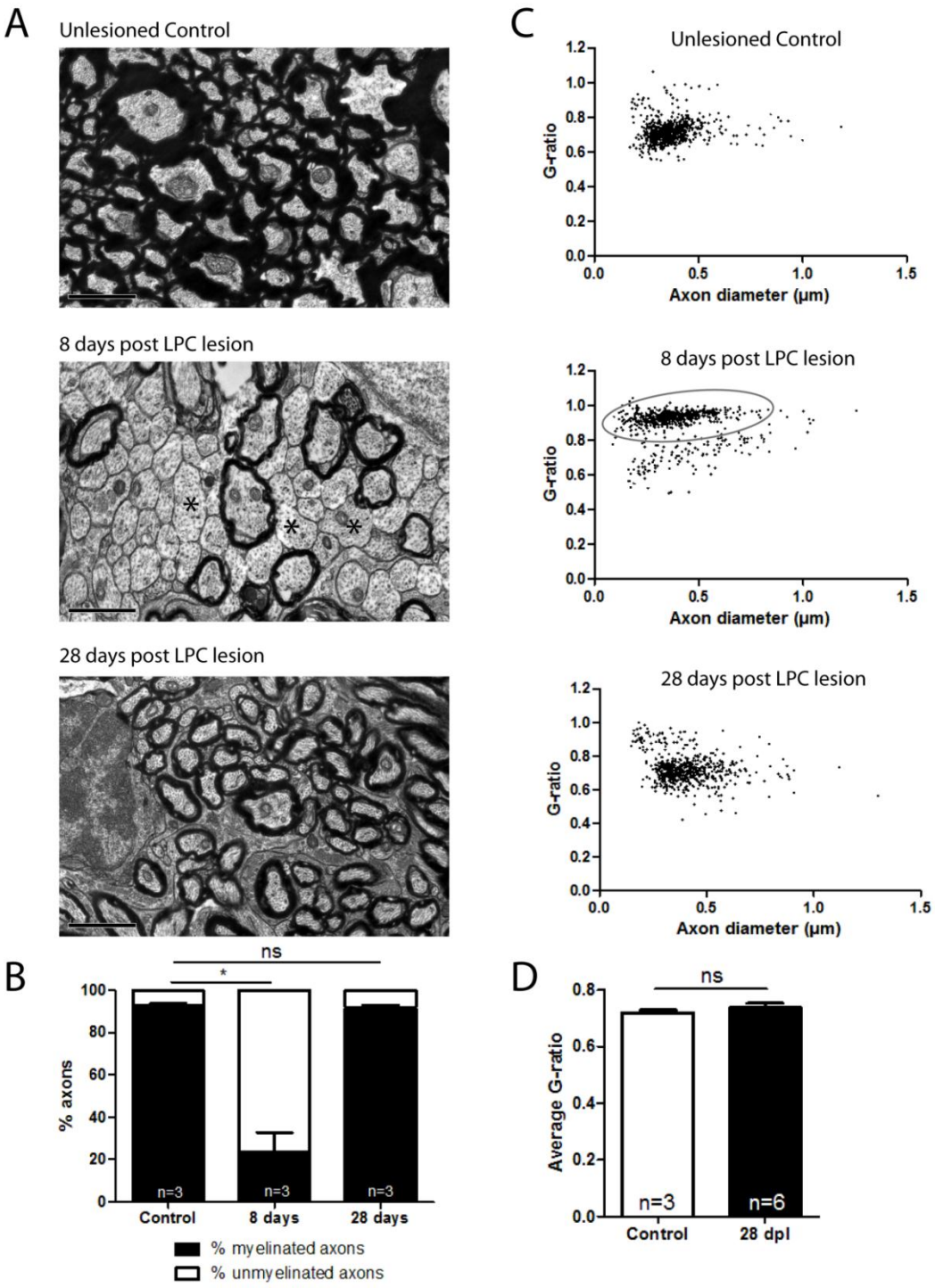

Figure 5.3: Electron microscopic evaluation of remyelination. (A) Cross sections through optic nerves and electron microscopic analysis thereof show many demyelinated axons at 8 dpl (asterisks) compared to unlesioned controls and complete regeneration at 28 dpl. (B) At 8 dpl the number of myelinated axons in the lesion area is significantly reduced to unlesioned controls ($p<0.05$, n=3, Kruskal Wallis test, Dunn's post-test), while there is no difference between remyelinated and control optic nerves. (C) Correlations of G-ratio and axon diameter show similar populations at 28 dpl and in unlesioned control, while most axons at 8 dpl have a much larger G-ratio indicating thinner myelin (circle). (D) Average diameter between unlesioned and remyelinated optic nerve is not different ($p>0.05$, n=3-6, Mann Whitney U-test). Error bars represent mean ± SEM. Scale bar: A = 1 µm.

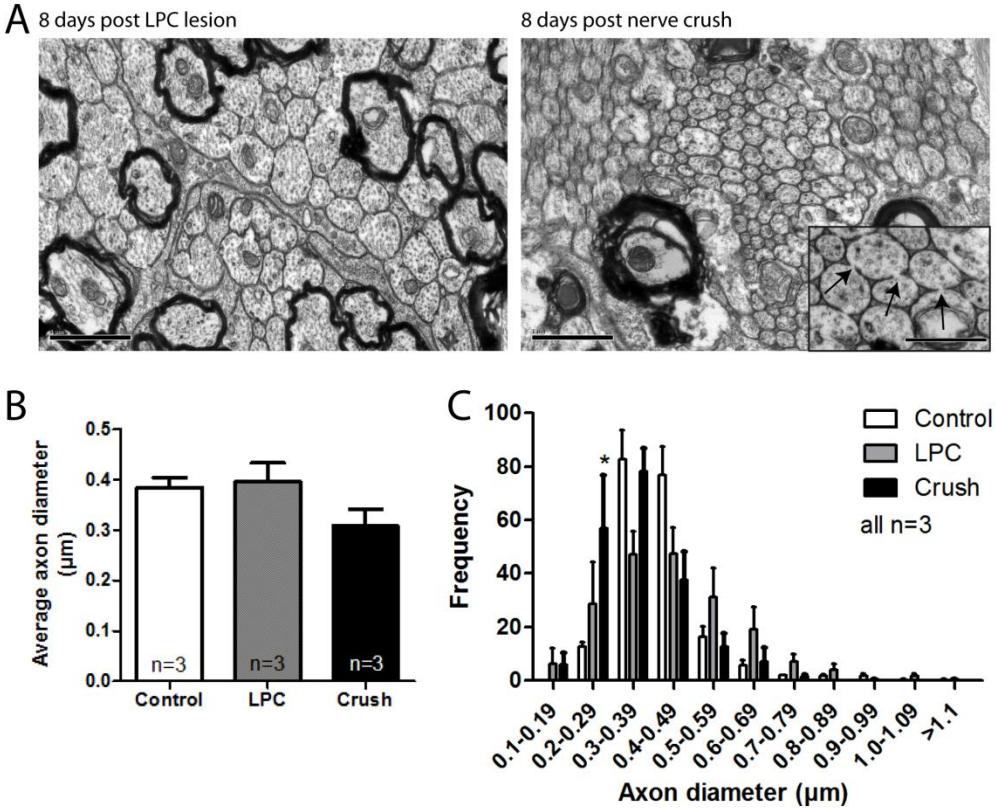

Figure 5.4: Electron microscopic analysis shows no axonal damage after LPC induced demyelinating lesions. (A) Electron microscopic analysis of cross sections through optic nerves show demyelinated axons of various axonal diameter compared to crushed optic nerve in which axons were severed and axonal diameter is smaller. Axons that are joined together (inset, arrows) are only observed after nerve crush and indicative of axonal sprouting. (B) Quantification of average axon diameter shows the presence of more small calibre axons after optic nerve crush compared to LPC treated optic nerves and unlesioned control. (C) Axons of small diameter are much more frequent after nerve crush compared to unlesioned controls and LPC treatment, and indicate no major axonal damage and sprouting during demyelination ($p<0.05$, n=3, Mann Whitney U-test). Error bars represent mean ± SEM. Scale bar: A = 1 µm; inset = 0.5 µm.

Remyelination in old zebrafish is impaired

During remyelination studies of the optic nerve of adult zebrafish (age 4 – 7 months) described previously in this thesis, I found that these are able to repair the myelin completely after demyelination, without any change in G-ratio. Remyelination capacity to this extent is uncommon and I wondered whether aged zebrafish would show the same efficiency in myelin repair. Previously lesioned animals were between 4 – 7 months ("young zebrafish"), and to investigate remyelination efficiency in aged animals further, I lesioned adult zebrafish older than 1.5 years ("old zebrafish"). The lesions were induced by placing a gelatine sponge soaked in LPC onto the optic nerve, as described above. I then used electron microscope analysis to measure G-ratios as an indicator of myelin thickness in optic nerve cross sections at 28 days post lesion in aged zebrafish. This analysis indicated that compared to unlesioned age-matched control and remyelinated optic nerve from young animals, the myelin sheath in old zebrafish at 28 dpl was much thinner (Figure 5.5-A). This difference was also notable when visually comparing myelin thickness in the lesioned area to another more distant area in the optic nerve of old zebrafish optic nerve at 28 dpl, suggesting that this is specific for the lesion area (Figure 5.5-A). The average G-ratio in the optic nerve of old zebrafish at 28 dpl was indeed significantly higher compared to young zebrafish at 28 dpl and old age-matched unlesioned controls ($p<0.05$, 3 animals per condition and 200-300 axons per animal, Mann Whitney U-test, Figure 5.5-B). This could be due to a higher proportion of unmyelinated axons present in the old zebrafish optic nerve; however the percentage of unmyelinated axons in old zebrafish at 28 dpl was comparable to young zebrafish at 28 dpl and old age-matched unlesioned controls, suggesting that a difference in proportion of myelinated axons was not the cause of a higher average G-ratio (Figure 5.5-C). Claudin k pixel intensity measurements in young and old zebrafish optic nerve were not different and suggest similar extent of myelination (Figure 5.5-D). In agreement with other rodent studies investigating remyelination in old animals, my results propose that old zebrafish are not able to repair myelin as effectively as their young counterparts, however whether this is a

problem of insufficient repair mechanisms or speed (and they would remyelinate fully after a longer time period) is not yet clear.

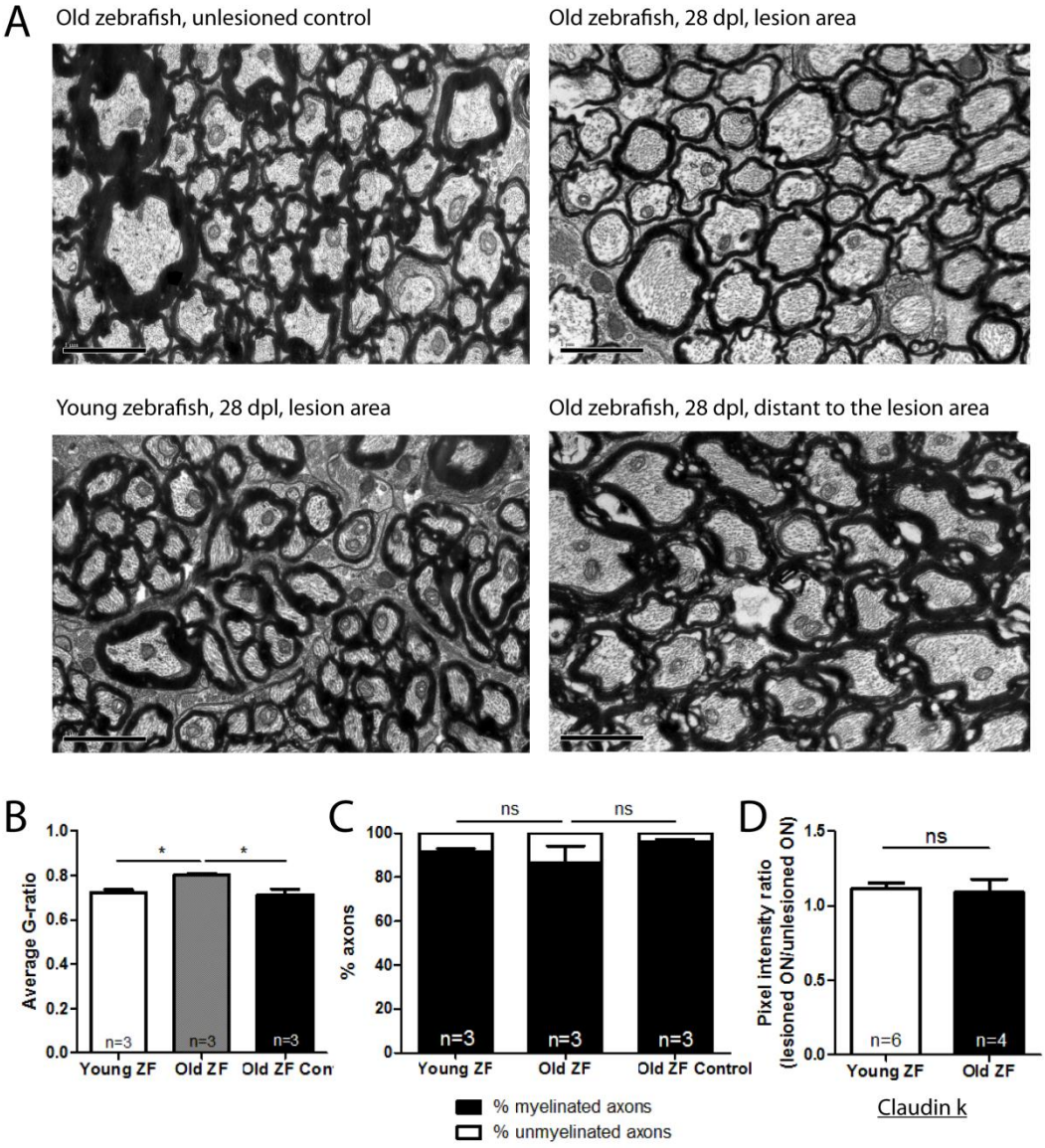

Figure 5.5: Remyelination in old zebrafish. (A) Electron microscopic analysis of cross sections through the lesion area in the optic nerves of young (4-7 months) and old (>1.5 years) zebrafish show differences in myelin thickness at 28 dpl. Old zebrafish present with much thinner myelin in the remyelinated lesion area compared to young remyelinated zebrafish, other areas in the old zebrafish optic nerve distant to the lesion site and unlesioned age-matched controls. (B) At 28 days after LPC-induced demyelination, axons in the lesion area of old zebrafish present with a significantly increased G-ratio compared to young zebrafish at 28 dpl and age-matched unlesioned controls ($p<0.05$, n=3, Mann Whitney U-test). (C) Percentage of unmyelinated axons in young and old zebrafish 28 days after LPC treatment compared to age-matched old zebrafish unlesioned controls shows no differences, suggesting that the higher average G-ratio is not a result of an increased proportion of unmyelinated fibres but instead of thinner myelin. (D) Claudin k pixel intensity in the lesion area at 28 dpl is not different between young and old zebrafish, indicating no differences in extend of myelination. Error bars represent mean ± SEM. Scale bars: A = 1 µm.

Origin of remyelinating cells

In mammalian studies, remyelination is thought to be carried out by oligodendrocyte precursor cells located in the white matter immediately surrounding the demyelinated area (Franklin et al., 1997) or from progenitor zones within the brain such as the subventricular zone (Nait-Oumesmar et al., 1999) and not from de-differentiation of mature oligodendrocytes and re-differentiation, which has been suggested in nerve regeneration studies in goldfish (Ankerhold and Stuermer, 1999). In order to determine where the cells responsible for remyelination in the zebrafish optic nerve originate, I first investigated proliferating cells in the optic nerve surrounding the demyelinating lesion by immunohistochemistry in cryostat sections. While I observed an increase of proliferating cell nuclear antigen (PCNA)-positive cells at 4 and 8 days post lesion compared to unlesioned controls ($p<0.05$, n=3-7, Kruskal Wallis test, Dunn's post-test), these did not co-label with the oligodendroglial cell marker *olig2*:DsRed, suggesting that cells of the oligodendroglial cell lineage were not proliferating around the lesion site (Figure 5.6-A). More likely, the increase in PCNA-positive cells was due to activation of immune cells which respond to the demyelinating injury. As the remyelinating cells did not seem to proliferate around the lesion area, I performed studies in which I treated lesioned fish with 5-Ethynyl-2'-deoxyuridine (EdU), which is a thymidine analogue that is incorporated into dividing cells during S-phase. In contrast to PCNA, which labels cells that are currently dividing at the point of analysis, EdU is incorporated into dividing cells at the point of *in vivo* administration and retained in the cells as they migrate from their point of division. EdU only has a very short bioavailability; pharmacokinetic studies investigating the clearance of EdU in mice following intravenous injection show that EdU is eliminated with a half-life of approximately 35min (Cheraghali et al., 1995). EdU treatment permits labelling of cells which divided at some point during the time of EdU application and their progeny. Due to the limited bioavailability of EdU, zebrafish needed to be treated frequently over a short period of time in order to label as many cells as possible. More specifically, I lesioned the optic nerve with LPC as previously described, injected the fish daily with EdU between post lesion day 3

and 10 and then analysed the remyelinated optic nerve at 28 dpl for oligodendrocytes with incorporated EdU (Figure 5.6-B). I found that in the lesioned optic nerve 9.3% ± 3.3% (mean ± SEM) of oligodendrocytes were also EdU-positive compared to the unlesioned control with 1% ± 1% (mean ± SEM) co-labelled cells (Figure 5.6-C,D). These findings suggest that some of the remyelinating cells are newly generated, though as the PCNA immunostaining was negative in oligodendroglial cells, they were not generated locally to the lesion. However, assumptions about whether local mature myelinating oligodendroglial cells are also capable of de- and re-differentiation and where those newly generated remyelinating cells originate from cannot be made.

Previous studies also demonstrate that peripheral myelinating Schwann cells can be involved in remyelination of the central nervous system. In the rodent spinal cord, Schwann cells are able to invade from the periphery to aid the remyelination process following focal toxin-induced lesions (Black et al., 2006) and upon transplantation into the spinal cord, they can migrate and remyelinate demyelinated axons (Baron-Van Evercooren et al., 1992). I therefore wondered whether the remyelination in fish was due to Schwann cell infiltration and tested this by making use of a transgenic zebrafish line, *Tg(FoxD3:GFP*), which labels neural crest-derived Schwann cells (Gilmour et al., 2002). When I analysed cryostat sections at 28 dpl, I found no GFP-positive cells in the remyelinated spinal cord, however labelled peripheral innervating nerves could be seen in muscle fascicles close by (Figure 5.7-A) confirming that transgene is still active in the adult zebrafish. Moreover, when I investigated cross sections of remyelinated optic nerve by EM, I also did not observe any Schwann cells (Figure 5.7-B), which can be easily distinguished from oligodendrocytes by their close association of nucleus and myelinated axon (one-to-one relationship) (Figure 5.7-C). Hence, neural crest-derived Schwann cells do not appear to play a role in this model of zebrafish optic nerve remyelination.

As remyelinating cells in the zebrafish optic nerve neither seemed to originate from local proliferation nor invasion of peripheral Schwann cells, I wondered whether

more distant sources such as the progenitor cell niches in the zebrafish brain could be a source for remyelination cells. In cryostat sections labelled with PCNA antibody to mark proliferating cells, I noticed an increase in proliferation in the periventricular progenitor zone in the midbrain at 8 days post LPC-induced demyelination. More specifically, PCNA+/olig2+ co-labelled cells situated immediately around the ventricle were significantly increased at 8 dpl compared to unlesioned controls ($p<0.05$, n=7, Kruskal Wallis test, Dunn's post-test, Figure 5.8-A,B). Since I had already shown that there is no local proliferation of *olig2*:DsRed-positive cells in the optic nerve immediately surrounding the optic nerve, these results might propose that following a demyelinating lesion in the optic nerve, the cells in the periventricular progenitor zone are able to respond to this injury, proliferate and migrate to the lesion where they differentiate into myelinating oligodendrocytes (Figure 5.8-C). To substantiate this theory further, I conducted a follow-on experiment in which I injected GFP-expressing lentivirus into the ventricle of adult zebrafish to try to label and track periventricular progenitor cells and immediately lesioned the optic nerve. This is to test whether in my model in response to the demyelinating lesion, repairing OPCs are derived from the periventricular progenitor cells and migrate to the optic nerve. Similar experiments have been conducted in zebrafish previously (Rothenaigner et al., 2011). They rely on the principle that lentiviral vectors driving GFP-expression will infect any cell they come in contact with and integrate into their genome. This method therefore permits to permanently label any cell close to the application site and track them and their progeny. In my experiments, I found that in the control injected fish, no lentivirus had been taken up by progenitor zone cells, suggesting that the cytomegalovirus (CMV) promoter which is active in rodent cells was possibly not recognised in zebrafish and difficulties with the use of lentiviral vectors in zebrafish has been previously recognised (Dr Bally-Cuif, personal communication). As such, I was not able to directly show proliferation and migration of the progenitor cells into the lesion area to test my hypothesis.

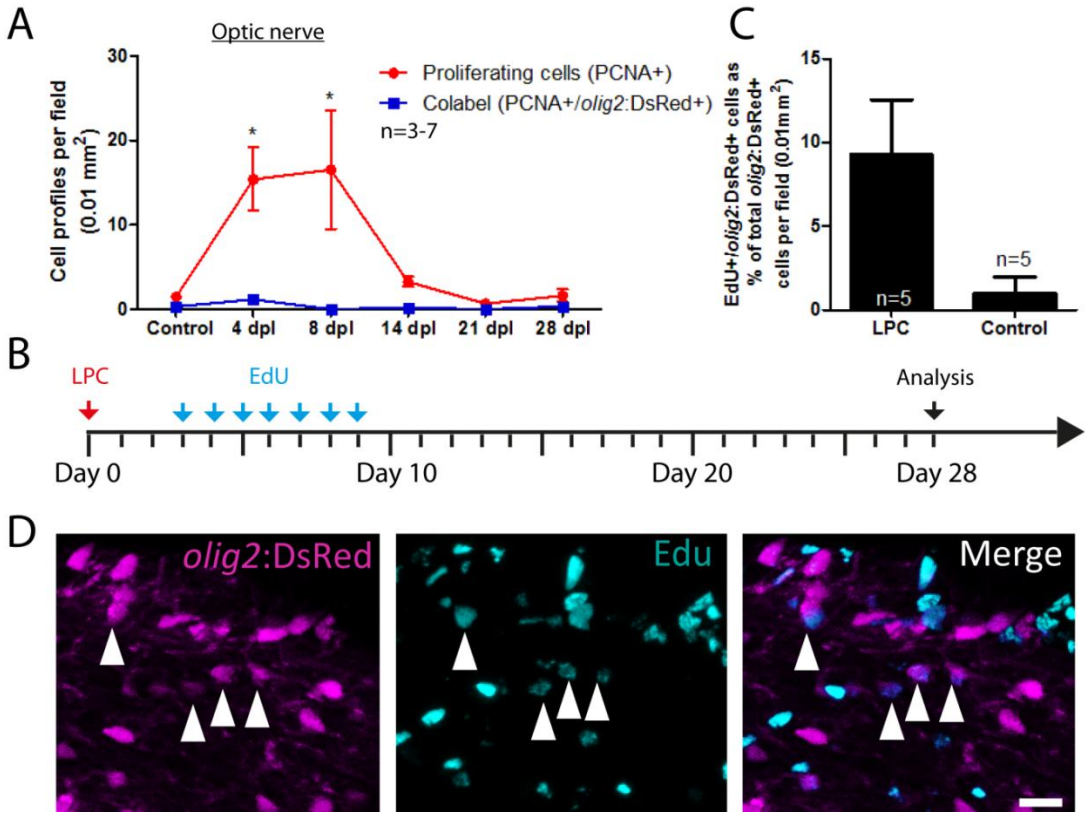

Figure 5.6: Origin of remyelinating cells. (A) Cryostat cross sections of lesioned optic nerve area were analysed for PCNA and *olig2:*DsRed co-label at various time points after LPC-induced demyelination. While PCNA+ cells counts are increased at 4 and 8 dpl compared to unlesioned controls ($p<0.05$, n=3-7, Kruskal-Wallis test, Dunn's post-test), no marked co-label with *olig2*:DsRed was observed, suggesting that this reflects immune cell response rather than oligodendroglial cell proliferation. (B) Schematic describes the experimental set-up: Zebrafish received daily EdU injections between post-lesion day 3 and 10; optic nerves were then analysed at 28 dpl. (C) In LPC lesioned optic nerve, some *olig2*:DsRed+ cells co-labelled with EdU, and although no statistical significance was found compared to the number of co-labelled cells in unlesioned control optic nerve, it suggests that these cells were newly generated. (D) Representative cryostat cross sections of lesioned optic nerve at 28 dpl show co-labelling of *olig2:*DsRed+ cells with EdU. Error bars represent mean ± SEM. Scale bar: D = 10 µm.

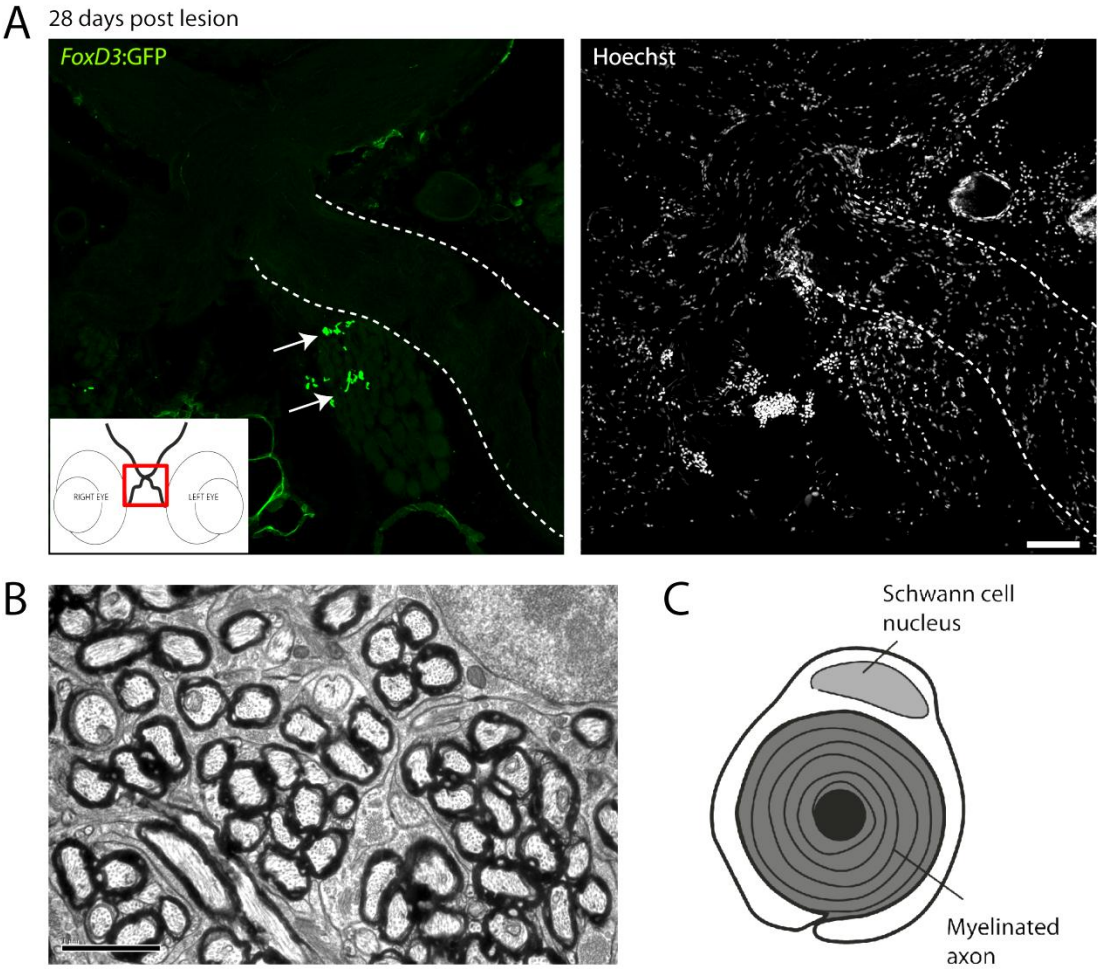

Figure 5.7: Schwann cells are not involved in optic nerve remyelination. (A) Cryostat cross sections through the optic chiasm (inset) of transgenic zebrafish labelling neural crest-derived Schwann cells at 28 dpl show no *FoxD3*:GFP+ cells in the remyelinated optic nerve. Peripheral innervating nerves in muscle fascicles around the nerve are detectable (arrows) and confirm transgenic expression in adult zebrafish of this line. (B) Schwann cells are also not detected in electron microscopic analysis of remyelinated optic nerve cross sections. (C) Schwann cells have a typical phenotype: the nucleus is closely associated with its myelinated axon. Scale bar: A = 100 µm, B = 1 µm.

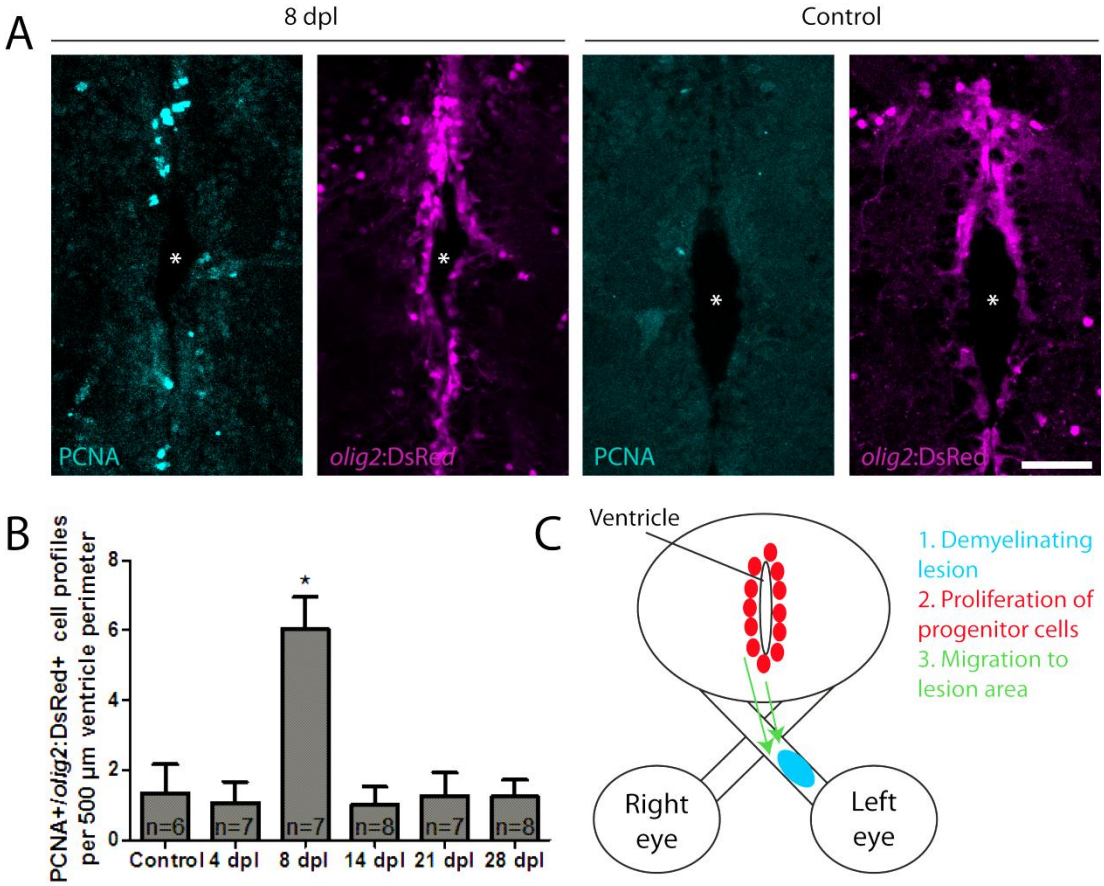

Figure 5.8: Increased proliferation in periventricular progenitor zone following optic nerve demyelination. (A) Cryostat cross sections through the brain of adult zebrafish show increased PCNA labelling of cells in the periventricular progenitor zone at 8 dpl suggesting increased proliferation. (B) These cells largely co-label with olig2 and are significantly different from the unlesioned control at 8 dpl ($p<0.05$, n=7, Kruskal Wallis test, Dunn's post-test). (C) Schematic shows suggested hypothesis of optic nerve remyelination in adult zebrafish: upon demyelination in the optic nerve, periventricular progenitor cells proliferate and migrate to the optic nerve to aid myelin repair. Error bars represent mean ± SEM. Scale bar: A = 25 µm.

Manipulation of optic nerve remyelination by treatment with Semaphorin 3A, a repelling oligodendrocyte precursor cell guidance molecule

In rodents, Semaphorin 3A (Sema3A) is thought to play a key role in regulating remyelination due to its repellent function in oligodendrocyte precursor cell recruitment. To investigate the role of Sema3A in zebrafish optic nerve remyelination I firstly aimed to determine if and where it is expressed in normal adult zebrafish brain and whether the levels in the optic nerve are altered following LPC-induced demyelination. As genome duplications during fish evolution have led to many genes being present in duplicate, I wondered whether both forms of Sema3A (Sema3Aa and 3Ab) could be detected in adult zebrafish. In situ hybridisation studies in cross sections of adult zebrafish brain (conducted by my colleague in the Becker lab, Karolina Mysiak), showed overlapping RNA expression of Sema3Aa and 3Ab in the tractus pretectomammilaris, the ventral and dorsal zone of the periventricular hypothalamus, the periventricular granular zone, the lateral valvula cerebelli and the torus longitudinalis (Figure 5.9-A). Overlapping expression was also observed in the cerebellum (data not shown). Immunohistochemical analysis with the Sema3A antibody showed labelling of similar structures, represented by sections of cerebellum (Figure 5.9-B), however antibody labelling was not very strong and barely detectable in structures such as the tractus pretectomammilaris. Co-labelling of normal adult zebrafish brain cross sections with anti-Sema3A antibody and markers for other cells present in the brain showed overlapping immunostaining with the neuronal marker acetylated tubulin (Figure 5.9-C), suggesting that like in mammals, Sema3A in zebrafish is expressed by neuronal cell bodies or axons in normal adult zebrafish brain. Co-labelling studies with Sema3A and *olig2*:DsRed-positive oligodendroglial cells in the zebrafish brain were negative.

Previous results from our laboratory have demonstrated that the number of OPCs present in an MS lesion inversely correlated with the density of cells expressing the chemorepellent Sema3A within the lesion (Boyd et al., 2013. In a model of focal LPC-induced demyelination in the mouse corpus callosum, an increase in Sema3A immunofluorescence staining at 3 days post lesion (and time point of maximal

demyelination), followed by decreasing Sema3A expression, which is limited to the lesion edge at 7 dpl. Sema3F expression within the lesion is also increased at 3dpl, however clears at a slower rate than Sema3A. At 14 dpl both Sema3A and 3F are absent from the lesion (Boyd et al., 2013). I therefore wondered whether Sema3A levels in the zebrafish optic nerve were also altered following LPC-induced demyelination. Indeed I observed a decreased Sema3A band at 110 kDa in western blot analysis of whole optic nerve lysates at early time points after LPC-induced demyelination (Figure 5.9-D,E). These results propose the hypothesis that following a demyelinating optic nerve lesion, endogenous Sema3A is reduced in the optic nerve to allow oligodendrocyte progenitor cell migration towards the lesion area (Figure 5.9-F) and subsequent remyelination.

Studies in our laboratory have shown that upon treatment with human recombinant Semaphorin 3A (rSema3A), the LPC-lesioned corpus callosum of mice did not remyelinate as effectively as in vehicle treated controls (Boyd et al., 2013). More detailed analysis demonstrated no change in cell death or oligodendrocyte proliferation and differentiation following rSema3A treatment, suggesting that the cause was indeed an inhibitory effect on oligodendrocyte precursor cell migration. To investigate whether similar mechanisms underpin zebrafish remyelination, I treated zebrafish with LPC-induced demyelinating lesions in the optic nerve with rSema3A. For the treatment time point I chose 8 days post lesion, as earlier characterisation of the demyelinating lesions showed that myelin and *olig2*:DsRed+ oligodendroglial cells were maximally reduced at this time point. Increasing numbers of *olig2*:DsRed+ cells in the lesion area after post-lesion day 8 in previous experiments suggested migration of *olig2*:DsRed+ cells into the lesion, and these were the ones I aimed to influence. In addition, endogenous Sema3A levels were also maximally reduced at 8 days after LPC as shown by the previous western bot. I then investigated the lesion area for *olig2*:DsRed+ oligodendroglial cells at 14 dpl, *MBP*:GFP+ cells at 21 dpl and electron microscopy at 28 dpl to assess effects on oligodendrocyte migration, differentiation and remyelination respectively (Figure 5.10-A). At 14 dpl the number of *olig2*:DsRed+ oligodendroglial cells in the lesion area was significantly reduced compared to vehicle treated zebrafish ($p<0.001$,

n=10, Mann Whitney-U test, Figure 5.10-B,C). The number of differentiated *MBP*:GFP+ oligodendrocytes in Sema3A treated zebrafish at 21 dpl was found not to be different to vehicle treated controls (Figure 5.10-D,E). This was a little surprising as a lower number of OPCs would have led to expect fewer differentiated oligodendrocytes. However, perhaps by 21dpl, the reduced chemorepellent effect of Sema3A allowed OPCs to migrate from around the treated optic nerve area and differentiate. Analysis of the lesion area by electron microscopy at 28 dpl showed that after treatment with rSema3A significantly less axons were remyelinated compared to vehicle treated animals (44.7% ± 10.18% myelinated axons compared to 89.9% ± 7.19%, mean ± SEM, $p<0.05$, n=5, Mann Whitney-U test, Figure 5.10-F,G). However, some unmyelinated small diameter axons were also observed in the lesioned optic nerve treated with rSema3A, which were reminiscent of re-growing axons and a possible indicator of axonal damage caused by toxicity of the treatment (Figure 5.10-G).

Taken together, these results suggest that perhaps some mechanisms underlying rodent remyelination may also be evident in zebrafish remyelination; however this is a hypothesis based on preliminary data only and would require more detailed analysis of the origin of endogenous Sema3A in adult zebrafish, possible signalling pathways involved in this remyelination process and putative effects of the rSema3A treatment on axons and other cells in the lesion area.

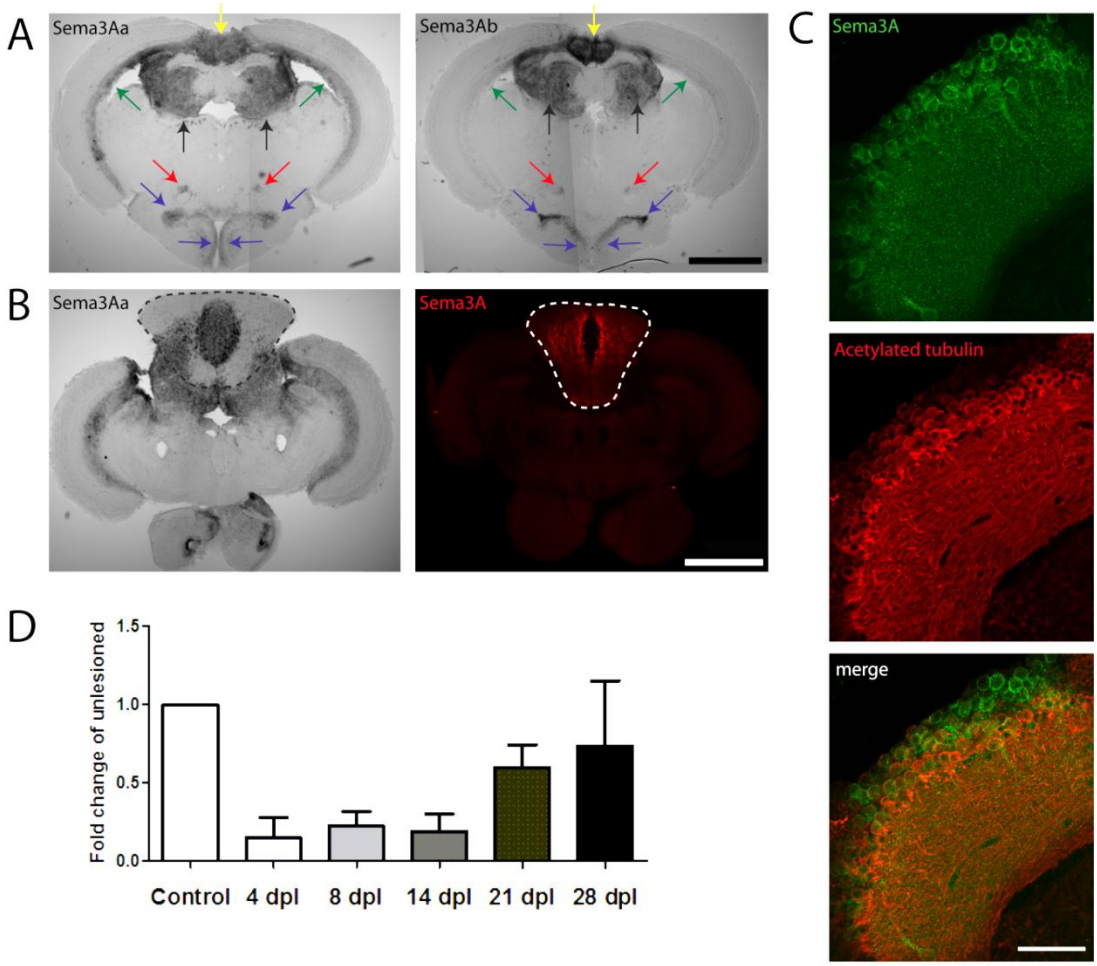

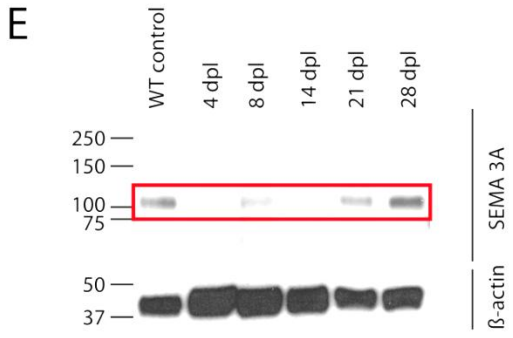

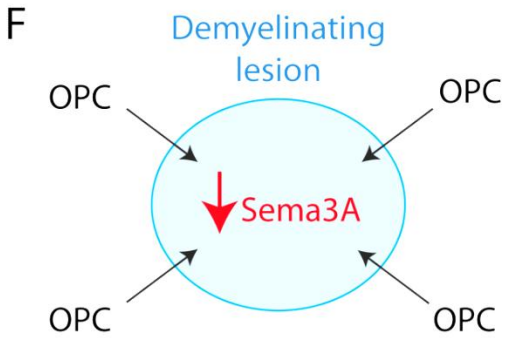

Figure 5.9: Endogenous Sema3A in zebrafish. (A) In cross sections of adult zebrafish brains Sema3Aa and 3Ab show overlapping in situ distribution patterns: Both Sema3Aa and 3Ab RNA is expressed in the tractus pretectomammilaris (red arrows), the ventral and dorsal zone of the periventricular hypothalamus (blue arrows), the periventricular granular zone (green arrows), the lateral valvula cerebelli (black arrows) and the torus longitudinalis (yellow arrow). (B) Overlapping staining of Sema3Aa RNA and anti-Sema3A antibody is observed in the cerebellum (marked area in brain cross sections). (C) Immunohistochemistry studies in cross sections show that Sema3A co-labels with neurons in the adult zebrafish brain. (D,E) A western blot and the quantification thereof show decreased levels of endogenous Sema3A (110kDa) at early time points after the lesion. (F) Schematic of hypothesis: Following demyelination, endogenous Sema3A is reduced to allow oligodendrocyte precursor cell (OPC) migration to the lesion area. Error bars represent mean ± SD. Scale bars: A,B = 500 µm, C = 100 µm.

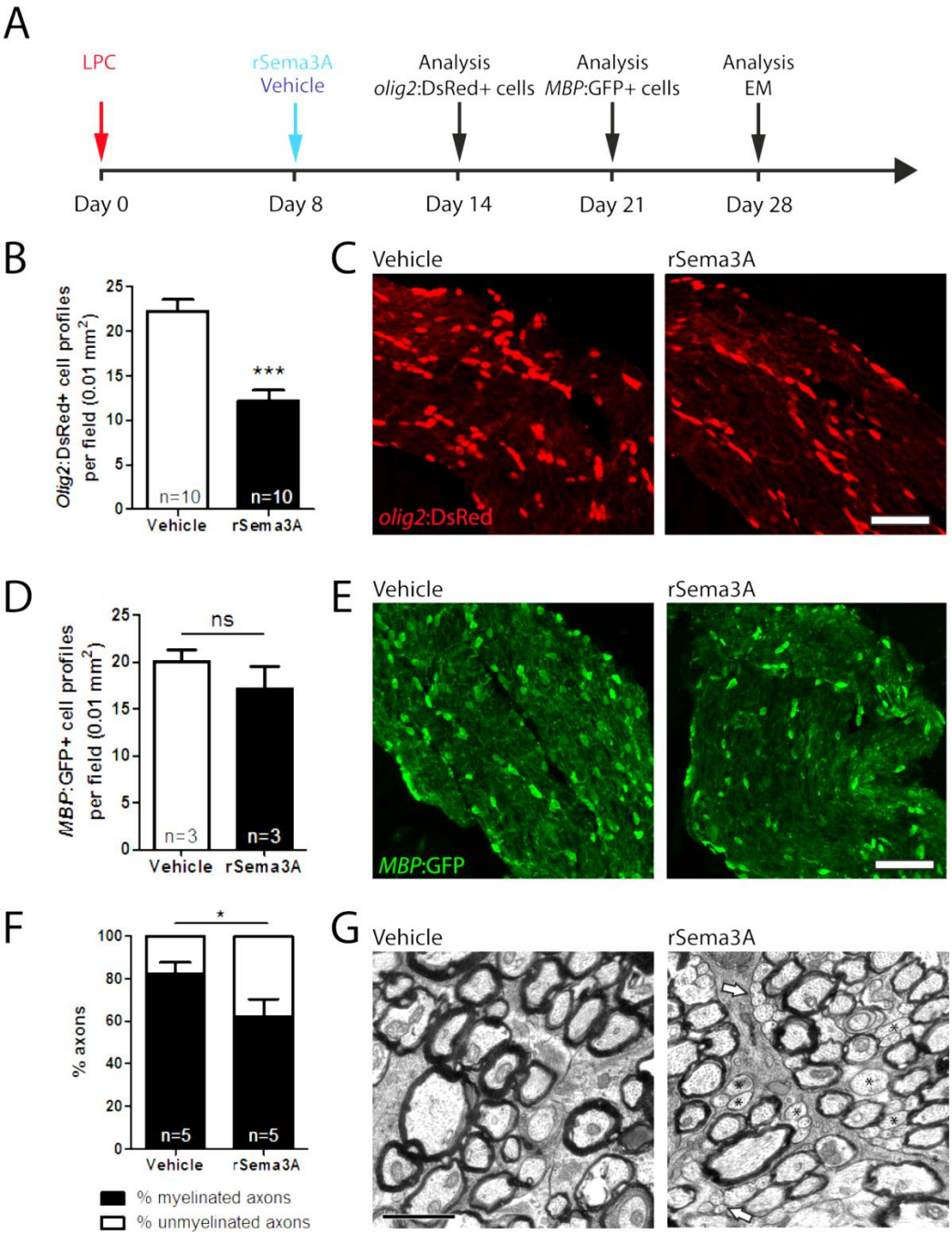

Figure 5.10: rSema3A treatment of lesioned optic nerve. (A) Schematic shows timeline of lesioning, treatment and analysis. (B) At 14 dpl *Olig2*:DsRed-positive oligodendroglial cells are reduced in the lesion area after rSema3A ($p<0.001$, n=10, Mann Whitney U-test). (C) Cryostat cross sections through the optic nerve lesion area at 14 dpl are representative of data shown in B. (D) At 21 dpl *MBP*:GFP-positive cells in the lesion area are not different after rSema3A treatment compared to vehicle treated controls. (E) Cryostat cross sections through the optic nerve lesion area at 21 dpl are representative of data shown in D. (F) At 28 dpl significantly fewer axons in the lesion site are myelinated after rSema3A treatment ($p<0.05$, n=5, Mann Whitney U-test). (G) Electron microscopic analysis of cross sections through the lesion site at 28 dpl show more unmyelinated axons (asterisks) after rSema3A treatment. Small diameter axons were also observed (arrows), indicating possible axon damage. Error bars represent mean ± SEM. Scale bars: C,E = 100 µm, G = 1 µm.

5.3 Discussion

Various experimental animal models are used to investigate pathological mechanisms underpinning demyelinating diseases and to identify targets for potential therapeutic intervention. It has been well established that zebrafish are extremely capable of regenerating various parts of their central nervous system (Becker and Becker, 2008; Fimbel et al., 2007; Kroehne et al., 2011), and as knowledge around myelin regeneration in this model organism is limited, I sought to characterise the time frame of de- and remyelination in focal demyelinating lesions in the adult zebrafish optic nerve as well as explore possible mechanisms of repair.

Remyelination of focal demyelinating lesions in the zebrafish optic nerve

Using this newly generated model of LPC-induced demyelination in the adult zebrafish optic nerve, I was able to show that maximal demyelination marked by the significant reduction in immunolabelling of the tight junction myelin protein Claudin k was present at 8 dpl and occurred simultaneously with a decrease of oligodendrocytes in the lesion site and an activation of microglia. Within 4 weeks, returning immunohistochemical markers for myelin and oligodendroglial cells suggested that the myelin had been repaired; and also microglia number had returned to levels comparable to controls. This time course is similar to that found in mammals following focal LPC-induced lesions (Foster et al., 1980; Hall, 1973), although mice show maximum demyelination already at 3 days following LPC injection and zebrafish only at 8 dpl; this might be due to temperature differences, as fish are kept at standard temperatures of 26.5°C. However both mice and zebrafish show complete remyelination at 28 dpl and this might possibly suggest homologous repair mechanisms between species. As zebrafish are more cost-effective and easier to handle than mice, and in addition have the benefit of easy transgenesis, rapid development and possibility of live imaging, it could be useful to validate candidate drugs from myelination screens in zebrafish larvae (Buckley et

al., 2010; Pogoda et al., 2006) in this adult zebrafish demyelination model to assess possible effects on remyelination (rather than developmental myelination) prior to moving onto mammalian model organisms.

Electron microscopic analysis of de- and remyelination studies is important to assess the quality and thickness of the myelin sheath and to determine the extent of myelin repair following injury. A useful tool in assessing myelin sheath thickness is the myelination ratio or G-ratio, as this takes into account the size of the axon, and is calculated by dividing the diameter of the axon by the diameter of the axon and its myelin sheath. Using electron microscopic analysis and G-ratios, it has been shown that remyelination in lesions of MS patients is associated with thinner myelin (Perier and Gregoire, 1965; Prineas and Connell, 1979), and this incomplete myelin repair is also reflected in rodent models of demyelination (Blakemore and Franklin, 2008). I could show that zebrafish are able to remyelinate their optic nerve with normal myelin thickness; this is a novel finding. Studies in the closely related goldfish demonstrate that regenerated fibres following optic nerve crush also regain their myelin sheath, however whether the regenerated myelin has the same thickness as pre-lesion is not known (Nona et al., 1992).

By comparison to the well remyelinated young zebrafish optic nerve, the same demyelinating lesions in the optic nerve of aged zebrafish led to remyelinated fibres with thinner myelin (higher G-ratios) but not a higher proportion of unmyelinated axons. It is unclear if old zebrafish are not able to remyelinate with normal thickness myelin or whether remyelination is just slower and a longer regenerative time period would result in full thickness remyelination. Nevertheless, this suggests a difference in ability to remyelinate between young and old zebrafish and supports the notion that regenerative capacity declines with age as has been investigated in various rodent models (Hampton et al., 2012; Shields et al., 1999). While regenerative capacity declines with age, remyelination failure is also thought to be a mechanistic problem as MS mostly occurs in young adults and neonatal demyelinating diseases like periventricular white matter injury also present with insufficient myelin repair (Segovia et al., 2008). It would therefore be interesting to

compare the highly effective mechanisms of remyelination in young zebrafish to a system in which myelin is not fully regenerated such as rodents or aged fish, and to establish differences in signalling and/or mechanism that could be responsible for decreased myelin repair capacity.

Although inability to remyelinate fully is not only dependent on age, it has become clear that general regeneration ability declines with age. In an attempt to understand the particular relationship between remyelination and ageing, research has focussed around the three possible stages which could impair successful remyelination in an aged organism. For successful remyelination to take place, OPCs need to migrate to the lesion site and differentiate. It has been suggested that in aged animals, fewer OPCs available for recruitment, slower recruitment rate or differentiation rate may be affected. Sim and colleagues investigated these questions in a model with toxin-induced demyelinating lesions in the caudal cerebellar peduncles (CCP) (Sim et al., 2002). When they compared the absolute numbers of OPCs available for recruitment in unlesioned young and old rats, they found no change in total number of OPCs expressing PDGF-α-receptor mRNA suggesting that the same number of OPCs is available for recruitment in both age groups. However by investigating OPC density in the lesion site, which was decreased in aged rats, and appearance of markers for differentiated oligodendrocytes, which appeared later in aged rats, they were able to show that changes in remyelination of old animals is most likely due to slower OPC recruitment and differentiation rate. Moreover, parabiosis experiments in which old mice were joined to young ones so that they shared the same blood supply demonstrated that remyelination in a young and an old mouse is equally effective if the old mouse had access to the environment of the young one. Ruckh et al. postulated that these effects might be due to changes in macrophage recruitment to the lesion site, which is decreased in old mice, and moreover they were able to show that mice lacking the chemokine receptor CCR2, which is required for macrophage chemotaxis, exhibited mildly abrogated remyelination (Ruckh et al., 2012). These studies open up possible pathways around macrophage recruitment, inflammatory signalling and oligodendrocyte differentiation that might be impaired

in successful remyelination and could potentially be targeted in therapeutic interventions. It would therefore be interesting to investigate whether microglia/macrophages recruitment to the lesion site in aged zebrafish is also altered, and might therefore explain the changes observed in remyelination.

Origin of remyelinating cells

The origin of remyelinating cells in the central nervous system has been focus of much research over recent years and is still not entirely clear. It has been shown that a minority of oligodendroglial cells survive a demyelinating insult, however as differentiated oligodendrocytes from both endogenous or transplanted sources appear incapable of remyelination (Keirstead and Blakemore, 1997; Targett et al., 1996) it is thought that remyelinating cells must originate from endogenous progenitor cells (Gensert and Goldman, 1997), which could either come from progenitor cells in the white matter around the lesion or from stem cell niches such as the periventricular progenitor zone. Recent studies using Cre-lox fate mapping analysis in mice, have shown that a widely distributed population of progenitors give rise to almost all remyelinating cells in artificially induced demyelinating lesions in the adult CNS, and that PDGFα/NG2+ progenitors can generate remyelinating Schwann cells, which contribute to CNS remyelination in mice (Zawadzka et al., 2010). To further investigate the origin of remyelinating cells in my zebrafish model, I used proliferation markers to assess proliferation of local and distant oligodendroglial cells, but also explored the possibility of contribution from other myelinating cells such as Schwann cells and cells involved in developmental myelination.

For this I performed pulse-chase experiments with the proliferation marker EdU, which is incorporated and retained by any dividing cell. In an attempt to label most proliferating cells, the fish received daily intraperitoneal EdU injections for 1 week shortly after induction of the optic nerve lesion. At 28 dpl, I found that approximately 10% of remyelinating *olig2*:DsRed+ oligodendrocytes in the lesion

area had incorporated the proliferation marker, suggesting that they were newly generated. These results are similar to those of my zebrafish optic nerve regeneration studies in chapter 3, but do not elucidate from where these newly generated cells originate. They could come from the optic nerve surrounding the lesion, but this is unlikely as I found no co-labelling of *olig2*:DsRed+ oligodendroglial cells with PCNA (proliferating cell nuclear antigen), in cross section of the optic nerve at various time points after the lesion, making it unlikely to have missed the time of OPC proliferation. This suggests that proliferation and recruitment of oligodendrocyte precursors directly surrounding the lesion are likely not involved in optic nerve remyelination and this is different to LPC-induced lesions in the rat spinal cord which show decreased remyelination if the surrounding OPCs have been destroyed by irradiation (Franklin et al., 1997). As the optic nerve is close to the progenitor zones within the brain, it could therefore be possible that while remyelination in the distant spinal cord requires local oligodendrocyte progenitors, optic nerve lesions could trigger OPC recruitment from the brain. It is not known whether oligodendrocytes in zebrafish can only originate from progenitor cells in the ventricular zone or whether parenchymal progenitor cells, such as NG2+ cells exist in zebrafish. A slowly dividing subpopulation of oligodendroglial lineage cells in the zebrafish telencephalon parenchyma has been found, which could potentially give rise to mature oligodendrocytes (Marz et al., 2010), indicting similarities to the NG2+ cells in mammals.

To further investigate the origin of remyelinating cells in the zebrafish optic nerve, I considered more distant areas, such as known proliferative zones in the brain as sources for the remyelinating oligodendrocytes. It has been well established that zebrafish are able to regenerate various CNS tissues and the reason for this has been attributed to a wide distribution of stem cell niches in the zebrafish brain (Kizil et al., 2012). I therefore investigated proliferation of progenitor cells in the periventricular progenitor zone in adult zebrafish following the LPC-induced demyelinating optic nerve lesion and observed an increased number of PCNA+/olig2+ progenitor cells at 8 dpl. This leads to the hypothesis that following the optic nerve lesion, progenitor cells in the brain proliferate, migrate to the optic

nerve and remyelinate the lesion site. This hypothesis is supported by the finding that in a model of demyelination in the corpus callosum in mice, following a demyelinating lesion, progenitor cells around the ventricle proliferate and migrate towards the lesion area (Nait-Oumesmar et al., 1999) and that in post-mortem brain tissue from MS patients an increased density and proliferation of GFAP+/PSA-NCAM+ radial glia-derived progenitor cells is observed in the subventricular granular zone (Nait-Oumesmar et al., 2007). While it is unknown whether precursor cells in zebrafish would be able to migrate the distance between the periventricular progenitor zone and the lesion site (approximately 500-600 µm), I found no increase in local oligodendrocyte proliferation around the lesion area suggesting that the cells must originate from more distant sources. Recent research shows that inflammation in the zebrafish CNS initiates a neuroregenerative response by inducing reactive proliferation of S100ß-positive progenitor cells in the periventricular progenitor zone, and moreover, this proliferative response was dampened upon administration of the immunosuppressant dexamethasone (Kyritsis et al., 2012). It has also been demonstrated that rodent and human OPCs and neural stem cells express many cytokine receptors; their ligands are found to be upregulated in experimental demyelinating lesions in rodents and MS tissue, suggesting that there may be a chemotactic/trophic response resulting in proliferation and migration of the progenitors (Carbajal et al., 2010; Dziembowska et al., 2005; Kelland et al., 2011; Nguyen and Stangel, 2001). Hence it would be interesting to investigate the role of inflammation in optic nerve remyelination and whether inflammatory signalling could be responsible for proliferation in the periventricular progenitor zone in response to injury. Several findings throughout my analysis would support this theory: Firstly, I found up- regulation of microglia along the entire optic tract of the lesioned side not just local to the lesion (Figure 5.11-A,B), and secondly the progenitor cells in the zebrafish brain possess long processes that are in close contact with the optic projection (Figure 5.11-A,C) and it would therefore be possible that they could directly respond to inflammatory signals with proliferation and migration to the lesion site. Furthermore, it has been demonstrated that LPC-induced demyelination in the mouse corpus callosum

resulted in proliferation of progenitor cells in the subventricular granular zone (SVZ) in young but not old animals (Decker et al., 2002), indicating that this potential mechanism of OPC recruitment is impaired with age and could explain a possible relationship between remyelinating and ageing. To assess this signalling mechanism more closely, I conducted an experiment for which I injected GFP-expressing lentivirus into the ventricle of lesioned zebrafish, assuming that periventricular progenitor cells would be infected and I could trace their proliferation and migration to the lesion site; however I found that progenitor cells did not take up the lentivirus, which might have been due to a promoter not recognised by zebrafish. All of these results taken together suggest that although the exact signalling mechanisms around OPC proliferation and migration remain unclear, a hypothesis involving OPC response in zebrafish to inflammatory cytokines may be plausible.

However, as I was only able to label ~10% of remyelinating oligodendrocytes with the proliferation marker EdU in my zebrafish demyelination model, this also raises the question where the remaining 90% of remyelination cells originate from and there are several possible explanations.

Firstly, Easter and colleagues showed that the goldfish optic nerve always contains a well-defined area of small calibre unmyelinated fibres, which originate from the peripheral edges of the retina and are the site where continuous axonal growth and myelination occurs throughout fish life (Easter et al., 1984; Easter et al., 1981). In the adult goldfish, this area occupies less than 1% of the optic nerve cross section (Easter et al., 1981). As this area must contain oligodendroglial cells that are capable of myelinating new axons, it raises the suggestion that perhaps these cells are involved in remyelination of artificially demyelinated optic nerve lesions. Throughout my studies, I also observed this well-defined area in electron microscopic cross sections of the zebrafish optic nerve (Figure 5.12). However in comparison to the demyelinating lesions, which would normally affect ~80% of the nerve cross section at the widest diameter, I found that this unmyelinated area was

very small and usually located on the nerve edge distant to the lesion site. As such it is questionable whether the cells involved in the myelination of these newly grown axons would be capable of remyelinating the entire experimentally demyelinated lesion. In addition, I have shown a loss of *olig2*:DsRed-positive cells, and it is possible that this loss also included some cells from the unmyelinated area. It is not clear which cells exactly myelinate the unmyelinated area and whether they are more progenitor-like and capable of proliferating, however it seems unlikely that they would be exclusively responsible for repairing the myelin in demyelinated lesion, suggesting that remyelinating cells must come from elsewhere. It would be difficult to test the presence of these cells as they would express the same oligodendroglial makers as other oligodendrocytes in the optic nerve. It could perhaps be useful to investigate distribution of oligodendrocyte progenitor cells (eg. olig2-positive but negative for MBP, a marker of differentiated oligodendrocytes) in cross sections of the optic nerve to see whether more progenitor cells are located around the physiologically unmyelinated area.

Secondly, studies in the closely related goldfish investigating the origin of myelinating oligodendrocytes in the regenerated optic nerve described no apoptosis and new generation of oligodendrocyte following optic nerve crush. Rather, it was thought that myelinating oligodendrocytes present around the lesion area might be able to undergo de-differentiation into precursor cells and re-differentiate into new mature oligodendrocytes capable of forming myelin sheaths (Ankerhold and Stuermer, 1999). By using a dye-labelling protocol, which allows the visualisation of single cells, they could show that some mature oligodendrocytes surviving in the lesion site lost their multiple processes and appeared more progenitor-like. As remyelination took place, these cells would again take on a more complex morphology with numerous processes reminiscent of internodes. Similarly experiments using primary mixed glial cultures demonstrated possible successful de-differentiation of oligodendroglial cells after treatment with basic fibroblast growth factor as there was an increase in O2A oligodendrocyte progenitor cells and a decrease of oligodendrocytes expressing markers of differentiation (Grinspan et al., 1993). These findings raise the possibility that de- and re-differentiation of

mature surviving oligodendrocytes might also contribute to myelin repair following focal injury, and could explain why I only observed EdU-labelling in 10% of oligodendroglial cells in the remyelinated lesions especially if these cells de-differentiate but do not proliferate, perhaps as they may not de-differentiate to an precursor state. It is also not clear, whether de-differentiation would be compatible with my finding of reduced *olig2*:DsRed-positive cells in the lesion area, as this transcription factor is expressed very early in the oligodendroglial lineage and would suggest de-differentiation to an early precursor state. To investigate this possibility, it could be useful to explore makers such as PDGF-α receptor, NG2 and nestin, which are known to label precursor cells.

It has also been shown that peripheral myelinating Schwann cells may be involved in CNS remyelination as they were observed in the regenerated goldfish optic nerve (Nona et al., 1992) and in rodent experimental de/remyelination models (Black et al., 2006; Blakemore, 1975; Felts and Smith, 1992; Gilson and Blakemore, 2002). This might suggest that peripheral myelinating Schwann cells can invade the CNS and aid remyelination. I investigated this possibility by making use of the transgenic zebrafish line *Tg*(*FoxD3:GFP*), which labels all neural crest-derived cells. At 28 dpl, when remyelination was complete according to myelin markers and electron microscopic analysis, I found no labelled cells in the remyelinated optic nerve, whereas labelled cells were readily detectable in peripheral nerves in the same animals. As such, neural crest derived cells are not likely to be involved in zebrafish optic nerve remyelination.

Lastly, technical aspects also have to be taken into account as the Edu/BrdU labelling protocols are limited by the bioavailability of the compounds and the toxicity of the anaesthetising agent to the zebrafish. Studies show that intravenously applied EdU has a half-life of less than one hour and raises questions about the effective labelling of cells dividing over a long time period (Cheraghali et al., 1995). To reliably label all proliferating cells, EdU would need to be injected intraperitoneally multiple times per day throughout the period of interest, but as fish tend to succumb to frequent use of anaesthetising agents this is experimentally

undesirable. Alternatively, the proliferation marker could also be administered by letting the fish swim in a diluted concentration; however in our laboratory this technique has been previously associated with weak EdU labelling.

In summary, although much progress has been made in other experimental models to determine the origin of remyelinating cells, further experiments are needed, especially to evaluate if all cells come from the same endogenous source and whether they are different between different areas of the central nervous system and even within species. For studies in the zebrafish it would therefore be helpful to develop a transgenic zebrafish line allowing lineage tracing of oligodendroglial cells following demyelinating lesions. For example, the photoactivatable fluorescent protein Kaede could be expressed under a myelinating oligodendrocyte specific promoter, eg. myelin protein zero. By placing a demyelinating lesion and photoconverting the Kaede in all existing myelinating oligodendrocytes in the optic nerve into a different fluorescent colour, it would presumably be possible to determine whether the remyelinating oligodendrocytes were newly generated (ie came from precursors and expressed the original, non-photoconverted transgene) or were a product of de- and re-differentiation (ie expressed the different photoconverted transgene). Such lines have been developed for selective labelling of neuronal networks in zebrafish (Sato et al., 2006), however to generate a specific line expressing Kaede under the oligodendrocyte specific promoter is difficult as variegated transgene expression would need to be absolutely excluded to avoid confusion between new and old myelinating cells. This technique may also bear limitations, such as insufficient UV-light needed for photo-conversion passing through the non-transparent adult zebrafish skull reach cells in the brain, or the de-differentiation of oligodendrocytes to very early progenitor stages where Kaede expression may be turned off, and then on re-differentiation the initial transgene would be re-expressed in the non-photoactivated colour. To bypass this problem, one could perhaps design a transgenic line in which a myelin marker, eg myelin basic protein, drives red fluorescent protein (RFP) and Cre expression, which in turn would excise a floxed stop-cassette in front of an *actin* promoter (or another general house-keeping gene) driving GFP expression. Under normal circumstances,

transgenic fish containing this construct should have RFP-labelled myelinating oligodendrocytes. Upon placement of the lesion, tamoxifen administration would lead to Cre expression and excision of the stop cassette, resulting in RFP and GFP-positive newly generated oligodendrocytes. This however, works on the principle that MBP is turned over very slowly in already myelinating cells, so after Cre expression the pre-existing myelinating cells would only express a small amount of GFP or none at all. Lineage tracing using the Cre/loxP system has already been successfully used in zebrafish to trace Müller glia in the retina as they undergo reprogramming and proliferation following injury (Ramachandran et al., 2010; Ramachandran et al., 2012).

Manipulation of remyelination with human recombinant Semaphorin 3A

The axonal guidance molecules Semaphorin 3A and 3F (Sema3A/3F) have a well described role in the recruitment of oligodendrocyte precursor cells in development, as Sema3A repels and Sema3F attracts OPCs (Spassky et al., 2002; Sugimoto et al., 2001), and it has been suggested that they might also occupy a key function in OPC recruitment during remyelination. Transcripts of *Sema3A* and *3F* were found up-regulated in lesions within post-mortem brain tissue of MS patients and also in a rodent demyelination model, with increased expression of Sema3F and Sema3A after the lesion (Williams et al., 2007). The semaphorin class 3 receptors neuropilins and plexins have also been identified on oligodendrocyte precursor cells and studies in an adult murine demyelination model demonstrated that lentiviral induced over-expression of Sema3A in lesions impaired OPC recruitment, while Sema3F accelerated OPC migration and remyelination rate (Piaton et al., 2011). Alignment studies of human and zebrafish Semaphorin 3A show high amino acid sequence identity (human Sema3A is 64.9% identical/77.3% similar to zebrafish Sema3Aa and 75.1% identical/85.2% similar to zebrafish Sema3Ab using EMBL clustal alignment analysis), which proposes evolutionary conservation and possibly similar signalling mechanisms of this protein in both species. To investigate the role of Sema3A in zebrafish optic nerve remyelination, I analysed Sema3A levels in

whole optic nerve lysates by western blot analysis. For this I used an antibody, which is commonly used in rodent studies to detect Sema3A. In an alignment of the antigen peptide recognised by the anti-Sema3A antibody and the zebrafish homologues of Sema3A, the sequences mostly overlapped and suggested that the antibody would most likely also recognise zebrafish Sema3A. In the western blot analysis, I observed a specific single band at 110kDa marked by the anti-Sema3A antibody, which was reduced at 4, 8 and 14 days post lesion. These findings are similar to observations made in our laboratory in rodent models of experimental demyelination. In rodent demyelinating lesions Sema3A protein was detected at 3 dpl, the time point of maximal demyelination, much reduced and limited to the lesion edge at 7 dpl and not detectable at 14 dpl (Boyd et al., 2013). It has been shown that in this rodent model migration of OPCs into the lesion area occurs from around post-lesion day 6, with their subsequent differentiation taking place at 10-14 dpl (Huang et al., 2011b). This suggests that the initial Sema3A expression response is suppressed at around the time that OPC migration into the lesion begins, perhaps correlating to the success of OPC recruitment and remyelination in rodents. My findings in zebrafish also support a hypothesis based around OPC recruitment, whereby Sema3A levels in the zebrafish optic nerve reduce to allow OPC migration towards the lesion area. Hence, my results might indicate that some remyelination mechanisms in zebrafish are perhaps homologous to those observed in mammals, allowing experimental demyelination in zebrafish to be used for investigation and identification of therapeutic targets to aid remyelination.

To further examine a possible role of Sema3A zebrafish remyelination I treated lesioned animals with human recombinant Semaphorin 3A (rSema3A) and found a decreased number of *olig2*:DsRed-positive oligodendroglial cells in the lesion area after treatment compared to vehicle treated controls at 14 dpl and fewer myelinated axons at 28 dpl. This might indicate a repelling effect on the migration of oligodendrocytes as described in previous studies, or could also be due to decreased cell proliferation, which has not been previously associated with Sema3A, or toxic effects. To exclude cell death, I attempted approaches including TUNEL and various anti-activated caspase 3 antibodies, but could not get these

protocols to work sufficiently in cryostat sections of zebrafish optic nerve. As Sema3A has also been associated with neuronal toxicity (Yasuhara et al., 2005), further experiments including neuronal tracer experiments to assess axonal damage could give valuable insight into the effects of exogenous Sema3A in zebrafish. Small axons reminiscent of re-growing axons observed in electron microscopy images suggest that axon damage might have occurred following rSema3A treatment; it would therefore be useful to test different treatment doses. To validate the effects of Sema3A on OPC migration following demyelinating lesions, it would be crucial to test whether Sema3A also exhibits effects on OPCs without a demyelinating lesion. Further it could be helpful to determine the dose of rSema3A needed to reach concentrations comparable to endogenous levels found in an unlesioned optic nerve; this could be achieved by treating optic nerve with different doses of rSema3A and determining Sema3A levels by whole optic nerve lysates in western blot. And lastly, one would need to exclude the effect of rSema3A treatment on cell survival, proliferation and differentiation to evaluate whether Sema3A solely influences OPC migration. It might also be useful to determine whether Sema3A receptors are expressed by oligodendrocytes and how they are regulated during optic nerve myelination.

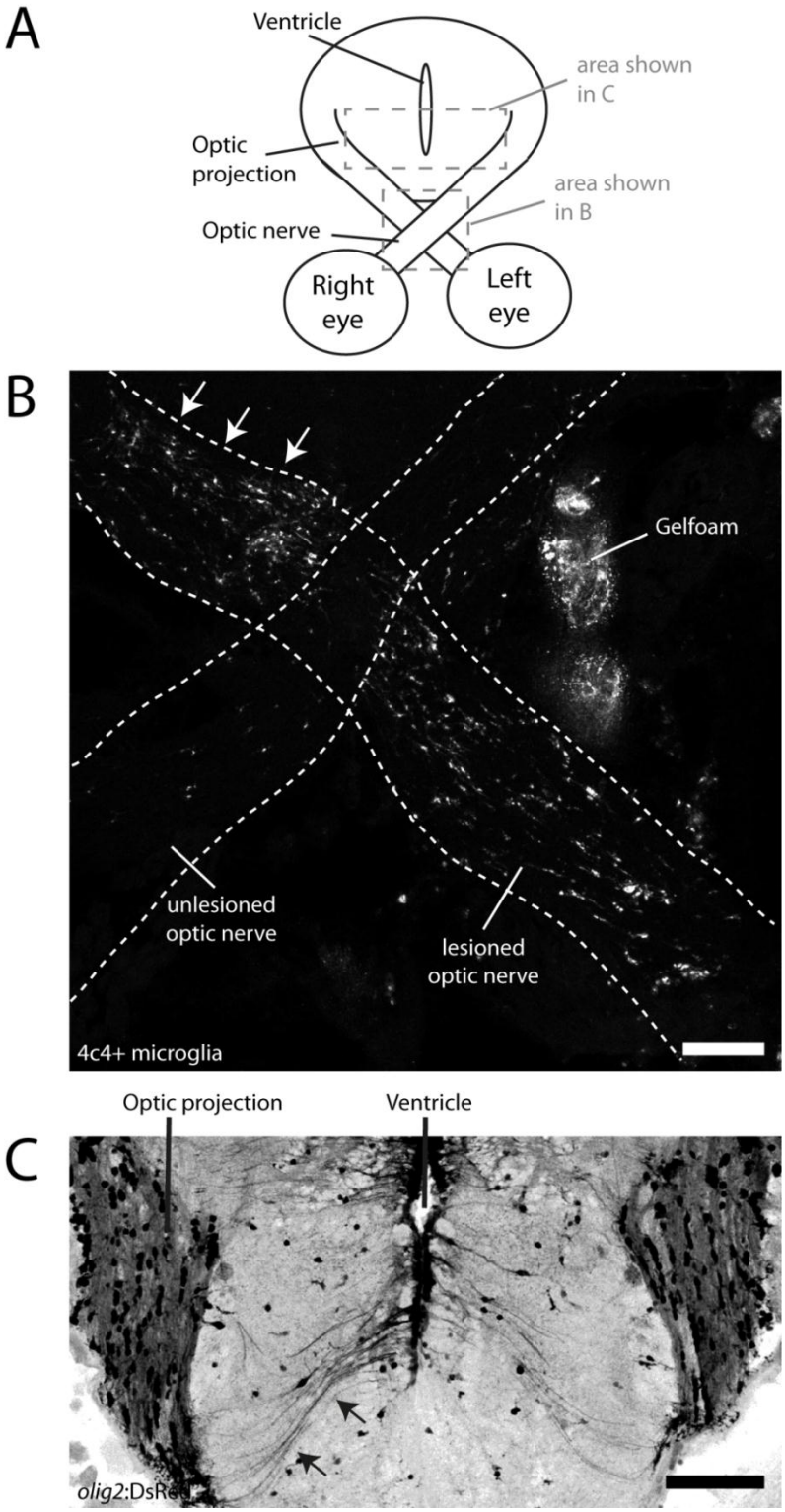

Figure 5.11: Microglia and ventricular progenitor cells following LPC-induced optic nerve demyelination. (A) Schematic shows location of images presented in B and C. (B) In a cross section of adult zebrafish optic chiasm at 8 dpl, an increase of microglia in around the lesion site and in the optic tract (arrows) is observed brains. (C) A cross sections of adult zebrafish brain show *olig2*:DsRed+ progenitor cells in the periventricular progenitor zone with long processes extending right up to the optic projection. The fluorescence was inverted to allow easier visualisation of the cell processes. Scale bar: B,C = 100 µm.

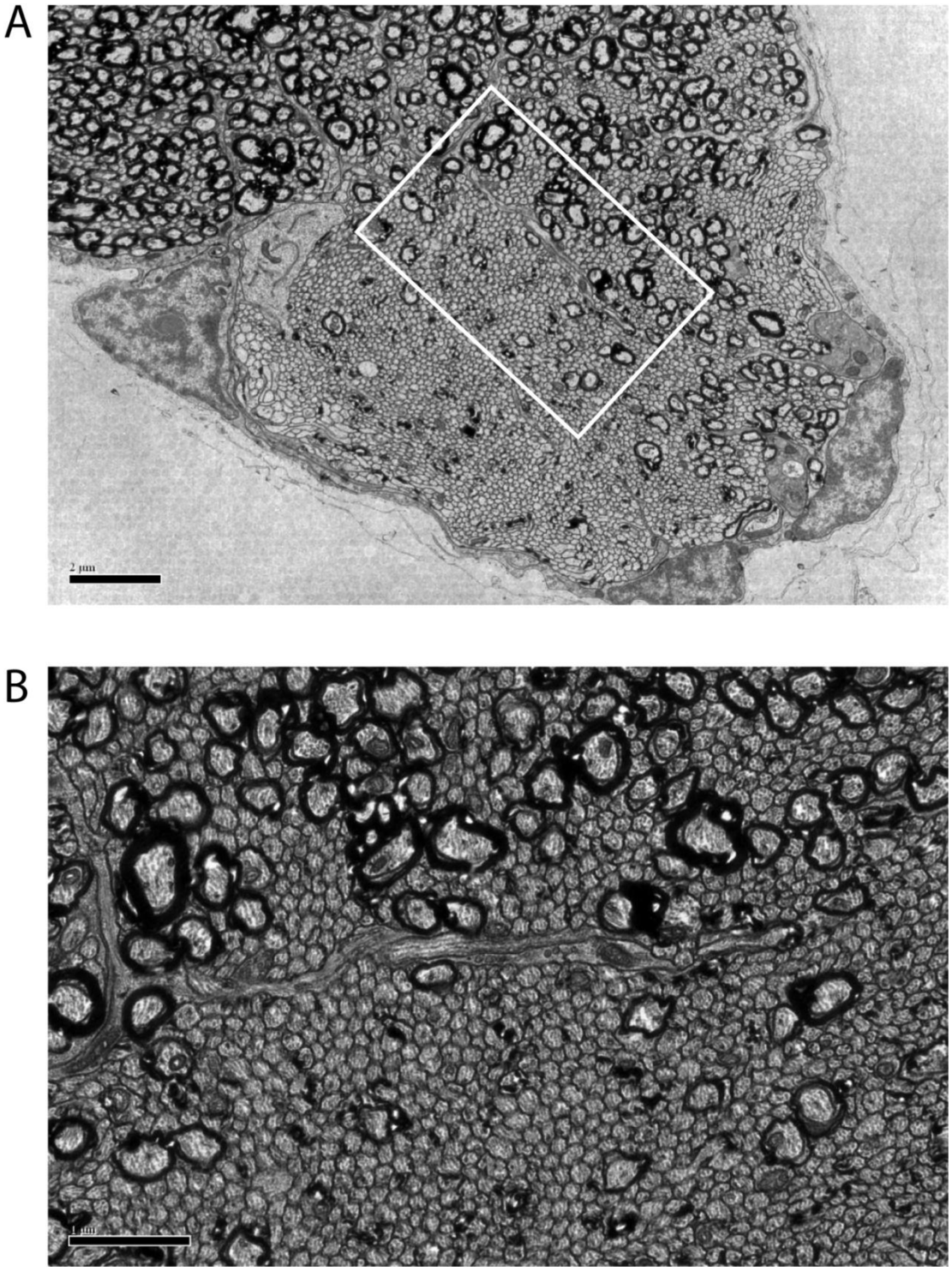

Figure 5.12: Unmyelinated area zebrafish optic nerve. (A) In electron microscopic analysis of optic nerve cross sections, a well-defined area of unmyelinated axons can be observed. In the closely related goldfish, this area occupies less than 1% of the cross section through the optic nerve (Easter et al., 1981). (B) Higher magnification of box in A. Scale bars: A = 1 µm, B = 2 µm.

CHAPTER 6 – Discussion

6.1 Zebrafish as a model to study demyelinating disease

Multiple sclerosis is an intriguing disease with no curative treatments and many experimental models have been developed to study various aspects of multiple sclerosis ranging from disease pathology and correlation with imaging modalities to targets for therapeutic intervention. These models include toxin-mediated demyelination, where locally applied myelinotoxic agents such as ethidium bromide or LPC cause focal demyelination in the spinal cord or brain in experimental animals including rodents, cats and primates (Blakemore, 1982; Hall, 1972; Woodruff and Franklin, 1999). In another model the cuprizone diet leads to demyelination in major myelinated tracts of the rodent brain (Blakemore, 1973a). The value of these toxin-mediated demyelination models lies mostly in their regenerative aspect, as the focal lesions remyelinate several weeks after the demyelinating insult by ethidium bromide or LPC or following cessation of the cuprizone diet with a known time course (Blakemore, 1973b; Ludwin, 1978). These models lend themselves to the exploration of myelin repair mechanisms, including the origin of remyelinating cells and efficiency of remyelination. As multiple sclerosis is thought to be immune mediated, demyelination models with viral- and auto-immune induced demyelination are studied for further understanding of disease pathology and more specifically to model immune cells within MS lesions. Murine models using Theiler virus-induced encephalomyelitis mirrors some immunological aspects of MS by presenting with chronic inflammation in the white and grey matter and resulting demyelination (reviewed in Oleszak et al., 1995). In contrast, experimental autoimmune encephalomyelitis (EAE) is induced by injecting a CNS-specific myelin protein such as myelin associated glycoprotein (MAG) or myelin oligodendrocyte protein (MOG) with adjuvants and mimics primarily the multifocal presentation of MS and its different clinical stages, though most changes occur in spinal cord or

brainstem and only rarely affect the hemispheres (reviewed in Glynn and Linington, 1989). As such these models have been used extensively to study the role of inflammatory cells and cytokines in MS pathology and to identify immunomodulatory targets for possible therapeutic intervention.

It has been previously suggested that zebrafish could potentially also be very useful in modelling demyelinating disease due to their transparency and rapid development at the larval stage (Buckley et al., 2008). While the myelin composition of fish is also similar to mammals with the major exception that myelin protein zero is found in the zebrafish CNS, it is not clear that the actual process of myelin formation is homologous, which is essential when attempting to model a human disease in animals. Studies investigating genes involved in regulating myelin formation in zebrafish suggest conservation of mechanisms between mammals and zebrafish (for examples see Kucenas et al., 2008; Park and Appel, 2003; Takada et al., 2010) and advances are being made constantly to understand this further. Live imaging in transgenic zebrafish larvae has revealed that myelinating oligodendroglial cells go through the same stages of axon glial contact formation and process extension as rodent oligodendrocytes *in vitro*, and this is could mean that homologous processes are likely involved (Czopka and Lyons, 2011). As such, this model platform may be useful to study the physiological processes of myelination. Moreover, zebrafish larvae have been successfully used to visualise myelin repair by oligodendrocytes. In zebrafish larvae expressing membrane-bound GFP under the oligodendrocyte specific promoter nkx2.2, laser ablation of myelinating oligodendrocytes resulted in compensation by neighbouring cells, which quickly extended new processes and migrated to the lesioned area (Kirby et al., 2006). Ablation over several muscle segments showed that oligodendrocyte precursor cells from not affected areas were capable of responding to the insult by migration to the lesion site. This highlights the importance for model organisms such as zebrafish, which bear the benefit of a transparent larval stage and are therefore suitable for *in vivo* live imaging. Similarly, I have shown in this thesis that by using an inducible genetic cell ablation approach, it is possible to specifically

ablate myelinating cells in the developing zebrafish, and that this system is able to generate new oligodendrocytes following the insult. These results are also consistent with findings in an experimental model of targeted genetic oligodendrocyte ablation in *Xenopus laevis* (Kaya et al., 2012).

These approaches to visualise oligodendrocyte response to injury in fish all have the common derivative of working with developing systems, however it is critical to differentiate between de novo myelination of developing axons and remyelination of ones that already were myelinated once, as developmental myelination capacity and mechanisms may be different to those implied during adult myelin repair. This difficulty might be overcome in models using developmental stages by measuring the rate of regeneration and comparing it to the rate of normal development, but could on a molecular level still involve developmental signals which may not be active or relevant in remyelination of the adult CNS. I therefore sought to develop experimental demyelinating lesions in adult zebrafish to study the events following myelin injury in a system in which developmental myelination is largely completed and which could be potentially useful to for *in vivo* live imaging of remyelination on a cellular level and to identify potential therapeutic targets to aid remyelination in scenarios where this is insufficient.

For this, I firstly characterised a novel myelin protein, Claudin k, which was identified in a microarray screen investigating differential myelin gene expression in hypomyelinating zebrafish (Schaefer, 2009) and evaluated its use as a tool to label myelin in zebrafish. To date many myelin proteins in zebrafish have already been described and are used in zebrafish myelination studies; these include myelin basic protein, myelin protein zero and DM20, a short isoform of proteolipid protein. Studies show that RNA transcripts for these proteins were detected in oligodendrocytes in the CNS of zebrafish larvae from 2 days post fertilisation onwards (Bai et al., 2011; Brosamle and Halpern, 2002) similar to Claudin k, however a transgenic line with variegated membrane bound GFP expression in myelinating glia using the GAL4-UAS system allowed visualisation of single

myelinating oligodendrocytes at various stages of myelination as well as flexibility to generate new transgenic lines by crossing this line into other effector lines for specific cell ablation (Davison et al., 2007).

Claudin k is specifically expressed in tight junctions of myelinating cells of the central and peripheral nervous system in zebrafish and I have used the transgenic line *Tg(claudin k:GAL4,UAS:GFP)* and specific Claudin k antibodies to describe the events occurring during developmental myelination and myelin regeneration in more detail. By being a constituent of tight junctions within the myelin sheath, a major function of Claudin k is to closely join the several lamellae of myelin, and its clear localisation to Schmidt-Lanterman incisures, mesaxon and paranodal loops suggests that the majority of Claudin k-containing tight junctions are located in close proximity to the cytoplasmic channels, which show similar distribution (Velumian et al., 2011). This suggests a function in early myelination as myelin wraps are beginning to form and was further confirmed by time course studies and comparison to other myelin markers such as myelin basic protein and myelin protein zero indicating that Claudin k was one of the earliest detectable markers in myelinated structures in developing embryos. While it is not clear how the compact myelin sheath is actually formed, whether several layers are loosely wrapped around the axon and then all compact together, or whether it is an integrated process whereby the inner layers are already compacting as outer layers are being formed, high resolution live imaging of CNS myelin formation is beginning to help us understand this intricate process better (Ioannidou et al., 2012; Sobottka et al., 2011). Studies have suggested specific functions of other myelin proteins during the myelination process, in particular a role of myelin basic protein and myelin protein zero during myelin compaction (Baumann and Pham-Dinh, 2001; Hartline and Colman, 2007) and hence support the theory that there is a dynamic but distinct timeline along which myelination is achieved during development. Furthermore, my studies in the adult zebrafish visual system demonstrated a difference between markers expressed in “loose” and “compact” myelin wrappings with myelin protein zero clearly absent from the myelinated retinal fibre layer, which only contains non-

compacted myelin wraps (Schweitzer et al., 2007). Hence, Claudin k is useful for studying axon-glial interaction as it is expressed early and throughout all myelination stages during zebrafish development. To investigate whether Claudin k would also be useful as a marker of myelin regeneration in adult zebrafish, I performed regeneration studies of the adult zebrafish optic nerve. I observed a reduction of myelin immunofluorescence across the optic nerve following crush injury, which regenerated within 4 weeks and is similar to previous findings in related fish studies (Ankerhold and Stuermer, 1999), and further suggests that Claudin k is also useful to track and quantify myelin during regeneration. Moreover, a novel transgenic line expressing a membrane bound GFP under the *claudin k* promoter using the GAL4:UAS system allowed the observation of single myelinating cells during the process of optic nerve regeneration. The GFP-positive cells observed in the lesion area were of a simple bipolar morphology at early time points after the optic nerve crush and had multiple processes and a complex morphology at later stages during regeneration. These findings are indicative of oligodendroglial cell differentiation throughout the regeneration process and show that myelin regeneration following optic nerve crush in zebrafish is unlikely to involve Schwann cells, which have been shown to invade the regenerating optic nerve of goldfish (Nona et al., 1992). My studies also showed that approximately 25% of oligodendrocytes in the lesion site were newly generated as they incorporated the proliferation marker BrdU. This is different to findings in the goldfish, in which less than 10% of oligodendrocytes were newly generated and myelination was thought to be carried out by de- and re-differentiation of oligodendrocytes in the lesion area (Ankerhold and Stuermer, 1999). These findings highlight the opportunities of Claudin k to visualise cellular events during de- and remyelination.

In summary, my studies show that Claudin k is a reliable and quantifiable marker of myelin in zebrafish, which compares to other, previously described myelin markers in zebrafish such as myelin protein zero and myelin basic protein, with the advantage that the variegated expression within the transgenic line allows visualisation of single cells and the GAL4:UAS system gives some flexibility in terms of generating new lines.

6.2 Zebrafish remyelination – homology to mammals

Previous studies on myelin regeneration in the closely related goldfish involve axon severance, and therefore do not investigate remyelination per se but rather myelination in a regenerating environment (Ankerhold and Stuermer, 1999). Hence I sought to develop experimental focal demyelinating lesions in the adult zebrafish to specifically study changes associated with de- and remyelination and for this I used the myelin toxin LPC to induce focal demyelinating lesions, which is commonly used in rodent experimental models. After LPC-mediated demyelination in the zebrafish optic nerve, without concurrent axonal damage, I observed a clear reduction of both immunohistochemical markers for myelin and oligodendrocytes and a regeneration of these within 4 weeks. This is consistent with remyelination time courses described in rodent models of LPC-induced demyelination (Foster et al., 1980; Hall, 1973) and might possibly hint towards some similarities in the repair mechanisms**.**

While immunohistological studies give some indication of the time line of myelin repair, a more accurate measurement is the G-ratio, which takes into account the myelin thickness in relation to the axon diameter it surrounds. It has been shown that in remyelinated MS plaques, also called “shadow plaques”, the regenerated myelin is much thinner (and thus presents with a higher G-ratio) compared to the normal appearing white matter and these findings are also reflected in some rodent experimental models of MS (Blakemore and Franklin, 2008; Hampton et al., 2012). In my remyelination model in the adult zebrafish optic nerve, I found that while the relative myelin thickness of remyelinated fibres was not different to before demyelination in young zebrafish, aged zebrafish seem to lack this regenerative capacity and presented with thinner myelin sheaths after 4 weeks of regeneration. This raises questions around whether old zebrafish truly remyelinate insufficiently or whether the process is just slower and a longer regenerative period would result in normal myelin sheath regeneration, given their generally high regeneration capacity. Studies in young and aged mice report similar findings, and that

remyelination in old age may be affected rather by slower remyelination rate than insufficient mechanisms (Shields et al., 1999). More specifically, changes in macrophage recruitment seem to be altered in aged mice, because when they were joined to young mice by parabiosis, the old mice were not only able to recruit from the macrophage pool of the young animal but also remyelinate the lesion area (Ruckh et al., 2012). As the aim of working with experimental disease models is to mimic the human pathology as precisely as possible, these findings question whether young animals are a useful in modelling remyelination since they present with a higher regenerative ability than humans, or whether aged organisms would indeed be more accurate. The answer is two-fold and involves different approaches of understanding demyelinating disease. For studies investigating why remyelination in multiple sclerosis is insufficient, one needs an experimental paradigm, which mimics this pathology most closely and where pathways can be potentially altered to explore enhancing treatment strategies. Experimental models, which model only certain aspects of the disease can also be very powerful tools if they allow screening of pathways involved in remyelination and testing of candidate target molecules. On the other hand, however, it would be interesting to compare the mechanisms of repair of young zebrafish with full remyelination capacity to other models with insufficient remyelination, and to explore differences within myelin repair mechanisms. For example it would be interesting to isolate remyelinating cells in the optic nerve of young and old zebrafish and perform transcriptional profiling which might elucidate differences in signalling pathways that could explain this differential remyelination capacity.

In the rodent central nervous system, there are two main areas from which oligodendrocytes can originate: firstly, OPCs expressing the progenitor markers NG2 and PDGF-receptor-α are widely distributed in the postnatal brain and can differentiate into myelinating oligodendrocytes upon injury (Kang et al., 2010; Zawadzka et al., 2010); and secondly the OPCs can arise from progenitor cells in the subventricular zone (SVZ) (Menn et al., 2006; Nait-Oumesmar et al., 1999). In the zebrafish, it is unclear whether oligodendrocytes can only originate from the

precursor cells in the periventricular progenitor zone, or whether parenchymal progenitor cells such as NG2+ cells exist in zebrafish. It has been shown that the zebrafish brain parenchyma contains a population of slowly dividing oligodendroglial progenitor cells (Marz et al., 2010). However it is not known which progenitor population gives rise to remyelinating cells in the zebrafish optic nerve or whether it is perhaps a contribution of both populations. Much research has been performed to determine the sources of OPCs responsible for remyelination in the rodent brain, and while results show that oligodendrocyte precursor cells from both regions are capable of remyelinating, there appears to be a difference in recruitment origin depending on the location of the lesion. Studies investigating myelin repair in demyelinating spinal cord lesions in rodents indicate that remyelination is carried out by oligodendrocyte precursor cells in the immediately surrounding white matter and surviving oligodendrocytes in the lesion site do not contribute to this process (reviewed in Blakemore and Keirstead, 1999). By contrast, in experimental demyelination models where the lesion is located in the brain an increased proliferation in the SVZ has been described, which is also observed in post-mortem brain of MS patients (reviewed in Nait-Oumesmar et al., 2008). It is thought that this proliferation in response to injury is triggered by Cdk2, a cyclin-dependent kinase which controls the cell cycle by promoting cell cycle exit and differentiation (Caillava et al., 2011). Cell tracing experiments showed that these proliferating progenitor cells were able to migrate to the lesion area, differentiate into myelinating oligodendrocytes and contribute to remyelination, however this was only observed for lesions within close vicinity of the ventricles, for example in the corpus callosum or the rostral migratory stream, but not for more distant lesions for example in the cerebellum. This suggests that perhaps, depending on the location of the demyelinating lesion, different sources of progenitor cells are activated; however the relative contribution of both SVZ-derived and adult progenitor cell populations and detailed signalling mechanisms remain unclear. In my studies in the zebrafish, I also observed an increased proliferation in the periventricular progenitor zone following optic nerve demyelination. Furthermore, I found an activation of microglia along the entire optic tract of the lesioned optic

nerve, which might suggest an inflammatory signalling mechanism as the periventricular progenitor cells possess very long processes that end in close proximity of the optic projection and could possibly directly respond to chemokines. This is supported by recent studies in the zebrafish, which report progenitor proliferation after the inflammatory agent zymosan was injected into the ventricle (Kyritsis et al., 2012). Further, it has been shown that OPCs of rodents express cytokine receptors that can mediate a chemotactic-induced proliferative and migratory response through their ligands which are up-regulated in demyelinating lesions of experimental animal models and within MS (Carbajal et al., 2010; Dziembowska et al., 2005; Kelland et al., 2011; Nguyen and Stangel, 2001). Experimental models also demonstrate that a depletion of macrophages reduces remyelination of spinal cord lesions (Kotter et al., 2001); and moreover induction of inflammation can enhance remyelination of chronically demyelinated areas (Foote and Blakemore, 2005) as well as myelination of the normally unmyelinated rodent retina by transplanted OPCs (Setzu et al., 2006), These finding support the hypothesis that inflammatory signalling seems to be an important mechanism for proliferation and recruitment of progenitor cells and subsequent successful remyelination, and together with my results might indicates that homologous signalling mechanisms may be involved in OPC recruitment in zebrafish. This might perhaps also question the need for anti-inflammatory treatment in human disease, especially as all approved therapies suppress and/or modulate the immune system and thereby possibly dampen the regenerative response. Closer investigation of the signalling mechanisms involved in remyelination, in particular the involvement of the immune system, could potentially present useful ways to specifically manipulate the immune response to dampen disease activity but aid regeneration. Further experiments in the zebrafish investigating the effect of optic nerve inflammation on cells of the progenitor zone and progenitor cell tracing following demyelinating optic nerve lesions would give more insight into whether recruitment mechanisms are homologous between species; and knockdown of various cytokine receptors expressed on OPCs in zebrafish could elucidate specific immunological signalling cascades. Moreover it could be interesting to explore demyelinating lesions in

various CNS locations to establish whether this system is similar to rodents in that there is no increased proliferation in the periventricular progenitor zone if the lesion area is not in close proximity.

Remyelination studies in rodents have revealed several pathways likely involved myelin repair through the regulation of oligodendroglial differentiation, such as Notch-Jagged and retinoid X receptor-ϒ signalling (Huang and Franklin, 2011; Huang et al., 2011b), some of which might also be implemented in fish. It has been shown that Notch mutant zebrafish are not able to generate myelinating oligodendrocytes from precursor cells and upon Notch overexpression increased oligodendrocyte development was observed (Park and Appel, 2003). Notch therefore appears to play a role in regulating specification of oligodendrocytes during development in zebrafish and hence could also be important in remyelination; however this has not been shown yet. Similarly, mechanisms of oligodendrocyte recruitment may also play a key role in successful remyelination. This possibility has been explored and it has been suggested that the guidance molecules Semaphorin 3A and 3F are able to guide oligodendrocyte precursor cells to the lesion area due to their respective chemo repelling and attracting properties (Williams et al., 2007). Indeed in rodent LPC-demyelination models overexpression studies of these molecules were able to show that Semaphorin 3A inhibits OPC recruitment to the lesion area and Semaphorin 3F aids OPC migration and therefore also remyelination (Piaton et al., 2011). Similarly, treatment with recombinant Semaphorin 3A and 3F also effectively altered remyelination in a mouse model of LPC-induced demyelination, without affecting cell survival, proliferation or differentiation, and therefore suggest a migratory effect (Boyd et al., 2013). In fish, the semaphorins have mainly been assigned a function in axon path finding; however the similarity between fish oligodendrocytes in terms of morphology and expressed markers, as well as remyelination time course opens potential questions about the role of class 3 semaphorins in myelin repair in zebrafish. To explore this further, I investigated Sema3A in the zebrafish optic nerve after demyelinating lesions and found reduced levels present at early time points after the lesion, suggesting a hypothesis based

around Sema3A negatively effecting OPC recruitment and homologous signalling mechanisms to mammals. Moreover, treatment with human recombinant Sema3A decreased the number of oligodendroglial cells and percentage of myelinated axons in the lesion area following demyelination, which is similar to results observed in rodent models (Boyd et al., 2013). However, to make clear statements about the exact signalling mechanisms and homologies to rodent systems, these studies would need to be extended. My studies show co-localisation of Sema3A expression with neuronal markers suggesting that, like in rodents it is produced in neuronal cell bodies and transported along the axon (de Wit et al., 2006). However, whether there is a local down-regulation in the lesion site after demyelination or a more global effect along the entire optic nerve is not clear. Western blots for Sema3A levels of different parts of the optic could give more insight into this. Furthermore, it is also not known whether high levels of Sema3A affects the axons in the optic nerve, as it has been previously suggested that Sema3A might be toxic to some kinds of neurons (Yasuhara et al., 2005). Axonal injury could be assessed by neuronal tracer experiments after Sema3A treatment where optic nerve axons are retrogradely labelled or by staining for phosphorylated or dephosphorylated neurofilament with SMI31 or SMI32 antibodies, as dephosphorylated neurofilament is associated with demyelinated axons. Alternative antibodies which detect axonal injury and may work in zebrafish include Amyloid precursor protein (APP). In addition, it would need to be determined whether Sema3A affects cell proliferation and differentiation and cell death analysis could ensure that Sema3A does not affect cell survival. Finally, knockdown of Sema3A in the zebrafish larvae could provide useful information about the role of Sema3A in OPC migration during development, and conditional knockdown in adult zebrafish could perhaps elucidate whether Sema3A affects myelin repair, as one would expect more OPC migration and perhaps faster or even more remyelination. Findings in our laboratory show that Sema3A knockdown mice remyelinate faster after LPC-induced lesions in the corpus callosum compared to control animals (Boyd et al., 2013). Hence, the investigation of remyelination in adult zebrafish with knocked

down Sema3A could perhaps support the hypothesis that some signalling mechanisms are homologous between zebrafish and mammals.

Taken together, my studies show that the time course of de- and remyelination between zebrafish and rodents is similar, and that perhaps homologous signalling mechanisms are implied in OPC recruitment and migration.

6.3 Clinical relevance of my findings

Although much research about disease pathology and possible therapeutic intervention in MS has been conducted, it still remains unclear what mechanisms cause the disease and how to treat it most effectively.

Experimental models of demyelinating disease have proven very useful in the search for therapeutic targets; the immunomodulators interferon-beta 1α, glatiramer acetate and the recently licensed fingolimod, which are currently the therapeutic mainstay for the relapsing-remitting form of MS (RRMS), and natalizumab, which is used for disease with more aggressive relapses, were initially validated in experimental animal models (reviewed in Denic et al., 2011). For example, studies in rodents and non-human primates clearly demonstrate that glatiramer acetate is able to suppress EAE by inhibiting cell proliferation in the spleen and cytokine response to auto-antigens, and animals treated with the drug showed less demyelination in the spinal cord compared to untreated EAE mice (Aharoni et al., 2008; Teitelbaum et al., 2004). Hence, through their ability to target immune cells and prevent lymphocyte migration into the CNS, as well as positively affect the blood-brain barrier integrity, which has been suggested by MRI imaging studies of patients with RRMS (Stone et al., 1995), these medical interventions are useful in suppressing inflammation and therefore potentially preventing and/or delaying progression and neurodegeneration. In my zebrafish-based demyelination model I observed an activation of microglia/macrophages following the demyelinating optic nerve lesion and hence it could be useful to study the effect of immunosuppression on remyelination. It would be particularly interesting to investigate whether inhibition of the immune response also leads to increased proliferation in the periventricular progenitor zone as recent studies have suggested that acute inflammation alone can trigger regeneration in the adult zebrafish brain (Kyritsis et al., 2012). Moreover, microglia/macrophage recruitment is impaired in old rats and investigation of the inflammatory response in my zebrafish-based demyelination model could lead to valuable information regarding the cause of insufficient myelin repair in old zebrafish.

Other groups are currently investigating immune-mediated mitochondrial injury, which has been associated with axonal damage and is thought to contribute to disease progression in MS. It has been shown that mitochondria are highly vulnerable to free radicals and Ca^{+} overload (Barrientos et al., 2011; Forte et al., 2007), and that suppression of mitochondrial oxidative stress might have long-term effects on neuroprotection (Qi et al., 2007). Studies in zebrafish propose the possibility of conducting screens to investigate mitochondrial function *in vivo*, which could be used to explore chemical compounds capable of preventing mitochondrial dysfunction (Stackley et al., 2011). Moreover, the recent development of transgenic zebrafish lines allowing real-time *in vivo* observation of mitochondria might also deliver new insights into pathology and help to devise neuroprotective mechanisms (Kim et al., 2008; Plucinska et al., 2012). Demyelinating optic nerve lesions in these transgenic lines could elucidate whether fish mitochondria are also vulnerable to demyelination and whether they possess different mechanisms to deal with oxidative stress compared to the mammalian mitochondria.

Another potential therapeutic strategy is to protect axons by enhancing remyelination by oligodendrocyte progenitor cells from endogenous sources and this has been the focus of much recent research (reviewed in Huang et al., 2011a). As axons are more vulnerable to inflammatory mechanisms when they are demyelinated, enhancing the process of remyelination could perhaps protect the axons from inflammatory injury and as such not only prevent axonal degeneration but also aid functional recovery after a demyelinating insult. As the remyelination process involves two major steps – the recruitment of oligodendrocyte precursors and their differentiation – enhancement of either of these might lead to increased remyelination capability. For example, studies in rodent demyelination models identified LINGO-1 as a negative regulator of oligodendrocyte differentiation and EAE mice treated with an antibody antagonist of LINGO-1 exhibited increased remyelination and functional recovery (Mi et al., 2007). A clinical trial investigating the use of a LINGO-1 antagonist in phase 1b has already been completed, however

the results remain to be reported (http://clinicaltrials.gov/ct2/show/NCT01244139). Similarly, it has been shown that signalling through the retinoid X receptor-ϒ positively affects oligodendrocyte maturation and increased remyelination, making this a potential therapeutic target although exact signalling mechanisms are yet unclear (Huang et al., 2011b). However as a licenced agonist of RXR-ϒ is already in clinical use for certain types of cancer, patient trials for RXR-ϒ as a treatment for MS may be conducted in the near future. Semaphorin 3A and 3F were shown to alter remyelination in rodent studies by affecting OPC recruitment through their respective repellent and attractive properties and although these molecules are currently far from being implemented in clinical practice, further investigation of these signalling pathways might lead to powerful targets that could be used for drug development (Williams et al., 2007). Using the experimental demyelination model in adult zebrafish described in this thesis, I was able to show that semaphorins may also play a role in oligodendrocyte recruitment in fish, highlighting possible similarities in remyelination mechanisms between species and the importance of this model organism for the discovery of therapy development.

Zebrafish are amendable to high throughput screening of chemical compound libraries due to their transparent larval stage, rapid development and capacity for transgenesis (Hao et al., 2010; Hong, 2009). These screens have already been implemented in the discovery of pro-myelinating substances (Buckley et al., 2010), and my work shows that as zebrafish possibly exhibit conserved remyelination mechanisms as rodents, findings made in fish can potentially be extrapolated to and benefit mammalian systems. Moreover, zebrafish have the potential for live imaging so that cellular events of remyelination can be followed by time lapse imaging. This method is widely used in larval zebrafish as they are transparent and technically easy to embed for *in vivo* live imaging, and I hypothesised that this methodology may also be possible in adult fish. For this I trialled a hand-held fibre optic confocal microscope with which I hoped to visualise single cells in the optic nerve. While it was possible to image individual transgenic cell bodies, the resolution was not high enough to observe cell processes and associated internodes

and moreover it would have been difficult to reliably image the same location to follow remyelination without a rig that would fix the position of the fish in relation to the fibre optic microscope. To further explore the possibility of single cell live imaging during remyelination, I wondered whether demyelination could be induced in the zebrafish tectum by local placement of LPC and subsequent confocal time lapse imaging through a tectal window. For this, I placed LPC onto the adult zebrafish optic tectum through a small hole in the skull and found that both loss of claudin k+ myelin and *olig2*:DsRed+ oligodendrocytes were present on the surface of the tectum as well as a local activation of microglia. By mounting the tectal surface of these adult zebrafish onto a coverslip, I was able to image single transgenic cells live under the confocal microscope, and as such this technique might be helpful in real-time imaging of cellular events occurring during remyelination in the adult zebrafish tectum, however a rig allowing water immersion and ventilation of the fish during live imaging over long periods of time would probably be necessary.

Taken together, my studies show that focal demyelinating lesions in the optic nerve of adult zebrafish facilitate the study of remyelination. This zebrafish-based model could be useful in exploring mechanisms involved in remyelination in organisms with high regenerative capacity and the possibility of *in vivo* live imaging of single cells. In addition, studies utilising mammalian experimental demyelination models could also benefit from the screening potential of larval zebrafish, which allows very fast, and often automated, assessment of the effects of chemical compounds on myelination. A strategy for the discovery of pro-myelinating substances could be to perform chemical compound screens in zebrafish larvae to determine initial candidate substances and test them in the adult zebrafish-based remyelination model, prior to moving onto rodent experimental models, which are more expensive and currently less amendable to spatial and temporal manipulation of gene expression and function. In addition, comparisons of mechanisms involved in remyelination between the regenerating optic nerve of young zebrafish and those in models with insufficient remyelination such as older zebrafish or rodents, for

example by transcriptional profiling of oligodendrocytes, could give valuable information about possible causes of remyelination failure.

6.4 Concluding remarks and future directions

In this thesis I propose adult zebrafish as a model to study remyelination after experimental demyelination. Zebrafish are being exploited for their high throughput screening potential of chemical compound libraries to discover putative substances that could enhance remyelination. However, it is unclear whether zebrafish and mammals share similar myelination and remyelination mechanisms and whether findings in the zebrafish could be extrapolated to mammals. The studies herein describe developmental myelination and myelin repair in zebrafish and show similarities of remyelination time course and possible signalling mechanisms in oligodendrocyte progenitor cell recruitment to findings made in experimental rodent models. Moreover, the data suggests that there is a differential myelin regeneration capacity between young and old zebrafish, which would lend itself to comparative studies of gene expression regulation and mechanisms of repair to determine why ageing impairs the remyelination process and what strategies zebrafish employ to be capable of regeneration. This may elucidate differences between complete and insufficient myelin repair mechanisms and as such might present potential targets for therapeutic intervention that could be useful in the treatment for MS.

ABBREVIATIONS

BSA	Bovine serum albumin
BrdU	Bromodeoxyuridine
CNS	Central nervous system
DAB	Diaminobenzidine
DMEM	Dulbecco's Modified Eagle Medium
dH_2O	Distilled water
DMSO	Dimethyl sulfoxide
dpf	Days post fertilisation
dpl	Days post lesion
DTR	Diphtheria toxin receptor
EAE	Experimental autoimmune encephalomyelitis
EdU	Ethynyl-deoxyuridine
EDTA	Ethylenediaminetetraacetic acid
EGTA	Ethylene glycol tetraacetic acid
EM	Electron microscopy
EtBr	Ethidium Bromide
GFP	Green fluorescent protein
hpf	Hours post fertilisation

LPC	Lysophosphatidolcholine
M	Molar
MAG	Myelin associated glycoprotein
MAPK	Mitogen-activated protein kinase
MBP	Myelin basic protein
min	Minute
ml	Millilitre(s)
µl	Microlitre(s)
MOG	Myelin/oligodendrocyte protein
MS	Multiple sclerosis
MTZ	Metronidazole
nl	Nanolitre(s)
NRP	Neuropilin
NTR	Nitroreductase
ON	Optic nerve
OPC	Oligodendrocyte progenitor/precursor cell
P0	Myelin protein zero
PBS	Phosphate buffered saline
PBStx	PBS containing Triton X-100
PBST	PBS containing Tween20
PCNA	Proliferating cell nuclear antigen

PFA	Paraformaldehyde
PI3K	Phosphoinositide-3-kinase
PLLN	Peripheral lateral line nerve
PLP	Proteolipid protein
PMP22	Peripheral myelin protein 22
PNS	Peripheral nervous system
PPMS	Primary progressive multiple sclerosis
PTU	N-phenylthiourea
RFP	Red fluorescent protein
rpm	Rotations per minute
RRMS	Relapsing-remitting multiple sclerosis
SD	Standard deviation
SEM	Standard error of the mean
SDS	Sodium dodecyl sulphate
SPMS	Secondary progressive multiple sclerosis
SVZ	Subventricular zone
TBS	Tris buffered saline
TBST	TBS containing Tween20
UAS	Upstream activating sequence
VEGF	Vascular endothelial growth factor
ZF	Zebrafish

REFERENCES

Abdul-Majid, K.B., Wefer, J., Stadelmann, C., Stefferl, A., Lassmann, H., Olsson, T., and Harris, R.A. (2003). Comparing the pathogenesis of experimental autoimmune encephalomyelitis in CD4-/- and CD8-/- DBA/1 mice defines qualitative roles of different T cell subsets. Journal of neuroimmunology *141*, 10-19.

Acs, P., and Komoly, S. (2012). Selective ultrastructural vulnerability in the cuprizone-induced experimental demyelination. Ideggyogyaszati szemle *65*, 266-270.

Adlkofer, K., Martini, R., Aguzzi, A., Zielasek, J., Toyka, K.V., and Suter, U. (1995). Hypermyelination and demyelinating peripheral neuropathy in Pmp22-deficient mice. Nature genetics *11*, 274-280.

Aharoni, R., Herschkovitz, A., Eilam, R., Blumberg-Hazan, M., Sela, M., Bruck, W., and Arnon, R. (2008). Demyelination arrest and remyelination induced by glatiramer acetate treatment of experimental autoimmune encephalomyelitis. Proceedings of the National Academy of Sciences of the United States of America *105*, 11358-11363.

Akitake, C.M., Macurak, M., Halpern, M.E., and Goll, M.G. (2011). Transgenerational analysis of transcriptional silencing in zebrafish. Developmental biology *352*, 191-201.

Almeida, R.G., Czopka, T., Ffrench-Constant, C., and Lyons, D.A. (2011). Individual axons regulate the myelinating potential of single oligodendrocytes in vivo. Development *138*, 4443-4450.

Amor, S., Baker, D., Groome, N., and Turk, J.L. (1993). Identification of a major encephalitogenic epitope of proteolipid protein (residues 56-70) for the induction of experimental allergic encephalomyelitis in Biozzi AB/H and nonobese diabetic mice. J Immunol *150*, 5666-5672.

Amor, S., Groome, N., Linington, C., Morris, M.M., Dornmair, K., Gardinier, M.V., Matthieu, J.M., and Baker, D. (1994). Identification of epitopes of myelin oligodendrocyte glycoprotein for the induction of experimental allergic encephalomyelitis in SJL and Biozzi AB/H mice. J Immunol *153*, 4349-4356.

Andrews, H.E., Nichols, P.P., Bates, D., and Turnbull, D.M. (2005). Mitochondrial dysfunction plays a key role in progressive axonal loss in Multiple Sclerosis. Medical hypotheses *64*, 669-677.

Ankerhold, R., and Stuermer, C.A. (1999). Fate of oligodendrocytes during retinal axon degeneration and regeneration in the goldfish visual pathway. Journal of neurobiology *41*, 572-584.

Ara, J., See, J., Mamontov, P., Hahn, A., Bannerman, P., Pleasure, D., and Grinspan, J.B. (2008). Bone morphogenetic proteins 4, 6, and 7 are up-regulated in mouse spinal cord during experimental autoimmune encephalomyelitis. Journal of neuroscience research *86*, 125-135.

Ariga, J., Walker, S.L., and Mumm, J.S. (2010). Multicolor time-lapse imaging of transgenic zebrafish: visualizing retinal stem cells activated by targeted neuronal cell ablation. Journal of visualized experiments : JoVE.

Asakawa, K., and Kawakami, K. (2008). Targeted gene expression by the Gal4-UAS system in zebrafish. Development, growth & differentiation *50*, 391-399.

Azim, K., and Butt, A.M. (2011). GSK3beta negatively regulates oligodendrocyte differentiation and myelination in vivo. Glia *59*, 540-553.

Back, S.A., Tuohy, T.M., Chen, H., Wallingford, N., Craig, A., Struve, J., Luo, N.L., Banine, F., Liu, Y., Chang, A.*, et al.* (2005). Hyaluronan accumulates in demyelinated lesions and inhibits oligodendrocyte progenitor maturation. Nature medicine *11*, 966-972.

Bai, Q., Sun, M., Stolz, D.B., and Burton, E.A. (2011). Major isoform of zebrafish P0 is a 23.5 kDa myelin glycoprotein expressed in selected white matter tracts of the central nervous system. The Journal of comparative neurology *519*, 1580-1596.

Baker, D., O'Neill, J.K., Gschmeissner, S.E., Wilcox, C.E., Butter, C., and Turk, J.L. (1990). Induction of chronic relapsing experimental allergic encephalomyelitis in Biozzi mice. Journal of neuroimmunology *28*, 261-270.

Bankston, A.N., Mandler, M.D., and Feng, Y. (2013). Oligodendroglia and neurotrophic factors in neurodegeneration. Neuroscience bulletin *29*, 216-228.

Barbin, G., Aigrot, M.S., Charles, P., Foucher, A., Grumet, M., Schachner, M., Zalc, B., and Lubetzki, C. (2004). Axonal cell-adhesion molecule L1 in CNS myelination. Neuron glia biology *1*, 65-72.

Baron-Van Evercooren, A., Gansmuller, A., Duhamel, E., Pascal, F., and Gumpel, M. (1992). Repair of a myelin lesion by Schwann cells transplanted in the adult mouse spinal cord. Journal of neuroimmunology *40*, 235-242.

Barres, B.A., and Raff, M.C. (1993). Proliferation of oligodendrocyte precursor cells depends on electrical activity in axons. Nature *361*, 258-260.

Barrientos, S.A., Martinez, N.W., Yoo, S., Jara, J.S., Zamorano, S., Hetz, C., Twiss, J.L., Alvarez, J., and Court, F.A. (2011). Axonal degeneration is mediated by the mitochondrial permeability transition pore. The Journal of neuroscience : the official journal of the Society for Neuroscience *31*, 966-978.

Barros, C.S., Nguyen, T., Spencer, K.S., Nishiyama, A., Colognato, H., and Muller, U. (2009). Beta1 integrins are required for normal CNS myelination and promote AKT-dependent myelin outgrowth. Development *136*, 2717-2724.

Baumann, N., and Pham-Dinh, D. (2001). Biology of oligodendrocyte and myelin in the mammalian central nervous system. Physiological reviews *81*, 871-927.

Bechtold, D.A., Miller, S.J., Dawson, A.C., Sun, Y., Kapoor, R., Berry, D., and Smith, K.J. (2006). Axonal protection achieved in a model of multiple sclerosis using lamotrigine. Journal of neurology *253*, 1542-1551.

Becker, C.G., and Becker, T. (2007). Growth and pathfinding of regenerating axons in the optic projection of adult fish. Journal of neuroscience research *85*, 2793-2799.

Becker, C.G., and Becker, T. (2008). Adult zebrafish as a model for successful central nervous system regeneration. Restorative neurology and neuroscience *26*, 71-80.

Becker, C.G., Meyer, R.L., and Becker, T. (2000). Gradients of ephrin-A2 and ephrin-A5b mRNA during retinotopic regeneration of the optic projection in adult zebrafish. The Journal of comparative neurology *427*, 469-483.

Benetti, F., Ventura, M., Salmini, B., Ceola, S., Carbonera, D., Mammi, S., Zitolo, A., D'Angelo, P., Urso, E., Maffia, M.*, et al.* (2010). Cuprizone neurotoxicity, copper deficiency and neurodegeneration. Neurotoxicology *31*, 509-517.

Bernardos, R.L., Barthel, L.K., Meyers, J.R., and Raymond, P.A. (2007). Late-stage neuronal progenitors in the retina are radial Muller glia that function as retinal stem cells. The Journal of neuroscience : the official journal of the Society for Neuroscience *27*, 7028-7040.

Bielenberg, D.R., Hida, Y., Shimizu, A., Kaipainen, A., Kreuter, M., Kim, C.C., and Klagsbrun, M. (2004). Semaphorin 3F, a chemorepulsant for endothelial cells, induces a poorly vascularized, encapsulated, nonmetastatic tumor phenotype. The Journal of clinical investigation *114*, 1260-1271.

Bingham, C.O., 3rd, and Austen, K.F. (1999). Phospholipase A2 enzymes in eicosanoid generation. Proceedings of the Association of American Physicians *111*, 516-524.

Birchmeier, C., and Nave, K.A. (2008). Neuregulin-1, a key axonal signal that drives Schwann cell growth and differentiation. Glia *56*, 1491-1497.

Birgbauer, E., Rao, T.S., and Webb, M. (2004). Lysolecithin induces demyelination in vitro in a cerebellar slice culture system. Journal of neuroscience research *78*, 157-166.

Bitsch, A., Schuchardt, J., Bunkowski, S., Kuhlmann, T., and Bruck, W. (2000). Acute axonal injury in multiple sclerosis. Correlation with demyelination and inflammation. Brain : a journal of neurology *123 (Pt 6)*, 1174-1183.

Black, J.A., Newcombe, J., Trapp, B.D., and Waxman, S.G. (2007). Sodium channel expression within chronic multiple sclerosis plaques. Journal of neuropathology and experimental neurology *66*, 828-837.

Black, J.A., Waxman, S.G., and Smith, K.J. (2006). Remyelination of dorsal column axons by endogenous Schwann cells restores the normal pattern of Nav1.6 and Kv1.2 at nodes of Ranvier. Brain : a journal of neurology *129*, 1319-1329.

Blakemore, W.F. (1973a). Demyelination of the superior cerebellar peduncle in the mouse induced by cuprizone. Journal of the neurological sciences *20*, 63-72.

Blakemore, W.F. (1973b). Remyelination of the superior cerebellar peduncle in the mouse following demyelination induced by feeding cuprizone. Journal of the neurological sciences *20*, 73-83.

Blakemore, W.F. (1975). Remyelination by Schwann cells of axons demyelinated by intraspinal injection of 6-aminonicotinamide in the rat. Journal of neurocytology *4*, 745-757.

Blakemore, W.F. (1982). Ethidium bromide induced demyelination in the spinal cord of the cat. Neuropathology and applied neurobiology *8*, 365-375.

Blakemore, W.F., Chari, D.M., Gilson, J.M., and Crang, A.J. (2002). Modelling large areas of demyelination in the rat reveals the potential and possible limitations of transplanted glial cells for remyelination in the CNS. Glia *38*, 155-168.

Blakemore, W.F., and Franklin, R.J. (2008). Remyelination in experimental models of toxin-induced demyelination. Current topics in microbiology and immunology *318*, 193-212.

Blakemore, W.F., and Keirstead, H.S. (1999). The origin of remyelinating cells in the central nervous system. Journal of neuroimmunology *98*, 69-76.

Boggs, J.M. (2006). Myelin basic protein: a multifunctional protein. Cellular and molecular life sciences : CMLS *63*, 1945-1961.

Bondan, E.F., Custodio, P.R., Lallo, M.A., Bentubo, H.D., and Graca, D.L. (2009). Ethidium bromide-induced demyelination in the sciatic nerve of diabetic rats. Arquivos de neuro-psiquiatria *67*, 1066-1070.

Boyd, A., Zhang, H., and Williams, A. (2013). Insufficient OPC migration into demyelinated lesions is a cause of poor remyelination in MS and mouse models. Acta neuropathologica.

Brand, A.H., and Perrimon, N. (1993). Targeted gene expression as a means of altering cell fates and generating dominant phenotypes. Development *118*, 401-415.

Brinkmann, B.G., Agarwal, A., Sereda, M.W., Garratt, A.N., Muller, T., Wende, H., Stassart, R.M., Nawaz, S., Humml, C., Velanac, V.*, et al.* (2008). Neuregulin-1/ErbB signaling serves distinct functions in myelination of the peripheral and central nervous system. Neuron *59*, 581-595.

Brosamle, C., and Halpern, M.E. (2002). Characterization of myelination in the developing zebrafish. Glia *39*, 47-57.

Bruck, W. (2005). The pathology of multiple sclerosis is the result of focal inflammatory demyelination with axonal damage. Journal of neurology *252 Suppl 5*, v3-9.

Brunner, C., Lassmann, H., Waehneldt, T.V., Matthieu, J.M., and Linington, C. (1989). Differential ultrastructural localization of myelin basic protein, myelin/oligodendroglial glycoprotein, and 2',3'-cyclic nucleotide 3'-phosphodiesterase in the CNS of adult rats. Journal of neurochemistry *52*, 296-304.

Buch, T., Heppner, F.L., Tertilt, C., Heinen, T.J., Kremer, M., Wunderlich, F.T., Jung, S., and Waisman, A. (2005). A Cre-inducible diphtheria toxin receptor mediates cell lineage ablation after toxin administration. Nature methods *2*, 419-426.

Buckley, C.E., Goldsmith, P., and Franklin, R.J. (2008). Zebrafish myelination: a transparent model for remyelination? Disease models & mechanisms *1*, 221-228.

Buckley, C.E., Marguerie, A., Roach, A.G., Goldsmith, P., Fleming, A., Alderton, W.K., and Franklin, R.J. (2010). Drug reprofiling using zebrafish identifies novel compounds with potential pro-myelination effects. Neuropharmacology *59*, 149-159.

Cai, J., Qi, Y., Hu, X., Tan, M., Liu, Z., Zhang, J., Li, Q., Sander, M., and Qiu, M. (2005). Generation of oligodendrocyte precursor cells from mouse dorsal spinal cord independent of Nkx6 regulation and Shh signaling. Neuron *45*, 41-53.

Caillava, C., Vandenbosch, R., Jablonska, B., Deboux, C., Spigoni, G., Gallo, V., Malgrange, B., and Baron-Van Evercooren, A. (2011). Cdk2 loss accelerates precursor differentiation and remyelination in the adult central nervous system. The Journal of cell biology *193*, 397-407.

Calabrese, M., Agosta, F., Rinaldi, F., Mattisi, I., Grossi, P., Favaretto, A., Atzori, M., Bernardi, V., Barachino, L., Rinaldi, L.*, et al.* (2009). Cortical lesions and atrophy associated with cognitive impairment in relapsing-remitting multiple sclerosis. Archives of neurology *66*, 1144-1150.

Campbell, G.R., and Mahad, D.J. (2011). Mitochondria as crucial players in demyelinated axons: lessons from neuropathology and experimental demyelination. Autoimmune diseases *2011*, 262847.

Carbajal, K.S., Schaumburg, C., Strieter, R., Kane, J., and Lane, T.E. (2010). Migration of engrafted neural stem cells is mediated by CXCL12 signaling through CXCR4 in a viral model of multiple sclerosis. Proceedings of the National Academy of Sciences of the United States of America *107*, 11068-11073.

Carre, J.L., Goetz, B.D., O'Connor, L.T., Bremer, Q., and Duncan, I.D. (2002). Mutations in the rat myelin basic protein gene are associated with specific alterations in other myelin gene expression. Neuroscience letters *330*, 17-20.

Catterall, W.A. (2012). Voltage-gated sodium channels at 60: structure, function and pathophysiology. The Journal of physiology *590*, 2577-2589.

Chang, A., Nishiyama, A., Peterson, J., Prineas, J., and Trapp, B.D. (2000). NG2-positive oligodendrocyte progenitor cells in adult human brain and multiple sclerosis lesions. The Journal of neuroscience : the official journal of the Society for Neuroscience *20*, 6404-6412.

Chang, A., Tourtellotte, W.W., Rudick, R., and Trapp, B.D. (2002). Premyelinating oligodendrocytes in chronic lesions of multiple sclerosis. The New England journal of medicine *346*, 165-173.

Chari, D.M., and Blakemore, W.F. (2002). Efficient recolonisation of progenitor-depleted areas of the CNS by adult oligodendrocyte progenitor cells. Glia *37*, 307-313.

Charles, P., Reynolds, R., Seilhean, D., Rougon, G., Aigrot, M.S., Niezgoda, A., Zalc, B., and Lubetzki, C. (2002). Re-expression of PSA-NCAM by demyelinated axons: an inhibitor of remyelination in multiple sclerosis? Brain : a journal of neurology *125*, 1972-1979.

Chastain, E.M., and Miller, S.D. (2012). Molecular mimicry as an inducing trigger for CNS autoimmune demyelinating disease. Immunological reviews *245*, 227-238.

Chelur, D.S., and Chalfie, M. (2007). Targeted cell killing by reconstituted caspases. Proceedings of the National Academy of Sciences of the United States of America *104*, 2283-2288.

Chen, H., Chedotal, A., He, Z., Goodman, C.S., and Tessier-Lavigne, M. (1997). Neuropilin-2, a novel member of the neuropilin family, is a high affinity receptor for the semaphorins Sema E and Sema IV but not Sema III. Neuron *19*, 547-559.

Cheraghali, A.M., Kumar, R., Knaus, E.E., and Wiebe, L.I. (1995). Pharmacokinetics and bioavailability of 5-ethyl-2'-deoxyuridine and its novel (5R,6R)-5-bromo-6-ethoxy-5,6-dihydro prodrugs in mice. Drug metabolism and disposition: the biological fate of chemicals *23*, 223-226.

Cohen, J.A., Coles, A.J., Arnold, D.L., Confavreux, C., Fox, E.J., Hartung, H.P., Havrdova, E., Selmaj, K.W., Weiner, H.L., Fisher, E.*, et al.* (2012). Alemtuzumab versus interferon beta 1a as first-line treatment for patients with relapsing-remitting multiple sclerosis: a randomised controlled phase 3 trial. Lancet *380*, 1819-1828.

Cohen, N.R., Taylor, J.S., Scott, L.B., Guillery, R.W., Soriano, P., and Furley, A.J. (1998). Errors in corticospinal axon guidance in mice lacking the neural cell adhesion molecule L1. Current biology : CB *8*, 26-33.

Coles, A.J., Twyman, C.L., Arnold, D.L., Cohen, J.A., Confavreux, C., Fox, E.J., Hartung, H.P., Havrdova, E., Selmaj, K.W., Weiner, H.L.*, et al.* (2012). Alemtuzumab for patients with relapsing multiple sclerosis after disease-modifying therapy: a randomised controlled phase 3 trial. Lancet *380*, 1829-1839.

Colman, D.R., Kreibich, G., Frey, A.B., and Sabatini, D.D. (1982). Synthesis and incorporation of myelin polypeptides into CNS myelin. The Journal of cell biology *95*, 598-608.

Compston, A., and Coles, A. (2002). Multiple sclerosis. Lancet *359*, 1221-1231.

Compston, A., and Coles, A. (2008). Multiple sclerosis. Lancet *372*, 1502-1517.

Costenbader, K.H., Gay, S., Alarcon-Riquelme, M.E., Iaccarino, L., and Doria, A. (2012). Genes, epigenetic regulation and environmental factors: which is the most relevant in developing autoimmune diseases? Autoimmunity reviews *11*, 604-609.

Craner, M.J., Newcombe, J., Black, J.A., Hartle, C., Cuzner, M.L., and Waxman, S.G. (2004). Molecular changes in neurons in multiple sclerosis: altered axonal expression of Nav1.2 and Nav1.6 sodium channels and Na+/Ca2+ exchanger. Proceedings of the National Academy of Sciences of the United States of America *101*, 8168-8173.

Curado, S., Stainier, D.Y., and Anderson, R.M. (2008). Nitroreductase-mediated cell/tissue ablation in zebrafish: a spatially and temporally controlled ablation method with applications in developmental and regeneration studies. Nature protocols *3*, 948-954.

Czepiel, M., Balasubramaniyan, V., Schaafsma, W., Stancic, M., Mikkers, H., Huisman, C., Boddeke, E., and Copray, S. (2011). Differentiation of induced pluripotent stem cells into functional oligodendrocytes. Glia *59*, 882-892.

Czopka, T., and Lyons, D.A. (2011). Dissecting mechanisms of myelinated axon formation using zebrafish. Methods in cell biology *105*, 25-62.

D'Urso, D., Ehrhardt, P., and Muller, H.W. (1999). Peripheral myelin protein 22 and protein zero: a novel association in peripheral nervous system myelin. The Journal of neuroscience : the official journal of the Society for Neuroscience *19*, 3396-3403.

Dal Canto, M.C., and Lipton, H.L. (1975). Primary demyelination in Theiler's virus infection. An ultrastructural study. Laboratory investigation; a journal of technical methods and pathology *33*, 626-637.

Dal Canto, M.C., and Lipton, H.L. (1977). Multiple sclerosis. Animal model:Theiler's virus infection in mice. The American journal of pathology *88*, 497-500.

Davison, J.M., Akitake, C.M., Goll, M.G., Rhee, J.M., Gosse, N., Baier, H., Halpern, M.E., Leach, S.D., and Parsons, M.J. (2007). Transactivation from Gal4-VP16 transgenic insertions for tissue-specific cell labeling and ablation in zebrafish. Developmental biology *304*, 811-824.

Dawson, M.R., Polito, A., Levine, J.M., and Reynolds, R. (2003). NG2-expressing glial progenitor cells: an abundant and widespread population of cycling cells in the adult rat CNS. Molecular and cellular neurosciences *24*, 476-488.

De Benedictis, L., Bizzoca, A., Corsi, P., Albieri, I., Consalez, G.G., and Gennarini, G. (2006). Activation profile of the F3/Contactin gene in the developing mouse cerebellum. Molecular and cellular neurosciences *32*, 403-418.

de Wit, J., Toonen, R.F., Verhaagen, J., and Verhage, M. (2006). Vesicular trafficking of semaphorin 3A is activity-dependent and differs between axons and dendrites. Traffic *7*, 1060-1077.

Debanne, D., Campanac, E., Bialowas, A., Carlier, E., and Alcaraz, G. (2011). Axon physiology. Physiological reviews *91*, 555-602.

Decker, L., Picard-Riera, N., Lachapelle, F., and Baron-Van Evercooren, A. (2002). Growth factor treatment promotes mobilization of young but not aged adult subventricular zone precursors in response to demyelination. Journal of neuroscience research *69*, 763-771.

Denic, A., Johnson, A.J., Bieber, A.J., Warrington, A.E., Rodriguez, M., and Pirko, I. (2011). The relevance of animal models in multiple sclerosis research. Pathophysiology : the official journal of the International Society for Pathophysiology / ISP *18*, 21-29.

Devaux, J., and Gow, A. (2008). Tight junctions potentiate the insulative properties of small CNS myelinated axons. The Journal of cell biology *183*, 909-921.

Dougherty, K.D., Dreyfus, C.F., and Black, I.B. (2000). Brain-derived neurotrophic factor in astrocytes, oligodendrocytes, and microglia/macrophages after spinal cord injury. Neurobiology of disease *7*, 574-585.

Druskovic, M., Suput, D., and Milisav, I. (2006). Overexpression of caspase-9 triggers its activation and apoptosis in vitro. Croatian medical journal *47*, 832-840.

Duncan, I.D., Brower, A., Kondo, Y., Curlee, J.F., Jr., and Schultz, R.D. (2009). Extensive remyelination of the CNS leads to functional recovery. Proceedings of the National Academy of Sciences of the United States of America *106*, 6832-6836.

Dutton, K.A., Pauliny, A., Lopes, S.S., Elworthy, S., Carney, T.J., Rauch, J., Geisler, R., Haffter, P., and Kelsh, R.N. (2001). Zebrafish colourless encodes sox10 and specifies non-ectomesenchymal neural crest fates. Development *128*, 4113-4125.

Dziembowska, M., Tham, T.N., Lau, P., Vitry, S., Lazarini, F., and Dubois-Dalcq, M. (2005). A role for CXCR4 signaling in survival and migration of neural and oligodendrocyte precursors. Glia *50*, 258-269.

Easter, S.S., Jr., Bratton, B., and Scherer, S.S. (1984). Growth-related order of the retinal fiber layer in goldfish. The Journal of neuroscience : the official journal of the Society for Neuroscience *4*, 2173-2190.

Easter, S.S., Jr., Rusoff, A.C., and Kish, P.E. (1981). The growth and organization of the optic nerve and tract in juvenile and adult goldfish. The Journal of neuroscience : the official journal of the Society for Neuroscience *1*, 793-811.

Edgar, J.M., McLaughlin, M., Werner, H.B., McCulloch, M.C., Barrie, J.A., Brown, A., Faichney, A.B., Snaidero, N., Nave, K.A., and Griffiths, I.R. (2009). Early ultrastructural defects of axons and axon-glia junctions in mice lacking expression of Cnp1. Glia *57*, 1815-1824.

Eichberg, J. (2002). Myelin P0: new knowledge and new roles. Neurochemical research *27*, 1331-1340.

Emery, B. (2010). Regulation of oligodendrocyte differentiation and myelination. Science *330*, 779-782.

England, J.D., Gamboni, F., Levinson, S.R., and Finger, T.E. (1990). Changed distribution of sodium channels along demyelinated axons. Proceedings of the National Academy of Sciences of the United States of America *87*, 6777-6780.

Fancy, S.P., Baranzini, S.E., Zhao, C., Yuk, D.I., Irvine, K.A., Kaing, S., Sanai, N., Franklin, R.J., and Rowitch, D.H. (2009). Dysregulation of the Wnt pathway inhibits timely myelination and remyelination in the mammalian CNS. Genes & development *23*, 1571-1585.

Fancy, S.P., Chan, J.R., Baranzini, S.E., Franklin, R.J., and Rowitch, D.H. (2011). Myelin regeneration: a recapitulation of development? Annual review of neuroscience *34*, 21-43.

Fancy, S.P., Kotter, M.R., Harrington, E.P., Huang, J.K., Zhao, C., Rowitch, D.H., and Franklin, R.J. (2010). Overcoming remyelination failure in multiple sclerosis and other myelin disorders. Experimental neurology *225*, 18-23.

Fang, C., Bourdette, D., and Banker, G. (2012). Oxidative stress inhibits axonal transport: implications for neurodegenerative diseases. Molecular neurodegeneration *7*, 29.

Fausett, B.V., and Goldman, D. (2006). A role for alpha1 tubulin-expressing Muller glia in regeneration of the injured zebrafish retina. The Journal of neuroscience : the official journal of the Society for Neuroscience *26*, 6303-6313.

Feldner, J. (2005). In vivo analysis of cell recognition molecules involved in axonal pathfinding of motor neurons in the trunk of embryonic zebrafish *Danio rerio*. In Biology (Hamburg: Universität Hamburg), pp. 118.

Felts, P.A., and Smith, K.J. (1992). Conduction properties of central nerve fibers remyelinated by Schwann cells. Brain research *574*, 178-192.

Ferent, J., Zimmer, C., Durbec, P., Ruat, M., and Traiffort, E. (2013). Sonic Hedgehog Signaling Is a Positive Oligodendrocyte Regulator during Demyelination. The Journal of neuroscience : the official journal of the Society for Neuroscience *33*, 1759-1772.

Ferguson, B., Matyszak, M.K., Esiri, M.M., and Perry, V.H. (1997). Axonal damage in acute multiple sclerosis lesions. Brain : a journal of neurology *120 (Pt 3)*, 393-399.

Fewou, S.N., Ramakrishnan, H., Bussow, H., Gieselmann, V., and Eckhardt, M. (2007). Down-regulation of polysialic acid is required for efficient myelin formation. The Journal of biological chemistry *282*, 16700-16711.

Ffrench-Constant, C., Miller, R.H., Burne, J.F., and Raff, M.C. (1988). Evidence that migratory oligodendrocyte-type-2 astrocyte (O-2A) progenitor cells are kept out of the rat retina by a barrier at the eye-end of the optic nerve. Journal of neurocytology *17*, 13-25.

Fimbel, S.M., Montgomery, J.E., Burket, C.T., and Hyde, D.R. (2007). Regeneration of inner retinal neurons after intravitreal injection of ouabain in zebrafish. The Journal of neuroscience : the official journal of the Society for Neuroscience *27*, 1712-1724.

Findley, M.K., and Koval, M. (2009). Regulation and roles for claudin-family tight junction proteins. IUBMB life *61*, 431-437.

Flores, A.I., Narayanan, S.P., Morse, E.N., Shick, H.E., Yin, X., Kidd, G., Avila, R.L., Kirschner, D.A., and Macklin, W.B. (2008). Constitutively active Akt induces enhanced myelination in the CNS. The Journal of neuroscience : the official journal of the Society for Neuroscience *28*, 7174-7183.

Fogarty, M., Richardson, W.D., and Kessaris, N. (2005). A subset of oligodendrocytes generated from radial glia in the dorsal spinal cord. Development *132*, 1951-1959.

Foote, A.K., and Blakemore, W.F. (2005). Inflammation stimulates remyelination in areas of chronic demyelination. Brain : a journal of neurology *128*, 528-539.

Forte, M., Gold, B.G., Marracci, G., Chaudhary, P., Basso, E., Johnsen, D., Yu, X., Fowlkes, J., Rahder, M., Stem, K.*, et al.* (2007). Cyclophilin D inactivation protects axons in experimental autoimmune encephalomyelitis, an animal model of multiple sclerosis. Proceedings of the National Academy of Sciences of the United States of America *104*, 7558-7563.

Foster, R.E., Kocsis, J.D., Malenka, R.C., and Waxman, S.G. (1980). Lysophosphatidyl choline-induced focal demyelination in the rabbit corpus callosum. Electron-microscopic observations. Journal of the neurological sciences *48*, 221-231.

Franklin, R.J. (2002a). Remyelination of the demyelinated CNS: the case for and against transplantation of central, peripheral and olfactory glia. Brain research bulletin *57*, 827-832.

Franklin, R.J. (2002b). Why does remyelination fail in multiple sclerosis? Nature reviews Neuroscience *3*, 705-714.

Franklin, R.J., and Ffrench-Constant, C. (2008). Remyelination in the CNS: from biology to therapy. Nature reviews Neuroscience *9*, 839-855.

Franklin, R.J., ffrench-Constant, C., Edgar, J.M., and Smith, K.J. (2012). Neuroprotection and repair in multiple sclerosis. Nature reviews Neurology *8*, 624-634.

Franklin, R.J., Gilson, J.M., and Blakemore, W.F. (1997). Local recruitment of remyelinating cells in the repair of demyelination in the central nervous system. Journal of neuroscience research *50*, 337-344.

Franklin, R.J., and Hinks, G.L. (1999). Understanding CNS remyelination: clues from developmental and regeneration biology. Journal of neuroscience research *58*, 207-213.

Franklin, R.J., Zhao, C., and Sim, F.J. (2002). Ageing and CNS remyelination. Neuroreport *13*, 923-928.

Fressinaud, C. (2005). Repeated injuries dramatically affect cells of the oligodendrocyte lineage: effects of PDGF and NT-3 in vitro. Glia *49*, 555-566.

Friese, M.A., and Fugger, L. (2009). Pathogenic CD8(+) T cells in multiple sclerosis. Annals of neurology *66*, 132-141.

Frost, E.E., Buttery, P.C., Milner, R., and ffrench-Constant, C. (1999). Integrins mediate a neuronal survival signal for oligodendrocytes. Current biology : CB *9*, 1251-1254.

Funfschilling, U., Supplie, L.M., Mahad, D., Boretius, S., Saab, A.S., Edgar, J., Brinkmann, B.G., Kassmann, C.M., Tzvetanova, I.D., Mobius, W.*, et al.* (2012). Glycolytic oligodendrocytes maintain myelin and long-term axonal integrity. Nature *485*, 517-521.

Gennarini, G., Cibelli, G., Rougon, G., Mattei, M.G., and Goridis, C. (1989). The mouse neuronal cell surface protein F3: a phosphatidylinositol-anchored member of the immunoglobulin superfamily related to chicken contactin. The Journal of cell biology *109*, 775-788.

Gensert, J.M., and Goldman, J.E. (1997). Endogenous progenitors remyelinate demyelinated axons in the adult CNS. Neuron *19*, 197-203.

Geren, B.B., and Schmitt, F.O. (1954). The Structure of the Schwann Cell and Its Relation to the Axon in Certain Invertebrate Nerve Fibers. Proceedings of the National Academy of Sciences of the United States of America *40*, 863-870.

Geretti, E., Shimizu, A., and Klagsbrun, M. (2008). Neuropilin structure governs VEGF and semaphorin binding and regulates angiogenesis. Angiogenesis *11*, 31-39.

Ghasemlou, N., Jeong, S.Y., Lacroix, S., and David, S. (2007). T cells contribute to lysophosphatidylcholine-induced macrophage activation and demyelination in the CNS. Glia *55*, 294-302.

Giger, R.J., Cloutier, J.F., Sahay, A., Prinjha, R.K., Levengood, D.V., Moore, S.E., Pickering, S., Simmons, D., Rastan, S., Walsh, F.S.*, et al.* (2000). Neuropilin-2 is required in vivo for selective axon guidance responses to secreted semaphorins. Neuron *25*, 29-41.

Gilmour, D.T., Maischein, H.M., and Nusslein-Volhard, C. (2002). Migration and function of a glial subtype in the vertebrate peripheral nervous system. Neuron *34*, 577-588.

Gilson, J.M., and Blakemore, W.F. (2002). Schwann cell remyelination is not replaced by oligodendrocyte remyelination following ethidium bromide induced demyelination. Neuroreport *13*, 1205-1208.

Givogri, M.I., Costa, R.M., Schonmann, V., Silva, A.J., Campagnoni, A.T., and Bongarzone, E.R. (2002). Central nervous system myelination in mice with deficient expression of Notch1 receptor. Journal of neuroscience research *67*, 309-320.

Glynn, P., and Linington, C. (1989). Cellular and molecular mechanisms of autoimmune demyelination in the central nervous system. Critical reviews in neurobiology *4*, 367-385.

Goldschmidt, T., Antel, J., Konig, F.B., Bruck, W., and Kuhlmann, T. (2009). Remyelination capacity of the MS brain decreases with disease chronicity. Neurology *72*, 1914-1921.

Griffiths, I., Klugmann, M., Anderson, T., Yool, D., Thomson, C., Schwab, M.H., Schneider, A., Zimmermann, F., McCulloch, M., Nadon, N.*, et al.* (1998). Axonal swellings and degeneration in mice lacking the major proteolipid of myelin. Science *280*, 1610-1613.

Grinspan, J. (2002). Cells and signaling in oligodendrocyte development. Journal of neuropathology and experimental neurology *61*, 297-306.

Grinspan, J.B., Reeves, M.F., Coulaloglou, M.J., Nathanson, D., and Pleasure, D. (1996). Re-entry into the cell cycle is required for bFGF-induced oligodendroglial dedifferentiation and survival. Journal of neuroscience research *46*, 456-464.

Grinspan, J.B., Stern, J.L., Franceschini, B., and Pleasure, D. (1993). Trophic effects of basic fibroblast growth factor (bFGF) on differentiated oligodendroglia: a mechanism for regeneration of the oligodendroglial lineage. Journal of neuroscience research *36*, 672-680.

Groves, A.K., Barnett, S.C., Franklin, R.J., Crang, A.J., Mayer, M., Blakemore, W.F., and Noble, M. (1993). Repair of demyelinated lesions by transplantation of purified O-2A progenitor cells. Nature *362*, 453-455.

Hagemeier, K., Bruck, W., and Kuhlmann, T. (2012). Multiple sclerosis - remyelination failure as a cause of disease progression. Histology and histopathology *27*, 277-287.

Hall, S.M. (1972). The effect of injections of lysophosphatidyl choline into white matter of the adult mouse spinal cord. Journal of cell science *10*, 535-546.

Hall, S.M. (1973). Some aspects of remyelination after demyelination produced by the intraneural injection of lysophosphatidyl choline. Journal of cell science *13*, 461-477.

Hall, S.M., and Gregson, N.A. (1971). The in vivo and ultrastructural effects of injection of lysophosphatidyl choline into myelinated peripheral nerve fibres of the adult mouse. Journal of cell science *9*, 769-789.

Hampton, D.W., Anderson, J., Pryce, G., Irvine, K.A., Giovannoni, G., Fawcett, J.W., Compston, A., Franklin, R.J., Baker, D., and Chandran, S. (2008). An experimental model of secondary progressive multiple sclerosis that shows regional variation in gliosis, remyelination, axonal and neuronal loss. Journal of neuroimmunology *201-202*, 200-211.

Hampton, D.W., Innes, N., Merkler, D., Zhao, C., Franklin, R.J., and Chandran, S. (2012). Focal immune-mediated white matter demyelination reveals an age-associated increase in axonal vulnerability and decreased remyelination efficiency. The American journal of pathology *180*, 1897-1905.

Hanafy, K.A., and Sloane, J.A. (2011). Regulation of remyelination in multiple sclerosis. FEBS letters *585*, 3821-3828.

Hao, J., Williams, C.H., Webb, M.E., and Hong, C.C. (2010). Large scale zebrafish-based in vivo small molecule screen. Journal of visualized experiments : JoVE.

Harrington, E.P., Zhao, C., Fancy, S.P., Kaing, S., Franklin, R.J., and Rowitch, D.H. (2010). Oligodendrocyte PTEN is required for myelin and axonal integrity, not remyelination. Annals of neurology *68*, 703-716.

Hartline, D.K., and Colman, D.R. (2007). Rapid conduction and the evolution of giant axons and myelinated fibers. Current biology : CB *17*, R29-35.

Hassen, G.W., Feliberti, J., Kesner, L., Stracher, A., and Mokhtarian, F. (2008). Prevention of axonal injury using calpain inhibitor in chronic progressive experimental autoimmune encephalomyelitis. Brain research *1236*, 206-215.

Hayasaka, K., Himoro, M., Sato, W., Takada, G., Uyemura, K., Shimizu, N., Bird, T.D., Conneally, P.M., and Chance, P.F. (1993). Charcot-Marie-Tooth neuropathy type 1B is associated with mutations of the myelin P0 gene. Nature genetics *5*, 31-34.

Hayashi, S., and McMahon, A.P. (2002). Efficient recombination in diverse tissues by a tamoxifen-inducible form of Cre: a tool for temporally regulated gene activation/inactivation in the mouse. Developmental biology *244*, 305-318.

He, Z., and Tessier-Lavigne, M. (1997). Neuropilin is a receptor for the axonal chemorepellent Semaphorin III. Cell *90*, 739-751.

Hendriks, J.J., Teunissen, C.E., de Vries, H.E., and Dijkstra, C.D. (2005). Macrophages and neurodegeneration. Brain research Brain research reviews *48*, 185-195.

Hong, C.C. (2009). Large-scale small-molecule screen using zebrafish embryos. Methods Mol Biol *486*, 43-55.

Huang, J.K., Fancy, S.P., Zhao, C., Rowitch, D.H., Ffrench-Constant, C., and Franklin, R.J. (2011a). Myelin regeneration in multiple sclerosis: targeting endogenous stem cells. Neurotherapeutics : the journal of the American Society for Experimental NeuroTherapeutics *8*, 650-658.

Huang, J.K., and Franklin, R.J. (2011). Regenerative medicine in multiple sclerosis: identifying pharmacological targets of adult neural stem cell differentiation. Neurochemistry international *59*, 329-332.

Huang, J.K., Jarjour, A.A., Nait Oumesmar, B., Kerninon, C., Williams, A., Krezel, W., Kagechika, H., Bauer, J., Zhao, C., Evercooren, A.B.*, et al.* (2011b). Retinoid X receptor gamma signaling accelerates CNS remyelination. Nature neuroscience *14*, 45-53.

Huxley, A.F., and Stampfli, R. (1949). Evidence for saltatory conduction in peripheral myelinated nerve fibres. The Journal of physiology *108*, 315-339.

Inder, T.E., and Huppi, P.S. (2000). In vivo studies of brain development by magnetic resonance techniques. Mental retardation and developmental disabilities research reviews *6*, 59-67.

Ioannidou, K., Anderson, K.I., Strachan, D., Edgar, J.M., and Barnett, S.C. (2012). Time-lapse imaging of the dynamics of CNS glial-axonal interactions in vitro and ex vivo. PloS one *7*, e30775.

Irvine, K.A., and Blakemore, W.F. (2008). Remyelination protects axons from demyelination-associated axon degeneration. Brain : a journal of neurology *131*, 1464-1477.

Jarjour, A.A., Zhang, H., Bauer, N., Ffrench-Constant, C., and Williams, A. (2012). In vitro modeling of central nervous system myelination and remyelination. Glia *60*, 1-12.

Jepson, S., Vought, B., Gross, C.H., Gan, L., Austen, D., Frantz, J.D., Zwahlen, J., Lowe, D., Markland, W., and Krauss, R. (2012). LINGO-1, a transmembrane signaling protein, inhibits oligodendrocyte differentiation and myelination through intercellular self-interactions. The Journal of biological chemistry *287*, 22184-22195.

Jeserich, G., and Rauen, T. (1990). Cell cultures enriched in oligodendrocytes from the central nervous system of trout in terms of phenotypic expression exhibit parallels with cultured rat Schwann cells. Glia *3*, 65-74.

Ji, Q., and Goverman, J. (2007). Experimental autoimmune encephalomyelitis mediated by CD8+ T cells. Annals of the New York Academy of Sciences *1103*, 157-166.

John, G.R., Shankar, S.L., Shafit-Zagardo, B., Massimi, A., Lee, S.C., Raine, C.S., and Brosnan, C.F. (2002). Multiple sclerosis: re-expression of a developmental pathway that restricts oligodendrocyte maturation. Nature medicine *8*, 1115-1121.

Johns, T.G., and Bernard, C.C. (1999). The structure and function of myelin oligodendrocyte glycoprotein. Journal of neurochemistry *72*, 1-9.

Johnson, A.J., Suidan, G.L., McDole, J., and Pirko, I. (2007). The CD8 T cell in multiple sclerosis: suppressor cell or mediator of neuropathology? International review of neurobiology *79*, 73-97.

Joosten, E.A., and Gribnau, A.A. (1989). Immunocytochemical localization of cell adhesion molecule L1 in developing rat pyramidal tract. Neuroscience letters *100*, 94-98.

Kabarowski, J.H., Xu, Y., and Witte, O.N. (2002). Lysophosphatidylcholine as a ligand for immunoregulation. Biochemical pharmacology *64*, 161-167.

Kang, S.H., Fukaya, M., Yang, J.K., Rothstein, J.D., and Bergles, D.E. (2010). NG2+ CNS glial progenitors remain committed to the oligodendrocyte lineage in postnatal life and following neurodegeneration. Neuron *68*, 668-681.

Katrych, O., Simone, T.M., Azad, S., and Mousa, S.A. (2009). Disease-modifying agents in the treatment of multiple sclerosis: a review of long-term outcomes. CNS & neurological disorders drug targets *8*, 512-519.

Kawasaki, T., Kitsukawa, T., Bekku, Y., Matsuda, Y., Sanbo, M., Yagi, T., and Fujisawa, H. (1999). A requirement for neuropilin-1 in embryonic vessel formation. Development *126*, 4895-4902.

Kaya, F., Mannioui, A., Chesneau, A., Sekizar, S., Maillard, E., Ballagny, C., Houel-Renault, L., Dupasquier, D., Bronchain, O., Holtzmann, I.*, et al.* (2012). Live imaging of targeted cell ablation in Xenopus: a new model to study demyelination and repair. The Journal of neuroscience : the official journal of the Society for Neuroscience *32*, 12885-12895.

Keirstead, H.S., and Blakemore, W.F. (1997). Identification of post-mitotic oligodendrocytes incapable of remyelination within the demyelinated adult spinal cord. Journal of neuropathology and experimental neurology *56*, 1191-1201.

Kelland, E.E., Gilmore, W., Weiner, L.P., and Lund, B.T. (2011). The dual role of CXCL8 in human CNS stem cell function: multipotent neural stem cell death and oligodendrocyte progenitor cell chemotaxis. Glia *59*, 1864-1878.

Kessler, O., Shraga-Heled, N., Lange, T., Gutmann-Raviv, N., Sabo, E., Baruch, L., Machluf, M., and Neufeld, G. (2004). Semaphorin-3F is an inhibitor of tumor angiogenesis. Cancer research *64*, 1008-1015.

Kim, M.J., Kang, K.H., Kim, C.H., and Choi, S.Y. (2008). Real-time imaging of mitochondria in transgenic zebrafish expressing mitochondrially targeted GFP. BioTechniques *45*, 331-334.

Kimmel, C.B., Ballard, W.W., Kimmel, S.R., Ullmann, B., and Schilling, T.F. (1995). Stages of embryonic development of the zebrafish. Developmental dynamics : an official publication of the American Association of Anatomists *203*, 253-310.

Kipp, M., van der Star, B., Vogel, D.Y.S., Puentes, F., van der Valk, P., Baker, D., and Amor, S. (2012). Experimental in vivo and in vitro models of multiple sclerosis: EAE and beyond. Multiple Sclerosis and Related Disorders, 15-28.

Kirby, B.B., Takada, N., Latimer, A.J., Shin, J., Carney, T.J., Kelsh, R.N., and Appel, B. (2006). In vivo time-lapse imaging shows dynamic oligodendrocyte progenitor behavior during zebrafish development. Nature neuroscience *9*, 1506-1511.

Kirschner, D.A., Inouye, H., Ganser, A.L., and Mann, V. (1989). Myelin membrane structure and composition correlated: a phylogenetic study. Journal of neurochemistry *53*, 1599-1609.

Kitagawa, K., Sinoway, M.P., Yang, C., Gould, R.M., and Colman, D.R. (1993). A proteolipid protein gene family: expression in sharks and rays and possible evolution from an ancestral gene encoding a pore-forming polypeptide. Neuron *11*, 433-448.

Kizil, C., Kaslin, J., Kroehne, V., and Brand, M. (2012). Adult neurogenesis and brain regeneration in zebrafish. Developmental neurobiology *72*, 429-461.

Knapp, P.E., Bartlett, W.P., and Skoff, R.P. (1987). Cultured oligodendrocytes mimic in vivo phenotypic characteristics: cell shape, expression of myelin-specific antigens, and membrane production. Developmental biology *120*, 356-365.

Kolodkin, A.L. (1996). Semaphorins: mediators of repulsive growth cone guidance. Trends in cell biology *6*, 15-22.

Kolodkin, A.L., Levengood, D.V., Rowe, E.G., Tai, Y.T., Giger, R.J., and Ginty, D.D. (1997). Neuropilin is a semaphorin III receptor. Cell *90*, 753-762.

Kotter, M.R., Li, W.W., Zhao, C., and Franklin, R.J. (2006). Myelin impairs CNS remyelination by inhibiting oligodendrocyte precursor cell differentiation. The Journal of neuroscience : the official journal of the Society for Neuroscience *26*, 328-332.

Kotter, M.R., Setzu, A., Sim, F.J., Van Rooijen, N., and Franklin, R.J. (2001). Macrophage depletion impairs oligodendrocyte remyelination following lysolecithin-induced demyelination. Glia *35*, 204-212.

Kotter, M.R., Zhao, C., van Rooijen, N., and Franklin, R.J. (2005). Macrophage-depletion induced impairment of experimental CNS remyelination is associated with a reduced oligodendrocyte progenitor cell response and altered growth factor expression. Neurobiology of disease *18*, 166-175.

Kroehne, V., Freudenreich, D., Hans, S., Kaslin, J., and Brand, M. (2011). Regeneration of the adult zebrafish brain from neurogenic radial glia-type progenitors. Development *138*, 4831-4841.

Kucenas, S., Snell, H., and Appel, B. (2008). nkx2.2a promotes specification and differentiation of a myelinating subset of oligodendrocyte lineage cells in zebrafish. Neuron glia biology *4*, 71-81.

Kuhlmann, T., Lingfeld, G., Bitsch, A., Schuchardt, J., and Bruck, W. (2002). Acute axonal damage in multiple sclerosis is most extensive in early disease stages and decreases over time. Brain : a journal of neurology *125*, 2202-2212.

Kuhlmann, T., Miron, V., Cui, Q., Wegner, C., Antel, J., and Bruck, W. (2008). Differentiation block of oligodendroglial progenitor cells as a cause for remyelination failure in chronic multiple sclerosis. Brain : a journal of neurology *131*, 1749-1758.

Kume, N., and Gimbrone, M.A., Jr. (1994). Lysophosphatidylcholine transcriptionally induces growth factor gene expression in cultured human endothelial cells. The Journal of clinical investigation *93*, 907-911.

Kyritsis, N., Kizil, C., Zocher, S., Kroehne, V., Kaslin, J., Freudenreich, D., Iltzsche, A., and Brand, M. (2012). Acute inflammation initiates the regenerative response in the adult zebrafish brain. Science *338*, 1353-1356.

Laeng, P., Molthagen, M., Yu, E.G., and Bartsch, U. (1996). Transplantation of oligodendrocyte progenitor cells into the rat retina: extensive myelination of retinal ganglion cell axons. Glia *18*, 200-210.

Lai, K., Kaspar, B.K., Gage, F.H., and Schaffer, D.V. (2003). Sonic hedgehog regulates adult neural progenitor proliferation in vitro and in vivo. Nature neuroscience *6*, 21-27.

Lal-Nag, M., and Morin, P.J. (2009). The claudins. Genome biology *10*, 235.

Larochelle, C., Alvarez, J.I., and Prat, A. (2011). How do immune cells overcome the blood-brain barrier in multiple sclerosis? FEBS letters *585*, 3770-3780.

Lassmann, H., Bruck, W., Lucchinetti, C., and Rodriguez, M. (1997). Remyelination in multiple sclerosis. Mult Scler *3*, 133-136.

Laursen, L.S., Chan, C.W., and ffrench-Constant, C. (2009). An integrin-contactin complex regulates CNS myelination by differential Fyn phosphorylation. The Journal of neuroscience : the official journal of the Society for Neuroscience *29*, 9174-9185.

Laursen, L.S., Chan, C.W., and Ffrench-Constant, C. (2011). Translation of myelin basic protein mRNA in oligodendrocytes is regulated by integrin activation and hnRNP-K. The Journal of cell biology *192*, 797-811.

Lee, K.K., de Repentigny, Y., Saulnier, R., Rippstein, P., Macklin, W.B., and Kothary, R. (2006). Dominant-negative beta1 integrin mice have region-specific myelin defects accompanied by alterations in MAPK activity. Glia *53*, 836-844.

Lee, X., Yang, Z., Shao, Z., Rosenberg, S.S., Levesque, M., Pepinsky, R.B., Qiu, M., Miller, R.H., Chan, J.R., and Mi, S. (2007). NGF regulates the expression of axonal LINGO-1 to inhibit oligodendrocyte differentiation and myelination. The Journal of neuroscience : the official journal of the Society for Neuroscience *27*, 220-225.

Lee, Y., Morrison, B.M., Li, Y., Lengacher, S., Farah, M.H., Hoffman, P.N., Liu, Y., Tsingalia, A., Jin, L., Zhang, P.W.*, et al.* (2012). Oligodendroglia metabolically support axons and contribute to neurodegeneration. Nature *487*, 443-448.

Lendahl, U., Zimmerman, L.B., and McKay, R.D. (1990). CNS stem cells express a new class of intermediate filament protein. Cell *60*, 585-595.

Li, C., Trapp, B., Ludwin, S., Peterson, A., and Roder, J. (1998). Myelin associated glycoprotein modulates glia-axon contact in vivo. Journal of neuroscience research *51*, 210-217.

Li, C., Tropak, M.B., Gerlai, R., Clapoff, S., Abramow-Newerly, W., Trapp, B., Peterson, A., and Roder, J. (1994). Myelination in the absence of myelin-associated glycoprotein. Nature *369*, 747-750.

Li, H., de Faria, J.P., Andrew, P., Nitarska, J., and Richardson, W.D. (2011). Phosphorylation regulates OLIG2 cofactor choice and the motor neuron-oligodendrocyte fate switch. Neuron *69*, 918-929.

Li, H., Lu, Y., Smith, H.K., and Richardson, W.D. (2007). Olig1 and Sox10 interact synergistically to drive myelin basic protein transcription in oligodendrocytes. The Journal of neuroscience : the official journal of the Society for Neuroscience *27*, 14375-14382.

Liang, X., Draghi, N.A., and Resh, M.D. (2004). Signaling from integrins to Fyn to Rho family GTPases regulates morphologic differentiation of oligodendrocytes. The Journal of neuroscience : the official journal of the Society for Neuroscience *24*, 7140-7149.

Lieberoth, B.C., Becker, C.G., and Becker, T. (2003). Double labeling of neurons by retrograde axonal tracing and non-radioactive in situ hybridization in the CNS of adult zebrafish. Methods in cell science : an official journal of the Society for In Vitro Biology *25*, 65-70.

Liebetanz, D., and Merkler, D. (2006). Effects of commissural de- and remyelination on motor skill behaviour in the cuprizone mouse model of multiple sclerosis. Experimental neurology *202*, 217-224.

Lindvall, O., and Kokaia, Z. (2010). Stem cells in human neurodegenerative disorders--time for clinical translation? The Journal of clinical investigation *120*, 29-40.

Linker, R.A., Lee, D.H., Demir, S., Wiese, S., Kruse, N., Siglienti, I., Gerhardt, E., Neumann, H., Sendtner, M., Luhder, F.*, et al.* (2010). Functional role of brain-derived neurotrophic factor in neuroprotective autoimmunity: therapeutic implications in a model of multiple sclerosis. Brain : a journal of neurology *133*, 2248-2263.

Lipton, H.L. (1975). Theiler's virus infection in mice: an unusual biphasic disease process leading to demyelination. Infection and immunity *11*, 1147-1155.

Loh, Y.H., Christoffels, A., Brenner, S., Hunziker, W., and Venkatesh, B. (2004). Extensive expansion of the claudin gene family in the teleost fish, Fugu rubripes. Genome research *14*, 1248-1257.

Loulier, K., Ruat, M., and Traiffort, E. (2006). Increase of proliferating oligodendroglial progenitors in the adult mouse brain upon Sonic hedgehog delivery in the lateral ventricle. Journal of neurochemistry *98*, 530-542.

Lucchinetti, C., Bruck, W., Parisi, J., Scheithauer, B., Rodriguez, M., and Lassmann, H. (1999). A quantitative analysis of oligodendrocytes in multiple sclerosis lesions. A study of 113 cases. Brain : a journal of neurology *122 (Pt 12)*, 2279-2295.

Ludwin, S.K. (1978). Central nervous system demyelination and remyelination in the mouse: an ultrastructural study of cuprizone toxicity. Laboratory investigation; a journal of technical methods and pathology *39*, 597-612.

Lyons, D.A., Pogoda, H.M., Voas, M.G., Woods, I.G., Diamond, B., Nix, R., Arana, N., Jacobs, J., and Talbot, W.S. (2005). erbb3 and erbb2 are essential for schwann cell migration and myelination in zebrafish. Current biology : CB *15*, 513-524.

Machold, R., Hayashi, S., Rutlin, M., Muzumdar, M.D., Nery, S., Corbin, J.G., Gritli-Linde, A., Dellovade, T., Porter, J.A., Rubin, L.L.*, et al.* (2003). Sonic hedgehog is required for progenitor cell maintenance in telencephalic stem cell niches. Neuron *39*, 937-950.

Macklin, W.B., Campagnoni, C.W., Deininger, P.L., and Gardinier, M.V. (1987). Structure and expression of the mouse myelin proteolipid protein gene. Journal of neuroscience research *18*, 383-394.

Mallet, V.O., Mitchell, C., Guidotti, J.E., Jaffray, P., Fabre, M., Spencer, D., Arnoult, D., Kahn, A., and Gilgenkrantz, H. (2002). Conditional cell ablation by tight control of caspase-3 dimerization in transgenic mice. Nature biotechnology *20*, 1234-1239.

Manrique-Hoyos, N., Jurgens, T., Gronborg, M., Kreutzfeldt, M., Schedensack, M., Kuhlmann, T., Schrick, C., Bruck, W., Urlaub, H., Simons, M.*, et al.* (2012). Late motor decline after accomplished remyelination: impact for progressive multiple sclerosis. Annals of neurology *71*, 227-244.

Martini, R., Mohajeri, M.H., Kasper, S., Giese, K.P., and Schachner, M. (1995). Mice doubly deficient in the genes for P0 and myelin basic protein show that both proteins contribute to the formation of the major dense line in peripheral nerve myelin. The Journal of neuroscience : the official journal of the Society for Neuroscience *15*, 4488-4495.

Marz, M., Schmidt, R., Rastegar, S., and Strahle, U. (2010). Expression of the transcription factor Olig2 in proliferating cells in the adult zebrafish telencephalon. Developmental dynamics : an official publication of the American Association of Anatomists *239*, 3336-3349.

Matsushima, G.K., and Morell, P. (2001). The neurotoxicant, cuprizone, as a model to study demyelination and remyelination in the central nervous system. Brain Pathol *11*, 107-116.

McKay, R. (1997). Stem cells in the central nervous system. Science *276*, 66-71.

McMurray, H.F., Parthasarathy, S., and Steinberg, D. (1993). Oxidatively modified low density lipoprotein is a chemoattractant for human T lymphocytes. The Journal of clinical investigation *92*, 1004-1008.

Menn, B., Garcia-Verdugo, J.M., Yaschine, C., Gonzalez-Perez, O., Rowitch, D., and Alvarez-Buylla, A. (2006). Origin of oligodendrocytes in the subventricular zone of the adult brain. The Journal of neuroscience : the official journal of the Society for Neuroscience *26*, 7907-7918.

Mi, S., Hu, B., Hahm, K., Luo, Y., Kam Hui, E.S., Yuan, Q., Wong, W.M., Wang, L., Su, H., Chu, T.H.*, et al.* (2007). LINGO-1 antagonist promotes spinal cord remyelination and axonal integrity in MOG-induced experimental autoimmune encephalomyelitis. Nature medicine *13*, 1228-1233.

Mi, S., Lee, X., Shao, Z., Thill, G., Ji, B., Relton, J., Levesque, M., Allaire, N., Perrin, S., Sands, B.*, et al.* (2004). LINGO-1 is a component of the Nogo-66 receptor/p75 signaling complex. Nature neuroscience *7*, 221-228.

Mi, S., Miller, R.H., Lee, X., Scott, M.L., Shulag-Morskaya, S., Shao, Z., Chang, J., Thill, G., Levesque, M., Zhang, M.*, et al.* (2005). LINGO-1 negatively regulates myelination by oligodendrocytes. Nature neuroscience *8*, 745-751.

Mi, S., Miller, R.H., Tang, W., Lee, X., Hu, B., Wu, W., Zhang, Y., Shields, C.B., Miklasz, S., Shea, D.*, et al.* (2009). Promotion of central nervous system remyelination by induced differentiation of oligodendrocyte precursor cells. Annals of neurology *65*, 304-315.

Miller, D.J., Duka, T., Stimpson, C.D., Schapiro, S.J., Baze, W.B., McArthur, M.J., Fobbs, A.J., Sousa, A.M., Sestan, N., Wildman, D.E.*, et al.* (2012). Prolonged myelination in human neocortical evolution. Proceedings of the National Academy of Sciences of the United States of America *109*, 16480-16485.

Mirsky, R., Woodhoo, A., Parkinson, D.B., Arthur-Farraj, P., Bhaskaran, A., and Jessen, K.R. (2008). Novel signals controlling embryonic Schwann cell development, myelination and dedifferentiation. Journal of the peripheral nervous system : JPNS *13*, 122-135.

Miyamoto, T., Morita, K., Takemoto, D., Takeuchi, K., Kitano, Y., Miyakawa, T., Nakayama, K., Okamura, Y., Sasaki, H., Miyachi, Y.*, et al.* (2005). Tight junctions in Schwann cells of peripheral myelinated axons: a lesson from claudin-19-deficient mice. The Journal of cell biology *169*, 527-538.

Monk, K.R., Naylor, S.G., Glenn, T.D., Mercurio, S., Perlin, J.R., Dominguez, C., Moens, C.B., and Talbot, W.S. (2009). A G protein-coupled receptor is essential for Schwann cells to initiate myelination. Science *325*, 1402-1405.

Monk, K.R., Oshima, K., Jors, S., Heller, S., and Talbot, W.S. (2011). Gpr126 is essential for peripheral nerve development and myelination in mammals. Development *138*, 2673-2680.

Montag, D., Giese, K.P., Bartsch, U., Martini, R., Lang, Y., Bluthmann, H., Karthigasan, J., Kirschner, D.A., Wintergerst, E.S., Nave, K.A.*, et al.* (1994). Mice deficient for the myelin-associated glycoprotein show subtle abnormalities in myelin. Neuron *13*, 229-246.

Morcos, Y., and Chan-Ling, T. (1997). Identification of oligodendrocyte precursors in the myelinated streak of the adult rabbit retina in vivo. Glia *21*, 163-182.

Münzel, E.J., Schaefer, K., Obirei, B., Kremmer, E., Burton, E.A., Kuscha, V., Becker, C.G., Brosamle, C., Williams, A., and Becker, T. (2012). Claudin k is specifically expressed in cells that form myelin during development of the nervous system and regeneration of the optic nerve in adult zebrafish. Glia *60*, 253-270.

Murray, P.D., McGavern, D.B., Sathornsumetee, S., and Rodriguez, M. (2001). Spontaneous remyelination following extensive demyelination is associated with improved neurological function in a viral model of multiple sclerosis. Brain : a journal of neurology *124*, 1403-1416.

Nait-Oumesmar, B., Decker, L., Lachapelle, F., Avellana-Adalid, V., Bachelin, C., and Baron-Van Evercooren, A. (1999). Progenitor cells of the adult mouse subventricular zone proliferate, migrate and differentiate into oligodendrocytes after demyelination. The European journal of neuroscience *11*, 4357-4366.

Nait-Oumesmar, B., Picard-Riera, N., Kerninon, C., and Baron-Van Evercooren, A. (2008). The role of SVZ-derived neural precursors in demyelinating diseases: from animal models to multiple sclerosis. Journal of the neurological sciences *265*, 26-31.

Nait-Oumesmar, B., Picard-Riera, N., Kerninon, C., Decker, L., Seilhean, D., Hoglinger, G.U., Hirsch, E.C., Reynolds, R., and Baron-Van Evercooren, A. (2007). Activation of the subventricular zone in multiple sclerosis: evidence for early glial progenitors. Proceedings of the National Academy of Sciences of the United States of America *104*, 4694-4699.

Nave, K.A., Lai, C., Bloom, F.E., and Milner, R.J. (1987). Splice site selection in the proteolipid protein (PLP) gene transcript and primary structure of the DM-20 protein of central nervous system myelin. Proceedings of the National Academy of Sciences of the United States of America *84*, 5665-5669.

Newbern, J., and Birchmeier, C. (2010). Nrg1/ErbB signaling networks in Schwann cell development and myelination. Seminars in cell & developmental biology *21*, 922-928.

Nguyen, D., and Stangel, M. (2001). Expression of the chemokine receptors CXCR1 and CXCR2 in rat oligodendroglial cells. Brain research Developmental brain research *128*, 77-81.

Nicholson, G.A., Valentijn, L.J., Cherryson, A.K., Kennerson, M.L., Bragg, T.L., DeKroon, R.M., Ross, D.A., Pollard, J.D., McLeod, J.G., Bolhuis, P.A.*, et al.* (1994). A frame shift mutation in the PMP22 gene in hereditary neuropathy with liability to pressure palsies. Nature genetics *6*, 263-266.

Noll, E., and Miller, R.H. (1993). Oligodendrocyte precursors originate at the ventral ventricular zone dorsal to the ventral midline region in the embryonic rat spinal cord. Development *118*, 563-573.

Nona, S. (1995). Regeneration in the Goldfish Visual System. In Webvision: The Organization of the Retina and Visual System, H. Kolb, E. Fernandez, and R. Nelson, eds. (Salt Lake City (UT)).

Nona, S.N. (1994). Regeneration in the Goldfish Visual System. In Webvision - The organisation of the retina and visual system, H. Kolb, Nelson, R., Fernandez, E., Jones, B.,, ed.

Nona, S.N., Duncan, A., Stafford, C.A., Maggs, A., Jeserich, G., and Cronly-Dillon, J.R. (1992). Myelination of regenerated axons in goldfish optic nerve by Schwann cells. Journal of neurocytology *21*, 391-401.

Nona, S.N., Thomlinson, A.M., and Stafford, C.A. (1998). Temporary colonization of the site of lesion by macrophages is a prelude to the arrival of regenerated axons in injured goldfish optic nerve. Journal of neurocytology *27*, 791-803.

Noseworthy, J.H., Lucchinetti, C., Rodriguez, M., and Weinshenker, B.G. (2000). Multiple sclerosis. The New England journal of medicine *343*, 938-952.

O'Meara, R.W., Michalski, J.P., and Kothary, R. (2011). Integrin signaling in oligodendrocytes and its importance in CNS myelination. Journal of signal transduction *2011*, 354091.

Okita, C., Sato, M., and Schroeder, T. (2004). Generation of optimized yellow and red fluorescent proteins with distinct subcellular localization. BioTechniques *36*, 418-422, 424.

Oleszak, E.L., Kuzmak, J., Good, R.A., and Platsoucas, C.D. (1995). Immunology of Theiler's murine encephalomyelitis virus infection. Immunologic research *14*, 13-33.

Omari, K.M., John, G., Lango, R., and Raine, C.S. (2006). Role for CXCR2 and CXCL1 on glia in multiple sclerosis. Glia *53*, 24-31.

Omari, K.M., John, G.R., Sealfon, S.C., and Raine, C.S. (2005). CXC chemokine receptors on human oligodendrocytes: implications for multiple sclerosis. Brain : a journal of neurology *128*, 1003-1015.

Orentas, D.M., Hayes, J.E., Dyer, K.L., and Miller, R.H. (1999). Sonic hedgehog signaling is required during the appearance of spinal cord oligodendrocyte precursors. Development *126*, 2419-2429.

Owens, G.P., and Bennett, J.L. (2012). Trigger, pathogen, or bystander: the complex nexus linking Epstein- Barr virus and multiple sclerosis. Mult Scler *18*, 1204-1208.

Park, H.C., and Appel, B. (2003). Delta-Notch signaling regulates oligodendrocyte specification. Development *130*, 3747-3755.

Patel, J.R., McCandless, E.E., Dorsey, D., and Klein, R.S. (2010). CXCR4 promotes differentiation of oligodendrocyte progenitors and remyelination. Proceedings of the National Academy of Sciences of the United States of America *107*, 11062-11067.

Patel, P.I., Roa, B.B., Welcher, A.A., Schoener-Scott, R., Trask, B.J., Pentao, L., Snipes, G.J., Garcia, C.A., Francke, U., Shooter, E.M.*, et al.* (1992). The gene for the peripheral myelin protein PMP-22 is a candidate for Charcot-Marie-Tooth disease type 1A. Nature genetics *1*, 159-165.

Patrikios, P., Stadelmann, C., Kutzelnigg, A., Rauschka, H., Schmidbauer, M., Laursen, H., Sorensen, P.S., Bruck, W., Lucchinetti, C., and Lassmann, H. (2006). Remyelination is extensive in a subset of multiple sclerosis patients. Brain : a journal of neurology *129*, 3165-3172.

Penderis, J., Shields, S.A., and Franklin, R.J. (2003). Impaired remyelination and depletion of oligodendrocyte progenitors does not occur following repeated episodes of focal demyelination in the rat central nervous system. Brain : a journal of neurology *126*, 1382-1391.

Pepinsky, R.B., Walus, L., Shao, Z., Ji, B., Gu, S., Sun, Y., Wen, D., Lee, X., Wang, Q., Garber, E.*, et al.* (2011). Production of a PEGylated Fab' of the anti-LINGO-1 Li33 antibody and assessment of its biochemical and functional properties in vitro and in a rat model of remyelination. Bioconjugate chemistry *22*, 200-210.

Perier, O., and Gregoire, A. (1965). Electron microscopic features of multiple sclerosis lesions. Brain : a journal of neurology *88*, 937-952.

Pfeiffer, S.E., Warrington, A.E., and Bansal, R. (1993). The oligodendrocyte and its many cellular processes. Trends in cell biology *3*, 191-197.

Pfriem, A., Pylatiuk, C., Alshut, R., Ziegener, B., Schulz, S., and Bretthauer, G. (2012). A modular, low-cost robot for zebrafish handling. Conference proceedings : Annual International Conference of the IEEE Engineering in Medicine and Biology Society IEEE Engineering in Medicine and Biology Society Conference *2012*, 980-983.

Piaton, G., Aigrot, M.S., Williams, A., Moyon, S., Tepavcevic, V., Moutkine, I., Gras, J., Matho, K.S., Schmitt, A., Soellner, H.*, et al.* (2011). Class 3 semaphorins influence oligodendrocyte precursor recruitment and remyelination in adult central nervous system. Brain : a journal of neurology *134*, 1156-1167.

Piaton, G., Williams, A., Seilhean, D., and Lubetzki, C. (2009). Remyelination in multiple sclerosis. Progress in brain research *175*, 453-464.

Plucinska, G., Paquet, D., Hruscha, A., Godinho, L., Haass, C., Schmid, B., and Misgeld, T. (2012). In vivo imaging of disease-related mitochondrial dynamics in a vertebrate model system. The Journal of neuroscience : the official journal of the Society for Neuroscience *32*, 16203-16212.

Pogoda, H.M., Sternheim, N., Lyons, D.A., Diamond, B., Hawkins, T.A., Woods, I.G., Bhatt, D.H., Franzini-Armstrong, C., Dominguez, C., Arana, N.*, et al.* (2006). A genetic screen identifies genes essential for development of myelinated axons in zebrafish. Developmental biology *298*, 118-131.

Poliak, S., Matlis, S., Ullmer, C., Scherer, S.S., and Peles, E. (2002). Distinct claudins and associated PDZ proteins form different autotypic tight junctions in myelinating Schwann cells. The Journal of cell biology *159*, 361-372.

Poss, K.D., Wilson, L.G., and Keating, M.T. (2002). Heart regeneration in zebrafish. Science *298*, 2188-2190.

Prayoonwiwat, N., and Rodriguez, M. (1993). The potential for oligodendrocyte proliferation during demyelinating disease. Journal of neuropathology and experimental neurology *52*, 55-63.

Prineas, J.W., and Connell, F. (1979). Remyelination in multiple sclerosis. Annals of neurology *5*, 22-31.

Pringle, N.P., Yu, W.P., Guthrie, S., Roelink, H., Lumsden, A., Peterson, A.C., and Richardson, W.D. (1996). Determination of neuroepithelial cell fate: induction of the oligodendrocyte lineage by ventral midline cells and sonic hedgehog. Developmental biology *177*, 30-42.

Pringproa, K., Rohn, K., Kummerfeld, M., Wewetzer, K., and Baumgartner, W. (2010). Theiler's murine encephalomyelitis virus preferentially infects immature stages of the murine oligodendrocyte precursor cell line BO-1 and blocks oligodendrocytic differentiation in vitro. Brain research *1327*, 24-37.

Puckett, C., Hudson, L., Ono, K., Friedrich, V., Benecke, J., Dubois-Dalcq, M., and Lazzarini, R.A. (1987). Myelin-specific proteolipid protein is expressed in myelinating Schwann cells but is not incorporated into myelin sheaths. Journal of neuroscience research *18*, 511-518.

Pugliatti, M., Sotgiu, S., and Rosati, G. (2002). The worldwide prevalence of multiple sclerosis. Clinical neurology and neurosurgery *104*, 182-191.

Qi, X., Lewin, A.S., Sun, L., Hauswirth, W.W., and Guy, J. (2007). Suppression of mitochondrial oxidative stress provides long-term neuroprotection in experimental optic neuritis. Investigative ophthalmology & visual science *48*, 681-691.

Qi, Y., Cai, J., Wu, Y., Wu, R., Lee, J., Fu, H., Rao, M., Sussel, L., Rubenstein, J., and Qiu, M. (2001). Control of oligodendrocyte differentiation by the Nkx2.2 homeodomain transcription factor. Development *128*, 2723-2733.

Quintana, F.J., Iglesias, A.H., Farez, M.F., Caccamo, M., Burns, E.J., Kassam, N., Oukka, M., and Weiner, H.L. (2010). Adaptive autoimmunity and Foxp3-based immunoregulation in zebrafish. PloS one *5*, e9478.

Raff, M.C., Abney, E.R., and Fok-Seang, J. (1985). Reconstitution of a developmental clock in vitro: a critical role for astrocytes in the timing of oligodendrocyte differentiation. Cell *42*, 61-69.

Raff, M.C., Miller, R.H., and Noble, M. (1983). A glial progenitor cell that develops in vitro into an astrocyte or an oligodendrocyte depending on culture medium. Nature *303*, 390-396.

Raine, C.S., and Wu, E. (1993). Multiple sclerosis: remyelination in acute lesions. Journal of neuropathology and experimental neurology *52*, 199-204.

Ramachandran, R., Reifler, A., Parent, J.M., and Goldman, D. (2010). Conditional gene expression and lineage tracing of tuba1a expressing cells during zebrafish development and retina regeneration. The Journal of comparative neurology *518*, 4196-4212.

Ramachandran, R., Reifler, A., Wan, J., and Goldman, D. (2012). Application of Cre-loxP recombination for lineage tracing of adult zebrafish retinal stem cells. Methods Mol Biol *884*, 129-140.

Ranscht, B. (1988). Sequence of contactin, a 130-kD glycoprotein concentrated in areas of interneuronal contact, defines a new member of the immunoglobulin supergene family in the nervous system. The Journal of cell biology *107*, 1561-1573.

Rao, M.S. (1999). Multipotent and restricted precursors in the central nervous system. The Anatomical record *257*, 137-148.

Raphael, A.R., and Talbot, W.S. (2011). New insights into signaling during myelination in zebrafish. Current topics in developmental biology *97*, 1-19.

Rash, J.E. (2010). Molecular disruptions of the panglial syncytium block potassium siphoning and axonal saltatory conduction: pertinence to neuromyelitis optica and other demyelinating diseases of the central nervous system. Neuroscience *168*, 982-1008.

Readhead, C., Takasashi, N., Shine, H.D., Saavedra, R., Sidman, R., and Hood, L. (1990). Role of myelin basic protein in the formation of central nervous system myelin. Annals of the New York Academy of Sciences *605*, 280-285.

Redwine, J.M., and Armstrong, R.C. (1998). In vivo proliferation of oligodendrocyte progenitors expressing PDGFalphaR during early remyelination. Journal of neurobiology *37*, 413-428.

Reimer, M.M., Sorensen, I., Kuscha, V., Frank, R.E., Liu, C., Becker, C.G., and Becker, T. (2008). Motor neuron regeneration in adult zebrafish. The Journal of neuroscience : the official journal of the Society for Neuroscience *28*, 8510-8516.

Reynolds, R., Roncaroli, F., Nicholas, R., Radotra, B., Gveric, D., and Howell, O. (2011). The neuropathological basis of clinical progression in multiple sclerosis. Acta neuropathologica *122*, 155-170.

Richardson, W.D., Kessaris, N., and Pringle, N. (2006). Oligodendrocyte wars. Nature reviews Neuroscience *7*, 11-18.

Richardson, W.D., Young, K.M., Tripathi, R.B., and McKenzie, I. (2011). NG2-glia as multipotent neural stem cells: fact or fantasy? Neuron *70*, 661-673.

Ritchie, J.M., and Rogart, R.B. (1977). Density of sodium channels in mammalian myelinated nerve fibers and nature of the axonal membrane under the myelin sheath. Proceedings of the National Academy of Sciences of the United States of America *74*, 211-215.

Roa, B.B., Garcia, C.A., Pentao, L., Killian, J.M., Trask, B.J., Suter, U., Snipes, G.J., Ortiz-Lopez, R., Shooter, E.M., Patel, P.I.*, et al.* (1993). Evidence for a recessive PMP22 point mutation in Charcot-Marie-Tooth disease type 1A. Nature genetics *5*, 189-194.

Rong, J.X., Berman, J.W., Taubman, M.B., and Fisher, E.A. (2002). Lysophosphatidylcholine stimulates monocyte chemoattractant protein-1 gene expression in rat aortic smooth muscle cells. Arteriosclerosis, thrombosis, and vascular biology *22*, 1617-1623.

Roos, M., Schachner, M., and Bernhardt, R.R. (1999). Zebrafish semaphorin Z1b inhibits growing motor axons in vivo. Mechanisms of development *87*, 103-117.

Rothenaigner, I., Krecsmarik, M., Hayes, J.A., Bahn, B., Lepier, A., Fortin, G., Gotz, M., Jagasia, R., and Bally-Cuif, L. (2011). Clonal analysis by distinct viral vectors identifies bona fide neural stem cells in the adult zebrafish telencephalon and characterizes their division properties and fate. Development *138*, 1459-1469.

Ruckh, J.M., Zhao, J.W., Shadrach, J.L., van Wijngaarden, P., Rao, T.N., Wagers, A.J., and Franklin, R.J. (2012). Rejuvenation of regeneration in the aging central nervous system. Cell stem cell *10*, 96-103.

Rus, H., Cudrici, C., David, S., and Niculescu, F. (2006). The complement system in central nervous system diseases. Autoimmunity *39*, 395-402.

Saavedra, R.A., Fors, L., Aebersold, R.H., Arden, B., Horvath, S., Sanders, J., and Hood, L. (1989). The myelin proteins of the shark brain are similar to the myelin proteins of the mammalian peripheral nervous system. Journal of molecular evolution *29*, 149-156.

Sabo, J.K., Aumann, T.D., Merlo, D., Kilpatrick, T.J., and Cate, H.S. (2011). Remyelination is altered by bone morphogenic protein signaling in demyelinated lesions. The Journal of neuroscience : the official journal of the Society for Neuroscience *31*, 4504-4510.

Saher, G., Brugger, B., Lappe-Siefke, C., Mobius, W., Tozawa, R., Wehr, M.C., Wieland, F., Ishibashi, S., and Nave, K.A. (2005). High cholesterol level is essential for myelin membrane growth. Nature neuroscience *8*, 468-475.

Sato, T., Takahoko, M., and Okamoto, H. (2006). HuC:Kaede, a useful tool to label neural morphologies in networks in vivo. Genesis *44*, 136-142.

Schaefer, K. (2009). Characterization of two novel myelin proteins. In Fakultät für Chemie und Pharmazie (Munich: Ludwig-Maximilians-Universtität München), pp. 124.

Schweitzer, J., Becker, T., Becker, C.G., and Schachner, M. (2003). Expression of protein zero is increased in lesioned axon pathways in the central nervous system of adult zebrafish. Glia *41*, 301-317.

Schweitzer, J., Becker, T., Schachner, M., Nave, K.A., and Werner, H. (2006). Evolution of myelin proteolipid proteins: gene duplication in teleosts and expression pattern divergence. Molecular and cellular neurosciences *31*, 161-177.

Schweitzer, J., Gimnopoulos, D., Lieberoth, B.C., Pogoda, H.M., Feldner, J., Ebert, A., Schachner, M., Becker, T., and Becker, C.G. (2007). Contactin1a expression is associated with oligodendrocyte differentiation and axonal regeneration in the central nervous system of zebrafish. Molecular and cellular neurosciences *35*, 194-207.

See, J.M., and Grinspan, J.B. (2009). Sending mixed signals: bone morphogenetic protein in myelination and demyelination. Journal of neuropathology and experimental neurology *68*, 595-604.

Segovia, K.N., McClure, M., Moravec, M., Luo, N.L., Wan, Y., Gong, X., Riddle, A., Craig, A., Struve, J., Sherman, L.S*., et al.* (2008). Arrested oligodendrocyte lineage maturation in chronic perinatal white matter injury. Annals of neurology *63*, 520-530.

Setzu, A., Ffrench-Constant, C., and Franklin, R.J. (2004). CNS axons retain their competence for myelination throughout life. Glia *45*, 307-311.

Setzu, A., Lathia, J.D., Zhao, C., Wells, K., Rao, M.S., Ffrench-Constant, C., and Franklin, R.J. (2006). Inflammation stimulates myelination by transplanted oligodendrocyte precursor cells. Glia *54*, 297-303.

Sharma, A., Verhaagen, J., and Harvey, A.R. (2012). Receptor complexes for each of the Class 3 Semaphorins. Frontiers in cellular neuroscience *6*, 28.

Sheikh, A.M., Nagai, A., Ryu, J.K., McLarnon, J.G., Kim, S.U., and Masuda, J. (2009). Lysophosphatidylcholine induces glial cell activation: role of rho kinase. Glia *57*, 898-907.

Sherman, D.L., and Brophy, P.J. (2005). Mechanisms of axon ensheathment and myelin growth. Nature reviews Neuroscience *6*, 683-690.

Shields, S.A., Gilson, J.M., Blakemore, W.F., and Franklin, R.J. (1999). Remyelination occurs as extensively but more slowly in old rats compared to young rats following gliotoxin-induced CNS demyelination. Glia *28*, 77-83.

Shin, J., Park, H.C., Topczewska, J.M., Mawdsley, D.J., and Appel, B. (2003). Neural cell fate analysis in zebrafish using olig2 BAC transgenics. Methods in cell science : an official journal of the Society for In Vitro Biology *25*, 7-14.

Sim, F.J., Zhao, C., Penderis, J., and Franklin, R.J. (2002). The age-related decrease in CNS remyelination efficiency is attributable to an impairment of both oligodendrocyte progenitor recruitment and differentiation. The Journal of neuroscience : the official journal of the Society for Neuroscience *22*, 2451-2459.

Simmons, T., and Appel, B. (2012). Mutation of pescadillo disrupts oligodendrocyte formation in zebrafish. PloS one *7*, e32317.

Sloane, J.A., Batt, C., Ma, Y., Harris, Z.M., Trapp, B., and Vartanian, T. (2010). Hyaluronan blocks oligodendrocyte progenitor maturation and remyelination through TLR2. Proceedings of the National Academy of Sciences of the United States of America *107*, 11555-11560.

Smith, G.S., Samborska, B., Hawley, S.P., Klaiman, J.M., Gillis, T.E., Jones, N., Boggs, J.M., and Harauz, G. (2013). Nucleus-localized 21.5-kDa myelin basic protein promotes oligodendrocyte proliferation and enhances neurite outgrowth in coculture, unlike the plasma membrane-associated 18.5-kDa isoform. Journal of neuroscience research *91*, 349-362.

Smith, K.J. (2007). Sodium channels and multiple sclerosis: roles in symptom production, damage and therapy. Brain Pathol *17*, 230-242.

Sobottka, B., Ziegler, U., Kaech, A., Becher, B., and Goebels, N. (2011). CNS live imaging reveals a new mechanism of myelination: the liquid croissant model. Glia *59*, 1841-1849.

Sommer, I., and Schachner, M. (1981). Monoclonal antibodies (O1 to O4) to oligodendrocyte cell surfaces: an immunocytological study in the central nervous system. Developmental biology *83*, 311-327.

Spassky, N., de Castro, F., Le Bras, B., Heydon, K., Queraud-LeSaux, F., Bloch-Gallego, E., Chedotal, A., Zalc, B., and Thomas, J.L. (2002). Directional guidance of oligodendroglial migration by class 3 semaphorins and netrin-1. The Journal of neuroscience : the official journal of the Society for Neuroscience *22*, 5992-6004.

Spomer, W., Pfriem, A., Alshut, R., Just, S., and Pylatiuk, C. (2012). High-throughput screening of zebrafish embryos using automated heart detection and imaging. Journal of laboratory automation *17*, 435-442.

Sriram, S. (2011). Role of glial cells in innate immunity and their role in CNS demyelination. Journal of neuroimmunology *239*, 13-20.

Stackley, K.D., Beeson, C.C., Rahn, J.J., and Chan, S.S. (2011). Bioenergetic profiling of zebrafish embryonic development. PloS one *6*, e25652.

Stadelmann, C., and Bruck, W. (2008). Interplay between mechanisms of damage and repair in multiple sclerosis. Journal of neurology *255 Suppl 1*, 12-18.

Steelman, A.J., Thompson, J.P., and Li, J. (2012). Demyelination and remyelination in anatomically distinct regions of the corpus callosum following cuprizone intoxication. Neuroscience research *72*, 32-42.

Stolt, C.C., Rehberg, S., Ader, M., Lommes, P., Riethmacher, D., Schachner, M., Bartsch, U., and Wegner, M. (2002). Terminal differentiation of myelin-forming oligodendrocytes depends on the transcription factor Sox10. Genes & development *16*, 165-170.

Stone, L.A., Frank, J.A., Albert, P.S., Bash, C., Smith, M.E., Maloni, H., and McFarland, H.F. (1995). The effect of interferon-beta on blood-brain barrier disruptions demonstrated by contrast-enhanced magnetic resonance imaging in relapsing-remitting multiple sclerosis. Annals of neurology *37*, 611-619.

Stratmann, A., and Jeserich, G. (1995). Molecular cloning and tissue expression of a cDNA encoding IP1--a P0-like glycoprotein of trout CNS myelin. Journal of neurochemistry *64*, 2427-2436.

Stys, P.K., Waxman, S.G., and Ransom, B.R. (1991). Na(+)-Ca2+ exchanger mediates Ca2+ influx during anoxia in mammalian central nervous system white matter. Annals of neurology *30*, 375-380.

Stys, P.K., Zamponi, G.W., van Minnen, J., and Geurts, J.J. (2012). Will the real multiple sclerosis please stand up? Nature reviews Neuroscience *13*, 507-514.

Su, K.G., Banker, G., Bourdette, D., and Forte, M. (2009). Axonal degeneration in multiple sclerosis: the mitochondrial hypothesis. Current neurology and neuroscience reports *9*, 411-417.

Sugimoto, Y., Taniguchi, M., Yagi, T., Akagi, Y., Nojyo, Y., and Tamamaki, N. (2001). Guidance of glial precursor cell migration by secreted cues in the developing optic nerve. Development *128*, 3321-3330.

Swanborg, R.H. (2001). Experimental autoimmune encephalomyelitis in the rat: lessons in T-cell immunology and autoreactivity. Immunological reviews *184*, 129-135.

Takada, N., and Appel, B. (2010). Identification of genes expressed by zebrafish oligodendrocytes using a differential microarray screen. Developmental dynamics : an official publication of the American Association of Anatomists *239*, 2041-2047.

Takada, N., Kucenas, S., and Appel, B. (2010). Sox10 is necessary for oligodendrocyte survival following axon wrapping. Glia *58*, 996-1006.

Targett, M.P., Sussman, J., Scolding, N., O'Leary, M.T., Compston, D.A., and Blakemore, W.F. (1996). Failure to achieve remyelination of demyelinated rat axons following transplantation of glial cells obtained from the adult human brain. Neuropathology and applied neurobiology *22*, 199-206.

Tasaki, I. (1939). The electro-saltatory transmission of the nerve impulse and the effect of narcosis upton the nerve fiber. Am J Physiol *127*, 211-227.

Taveggia, C., Thaker, P., Petrylak, A., Caporaso, G.L., Toews, A., Falls, D.L., Einheber, S., and Salzer, J.L. (2008). Type III neuregulin-1 promotes oligodendrocyte myelination. Glia *56*, 284-293.

Tawk, M., Makoukji, J., Belle, M., Fonte, C., Trousson, A., Hawkins, T., Li, H., Ghandour, S., Schumacher, M., and Massaad, C. (2011). Wnt/beta-catenin signaling is an essential and direct driver of myelin gene expression and myelinogenesis. The Journal of neuroscience : the official journal of the Society for Neuroscience *31*, 3729-3742.

Tegla, C.A., Cudrici, C., Rozycka, M., Soloviova, K., Ito, T., Singh, A.K., Khan, A., Azimzadeh, P., Andrian-Albescu, M., Niculescu, F.*, et al.* (2011). C5b-9-activated, K(v)1.3 channels mediate oligodendrocyte cell cycle activation and dedifferentiation. Experimental and molecular pathology *91*, 335-345.

Teitelbaum, D., Aharoni, R., Klinger, E., Kreitman, R., Raymond, E., Malley, A., Shofti, R., Sela, M., and Arnon, R. (2004). Oral glatiramer acetate in experimental autoimmune encephalomyelitis: clinical and immunological studies. Annals of the New York Academy of Sciences *1029*, 239-249.

Theiler, M. (1934). Spontaneous Encephalomyelitis of Mice--a New Virus Disease. Science *80*, 122.

Thomas, J.L., Spassky, N., Perez Villegas, E.M., Olivier, C., Cobos, I., Goujet-Zalc, C., Martinez, S., and Zalc, B. (2000). Spatiotemporal development of oligodendrocytes in the embryonic brain. Journal of neuroscience research *59*, 471-476.

Thornberry, N.A., and Lazebnik, Y. (1998). Caspases: enemies within. Science *281*, 1312-1316.

Trapp, B.D., Andrews, S.B., Cootauco, C., and Quarles, R. (1989). The myelin-associated glycoprotein is enriched in multivesicular bodies and periaxonal membranes of actively myelinating oligodendrocytes. The Journal of cell biology *109*, 2417-2426.

Trapp, B.D., Ransohoff, R., and Rudick, R. (1999). Axonal pathology in multiple sclerosis: relationship to neurologic disability. Current opinion in neurology *12*, 295-302.

Trojano, M., Paolicelli, D., Tortorella, C., Iaffaldano, P., Lucchese, G., Di Renzo, V., and D'Onghia, M. (2011). Natural history of multiple sclerosis: have available therapies impacted long-term prognosis? Neurologic clinics *29*, 309-321.

Tse, C., Xiang, R.H., Bracht, T., and Naylor, S.L. (2002). Human Semaphorin 3B (SEMA3B) located at chromosome 3p21.3 suppresses tumor formation in an adenocarcinoma cell line. Cancer research *62*, 542-546.

Tsunoda, I., and Fujinami, R.S. (2010). Neuropathogenesis of Theiler's murine encephalomyelitis virus infection, an animal model for multiple sclerosis. Journal of neuroimmune pharmacology : the official journal of the Society on NeuroImmune Pharmacology *5*, 355-369.

Vallstedt, A., Klos, J.M., and Ericson, J. (2005). Multiple dorsoventral origins of oligodendrocyte generation in the spinal cord and hindbrain. Neuron *45*, 55-67.

van den Pol, A.N., and Kim, W.T. (1993). NILE/L1 and NCAM-polysialic acid expression on growing axons of isolated neurons. The Journal of comparative neurology *332*, 237-257.

van Noort, J.M., Baker, D., and Amor, S. (2012). Mechanisms in the development of multiple sclerosis lesions: reconciling autoimmune and neurodegenerative factors. CNS & neurological disorders drug targets *11*, 556-569.

Vandenberg, J.I., and Waxman, S.G. (2012). Hodgkin and Huxley and the basis for electrical signalling: a remarkable legacy still going strong. The Journal of physiology *590*, 2569-2570.

Velumian, A.A., Samoilova, M., and Fehlings, M.G. (2011). Visualization of cytoplasmic diffusion within living myelin sheaths of CNS white matter axons using microinjection of the fluorescent dye Lucifer Yellow. NeuroImage *56*, 27-34.

Vercellino, M., Masera, S., Lorenzatti, M., Condello, C., Merola, A., Mattioda, A., Tribolo, A., Capello, E., Mancardi, G.L., Mutani, R*., et al.* (2009). Demyelination, inflammation, and neurodegeneration in multiple sclerosis deep gray matter. Journal of neuropathology and experimental neurology *68*, 489-502.

Virchow, R. (1854). Über das ausgebreitete Vorkommen einer dem Nervenmark analogen Substanz in den tierischen Geweben. Virchows Arch Pathol Anat, 562-572.

Waehneldt, T.V. (1990). Phylogeny of myelin proteins. Annals of the New York Academy of Sciences *605*, 15-28.

Waehneldt, T.V., Matthieu, J.M., and Jeserich, G. (1986). Appearance of Myelin proteins during vertebrate evolution. Neurochemistry international *9*, 463-474.

Wang, J., Hamm, R.J., and Povlishock, J.T. (2011a). Traumatic axonal injury in the optic nerve: evidence for axonal swelling, disconnection, dieback, and reorganization. Journal of neurotrauma *28*, 1185-1198.

Wang, J., Panakova, D., Kikuchi, K., Holdway, J.E., Gemberling, M., Burris, J.S., Singh, S.P., Dickson, A.L., Lin, Y.F., Sabeh, M.K.*, et al.* (2011b). The regenerative capacity of zebrafish reverses cardiac failure caused by genetic cardiomyocyte depletion. Development *138*, 3421-3430.

Wang, S., Bates, J., Li, X., Schanz, S., Chandler-Militello, D., Levine, C., Maherali, N., Studer, L., Hochedlinger, K., Windrem, M.*, et al.* (2013). Human iPSC-Derived Oligodendrocyte Progenitor Cells Can Myelinate and Rescue a Mouse Model of Congenital Hypomyelination. Cell stem cell *12*, 252-264.

Wang, S., Sdrulla, A.D., diSibio, G., Bush, G., Nofziger, D., Hicks, C., Weinmaster, G., and Barres, B.A. (1998). Notch receptor activation inhibits oligodendrocyte differentiation. Neuron *21*, 63-75.

Warf, B.C., Fok-Seang, J., and Miller, R.H. (1991). Evidence for the ventral origin of oligodendrocyte precursors in the rat spinal cord. The Journal of neuroscience : the official journal of the Society for Neuroscience *11*, 2477-2488.

Waxman, S.G., Kocsis, J.D., and Nitta, K.C. (1979). Lysophosphatidyl choline-induced focal demyelination in the rabbit corpus callosum. Light-microscopic observations. Journal of the neurological sciences *44*, 45-53.

Waxman, S.G., and Ritchie, J.M. (1985). Organization of ion channels in the myelinated nerve fiber. Science *228*, 1502-1507.

Westerfield, M. (1995). The zebrafish book (Eugene, OR: University of Oregon Press).

White, Y.A., Woods, D.C., and Wood, A.W. (2011). A transgenic zebrafish model of targeted oocyte ablation and de novo oogenesis. Developmental dynamics : an official publication of the American Association of Anatomists *240*, 1929-1937.

Wilkins, A., Chandran, S., and Compston, A. (2001). A role for oligodendrocyte-derived IGF-1 in trophic support of cortical neurons. Glia *36*, 48-57.

Wilkins, A., Majed, H., Layfield, R., Compston, A., and Chandran, S. (2003). Oligodendrocytes promote neuronal survival and axonal length by distinct intracellular mechanisms: a novel role for oligodendrocyte-derived glial cell line-derived neurotrophic factor. The Journal of neuroscience : the official journal of the Society for Neuroscience *23*, 4967-4974.

Williams, A., Piaton, G., Aigrot, M.S., Belhadi, A., Theaudin, M., Petermann, F., Thomas, J.L., Zalc, B., and Lubetzki, C. (2007). Semaphorin 3A and 3F: key players in myelin repair in multiple sclerosis? Brain : a journal of neurology *130*, 2554-2565.

Wolburg, H. (1978). Growth and myelination of goldfish optic nerve fibers after retina regeneration and nerve crush. Zeitschrift fur Naturforschung Section C: Biosciences *33*, 988-996.

Wolburg, H. (1980). Myelinated axons of ganglion cells in the retinae of teleosts. Cell and tissue research *210*, 517-520.

Wolburg, H. (1981). Myelination and remyelination in the regenerating visual system of the goldfish. Experimental brain research Experimentelle Hirnforschung Experimentation cerebrale *43*, 199-206.

Wolswijk, G. (1998). Chronic stage multiple sclerosis lesions contain a relatively quiescent population of oligodendrocyte precursor cells. The Journal of neuroscience : the official journal of the Society for Neuroscience *18*, 601-609.

Wolswijk, G. (2002). Oligodendrocyte precursor cells in the demyelinated multiple sclerosis spinal cord. Brain : a journal of neurology *125*, 338-349.

Woodruff, R.H., and Franklin, R.J. (1999). Demyelination and remyelination of the caudal cerebellar peduncle of adult rats following stereotaxic injections of lysolecithin, ethidium bromide, and complement/anti-galactocerebroside: a comparative study. Glia *25*, 216-228.

Wu, G.F., and Alvarez, E. (2011). The immunopathophysiology of multiple sclerosis. Neurologic clinics *29*, 257-278.

Wulf, P., Bernhardt, R.R., and Suter, U. (1999). Characterization of peripheral myelin protein 22 in zebrafish (zPMP22) suggests an early role in the development of the peripheral nervous system. Journal of neuroscience research *57*, 467-478.

Wyatt, C., Ebert, A., Reimer, M.M., Rasband, K., Hardy, M., Chien, C.B., Becker, T., and Becker, C.G. (2010). Analysis of the astray/robo2 zebrafish mutant reveals that degenerating tracts do not provide strong guidance cues for regenerating optic axons. The Journal of neuroscience : the official journal of the Society for Neuroscience *30*, 13838-13849.

Yang, P., Peairs, J.J., Tano, R., Zhang, N., Tyrell, J., and Jaffe, G.J. (2007). Caspase-8-mediated apoptosis in human RPE cells. Investigative ophthalmology & visual science *48*, 3341-3349.

Yasuhara, T., Shingo, T., Muraoka, K., Kameda, M., Agari, T., Wenji, Y., Hishikawa, T., Matsui, T., Miyoshi, Y., Kimura, T.*, et al.* (2005). Toxicity of semaphorin3A for dopaminergic neurons. Neuroscience letters *382*, 61-65.

Ye, F., Chen, Y., Hoang, T., Montgomery, R.L., Zhao, X.H., Bu, H., Hu, T., Taketo, M.M., van Es, J.H., Clevers, H.*, et al.* (2009). HDAC1 and HDAC2 regulate oligodendrocyte differentiation by disrupting the beta-catenin-TCF interaction. Nature neuroscience *12*, 829-838.

Yoshida, M., and Colman, D.R. (1996). Parallel evolution and coexpression of the proteolipid proteins and protein zero in vertebrate myelin. Neuron *16*, 1115-1126.

Yuan, L., Moyon, D., Pardanaud, L., Breant, C., Karkkainen, M.J., Alitalo, K., and Eichmann, A. (2002). Abnormal lymphatic vessel development in neuropilin 2 mutant mice. Development *129*, 4797-4806.

Zawadzka, M., Rivers, L.E., Fancy, S.P., Zhao, C., Tripathi, R., Jamen, F., Young, K., Goncharevich, A., Pohl, H., Rizzi, M.*, et al.* (2010). CNS-resident glial progenitor/stem cells produce Schwann cells as well as oligodendrocytes during repair of CNS demyelination. Cell stem cell *6*, 578-590.

Zhang, H., Jarjour, A.A., Boyd, A., and Williams, A. (2011). Central nervous system remyelination in culture--a tool for multiple sclerosis research. Experimental neurology *230*, 138-148.

Zhang, H., Vutskits, L., Calaora, V., Durbec, P., and Kiss, J.Z. (2004). A role for the polysialic acid-neural cell adhesion molecule in PDGF-induced chemotaxis of oligodendrocyte precursor cells. Journal of cell science *117*, 93-103.

Zhang, Y., Argaw, A.T., Gurfein, B.T., Zameer, A., Snyder, B.J., Ge, C., Lu, Q.R., Rowitch, D.H., Raine, C.S., Brosnan, C.F.*, et al.* (2009). Notch1 signaling plays a role in regulating precursor differentiation during CNS remyelination. Proceedings of the National Academy of Sciences of the United States of America *106*, 19162-19167.

Zhang, Y., Zhang, J., Navrazhina, K., Argaw, A.T., Zameer, A., Gurfein, B.T., Brosnan, C.F., and John, G.R. (2010). TGFbeta1 induces Jagged1 expression in astrocytes via ALK5 and Smad3 and regulates the balance between oligodendrocyte progenitor proliferation and differentiation. Glia *58*, 964-974.

Zhang, Y.W., Denham, J., and Thies, R.S. (2006). Oligodendrocyte progenitor cells derived from human embryonic stem cells express neurotrophic factors. Stem cells and development *15*, 943-952.

Zhou, W., and Hildebrandt, F. (2012). Inducible podocyte injury and proteinuria in transgenic zebrafish. Journal of the American Society of Nephrology : JASN *23*, 1039-1047.

Zhou, Y., Gunput, R.A., and Pasterkamp, R.J. (2008). Semaphorin signaling: progress made and promises ahead. Trends in biochemical sciences *33*, 161-170.

Zhu, X., Hill, R.A., Dietrich, D., Komitova, M., Suzuki, R., and Nishiyama, A. (2011). Age-dependent fate and lineage restriction of single NG2 cells. Development *138*, 745-753.

Zuo, H., and Nishiyama, A. (2013). Polydendrocytes in development and myelin repair. Neuroscience bulletin *29*, 165-176.